

1. Introduction

According to the International Air Transport Association (IATA) [1], in year 2018 the global airline industry comprised over 2000 airlines operating more than 23,000 aircraft, providing service to over 21,000 city pairs. The world's airlines have flown almost 35 million scheduled flight departures and carried over 4.3 billion passengers. The growth of world air traffic has demonstrated an average growth of approximately 5% per year over the past 30 years, with substantial variations due to both changing economic conditions and differences in economic growth in different regions of the world. Historically, the annual growth in air travel has been about twice the annual growth in world's GDP. Even with relatively conservative expectations of economic growth over the next decades, a continued 4-5% annual growth in global air travel will lead to a doubling of total air travel during this period.

Despite such developments, since the beginning of the commercial aircraft operations, the aviation industry has been characterized as a low profit margin business. Several reasons, specific to this activity, are attributed to this phenomenon. Ferocious fares competition, narrow band of product differentiation, extremely regulated industry, government policies and strong power of suppliers (manufacturers, travel agencies and fuel providers) are frequently pointed as main reasons of the marginal economic performance of airlines [2]. In fact, since the 80's, the average world airlines profit margin has demonstrated a narrow variation, from -5% to 10%, meaning that the impact of efficient operations of the fleets in the assigned networks is crucial for the survival of the business [3]. This is observed in Fig. 1.1, which shows the global airlines profitability since the year 2000.

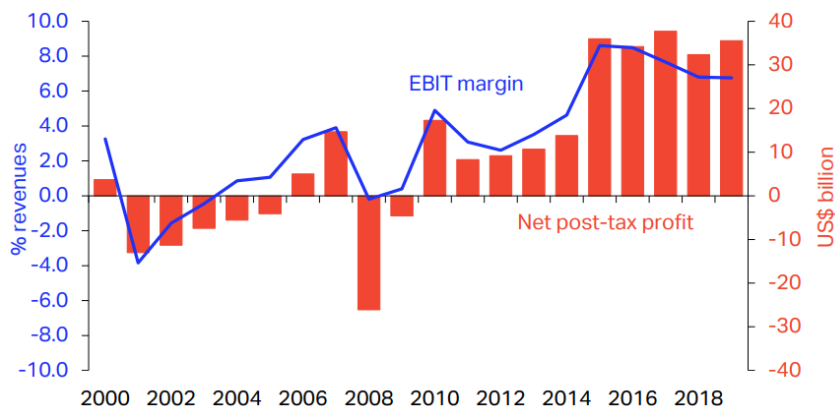


Figure 1.1: Global airlines profit margin since year 2000 [2]

Under this context, the usual initial approach adopted by airlines, with the objective to increase the profit margin, is the adoption of methods to reduce operational costs. In the flight operations domain, this is mainly related to the reduction of the trip fuel burn and trip time.

Trip fuel reduction links with an important aspect that has been recently impacting the industry: The global commitment on mitigation of aviation greenhouse gas emissions, established at the United Nations Climate Conference held in 2009 at Copenhagen [4]. This commitment was set after findings reported by the Aviation Working Group of Intergovernmental Panel on Climate Change in 1999 where aviation was found to contribute to 2.5% on global CO₂ emissions with a growing tendency in the following years [5]. In fact, a recent study conducted by Fregnani and Mattos shows that the share contribution of aviation in global emissions would increase up to 15% by the year 2050, if the other transport modals turn to electrical energy as the main source of energy and the aviation industry keeps its dependence strictly on fossil fuels [6]. Since then, discussions have evolved on the search for effective solutions with the objective of reducing the participation of aviation industry in global gas emissions. In the final report of the Copenhagen Conference, the following goals were agreed by the main aviation industry stakeholders (airlines, manufacturers, airports and air navigation service providers):

1. Improvement in fuel efficiency of 1.5% per year from 2009 to 2020 (measures under industry control, linked to operational procedures and basic infrastructure improvements).
2. Carbon-neutral growth at 2020 (when fuel CO₂ emissions are neutralized).
3. Reduction in CO₂ emissions to 50% of 2005 levels by 2050.

Here the term “fuel efficiency” is defined as the mass of fuel burned per passenger kilometer transported and is directly proportional to the level of greenhouse gas emissions, including CO₂. Toward the improvement (reduction) of this quantity, the aviation industry has since then driven to invest hard and continuously on new technologies (aircraft design and biofuels) and infrastructure (airports and air traffic management), in addition to the improvement of operational procedures. Focus on fuel efficiency became the main goal of all industry stakeholders, not only driven by fuel prices, but also considering the environmental aspects. Fig. 1.2 shows the estimation of added contribution of each of these components on the total emissions on yearly basis, considering an average of 5% growth on world traffic demand [1].

Based on these goals, a few years later, the International Air Transport Association, representing airlines, announced the so-called “Four-pillar” Strategy [7] [8], with the objective to guide the industry stakeholders toward the 2050 emissions reduction goal, via specific areas of development as shown in Table 1.1. In this framework, the development of market-based measures, including establishment of global offset mechanisms, was also included as an alternative solution toward the 2050 target. In fact, this was recently proposed in a global level by the International Civil Aviation Organization (ICAO) in 2018, with the development of the Carbon Offsetting and Reduction Scheme for International Aviation (CORSIA) Program [9].

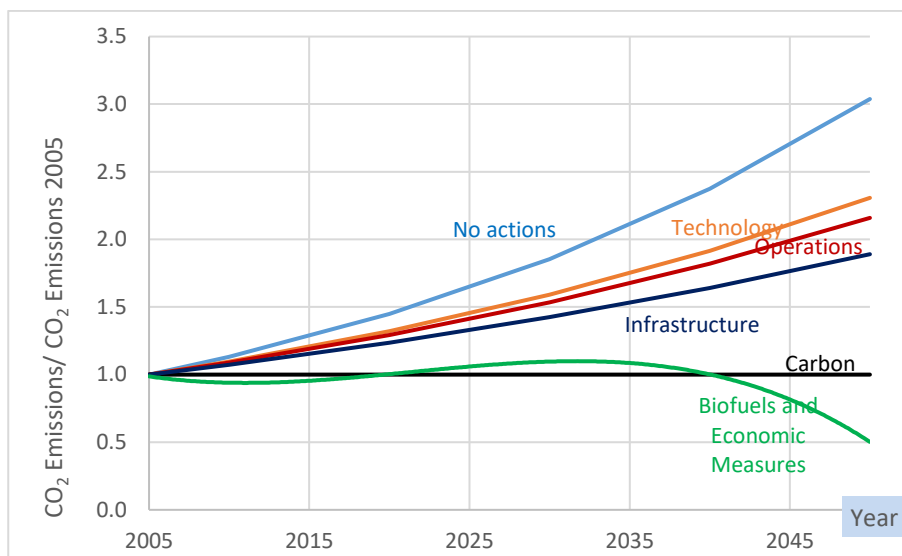


Figure 1.2: Aviation industry emissions reduction roadmap [8]

Table 1.1: Global strategies for reducing aviation fuel uses and emissions

| Technology | Flight Operations | Infrastructure | Market Base Measures |
|--------------------------------------|----------------------------------|---------------------------------------|------------------------------|
| New airframe and engine technologies | Improved operational procedures | More efficient air traffic management | Global offset mechanisms |
| Retrofits | More efficient flight procedures | More efficient airports | Positive economic incentives |
| Sustainable aviation fuels | Weight reduction | | Public-private initiatives |

Among the Four Pillars, the technology related initiatives are considered the main contributors for achieving the desired 2050 objectives in emission reduction [8]. Its achievement strongly depends on the development and implementation of new aircraft design methodologies using higher fidelity computational tools. In fact, aircraft and the engine manufacturers have been investing heavily to produce the airplanes as fuel efficient as possible. The main areas identified to have direct impact on fuel efficiency are airframe (aerodynamics, structures, equipment systems and new configurations) and engines technologies. It can be easily observed that each subsequent generation of airplane has better weight-to-drag ratios, improved wing performance, and the engines that use less fuel. These efficiencies can be measured and are part of the proposition airlines evaluate when deciding to acquire or lease new airplanes.

This effort may be verified along the aviation history since new aircraft designs have always driven toward more and lower fuel efficiency values. A study conducted by the Air Transport Actions Group (ATAG) [10], considering several air transport aircraft data, concluded that over the last 50 years, since the operations of the first generation of jet transport aircraft (Comet 4), the fuel efficiency has been reduced by over 82% when compared with the current designs. Figure 1.3 shows the results of such study.

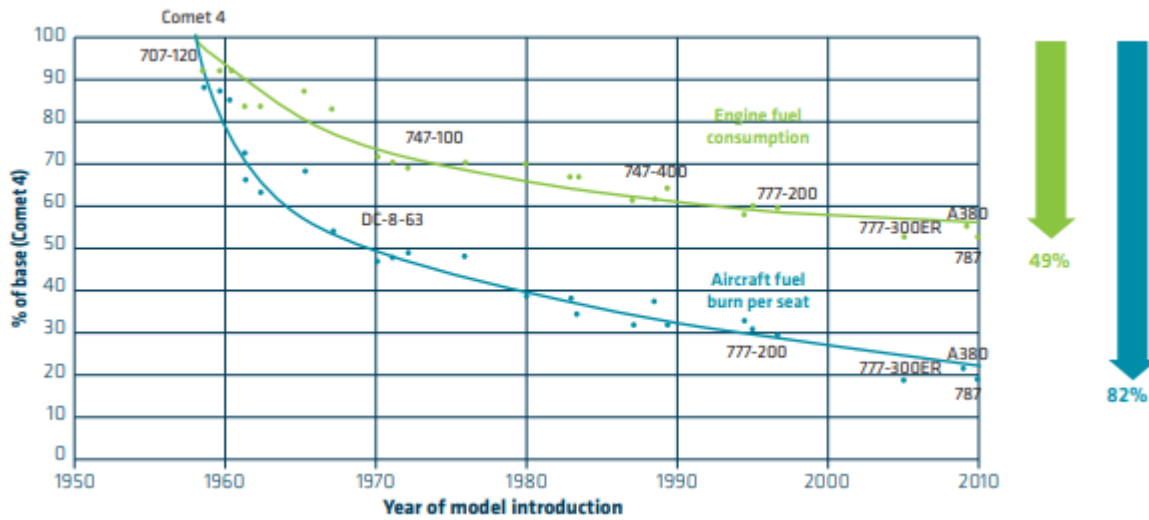


Figure 1.3: Fuel efficiency improvement since the first commercial jet [10]

It is worth mentioning that from 1970 onward, fuel efficiency was further enhanced with the development of flight management systems which automatically set the most efficient cruise speed and engine power settings based on fuel and other operational costs involved. Recently, airlines

have developed a range of operational, maintenance and planning procedures to ensure that their current technology aircraft are flying to their optimal levels of efficiency [7] [10]. Nowadays aircraft are equipped with the 4th generation of jet engines and carbon fiber fuselages (such as the Boeing 787 and the Airbus 350), offering 20% improvement in fuel efficiency over 1990's levels.

Tables 1.2 and 1.3 show the list of proposed technological improvements (airframe and engines related) and their associated fuel efficiency reduction related to 2005 levels. It is noticeable that up to 30% reduction on fuel efficiency may be achievable after 2020, most of them related to engines technologies [2] [7].

Table 1.2: Airframe technologies development impact on fuel efficiency

| Group | Concept | Technology | Applicability | Fuel Efficiency Reduction Benefit | TRL in 2014 | Expected Availability |
|------------------------|---|----------------------------------|---------------|-----------------------------------|-------------|-----------------------|
| Aircraft Configuration | Truss braced wing | | After 2020 | 10 to 15% | 2 | 2028 |
| | Hybrid wing-body | | After 2020 | 10 to 15% | 4 | 2026 |
| | Cruise efficient stall | | After 2020 | < 1% | 3 | 2027 |
| | Flying without landing gear | | After 2030 | 10% to 20% | 1 | 2032 |
| Aerodynamics | Advanced Wingtip | Wingtip fence | Retrofit | 1% to 3% | 9 | 2012 |
| | | Blended winglet /Sharklets | Retrofit | 3% to 6% | 9 | 2012 |
| | | Raked wingtip | Retrofit | 3% to 6% | 9 | 2012 |
| | | Split winglets (scimitar tips) | Retrofit | 2% to 6% | 7 | 2022 |
| | | Spiroid wingtip | After 2020 | 2% to 6% | 7 | 2022 |
| | High Lift Devices | High lift / Low Noise | After 2020 | 1% to 3% | 4 | 2026 |
| | | Variable Camber Trailing Edge | Before 2020 | 1% to 2% | 9 | 2012 |
| | | Dropped spoiler | Before 2020 | 1% to 2% | 9 | 2012 |
| | | Hingeless flap | After 2030 | 1% to 2% | 3 | 2027 |
| | Drag reduction | Drag coating | Retrofit | < 1% | 9 | 2012 |
| | | Turbulent flow coating (riblets) | Retrofit | 1% | 8 | 2015 |
| | | Graphic Films | Retrofit | 1% | 9 | 2012 |
| | Natural Laminar Flow | | After 2020 | 5% to 10% | 7 | 2022 |
| | Hybrid Laminar Flow | | After 2020 | 10% to 15% | 7 | 2022 |
| | Variable Camber | | Before 2020 | 1% to 3% | 8 | 2015 |
| | Variable Camber with new control surfaces | | After 2020 | 1% to 5% | 5 | 2024 |
| Structures | Active Load Alleviation | | Before 2020 | 1%to 5% | 9 | 2012 |
| | Composite Primary Structures | | Before 2020 | 1% to 3% | 9 | 2012 |
| | Smart wing/actuators | | After 2020 | < 1% | 6 | 2023 |
| | Morphing wings | | After 2030 | 2% to 8% | 5 | 2024 |

Table 1.3: Engine technologies development impact on fuel efficiency

| Group | Concept | Technology | Applicability | Fuel Efficiency Reduction Benefit | TRL in 2014 | Expected Availability |
|---------------------------|--------------------------------|----------------------------|---------------|-----------------------------------|-------------|-----------------------|
| New Engine Architecture | Geared Turbofans | | Before 2020 | 10%-15% | 7 | 2016 |
| | Advanced Turbofans | | Before 2020 | 10%-15% | 7 | 2016 |
| | Counter rotating fan | | After 2020 | 15%-20% | 3 | 2019 |
| | Open Rotor | | After 2020 | 15%-20% | 5 | 2019 |
| | New engine core concepts | | After 2030 | 25%-30% | 2 | 2026 |
| | Embedded Distributed Fan | | After 2030 | Less than 1% | 2 | 2026 |
| Advanced Concepts | Fan | Component Improvements | Before 2020 | 2%-6% | 8 | 2013 |
| | | Zero Hub | Before 2020 | 2%-4% | 7 | 2016 |
| | | High BPR | Before 2020 | 2%-6% | 7 | 2016 |
| | | Variable Nozzle | After 2020 | 1%-2% | 7 | 2016 |
| | Combustor | Variable Flow Splits | After 2020 | 1%-2% | 5 | 2020 |
| | | Ultra-compact low emission | Before 2020 | 1%- 2% | 5 | 2020 |
| | | Advanced | Before 2020 | 5%-10% | 8 | 2013 |
| | Compressor | Bling concept | After 2030 | 1%-3% | 3 | 2023 |
| | | Bisk Concept | After 2020 | 1%-3% | 7 | 2016 |
| | | Variable Geometry Chevron | After 2020 | Less than 1% | 5 | 2020 |
| Nacelles and Installation | Buried engines | | After 2020 | 1%-3% | 5 | 2020 |
| | Reduced nacelle weight | | Before 2020 | 1%-3% | 7 | 2016 |
| Engines Cycles | Adaptive Cycles | | After 2030 | 5%-15% | 2 | 2030 |
| | Pulse Detonation | | After 2030 | 5%-15% | 2 | 2030 |
| Others | Boundary Layer Ingestion Inlet | | After 2020 | 1%-3% | 3 | 2023 |
| | Ubiquitous Composites | | After 2020 | 10%-15% | 3 | 2023 |
| | Adaptive flow control | | After 2020 | 10%-20% | 2 | 2026 |

According to ICAO, flight operations related initiatives (the second pillar) would have potential to reduce emissions in a range of 2% to 6%, despite technology improvements [5]. Emissions are directly proportional to trip fuel burn, this means for airlines direct investments on flight path management, enhancements on flight planning methods and the adoption of fuel conservation programs should be carried out. With the oil crisis in the 70's, such procedures and methods have been developed by aircraft manufacturers and airlines with the objective to reduce fuel burn, and nowadays, they have been enhanced by high performance computer dedicated applications. Some examples are: fuel reserves management, empty weight management, center of gravity management, optimized flight planning systems, optimized strategies for climb, cruise and descent phase on speed and altitude management, among others [11] [12].

It should be noted that although the magnitude of such reductions seems to be small, the impact of such reductions in the whole network served by a fleet throughout a year is significant, since the multiplication factors are large. For example, 1% of trip fuel burn reductions on a Boeing 737-800 fleet, considering 13 hours of daily utilization and average sector of 600 nm (typical for a large Low-Cost Carrier), represents savings about 56.9 tons of jet fuel per year per aircraft. A fleet of 100 aircraft, would represent annual savings of about 3.7 Million US\$, considering an average fuel price of 0.65 US\$/kg. Although the magnitude of investments in such kind of initiatives is normally

lower than acquiring new aircraft quipped with leading technologies, its success is highly dependable on the implementation of company policies and staff training, which are sometimes hard to be fully effective due to cultural aspects and resistance of change [12].

The third pillar, related to aviation infrastructure initiatives (Air Traffic Management and Airport operations related), have potential to reduce aviation emissions by 12% [5]. This area, initially considered complementary on flight operations initiatives, has direct impact on the operations of aircraft which deals with the trajectories management of traffic flows evolving in a certain region. Moreover, the integration of onboard and ground systems (CNS/ATM technologies) have driven the efficient use of the airspace for the benefit of all stakeholders (airlines, airports and air navigation service providers). The main objective here is to reduce the delays associated with airspace capacity and infrastructure constraints. The more delays aircraft experience while maneuvering, the more fuel is burned and lower fuel efficiency. Therefore, the minimization of gate to gate time represents less fuel burnt and then less emissions.

In addition to the environmental aspects described above, optimization methods have been widely researched to improve airline's network efficiency toward profit maximization. Most optimization methods are related to total operational cost minimization and therefore indirectly related to the reduction of fuel burn. Such methods are developed to be applied on airline's network planning phase, in which three main processes blocks are considered [13], as shown in Fig. 1.4.

The first block is related to the process called Route Assignment (or Schedule Generation). The route allocation along the city pairs is determined according to the estimated or actual passenger and cargo demand, taking into consideration airport constraints, such as operational hours or infrastructure issues. At this stage, gravitational demand forecast models are frequently adopted when traffic data between cities is absent [14] [15].

It is worth mentioning that the aircraft types used in this block are selected based on preliminary studies conducted by the airline's fleet planning departments, frequently assisted by manufacturer's marketing teams. Usually, families of existing aircraft from one or more manufacturers are tested into the network produced at this phase, through experimental trials, to determine the highest potential profit configuration. In each run, once the fleets are selected, the amount of frequencies for each city pair is determined for each aircraft type based on their specific capacity, design range and a preliminary estimation of direct operational costs, as function of the sector distance. In this type of problem, the optimization models, typically falling into the Mixed Integer Linear Programming (MILP) class, are designed with the objective to exhaust a given

demand for each sector, based on a specific load factor and market share for each city-pair [16]. The objective function is frequently set for revenue or yield maximization, considering a pre-determined average fare [17] [18].

The second block is related to the process called Fleet Assignment (or Aircraft Scheduling). There, the optimum time schedules of each city-par (slots) are determined and assigned to each tail number (of each aircraft type), according to the frequencies determined for each route resulting from block 1 optimization. In this process, aircraft maintenance requirements and airport specific operational limitations (such as compatibility, presence of maintenance base, handling services, fuel availability are taken into consideration on the optimization problem. In this block, the objective function is usually set to optimize the fleet size [19].

After the network is implemented, airlines frequently assign the aircrafts which present the lowest performance degradation and empty weight combination to the longest routes, where the Maximum Takeoff Weight (*MTOW*) limit is frequently reached. This practice may also be introduced as new constraint into the block 2 optimization, whenever the aircraft schedule is reviewed on a frequent basis. The third and last block is related to the process called Crew Assignment, where pilots and commercial crew members are allocated to each flight, complying with labor regulations and crew technical constraints, on a rostering/pairing scheme. In this block, the objective function is frequently set to minimum crew numbers.

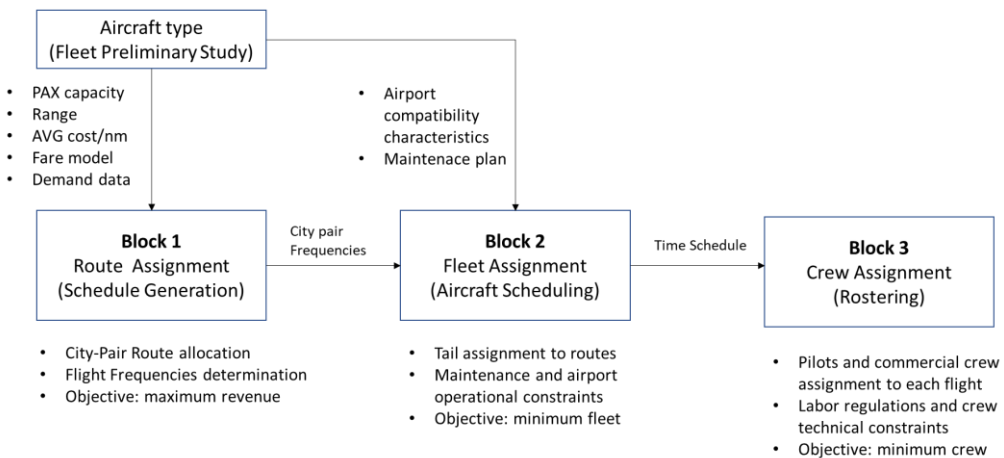


Figure 1.4: Typical network planning process adopted by airlines

These three blocks are interdependent, where outputs from each block are the necessary inputs for the subsequent block. However, each block has its own objective functions which impact on

the total profit of the network. Because of this, some models are built to solve all blocks in a single step, where the minimization of costs or maximization of revenues are set as global objective functions [13]. However, this unified resolution method, applied to optimize the entire process, leads to large-scale problems sometimes involving non-linear programming algorithms and therefore significant computational power may be required for the complete solution [20]. Nevertheless, airlines preference is to solve each block separately to have faster and less complex to model solutions, even if a sub-optimum solution is reached.

As earlier mentioned, the selection of the aircraft fleet types suited to the network is most of the times performed prior to the optimization of block 1, which has strong influence on flight frequencies. The determination of the optimal flight network and associated frequencies is a key step for airlines to elaborate their strategic planning, from market determination to aircraft and crew rostering. An optimal solution for this block facilitates the solution for the others. Furthermore, if in this optimization, the optimum aircraft types could be associated with the assigned network, the goal for maximum revenue and/or minimum operational costs would even be further improved. In other words, the network optimization is normally carried out separately from the aircraft optimization in the airline planning process.

1.1 Commercial transport aircraft (“airliners”)

Airliners are defined as airplanes designed for carrying passengers and cargo in commercial air transport services. Depending on the number of seats and type of mission, they are be classified into four size categories as described below:

Wide-body airliners

Also known as a twin-aisle aircraft, this is a jet airliner with a fuselage wide enough (typically 5m to 8m diameter) to accommodate two passenger aisles with seven or more seats abreast, with seating capacity between 250 to 500 passengers. These aircraft are usually allocated on long-haul flights between airline hubs and major cities where high a volume of passengers travelling in a single trip is a factor to consider. Examples of aircraft in this category flying now adays are: Boeing 747, Boeing 767, Boeing 777, Boeing 787, Airbus A300/A310,

Airbus A330, Airbus A340, Airbus A350, Airbus A380, Lockheed L-1011 TriStar, McDonnell Douglas DC-10, McDonnell Douglas MD-11, Ilyushin Il-86 and Ilyushin Il-96.

Narrow-body airliners

This is a class of airliner is designed to accommodate passengers in single-aisle configuration fuselage (typically 2m to 4m diameter), with four to six abreast and seating capacity between 120 to 250 passengers . These are medium size aircraft generally used for short/medium-haul flights, in hub-and-spoke or fully connected networks, where higher route frequencies are important factors to be considered. Examples of narrow-body airliners flying now adays are: Airbus A220, Airbus A320, Boeing 717, Boeing 737, Embraer E-Jets (190/195 E1 and E2 series), and Tupolev Tu-204/214, McDonnell Douglas DC-9, McDonnell Douglas MD-80, McDonnell Douglas MD-90, Tupolev Tu-154, Ilyushin IL-18 and Ilyushin IL-62.

Regional airliners

This class of airliner is designed to accommodate between 35 to 120 passengers in a single isle configuration, with three to six abreast and may be powered by either turbofans or turboprop engines. These are also medium-sized airliners typically used to feed traffic from smaller cities into the large airline hubs where shorter routes and lower passenger demands are expected. These aircraft are frequently operated by smaller airlines that are contracted as “feeders” to the main carriers, which should offer equivalent level of services to passengers than the last ones. Typical aircraft in this category include : Bombardier CRJ series, Embraer ERJ 145 regional jets series, Embraer 120, Bombardier "Q" (DASH-8) series, ATR 42/72 and Saab 340/2000.

Commuter airliners

This class of airliner is designed to accommodate less than 19 passengers in typical short-haul regional feeder missions, normally powered by turboprop engines. Depending on local and national regulations, a commuter aircraft may not qualify as an airliner and may not be subject to the regulations applied to larger aircraft. In this class of aircraft normally operators do not offer amenities as lavatories and galleys, and most of the times do not carry a flight attendant. Examples of aircraft in this category are Fairchild Metro, Jetstream 31, Embraer EMB 110

Bandeirante, Cessna C208 Caravan and Pilatus PC-12. Smaller twin piston-engined aircraft made by Cessna, Piper, and Beechcraft are also sometimes used as commuter aircraft.

To illustrate the design diversity such airliners, **Table 1.4** shows some of the technical characteristics of reference aircraft in each category.

Table 1.4 : Technical characteristics of reference airliners [21]

| Size category | Wide body | Narrow-body | Regional | Commuter |
|--|---------------------------------------|---------------------------------------|--|---|
| Model | Boeing 777-300ER | Airbus A320-200 | Embraer 190-100 LR | Beechcraft 1900 |
| Engines (number) | GE90-115B1 (2) turbofan 512kN each | CFM56-5 (2) turbofan 120kN each | GE CF34-10E (2) turbofan 82.3kN each | PT6A-67D (2) Turboprop 955kW each |
| Design Range [nm] | 7,370 | 3,300 | 2,300 | 1,356 |
| Take-off distance @ MTOW/ISA/sea level | 3,200 | 2,090 | 2,056 | 1,161 |
| Maximum Certified Cruise Altitude [ft] | 43,100 | 41,000 | 41,000 | 25,000 |
| Typical Long-Range Cruise Speed | Mach 0.84 | Mach 0.78 | Mach 0.78 | 280 kt |
| Passenger capacity | 386 (3 class) | 150 (1 class) | 114 (1 class) | 19 (1 class) |
| Fuselage length [m] | 73.9 | 37.6 | 36.2 | 17.6 |
| Wingspan [m] | 64.8 | 35.8 | 28.7 | 17.6 |
| Wing area [m^2] | 427.8 | 122.6 | 92.5 | 28.0 |
| Tail height [m] | 18.5 | 11.8 | 10.6 | 4.7 |
| Wing Sweep angle [$^\circ$] | 31.7 | 25.0 | 23.0 | 0.0 |
| Cabin height [m] | 5.9 | 4.1 | 3.3 | 4.7 |
| Cabin width [m] | 6.2 | 3.9 | 3.0 | n/a |
| OEW [kg] | 167,800 | 42,600 | 27,720 | 7,764 |
| MZFW[kg] | 239,950 | 62,500 | 40,800 | 7,765 |
| MTOW [kg] | 351,500 | 78,000 | 50,300 | 7,563 |
| MLW[kg] | 251,900 | 66,000 | 43,000 | 7,604 |
| Max Fuel Capacity [lt] | 121,283 | 27,200 | 16,013 | 2,022 |

1.2 Aircraft conceptual design

Some aspects related to the conceptual design of commercial transport airplanes shall be mentioned at this point. In this phase, the aircraft configuration that best meets all the requirements related to market, certification and manufacturing (or others established by the aircraft manufacturer) is chosen, evaluating numerous alternative design concepts potentially satisfying an initial statement of design requirements. The conceptual design process is iterative in nature where concepts are evaluated, compared to the requirements, revised, reevaluated, and so on until convergence to one or more satisfactory concepts is achieved (Fig.1.5). Inconsistencies among the requirements are often exposed, so that the products of conceptual design frequently include a set of revised requirements. Conceptual design traditionally performs mission analysis, sizing, and configuration down-select of candidate designs via empirical or low-fidelity physics analyses. The geometry parameters at this stage can, in practice define the overall shape or even the outer modeling of the aircraft to a degree sufficient for aerodynamic and flight analyses, or for simple structural analyses, such as Simple Bending/Torsion Beam Theory.

According to Magalhães and Mattos [22] when selecting a group of aircraft design methodologies to automate the conceptual design, there are two basic questions that must be answered: what disciplines should be considered and to what level of detail each of them should be treated. The first one shall be addressed, from the very beginning, under the airline perspective in which profit means its survival and is the major topic of interest. Once the airfare is normally determined by market laws and yield management models, the airplane best design is the one that provides minimum acquisition and operating costs, which leads to the necessity of a cost estimating module in the design framework.

A large fraction of airplane operating costs comes from its fuel consumption (according to IATA [7], between 25% to 50% of the total operational costs depending on the airline business model), which is derived exclusively from aircraft mission performance. So, the aircraft performance module shall be the core of the optimization framework. However, in order to develop a performance module other module, it is also necessary to develop the modules related flight physics disciplines, providing key input parameters to performance computations, which are: aerodynamics (providing aerodynamic coefficients), propulsion (providing net thrust and full flow) and stability and control. These for their turn, are based on an initial geometry definition

module. These are the core modules for any airplane design framework. Improvements can be made, once the initial set is complete, to incorporate a structural layout and analysis module, which would enable a more accurate calculation of airplane weight and other sophisticated elements (i.e. assessment of aeroelastic characteristics, noise, etc....).

Once the minimum set of modules is defined, the second question may be addressed: how deep the selected disciplines should be developed. This is related to the compromise between project development costs, time and level of accuracy required at the conceptual design phase. This is highly dependent on the available resources (human and infrastructure) and the budget allocated to the project. An interesting aspect to consider while interest in new materials and unusual configurations for future airplanes, these methodologies are being constantly revised.

Frequently based on a point mass models, performance computations rely on analytical approaches of the main flight physics disciplines (aerodynamics, propulsion, stability, control and performance) [23] [24] and in order to estimate fuel consumption, for a given mission and geometry. After some iterations, designers can determine, with a certain margin of error, the size and weight of the major aircraft components (fuselage, wing, empennage). Frequently, numerical optimization techniques are applied in this process with the objective to select engines, define the airplane layout and establish system architectures [25]. In the conceptual design phase, the engine is selected, aircraft layout containing access panels and structural shape is defined, the airplane is sized, and system architectures are established. After this phase, the aircraft configuration concept will look like the image shown in Fig. 1.6 [26].

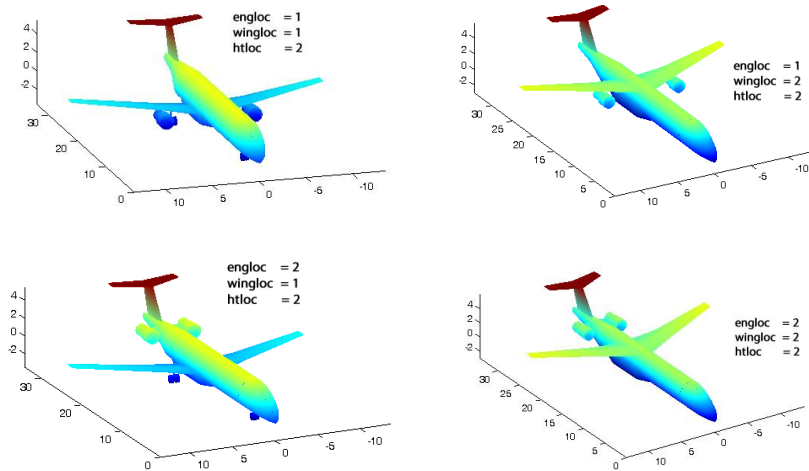


Figure 1.5: Conceptual design configurations study [12]

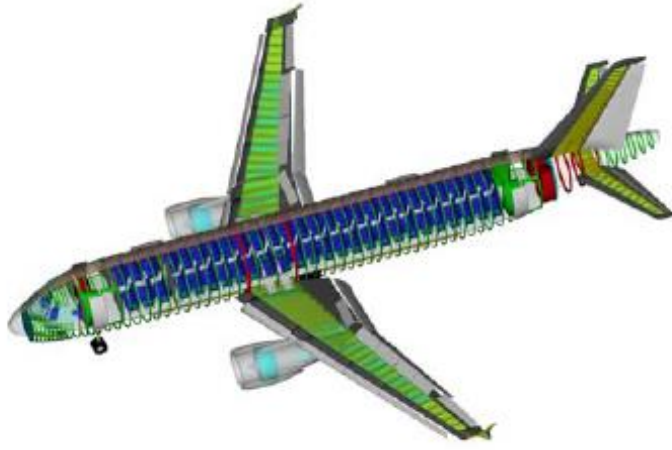


Figure 1.6: Aircraft layout after the conceptual design is finished [27]

Typically, the conceptual design process is carried out by aircraft manufacturers (and frequently by the academia) through optimization of averaged direct operational cost in each set of stage lengths (or ranges), carefully chosen by the project team. Considerations about the suitability of the product into a realistic airline network are usually not considered. With the objective to capture more realistic design scenarios, a common approach is to conduct surveys with airlines to incorporate their specific requirements into the project. Airline representatives are usually allocated into an aircraft development program council to provide regular feedbacks on design reviews. However, different airlines present different requirements for their fleets, highly influenced by their business model and operational profile, sometimes not explicit to this kind of committee for strategic reasons. Because of this, families of aircraft types (variants from a standard model) are offered to customers, in order to provide a range of solutions for different airline profiles and business models [12].

Until the 90's, the tools used for the aircraft conceptual design were limited by computational power. Simplistic models were developed in the several aeronautical disciplines, and therefore lower fidelity, in the sake of computational costs. Because of that, aircraft designers most times restricted mission requirements and performed optimizations focused on subsystems, ignoring the high degree of dependency that exists between airplane and network, resulting in a sub-optimization of systems functionalities.

With the increase of the computational power, the aircraft conceptual design process is nowadays carried out by manufacturers using Multidisciplinary Design Optimization (MDO)

frameworks. A great deal of computational analysis is required to obtain optimum configurations to satisfy many objectives and design constraints. Disciplines such as aerodynamics, propulsion, flight mechanics, structures and aeroelasticity, among others, are frequently considered in the optimization framework to obtain more realistic geometries of flight vehicles in addition to mission analysis into the network. Because of the increased complexity of such kind of methodology, significant efforts of computational analysis are required to obtain optimum configurations to satisfy many objectives and design constraints. Nowadays, many design variables (and types) may be employed, and advanced optimization algorithms that enable complex models of the aeronautical disciplines can be considered.

With the objective to produce realistic results, the airplane representation used in design framework is considerably more complex and sophisticated than that utilized by many authors. For example, Taylor [28] or Bower and Kroo [29] ran optimizations with only a single objective cost function and adopting just three aircraft design parameters (range, lift-to-drag ratio, and cruise speed), associated with simplistic frameworks with few disciplines. However, in recent studies, Mattos et. al [12] [30] proposed several design variables, constraints and features to be considered in the conceptual design framework as listed below:

- Geometric variables: front fuselage, tailcone, fuselage cross-section shape and dimensions, wing planform characteristics and wing airfoil geometries, wing structural sizing, vertical and horizontal tail characteristics, winglets, and landing gear sizing.
- Topology: engine location, wing location, number of engines, engine positioning to avoid hot exhaust gases hitting flaps and fan debris reaching fuel tanks, wing structure layout, seating abreast, number of aisles, main and nose landing gear location and sizing to comply with engine clearances from ground, and tail configuration.
- Propulsion: engine by-pass ratio, overall pressure ratio, fan pressure ratio, turbine inlet temperature, and fan diameter.
- Environmental constraints: noise footprint and engine emissions.
- Certification and performance requirements: 2nd segment climb, rate of climb, cruise speed, initial cruise altitude, time to climb, landing climb, takeoff climb, wing spanwise location where stall starts, landing and takeoff field lengths, flap settings, and fuel storage.

In addition, considering the complex network theory [31], the main indicators reflecting the statistical features of air transport network structure may be included in the framework such as degree of nodes, average degree, average path length, density and clustering coefficient [32]. Airports characteristics in the network may also be included in the mission profile computation. Information such as noise levels constraints for operating airplanes, runway length, elevation and environmental conditions could be set as fixed parameters in the framework.

In summary, there is a need for integrated design where both aircraft or family of aircraft and air transport networks are simultaneously optimized. For realistic results, a mandatory detailed representation of the airplane with accurate and concise mission performance calculations must be done, which must consider operational characteristics of airlines in their aerial network.

This should be carried out with a detailed description of the optimized configuration, not just representing the airplane with a few parameters, but with precise and concise mission performance calculations considering operational characteristics of airlines, taken into consideration fuel efficiency enhancements techniques, in the whole network. In addition, the cost of design and production of such aircraft models should be included in the optimization process, with the objective to balance the economic benefits between the airlines and the aircraft manufacturer.

1.3 Objective

This research proposes an innovative methodology for development of a Multidisciplinary Design Optimization (MDO) framework that integrates a highly detailed airplane model simultaneously with the optimum airline network. Under this scope, the following achievements are envisioned:

- I. Development of a detailed Airplane Calculator Module, incorporating typical disciplines used in the conceptual design phase.
- II. Development of a Network/Mission Analysis Module with the objective to calculate trip fuel and time on each sector of an aerial network, considering a realistic airline operational scenario, selected average load factor and market share.
- III. Development of the appropriate MDO framework, incorporating both modules, with the objective to run simulations considering the following cases:

- a. Determination of the optimal airplane design that fits into a fixed airline network and given passenger demand, on a test set of airports.
- b. Determination of optimal aerial airline network for a selected airplane type, considering an appropriate passenger demand model, on a test set of airports.
- c. Determination of the optimal design of network, considering an appropriate demand model, and fleet of three airplane types (typical airline classification for fleet purchase) at the same time, on a typical domestic airline set of airports.

1.4 Research contribution

The major contributions of the present research are outlined as follows:

- I. Integration of the aircraft and airline network designs in the same optimization process.
- II. Several design parameters are used to represent the airplane in finest detail with accurate aerodynamic, stability and control, and propulsion characteristics, necessary for realistic mission analysis. Aircraft are generated according to the following design features:
 - a. An Artificial Neural Network (ANN) system is employed to calculate the aerodynamic characteristics of the airplane configurations, based on full potential formulation with viscous correction. The use of the ANN enabled a high degree of accuracy and fidelity for the aerodynamics of the present work, allowing performance calculations in such a level never achieved in conceptual design before.
 - b. Verification of regulatory performance requirements: climb rate at 2nd segment, missed approach, takeoff field length, landing field length, climb rate at service ceiling, cruise speed, and adequate fuel storage.
 - c. Verification of noise signatures at ICAO Annex 16 standard certification points (sideline, approach, and takeoff).
 - d. Innovative method for turbofan engine weight calculation.
 - e. Realistic landing gear sizing and integration into the configuration avoiding flaps being affected by wake generated by wheels and hit by engine hot exhaust gases.
 - f. Proper sizing of wheel tires selected from tables containing internal pressure, loads, speed and other parameters. Main landing gear trunnion is positioned between the rear and auxiliary spars of the inner wing.

- g. Ditching requirements are considered for fuselage cross-section sizing.
 - h. Engines of underwing configurations are positioned in such a way to avoid uncontained fan debris to hit fuel tanks.
- III. A database of airplanes with the most distinguished characteristics is employed in the optimization of both aircraft and network integrated. Optimal fleet is then found from the airplanes from this database, ensuring faster convergence of the optimization process in this way.
- IV. Realistic airline mission performance calculation, considering:
- a. Airline operational characteristics.
 - b. Consideration of average ground and in-flight delay times per airport. Associated costs modeled as function of Maximum Takeoff Weight (*MTOW*).
 - c. Payload-range envelope limitations.
 - d. Calculation of maximum performance limit takeoff and landing weights according to regulatory requirements.
- V. The determination of the optimum network considers a two-stop route model and three airplane types making up the airline fleet. This is solved in a sub-procedure for obtaining the network with maximum profit.
- VI. Optimal airplane fleets are obtained considering maximization of Network Profit (airline objective) and Net Present Value (aircraft manufacturer objective). A genetic algorithm is used for such multi-objective optimization context.
- VII. Net Present Value (*NPV*) calculations are derived from a realistic aircraft program and adapted to each aircraft generated as function of Maximum Takeoff Weight (*MTOW*), number of passengers, wing area, engine diameter and engines maximum thrust at sea level.
- VIII. Aircraft sales price, used in the *NPV* calculations, modeled as function of Maximum Takeoff Weight (*MTOW*).
- IX. Crew salaries, used in the Direct Operational Cost (*DOC*) calculations, modeled as function of Maximum Takeoff Weight (*MTOW*).

1.5 Chapters structure

This study is organized into five chapters, bibliographical references and annexes. The chapter summaries are described as follows.

- Chapter 1 – Motivation and concepts introduction.
- Chapter 2 – Literature Review: presents the state-of-art of the existing Multidisciplinary Design Optimization (MDO) frameworks, airline network optimization methods and integrated aircraft and network optimization research.
- Chapter 3 – Methodology: presents the methods and procedures used for the development of: (i) a detailed aircraft calculation model considering five design disciplines (aerodynamics, propulsion, stability and control, weight estimation, tail sizing and landing gear sizing), (ii) a network calculation module considering two disciplines (network optimization and mission analysis) and (iii) the proposed MDO integration framework for simultaneous aircraft and network optimization.
- Chapter 4 – Results: presents the results of the proposed optimization framework considering three distinct scenarios:
 - (i) Optimization of one airplane design that fits into a fixed airline network, serving six Brazilian airports.
 - (ii) Optimization of an aerial airline network serving twenty Brazilian airports, considering a given airplane model.
 - (iii) Simultaneous optimization airplane and a network at the same time, considering five and ten airports networks.
 - (iv) Simultaneous optimization fleet of three airplane types and a network at the same time, serving twenty major Brazilian airports. In all cases, a comparison with the results produced by a reference aircraft is performed.
- Chapter 5 – Conclusions: presents the final considerations regarding the developed MDO framework, including the analysis of the achieved objective and model restrictions. Future developments and improvements of such framework are also proposed.

2. Literature review

2.1 Multidisciplinary design optimization

The Multidisciplinary Design Optimization (MDO) is an engineering design methodology in which the main objective is to determine numerically the optimal engineering design which involves several disciplines and/or subsystems, submitted to constraints and fixed parameters. This method allows the considering of interaction between disciplines as a synergetic driver into the best design solution. In fact, Sobiesczanski-Sobieski in 1993 defines for the first time, the term MDO as “*an emerging field of knowledge in which a methodology for the design of complex engineering systems are governed by mutually interacting physical phenomena and made up of distinct interacting subsystems*” with the key characteristic of “*synergism of the disciplines and subsystems*” [33].

Considering the solution of the MDO framework early in the conceptual design process, taking advantage of advanced computational analysis tools, designers can simultaneously improve the design and reduce the time and cost of the design cycle [34] [12]. According to Reymer [35], MDO techniques are capable of reducing the weight and cost of an aircraft design concept in the conceptual design phase considering minor changes to the design variables, and no additional downstream costs.

The idea of integrated engineering design frameworks was first introduced by the academia (and promptly adopted by the aeronautical industry) with the research conducted by Schmit [36] and Haftka [37] where several disciplines in wing structural optimizations were included. Some years later, the initial applications using the Multidisciplinary Design Optimization (MDO) concept, considering the integration of wing design disciplines (aerodynamics, structures and flight controls) were adopted in the work of Ashley [38] and Grossman et.al [39].

The research on multidisciplinary design architectures and optimization methods started to gain momentum during the 90’s, when computational power started to permit complex problem solvings at resonable costs. Some relevant research studies in the field are worth mentioning:

Haftka et. al [40] performed the first framework for indisciplinary analysis, considering the computational challenges for non-linear algebraic equations and coupled systems. Cramer et. al [41]

formalized the monolithic frameworks and necessary computational methods to find the global minima, based on gradient formulations.

Balling and Sobieski [42] studied several monolithic approaches and estimated their computational costs based on gradient methods. In their research, they have also identified that aircraft design may vary in single level and multilevel optimization. In single level approach, both disciplinary and system design variables are determined by the system optimizer, while in the second one, system and design variables have their own optimizers. In addition, this study identifies simultaneous analysis design (SAND) or nested analysis design (NAND) as suitable strategies to handle system variables in complex problems. In the SAND approach, both disciplinary design and state variables are determined by the optimizer, while in NAND, only disciplinary design variables are determined by it. In the first case, the optimum solution may be reached in less interactions, although providing a high computational cost.

Alexandrov and Hussaini [43] presented a complete research on possible monolithic and distributed architectures, optimization methodologies and convergence properties. In the same year, Sobieski and Haftka [44] also presented an extensive survey on mathematical modeling, design analysis, approximation concepts and systems sensitivities.

Kroo and Shevell [45] described several aeronautical design optimization formulations and their integration. Isikveren [46] presented, in his doctorate thesis, the first MDO framework applied for the whole aircraft design process. Recent research studies made use of such variety of frameworks developed by the above authors, on environmental- aeronautical applications. For example, Henderson [47] developed an environmental design framework to design and optimize aircraft for specific environmental metrics on engine emissions. Magalhães and Mattos [48] developed an MDO framework to consider the noise impact on aircraft conceptual design of three different mission profiles.

The core of the MDO framework is the analysis block, composed of a set of relevant disciplines most times dependent on each other. This block is responsible for integrating the inputs of outputs of each discipline, considering their specific design variables, and producing a desired output to be used as objective function in the optimization cycle. Depending on the type of the simulation architecture, the outputs from certain disciplines may be the inputs of others. Fig. 2.1 shows a classic example on how the output and input variables for each discipline may interact producing a main output in the range of an aircraft. In this analysis, four main blocks of disciplines are integrated: structures, aerodynamics, propulsion and performance.

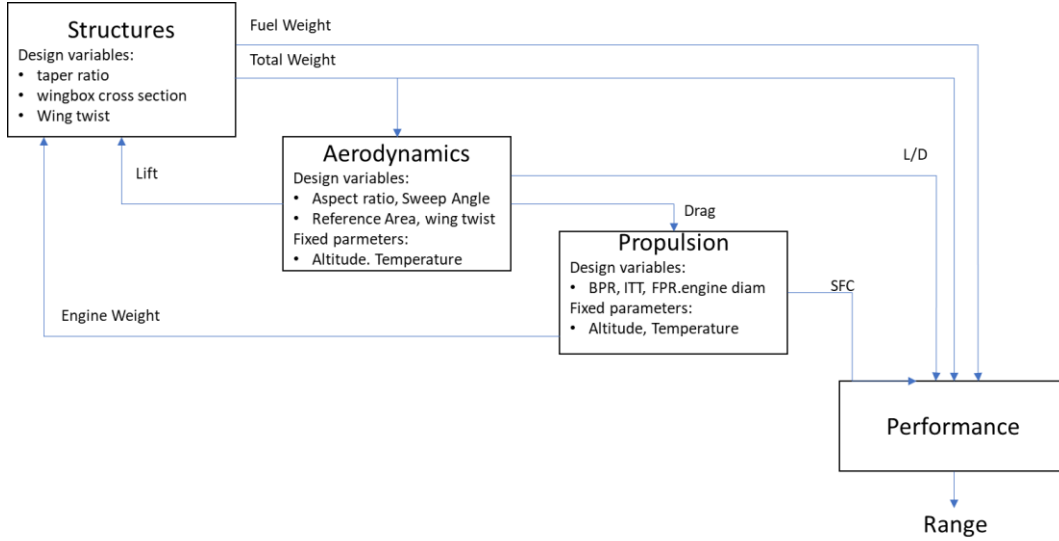


Figure 2.1: Block analysis for range computation

Many forms of approximation methods were developed to model disciplines in order to enhance the speed of the optimization when heavy computations are required. Empirical formula like the Class-I and -II methodologies proposed by Torenbeek [23] and Loftin [49] for drag and weight estimation are still extensively used for modeling because they provide faster results.

Surrogate techniques have been increasingly adopted in MDO frameworks to model the physics with enough precision and reducing the computational time of complex and heavy calculations [50] [34]. The aim of this technique is to represent the original model based on sampling data. They are recommended to be used when the inner physics of a certain system is not well known (or even understood), but the input-output behavior is well defined. The surrogate is constructed based on modeling the response of the system to a limited number of intelligently chosen data points in the design space. Its accuracy depends on the number and location of samples in the design space [50]. When only a single design variable is involved, the surrogate model resumes on the statistical curve fitting [51]. Considering multivariable problems, the most used methods are polynomial response surfaces [52], Radial Basis Functions [53], Support-vector machines [54] and space mapping [55]. More recently, Kriging interpolation [56], Bayesian Networks [57] and Artificial Neural Networks [58] have been providing satisfactory results on aerospace systems modeling. Fig. 2.2 shows the generic formulation of the MDO framework, considering its basic components: analysis, optimization and design of experiments.

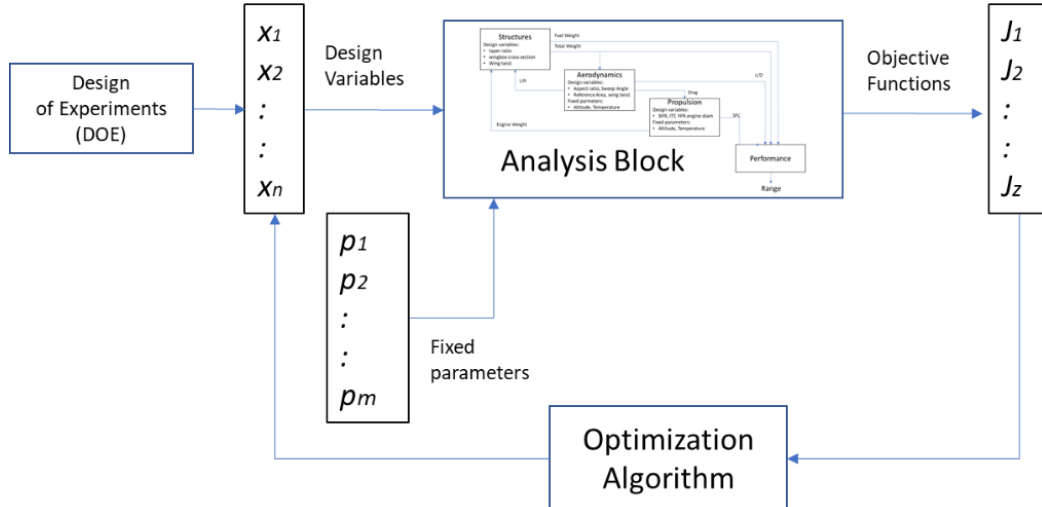


Figure 2.2: Generic MDO framework

Considering this framework, for a given J vector of objective functions, x vector of design parameters and fp vector of fixed parameters, the following generic mathematical formulation is applied:

$$\text{Minimize } \mathbf{J}(\mathbf{x}, \mathbf{fp}) \quad (\text{Eq. 1})$$

$$\text{Submitted to: } \mathbf{g}(\mathbf{x}, \mathbf{fp}) \leq \mathbf{0} \quad (\text{Eq. 2})$$

$$\mathbf{h}(\mathbf{x}, \mathbf{fp}) = \mathbf{0} \quad (\text{Eq. 3})$$

$$\mathbf{x}_{LB} \leq \mathbf{x} \leq \mathbf{x}_{UB}$$

Where: $\mathbf{J} = [\mathbf{J}_1(\mathbf{x}), \dots, \mathbf{J}_z(\mathbf{x})]^T$

$$\mathbf{x} = [\mathbf{x}_1, \dots, \mathbf{x}_n]^T$$

g and h are constraint functions

\mathbf{x}_{LB} and \mathbf{x}_{UB} are upper and lower limits of the design variables

In the MDO concept, the optimization algorithm is responsible for evaluating the value of each objective function, output from the analysis models, in each interactive cycle and adjust the values of the design variables, according to a certain algorithm, in order to seek the direction of the

minimum global solution. Depending on the type of disciplines integrated into the framework, the objective functions may be conflicting, and then slowing the convergence search toward the global minima. Optimization techniques will be explored in Session 2.2.

In order to provide the design variables space of exploration in which the optimizer runs, a design of experiments (DOE) [59] shall be provided in MDO frameworks. This statistical technique is commonly used in systematic approaches, such as in Monte Carlo simulations, where there is a need to determine the relationship between factors affecting a process and the output of that process (in this case, the process is the optimization algorithm itself). Among several types, the space fillers sampling methods (such as Latin Hypercube [60], Sobol [61] and Random Sampling) are frequently used in MDO problems. The Latin Hypercube (Fig. 2.3), derived from the 2D Latin Square which provides a single random sample on each dimensional row, is very popular in complex optimization problems, since it provides fewer design points and faster convergence times in multiple design variables environments [62].

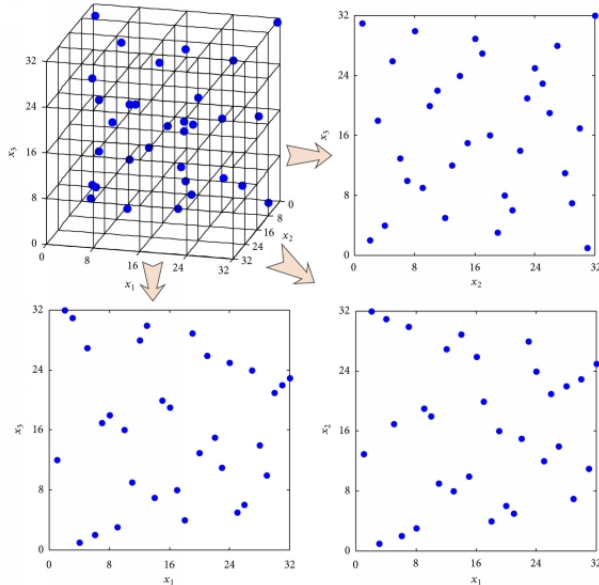


Figure 2.3: Latin Hypercube sampling [60]

According to Martins and Lambe [34], the most important considerations when implementing MDO are the description of the problem to be solved and how to organize the discipline analysis models, approximation models (if any), and optimization algorithm related to the problem formulation so that an optimal design is achieved. Such a combination of problem formulation

and organizational strategy is referred to as MDO architecture, defining how the different models are coupled and the optimization problem is solved. Two kinds of MDO framework architectures are frequently used by the industry (and academy):

- Monolithic architectures – where a single optimization problem is solved at once.
- Distributed architectures – where the overall problem is discomposed into multiple sub-optimization blocks, before going through the overall optimization.

The most intuitive monolithic architecture for engineers, and one of the first to be considered in MDO frameworks, is the so called Multidisciplinary Feasible (MDF). In this architecture, several discipline analyses, wrapped together in a Multidisciplinary Analysis (MDA) block, are executed in a certain sequence from which outputs are computed and aggregated into the final objective functions. An example of MDF framework is shown in Fig. 2.4, represented in the so-called Extended Design Structure Matrix (XDSM) format [63], considering three disciplines (Analysis 1,2 and 3), four design variables (x_i), three coupling variables between disciplines (y_i), a constraint vector I and a single objective function (f).

The analysis execution sequence is numbered from zero to seven. This framework always returns a system design that satisfies the consistency constraints, what is desirable in terms of engineering [34]. However, depending on the complexity of the disciplines, the analysis procedure may be time consuming. Also, during the optimization process, gradients of the coupled systems may be challenging to compute. This may be mitigated by the aggregation of the coupling variables to reduce the information transfer among the disciplines, in the so-called Individual Discipline Feasible (IDF) approach. In this case, constraints are rewritten as function of the design variables. This permits discipline analyses to be executed in parallel from which outputs are computed and aggregated into the final objective functions, as shown in Fig. 2.5.

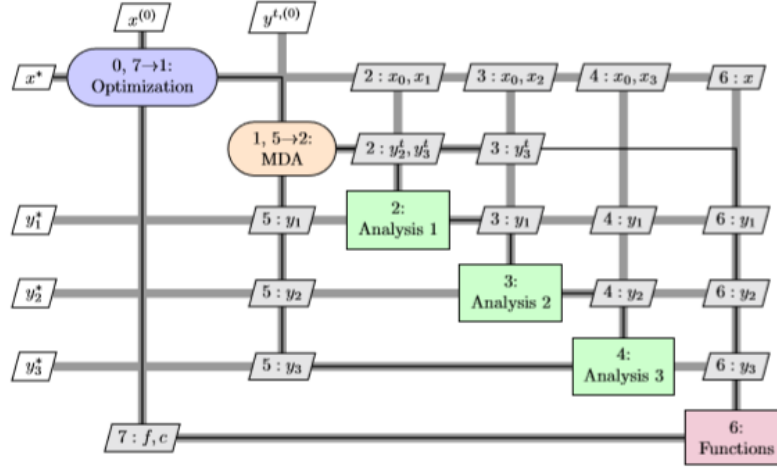


Figure 2.4: Example of Multidisciplinary Feasible Framework (MDF) [34]

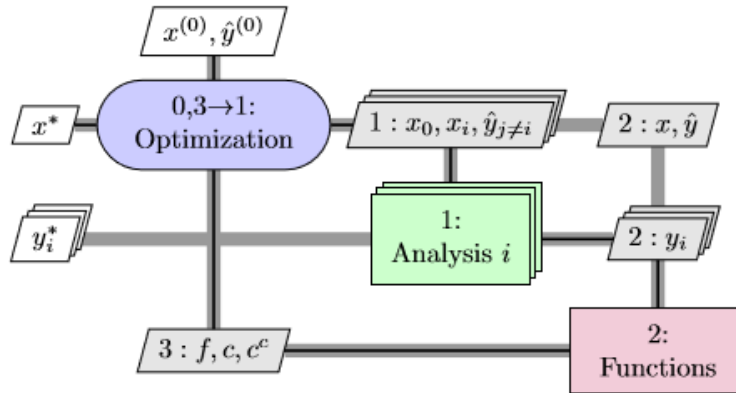


Figure 2.5: Example of Individual Discipline Feasible framework (IDF) [34]

Typical industrial practices involve breaking up the design of large and complex systems to specific engineering teams, that may be geographically distributed and have control of their own design procedures. For this reason, the distributed architectures are the most commonly used by the industry, although researchers are dedicated to investigating both [64]. An example of such framework is the Collaborative Optimization (CO) as shown in Fig 2.6, where a sub-optimization process is applied at a certain discipline analysis level. In this framework, the discipline sub-optimization problems are made independent of each other by using copies of the coupling and shared design variables. These copies are then shared with all the disciplines during every iteration of the solution procedure [34].

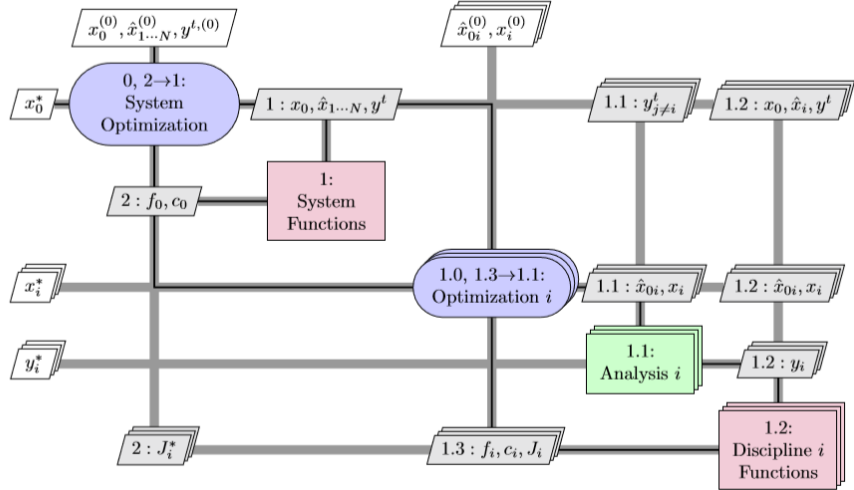


Figure 2.6: Example of Collaborative Optimization framework (CO) [34]

As extensions to the above classifications, Balling and Sobieski [42] define the concept of simultaneous analysis and design (SAND) or nested analysis design analysis (NAND) frameworks. In SAND, both design and state variables are determined by the optimization process, mostly used in distributed architectures, while in NAND, only the design variables are determined by it. It should be noted that different architectures and optimization methods may be used to solve a given optimal design problem. However, the correct definition of the type of architecture adopted is a key factor for the effectiveness of convergence of the optimization process [65] and has a significant influence on the final design. For example, if the calculations permit a given architecture to be run parallel, a distributed architecture is always preferred over a monolithic architecture for the sake of increased computational expense [34].

2.2 Design optimization techniques

The design optimization process is a consolidated activity of any engineering branch. Optimization methods have been in use since the 50's and have been combined with design synthesis and parametric analysis in the aerospace industry aiming to provide the best technical and/or economical solution to engineering problems. According to Sobieski [33], an optimization method is necessary whenever at least two opposing trends exist as function of the design variables during the analysis process. Optimization algorithms work under the same basic principle: in each cycle, the design parameters are adjusted, according to a certain function based on the evaluation

of the objective functions, seeking the direction of a minimum (or global) global solution. In early stages, when computer power is limited, graphical methods were used to find the minimum (or maximum) of multivariate function [66].

The selection of the suitable optimization method to be used in the airplane conceptual design process requires a careful analysis of the nature of the problem. The first aspect to consider is that calculations usually rely on information from several different types of objective functions and constraints which may or may not be continuous and differentiable. This might be a showstopper for some methods, where first and second order derivatives are most of the times required. Secondly, consideration of computational costs: an automated algorithm may take from few minutes to hours on running a single case depending on the level of fidelity of the models required for the results. This might be an issue considering the timelines of the project. Finally, the optimization method must be flexible enough to tackle both single-objective and multi-optimization problems with good converging characteristics. The designer should be able to perform some level of sensitivity analysis when multiple objectives are inserted into the optimization problem, like a Pareto front analysis [22]. Several techniques and methods have been developed over the years to address this issue, classified in two major groups: gradient-based methods and gradient-free methods, as shown in Fig.2.7.

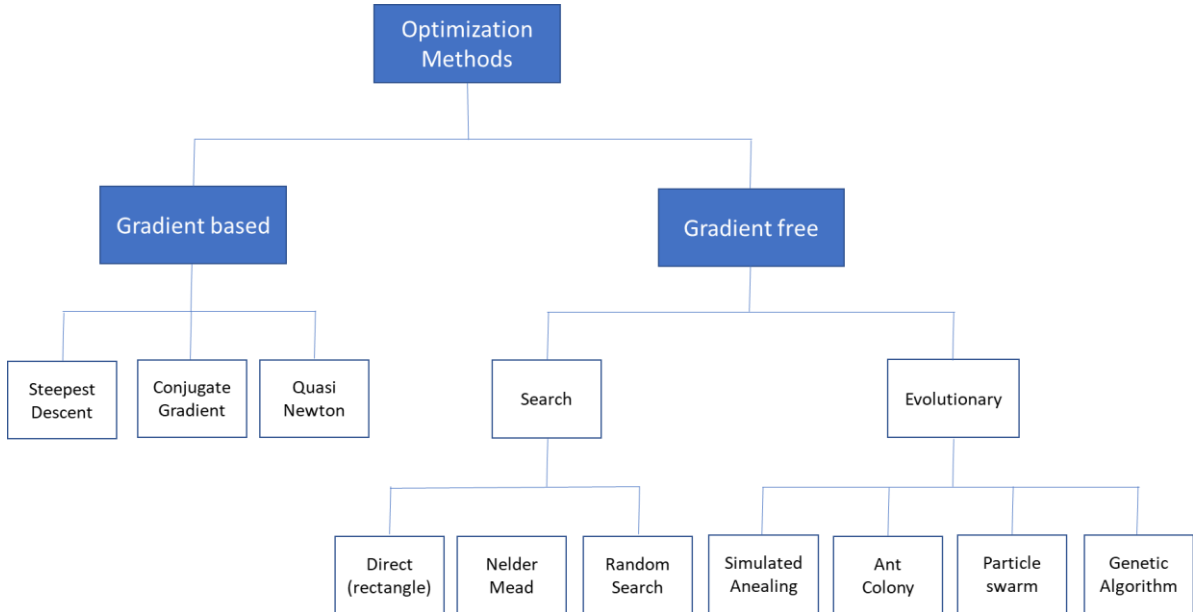


Figure 2.7: Types of Optimization Algorithms [65]

Initially, MDO problems were formulated considering single objective functions, continuous design variables and few disciplines, typical from aero-structural formulations. Under these scenarios, gradient-based and search algorithms were suitable. Since they are relatively simple to implement and capable of finding the local optima with high reliability, these methods became extremely popular in early 80's when computer power started to improve.

However, in such methods, the search for the global minima may get stuck when multiple peaks and valleys are present in the design space – a common characteristic in complex multi-objective/multi-variables and non-linear problems. Depending on the setting of initial conditions of design variables, the results may be trapped into local solutions. Also, these methods require the continuous and differentiable functions for evaluation of gradients (1st and 2nd order), which is sometimes difficult or not possible to calculate (i.e. discrete or step functions) [67]. This may cause difficulties on the convergence depending on the size of calculation steps adopted. Some examples of gradient based methods are: adjoint equations [68], steepest descent [69], conjugate gradient [70] and sequential quadratic programming [67]. With the increasing complexity of the MDO frameworks (multi-objective problems and increasing number of design variables), other optimization methods started to be formulated, such as in the research conducted by Tappeta and Renauld [71] on collaborative optimization and Miettinen [72] on non-linear multi-objective methods. Also, with the increasing number of disciplines, decomposition methods were integrated into these algorithms [73].

Later in 90's, with the increase of computational power, gradient-free search methods introduced in MDO frameworks. Among these, evolutionary algorithms have been demonstrated to be efficient for complex MDO problems involving different types of design variables. The main characteristic of such methods is the capability to evolve to better design variables at each optimization cycle, seeking the global minimum solution, based on a nature-inspired logic set to evaluate the objective (fitness) functions [74]. The most popular algorithms of this class are:

- Simulated annealing (SA).
- Particle swarm optimization (PSO).
- Ant colony optimization (ACO).
- Genetic algorithms (GA).

The Simulated Annealing (SA) algorithm is inspired on searching for lower entropy thermal equilibrium in metallic structures, using a statistical random search logic. In this method, the

acceptance of a new design worse than the previous one is occasionally and probabilistically allowed, increasing the chances to escape from local minima. Because of that, the speed of convergence might be slower than other methods, depending on the initial setting conditions of the system. This method is designed and mostly applied in single objective optimizations [75].

The Particle Swarm Optimization (PSO) algorithm iteratively improves a candidate solution with regard to a given measure of quality. In general, it presents a fast convergence and may deal with multiple objectives. It solves a problem by having a population of candidate solutions, modeled as flying particles, and moving these particles around in the search-space according to simple mathematical formula over the particle's position and velocity. Each particle's movement is influenced by its local best known position, but is also guided toward the best known positions in the search-space, which are updated as better positions are found by other particles. This is expected to move the swarm toward the global minimum [76]. However, some studies show that the algorithm may still lead to early convergence or particles spread, very dependent on empirical data to set up initial conditions [77] [78].

Ant colony optimization (ACO) is an algorithm based on behavior of ants in a colony. Artificial ants (simulation agents) seek optimal solutions by moving through a parameter space representing all possible solutions. Real ants lay down pheromones directing each other to resources while exploring their environment. The simulated ants record their positions and the quality of their solutions, so that in later simulation iterations, more ants locate better solutions [79]. Initially idealized for shortest path routing problems, ant colony optimization may be applied for the search of single objective optimum searches. According to recent studies [80] [78], although the convergence is mathematically proven, it is difficult to determine its time to reach the global minima.

Evolutionary optimization methods are known to handle noisy, non-smooth responses and are able to operate efficiently in large problems. Among them, Genetic Algorithms (GA) offer an alternative to the solution of complex and diverse frameworks, since they are simple to couple with the analysis modules, and do not incur the cost of computing the derivatives and can handle different types of design variables and constraints [81] [74].

GA methods are based on the natural biological evolution which operates on populations of potential solutions applying the principle of survival of the fittest to produce better approximations to a solution. It has been demonstrated to work with acceptable levels of robustness on multi-objective/multivariable problems, aiming to reduce the number of qualitative decisions required

and with increase in the number of design variables [74] [82]. At each generation, a new set of approximations is created by the process of selecting individuals according to their level of fitness in the problem domain and breeding them together using operators borrowed from natural genetics. This process leads to the evolution of populations of individuals that are better suited to their environment than the individuals that they were created from (just as in natural adaptation). Individuals are encoded as strings (chromosomes) composed over some alphabet(s), so that the genotypes (chromosome values) are uniquely mapped onto the decision variable (phenotypic) domain. The genetic characteristics of an individual are stored in a chromosome, which is represented by the set of chosen design parameters. The GA algorithm standard flowchart is displayed in Fig.2.8 [83].

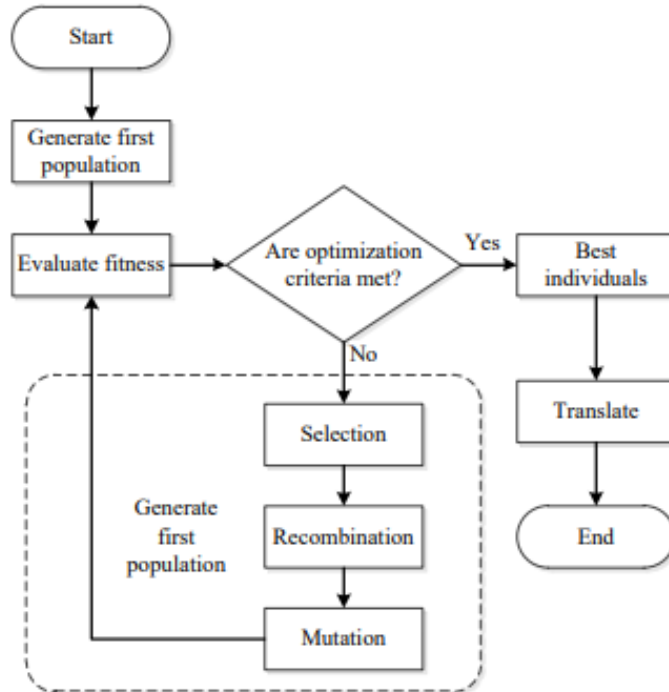


Figure 2.8: GA standard flowchart [74]

The selection, mutation and crossover mechanisms in GA are particularly important to prevent the process from ending up in a local minimum. GA methods may be used to create new designs with features that were absent not only in the parent pairs but anywhere in the entire parent generation. This amounts to extending design space by adding new variables and is entirely beyond

the capability of gradient-directed search allowing the escape from a local minima trap [44]. They differ substantially from more traditional search and optimization methods as follows:

1. Ability to generate population with parallel processing.
2. Does not require derivative information or other auxiliary knowledge. Only the objective function and corresponding fitness levels are needed.
3. Uses probabilistic transition rules, not deterministic ones.
4. Works on an encoding of the parameter set rather than the parameter set itself.
5. Allows the use of continuous, discrete, and integer design variables in the same optimization process. This feature is especially interesting in aircraft design and sizing need to be integrated with network parameters in a single optimization process.
6. Has no requirement for objective functions and constraints to be continuous (no gradient calculations involved in the optimization process).

It is important to note that GA methods provide several potential solutions to a given problem and the choice of final solution is left to the user (or decision maker). In cases where a problem does not have one individual solution, for example a family of Pareto-optimal solutions, (as is the case in multi-objective optimization), GA methods are potentially useful for identifying these alternative solutions simultaneously. Genetic algorithms are now of generalized use in optimization problems, including aircraft design and air transport networks [29] [84] [48] [85] [86]. However, one drawback is that stochastic algorithms in general can have difficulty obeying equality constraints. In addition, GA is sensitive to the initial population used. Wide diversity of feasible solutions is what is usually wanted.

The Multi-objective Genetic Algorithms (MOGA) are extensions of the standard GA [87] [88], based on controlled elitism concepts applied on multi-objective context. Its efficiency is ruled by two inherent operators (crossover and mutation) and the use of elitism, i. e., the best organism from the current generation to carry over to the next. The direction of improvement is always evaluated by comparing the fitness of the individual from generation with the fitness of its parents belonging to the previous generation. The new individuals are then created by moving in a randomly weighted direction that lies within the ones individuated by the given individuals and his parents. The crossover operator of GA may exploit structures of good solutions with respect to different objectives to create new non-dominated solutions in unexplored parts of the Pareto front. In such algorithms, the user constraints always lead to objective function penalization and allow concurrent evaluation of independent individuals [74]. The first multi-objective GA was the so-

called Vector Evaluated Genetic Algorithms [89]. Afterwards, several variations of multi-objective evolutionary algorithms were developed such as Multi-objective Genetic Algorithm (MOGA) [90], Niched Pareto Genetic Algorithm [91], Random Weighted Genetic Algorithm [92], Strength Pareto Evolutionary Algorithm [93] and Multi-objective Evolutionary Algorithm [94], among others.

Kalyanmoy et. al [95] proposed the Non-Dominated Sorting Genetic Algorithm (NSGA) as an improvement of the standard GA. In this method, a non-dominated sorting procedure is used on a modified elitism rule: the solution adopts an Elitism-preserving approach, storing all non-dominated solutions discovered so far, beginning from the initial population, enhancing the convergence properties toward the true Pareto-optimal set. In addition, the constraint handling method does not use penalty parameters. Therefore, this algorithm implements a modified definition of dominance to solve constrained multi-objective problems more efficiently. The main advantage of using this method on network and aircraft multi-objective design optimization problem is a slightly faster convergence on complex modeling when compared to MOGA [90], using both continuous and discrete variables [86].

An interesting compilation of characteristics of these GA algorithms was performed by Deb [96]. In this study, comparisons considering different methods were performed in several test functions of great complexity. The results have consistently shown the Fast Dominating Non-Sorting Algorithm (NSGA-II) [97] providing faster convergence to the Pareto Front and better spread of solutions. In fact, this was also observed in the study performed by Fregnani and Mattos [86].

Notwithstanding their effectiveness, the non-gradient methods also have their drawbacks. They may generate a large number of cycles in the analysis, due to their evolutionary characteristics and exploration of the whole design space at each run, when compared with gradient methods. Therefore, their use is limited by the computational costs, which is sometimes a critical factor in the research. In addition, these methods may lead to different designs each time they are run and the convergence is not completely mathematically proven in most of the cases [66] [74] [44]. This was demonstrated by Zingg et. al [98] in study where a genetic algorithm is compared with a gradient-based (adjoint) algorithm on several single and multi-objective aerodynamic shape optimization problems. Results demonstrated that both algorithms reliably converge to the same optimum, depending on the nature of the problem, the number of design variables, and architecture chosen, the genetic algorithm requires from 5 to 200 times as many function evaluations.

Finally, Martins and Lambe [63] [34] concluded that, for complex MDO frameworks, using non-gradient methods likely lead to better final designs than gradient optimizers, due to the last one presenting higher possibility to converge to a local minimum early in the design process. However, if gradients can be computed efficiently, the computational cost of the gradient-based optimization may be far less than that of the global optimization because the discipline analyses do not need to be run as many times.

2.3 Air transport network optimization

The Airline Deregulation Act, released in late 1978 by the North American government, presented a set of economic and operational measures tailored to lower the level of control on airfares, routes and stimulate the entry of new airlines into the aviation market. Consequently, the power of civil aviation regulators over fares was eliminated, establishing market forces for the first time in the history of airline industry. Ever since, this model has been quickly replicated in other countries as a form to support the growing passenger demands worldwide. Because of free competition between airlines, Hub-and-Spoke networks have evolved as the minimum cost configuration for Legacy Airlines while fully connected networks have become the emerging solution for the Low-Cost Carriers in their competition for growing markets. Since the 90's, boosted by these industry trends and the increasing computational power, a wide range of research initiatives were conducted on network optimization techniques with the objective to reduce costs or maximize profit for airlines [17].

These initiatives included initially the route assignment problems (Block 1, as defined in Chapter 1) once there was a strong interest to compare the optimum efficiency of the Hub-and-Spoke against point-to-point route systems. This was particularly helpful to support the low-cost airlines, raising worldwide in the end of 90's, which adopted the point-to-point solution for their networks [3]. In this kind of problem, the demands between city pairs are identified and thus potential flights between airport pairs are defined. It is crucial to address airports restrictions in this process (i.e. time of operations restrictions) – to prevent the inclusion of operationally impossible flights in the solution. As previously mentioned, in this phase, the flight frequencies for each route are also determined. Some important research studies on this topic are worth mentioning:

Aykin [99] studied hub location and routing, proposing an interactive heuristic method to solve both problems separately in a simple network system. This was one of the first studies to focus on hub allocation optimization and optimum spoke routes.

The Hub-and-Spoke Network problem for an air cargo delivery fleet to determine the optimal network structure is presented by Yang and Kornfeld [100]. This study shows that a pure hub-and-spoke may not represent the optimal solution always and that other parameters such as aircraft type, cargo demand, and city location can influence the outcome. However, it uses simplistic models considering only flight-time operating costs and direct distance between city pairs.

Campbell [101] performed a study presenting an integer programming formulation for four types of hub-allocation problems, featuring discrete hub centers and one-stop models for that.

Ahuja et. al [102] presented a detailed study about applications for network optimization problems in several fields of operational research, including the ones related to transportation. This study was one of the first to explore the cost minimization problem in complex network route assignment problem using a Mixed Integer Linear Programming (MILP) computational method.

Jaillet et. al [103], in their innovative study, presented a flow-based linear model for designing networks based on minimum cost optimization. In this research, heuristic methods were proposed to solve a Mixed Integer Linear Problem (MILP), presenting as output the associated frequencies to the routes located for one or more types of aircraft. The proposed model was able to predict the occurrence of hubs if they reveal to be cost effective for the aircraft fleets considered.

A reference research on network types and respective key performance indicators was performed by Lederer et. al [31], where analytic expressions for passengers and airline costs were derived for several network types. Parametric studies were conducted to evaluate the effect of distances, demands and frequencies on profit with the aim of profit optimization.

Later in years 2000, with a significant increase of computational power, an investigation was started into the coupled solution of route assignment and flight scheduling.

Evans et. al [104] proposed a model for network optimization coupled to flight scheduling and constraints on airport capacity, including passenger demand via gravitational model, airline competition, flight delay, and airline cost in the optimization model and three aircraft types.

Caetano and Gualda [13] also proposed a solution for jointly route assignment and fleet scheduling using a simplified linear program model. In a subsequent study, these authors described the so-called transport momentum methodology as a proxy for operational costs that are tailored for solving fleet assignment problems encompassing scheduling [105].

Sawai [106] proposes an innovative method that creates a new type of small-world network (based on communication theory) with less average path-length and larger clustering coefficients than the ones obtained via conventional route assignment methods, inspired on an Ant-Colony Optimization (ACO) algorithm.

Pita et. al [107] presented a mixed-integer linear optimization model for integrated flight scheduling and fleet assignment considering aircraft and passenger delay costs. In this model, for the first time, the objective function was set to maximize the expected profits of an airline that faces a given origin/destination-based travel demand and operates in congested, slot-constrained airports.

Bing [32] developed key performance metrics to evaluate the efficiency of transport networks featuring any kind of topology, suggested to be used as objective functions on future route and aircraft scheduling optimization research studies.

Gurkan et. al [20] proposed a nonlinear mixed integer programming model considering fuel consumption and CO₂ emission cost in terms of objective function. For the first time, cruise speed control is integrated into the three blocks of airline operations planning (Fig.1). This innovative method enabled the construction of a schedule to increase utilization of fuel-efficient aircraft and even to decrease total number of aircraft needed while satisfying the same service level and maintenance requirements for aircraft scheduling.

Dong et.al [108] proposed an integrated route scheduling and fleet assignment problem based on two coupled mixed integer programming models considering itinerary price elasticity and proposing heuristic algorithm to solve the problem.

As earlier mentioned, passenger demand is another important input to be considered in the network optimization process. In the last decades, gravitational models became popular to determine passenger demand in air transportation mainly because of their simplicity and forecast capacity using historical econometric variables related to the cities involved and time-geometric parameters. These models, analog to the gravitational law of physics, consider as ‘bodies’ the cities associated with the departure and arrival routes of the airports, the ‘mass’ equivalent to the amount of populations involved on each city, and the ‘distance’ is the geometric distance (great circle) between them. In fact, the first models considered the passenger demand as proportional to the product of populations divided by square of the distance.

Before the 50’s, gravitational models have been used in urban transport engineering, leaving its application to the analysis of long-distance mobility to geographers, on demand studies of the

dominant modes of transportation (road and rail transport). However, the application of gravity models to air transport networks started with the academic work of Taaffe [109] and Taaffe & King [110] studying mobility of passengers among major cities in the United States, using a logarithmic regression analysis. This methodology was later endorsed by Kanafani [111] as a suitable option where actual demand values are unknown or missing.

Jaillet et. al [103], in their already mentioned study on route assignment using a MILP formulation, proposed the use of the basic gravitational models to estimate the demand on this kind of problem. In this approach, the authors use the basic two-variable gravitational formulation, considering city-pair populations and great circle distance, on running the network optimization for fifty US airports. Later on, Ceha and Ohta [112] used the same formulation to predict the demand for air passengers on scheduled commercial flights in US.

Wojan [15] also determined the characteristics of the optimum airline networks using a modified gravitational model, considering population product only. In his work, the demand and cost conditions of an airline have been identified as one of the main determinants of network topology.

More recently, gravity models started to include geo/socio-economic and air transport variables, besides population and distance, since research studies soon perceived the low adherence of actual demand data considering these two variables only. Geo/socio-economic factors were identified to imply social and economic, industrial/business activities, geographical features related to cities served by the air transport system and competition between airports. Several variables of such kind started to be considered in the model such as: wealth (measured by GDP), employment rate, structure of the productive sector, competitiveness index, level of deregulation of air market [113], border effect factor [114], composition of society, proximity to airport hub, tourist factor, and catchment area of big cities. For example, Grosche et. al [14] proposed an extended gravitational model considering population, catchment area, buying power index, gross domestic income, time to travel and distance between city pairs, using data from twenty-eight European airports for calibration.

Factors related to air transport service were later included, such as: historical volumes of traffic at the airport, intensity of traffic flow between two cities, flight time, ticket cost, type of airport (flights, frequencies and chairs offered by airlines) and quality of service (offered by airlines).

Under this perspective, Bhadra and Kee [115] analyzed the demand and changes in the market for air travel passengers in the United States. Piermartini and Rousová [113] proposed a modified

gravity model to explain bilateral international passenger traffic and estimated the impact of the deregulation of air transport services for passengers. In this line of research, Hazdeline [114] performs the analysis of border effects in the domestic and international air transportation of passengers in Canada. Doganis [3], however, proposed a different approach, estimating the passenger demand of airports as function of airfares, frequency and scheduled traffic.

More recently, Olariaga et.al [116] analyzed the flow of domestic passengers by air transportation between twelve airports of a Colombian air transport network, expanding Grosche's model to specific characteristics of the arrival airports.

2.4 Integrated aircraft and network optimization

Although many research studies have been conducted on airline network optimization problems, especially on route and tail assignment, few studies integrated aircraft design characteristics and performance to realistic mission analysis for each city pair considered [28] [29]. The research on integration of entire airline networks with aircraft design variables started to be developed in the last fifteen years and was enabled with the increase of computational power and development of robust optimization solvers which are capable of handling multivariable, multi-objective functions and are submitted to non-linear constraints [63] [117]. The inclusion network and mission analysis modules into the aircraft design MDO framework is a complex task which involves several operational variables and extremely dependent of aircraft performance related disciplines (such as aerodynamics, structures and propulsion) and non-linear equations.

In fact, initial studies show that the direct coupling of aircraft design and airline fleet-route allocation frequently use mixed-integer and nonlinear programming formulations and require diverse types of design variables, constraints and disciplines. This would require a decomposition approach, using disciplines sub-optimizations, in order to facilitate the resolution of such framework [118] [119]. Some key studies on this approach are mentioned in the following paragraphs.

Roth and Crossley [120] proposed the use of genetic algorithms, combined with a gradient based method, for aircraft design optimization in specific mission profiles, providing the first insight in such kind of problem. Isikveren [46] expanded this concept including range optimization and computing fuel consumption with semi-empirical formulations. Cavalcanti et. al [121]

proposed a multi-objective optimization of wing planform carried out by the minimization of the block time and block fuel for a given mission. Versiani et. al [122] proposed a design framework to optimize families of aircraft for a given mission profile using genetic algorithms.

Taylor and Weck [123] [28] presented, for the first time, the benefits of optimizing an integrated air transportation network and vehicle design, concurrently defined. This study focused exclusively on the design of an air transportation network for overnight package delivery on two turn-around hub configurations connecting seven U.S. cities. By concurrently optimizing both the vehicle (simplified model base on Breguet Range equation) and network for a selected few cities with fixed demand, it was possible to obtain a minimum of a ten percent improvement in operational costs over the one obtained by optimizing the network design using a set of pre-defined aircraft. This was accomplished by embedding a linear programming solver in the perturbation step of simulated annealing algorithm to solve the substantial number of linear constraints imposed by the capacity and demand requirements of the network.

Afterwards, Mane et. al [124] conducted a research proposing to split aircraft design and airline allocation problems, on a systems-of systems approach. The aircraft design block first optimized a new aircraft for a specified design mission range and payload. The designed aircraft along with the existing set in fleet were allocated to the route network via a MILP problem. This study also compared the decomposition approach with solving the coupled problem as an MINLP problem using algorithms like genetic algorithms and Branch and Bound.

Bower and Kroo [29] developed a methodology for aircraft design considering demands of a given aerial network. In their design approach, the objectives are the minimization of direct operating costs and airplane emissions (CO_2 and NO_x). For this purpose, a hierarchical decomposition was used with discipline-specific optimization algorithms using simplistic models. A modified version of a multi-objective genetic algorithm is implemented in the system level aircraft design subspaces. Results were presented for a test problem that involved designing a single aisle commercial aircraft for a route network consisting of four cities and eight route segments, using eighteen design variables.

The problem of simultaneous aircraft-design and airline-aircraft allocation is also explored by Nusawardhana and Crossley in a reference study [125] in which the problem formulation specifies that the airliner allocates "variable" resources and aircraft manufacturer develops a new aircraft based on a set of "variable" design specifications. The optimization is carried out by a framework that combines dynamic programming, nonlinear programming and linear integer programming.

The aircraft design part uses simplistic models of performance proposed by Raymer [35]. Later on these authors proposed an improved mathematical formulation to solve simultaneously the aircraft design and fleet allocation problem (tail assignment) using a monolithic approach and a heuristic optimization solution, for a given airline network [119].

Siqueira et al. [126] proposed a Multi-disciplinary Design Optimization (MDO) framework to select the optimum conceptual aircraft design for an existing scheduled (fixed) airline network. Braun et al. [127] demonstrated the evaluation of future aircraft optimizing network and fleet assignment at the same time.

Davendralingam and Crossley [128] presented a joint conceptual framework on concurrently design aircraft and the operational network by incorporating established passenger demand models, using an MDF approach. A conceptual scenario involving six airports is formulated and solved to exhibit the methodology employed and showing reflexivity of demand. In preliminary studies [129], the authors investigated the impact of aircraft design choices on target market capture decisions and on demand itineraries and economic risks.

Hwang et al. [130] studied a method for simultaneous design and mission allocation optimization, using a modular approach on aerodynamics, propulsion and aircraft performance surrogates into a mission analysis tool, using a gradient-based optimization. A three-route test problem was executed with one design aircraft, showing a 200 to 400% profit increase when compared with a standard airliner. Extending this work, Hwang and Martins [131] expanded the analysis for a 128-route framework, considering a parallel computing technique.

Later, Hwang [132] et al. integrated the above methods on a concurrent optimization encompassing aircraft design, mission profiles, and the allocation of aircraft to routes in an airline network. To enable the solution of this complex approach, a gradient-based optimization approach was adopted with a parallel computational framework, which boosts the computation of derivatives in the multidisciplinary analysis. A surrogate model for the CFD analysis is retrained in each optimization iteration given the new set of shape design variables. The resulting optimization problem contains over 6,000 design variables and 23,000 constraints, and it is solved in approximately 10 hours on a machine with 128 processors.

The optimization revealed a 27% increase in airline profit when compared with the allocation-mission-design optimization to allocation only optimization. Afterwards, Roy et al. [133] [134] proposed the aircraft allocation optimization into this framework, introducing a Mixed Integer Non-Linear Problem (MINLP) to the problem, increasing the complexity of the solution search.

In a preliminary study, the authors proposed a framework based on the so-called Efficient Global Optimization, a special gradient-based algorithm applied in the design space, to solve this problem [135].

Finally, Roy et al. [136] studied the inclusion operational and revenue management variables (such as fare, booking limits, demand and aircraft count constraints), using a genetic algorithm as heuristic method combined with a Branch-and-Bound method (gradient based), in a monolithic approach for network optimization. This approach solves a 11-route problem, providing significant improvements on airlines objectives using a standard single aisle aircraft.

It is worth mentioning that all the above research studies directed the optimization frameworks considering the minimization of global network operational costs or profit, in single objective functions. No studies have been conducted with regard to multiobjective approaches. Also, at the moment, there are no studies in the literature considering the minimization of aircraft development and production costs taken into the integrated aircraft and network optimization framework. However, in an interesting research paper, Wilcox and Wakayama [137] used a monolithic framework to design a family of aircraft in a common framework, sharing parts of selected mission requirements, where design and manufacturing costs are considered in the objective function.

Finally, in a most recent study, Fregnani et al. [138] included the airline operational perspective in the optimization framework, demonstrating the great impact in the minimization of the Direct Operational Cost (DOC) due to the high degree of dependency between aircraft and the airline optimized network.

3. Methodology

In this research, the adoption of a “*hybrid MDF-CO*” MDO architecture with the objective to optimize simultaneously, the aircraft and network designs is proposed, as shown in Fig. 3.1. In fact, this model represents an improvement of the methodology proposed by Bower and Kroo [29], differing from the detailed airplane configuration and to the fidelity of some aeronautical disciplines considered in the optimization process. Two major design analysis blocks are presented:

- I. The Aircraft Framework: in which the disciplines related to the aircraft design (aerodynamics, propulsion, MTOW/OEW estimation, stability and control and noise)

- are integrated providing the necessary coupling variables for the Network Framework disciplines calculation (such as drag, thrust and weights) in each calculation cycle;
- II. The Network Framework: in which the disciplines related to network optimization, mission performance and airline economics are integrated, producing the output variables (network profit, network direct operational costs (DOC), net present value of total development/production cash flow (NPV) and estimated number of aircraft) which will be used in selected objective functions.

These frameworks are executed in series, such like in the MDF approach, and wrapped into an optimization cycle. First the Aircraft Framework is executed, determining the aircraft design to be used in the Network Framework. However, the execution of the last one is conditioned to the evaluation of an Airplane Design Check block, where the feasibility of the selected aircraft design is verified considering certification and operational requirements. If not complying with such requirements, the design under analysis is considered to have failed and a new one is then restarted in the optimization cycle. It is worth mentioning that a sub-optimization process is executed inside the Network Framework (Network Optimization Block) in order to determine the optimum airline network at each cycle, considering a certain passengers demand model (when the demand is not known directly) and the aircraft design under evaluation, like a CO framework.

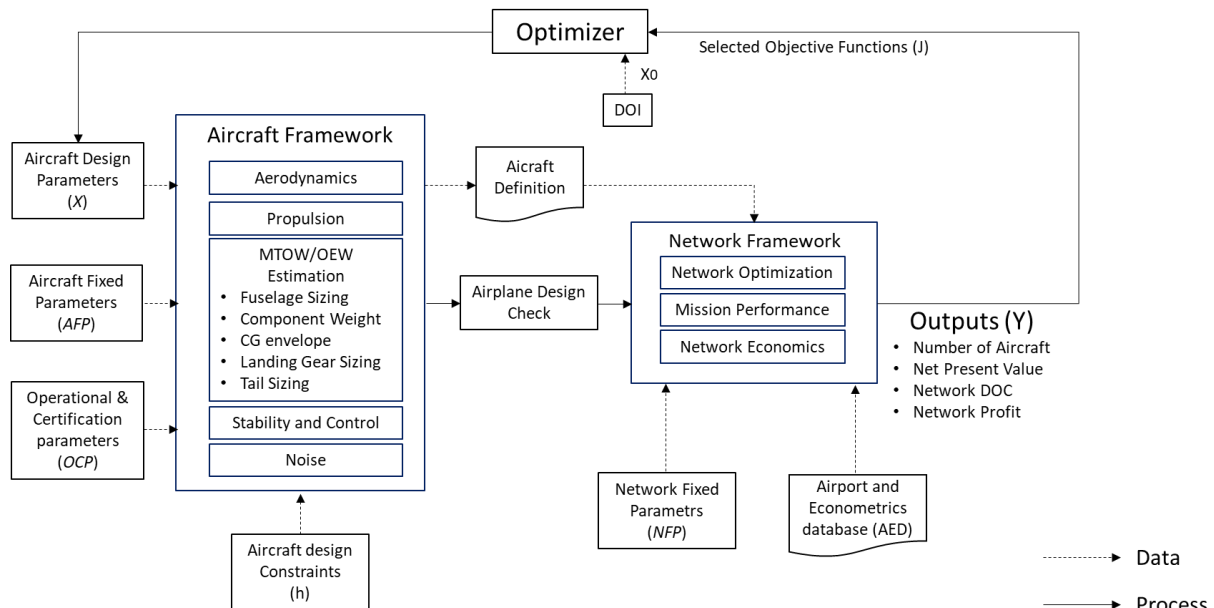


Figure 3.1: Proposed “Hybrid MDF-CO” MDO framework.

Airplanes generated in each calculation cycle are defined as a set of design and fixed parameters mostly related to airframe and engine geometric characteristics. Table 3.2 shows the selected aircraft design parameters (x_i), and its allowed design interval (from x_{lb} to x_{ub}), produced in each calculation cycle. This design interval is constructed taking into consideration the variation from a baseline aircraft design, which will be used in this research for comparison purposes.

The baseline aircraft corresponds to a mid-size regional jet (78 passengers in single class configuration), designed according to basic design requirements as shown in Table 3.1. Figure 3.2 shows some of the aircraft views. For the sake of comparison, the design parameters values associated with the baseline aircraft are also shown in Table 3.2.



Figure 3.2: Baseline Aircraft (78 passengers, single class)

Table 3.1: Baseline aircraft design requirements

| Basic Mission Requirements | Symbol | Value |
|---|----------------------------|-------|
| Maximum Cabin Passengers Capacity | <i>MaxPax</i> | 78 |
| Maximum Certified Cruise Altitude Ceiling [ft] | <i>MaxAlt</i> | 41000 |
| Design Range, Full passengers @ 100kg, ISA conditions [nm] | <i>RANGE</i> | 1600 |
| Design Landing Field Length, @ sea level, ISA conditions [m] | <i>LFL</i> | 2000 |
| Design Takeoff Field Length @ sea level, ISA conditions [m] | <i>TOFL</i> | 2500 |
| Operational Empty Weight [kg] | <i>OEW</i> | 21800 |
| Maximum Zero Fuel Weight [kg] | <i>MZFW</i> | 31700 |
| Maximum Taxi Weight [kg] | <i>MTW</i> | 38890 |
| Maximum Takeoff Weight [kg] | <i>MTOW</i> | 38790 |
| Maximum Fuel Capacity @ 0.81kg/l fuel density [kg] | <i>MAXFUEL</i> | 9428 |
| Maximum lift coefficient at undeflected flap/gear up airplane configuration | <i>CL_{MAX}</i> | 1.65 |
| Maximum lift coefficient at landing flaps/gear down configuration | <i>CL_{MAX LD}</i> | 2.20 |
| Maximum lift coefficient at takeoff flaps/gear down configuration | <i>CL_{MAX TO}</i> | 2.00 |
| Number of engines installed in the aircraft | <i>n_e</i> | 2 |
| Maximum Takeoff Thrust @ sea level / ISA conditions [lbf] | <i>MAXRATE</i> | 14200 |

Table 3.2: Aircraft/Engine design parameters

| <i>i</i> | Design Parameter (X_i) | Symbol | Allowed design interval (X_{lb} to X_{ub}) | Baseline Aircraft value |
|----------|---|---------------|--|-------------------------|
| 1 | Wing reference area [m^2] | wS | 72 to 130 | 72.72 |
| 2 | Wing aspect ratio | wAR_w | 7.5 to 10 | 8.6 |
| 3 | Wing taper ratio | wTR | 0.25 to 0.50 | 0.44 |
| 4 | Wing quarter-chord sweepback angle [°] | $wSweep1/4$ | 15 to 35 | 23.5 |
| 5 | Wing twist Angle [°] | $wTwist$ | -5 to -2 | -3 |
| 6 | Wing kink semispan position [%] | $KinkPos$ | 0.32 to 0.40 | 0.32 |
| 7 | Engine by-pass ratio | BPR | 4.5 to 6.5 | 5.0 |
| 8 | Engine fan diameter [m] | $eDiam$ | 1.0 to 2.0 | 1.425 |
| 9 | Engine overall pressure ratio | OPR | 25 to 30 | 28.0 |
| 10 | Engine turbine inlet temperature [K] | $eTIT$ | 1350 to 1500 | 1405 |
| 11 | Engine fan pressure ratio | FPR | 1.4 to 2.5 | 1.6 |
| 12 | Number of passengers (single class, pitch 32") | $Npax$ | 70 to 130 | 78 |
| 13 | Number of seat abreast | $Nseat$ | 4 to 5 | 4 |
| 14 | Design range, full pax @ 100kg, ISA conditions [nm] | $RANGE$ | 1000-2500 | 1600 |
| 15 | Engine design point pressure altitude [ft] | eHp | 33000 to 43000 | 41000 |
| 16 | Engine design point Mach number | eM | 0.74 to 0.82 | 0.78 |
| 17 | Engine position flag | $ePos$ | 0= tail, 1=under wing | 1 |
| 18 | Winglet presence flag | $WingletPres$ | 0= none, 1= with | 1 |
| 19 | Slat presence flag | $SlatPres$ | 0=none, 1=with | 1 |
| 20 | Horizontal tail position | HTP | 0=tail 1=fuselage | 1 |

Considering the Aircraft Framework, in each calculation cycle, aircraft fixed parameters (*AFP*) and operational/certification fixed parameters (*AOCFP*) are set as constant values to be used in the discipline computations, which are also common to the baseline aircraft design. They are listed in Tables 3.3 and 3.4.

Table 3.3: Aircraft fixed parameters

| <i>i</i> | Fixed parameter (AFP_i) | Symbol | Adopted value |
|----------|--|-------------|---------------|
| 1 | Number of galley stations | $Ngalleys$ | 2 |
| 2 | Number of aisles in the cabin | $Naisles$ | 1 |
| 3 | Aisle width [m] | $AisleW$ | 0.50 |
| 4 | Passengers seat width [m] | $SeatW$ | 0.46 |
| 5 | Passengers seat pitch [in] | $SeatPitch$ | 32 |
| 6 | Passengers cabin internal height (m) | $CabHt$ | 2.0 |
| 7 | Airfoil incidence at wing root [°] | $inc\ root$ | 2 |
| 8 | Wing Dihedral [°] | $wDih$ | 3 |
| 9 | Miscellaneous drag factor (%) | $Dmisc$ | 3.5 |
| 10 | Dynamic pressure efficiency on horizontal tail [%] | $qHTeff$ | 90.0 |
| 11 | Engine minimum clearance to ground [m] | $eCLR$ | 0.40 |
| 12 | Number of engines installed in the aircraft | n_e | 2 |
| 13 | Approach flap deflection | $FlapAPP$ | 15 |
| 14 | Takeoff flap deflection | $FlapTO$ | 35 |
| 15 | Landing flap deflection | $FlapLD$ | 45 |
| 16 | Engine's time between overhaul [h] | $eTBO$ | 2500 |

Table 3.4: Aircraft operational and certification fixed parameters

| <i>i</i> | Fixed parameter (AOC_i) | Symbol | Adopted value |
|----------|---|----------------|---------------|
| 1 | Residual rate of climb [ft/min] | <i>RROC</i> | 300 |
| 2 | Buffet margin (g) | <i>BuffMGN</i> | 1.3 |
| 3 | Speed Limit Hp<10000ft – indicated airspeed [kt] | <i>SPDLIM</i> | 250 |
| 4 | Maximum aircraft certified altitude [ft] | <i>Ceiling</i> | 41000 |
| 5 | Maximum certified speed (Mach/indicated airspeed in kt) | <i>MMO/VMO</i> | 0.82/340 |

In the Network Framework side, network fixed parameters (NFP) are set as constant values representing airline's data considered in network computations. They are listed in Table 3.5.

Table 3.5: Network fixed parameters

| <i>i</i> | Fixed parameter (NFP_i) | Symbol | Adopted value |
|----------|---|----------------|---------------|
| 1 | Aircraft average daily utilization [h] | <i>DU</i> | 13 |
| 2 | Average turnaround time [min] | <i>TAT</i> | 45 |
| 3 | Takeoff and climb-out fuel allowance [kg] | <i>TOFA</i> | 200 |
| 4 | Takeoff and climb-out time allowance [min] | <i>TOTA</i> | 3 |
| 5 | Approach and landing fuel allowance [kg] | <i>AFA</i> | 100 |
| 6 | Approach and landing time allowance [min] | <i>ATA</i> | 2 |
| 7 | Go-around fuel allowance [kg] | <i>GAFA</i> | 200 |
| 8 | Go-around time allowance [min] | <i>GATA</i> | 3 |
| 9 | Regulatory holding time [min] | <i>HOLDT</i> | 30 |
| 10 | Minimum cruise time [min] | <i>MINCRZT</i> | 3 |
| 11 | Taxi-out time [min] | <i>TOT</i> | 10 |
| 12 | Taxi in time [min] | <i>TIT</i> | 5 |
| 13 | Turnaround time [min] | <i>TAT</i> | 35 |
| 14 | Total passenger's weight, with baggage [kg] | <i>PAXWT</i> | 110 |

In addition, an airport and econometrics database (AED) supports the optimum network and mission performance disciplines, providing airport and city econometric related data used in their calculations. The parameters provided for each airport in this database are listed in Table 3.6:

Table 3.6: Airport and econometrics database parameters

| <i>i</i> | Parameter | Symbol |
|----------|---|--------------|
| 1 | IATA's 3-letter code airport designator | <i>APRID</i> |
| 2 | City Name | <i>City</i> |
| 3 | Airport's reference point latitude [$^{\circ}$] | <i>LAT</i> |
| 4 | Airport's reference point longitude [$^{\circ}$] | <i>LON</i> |
| 5 | Airport's reference point elevation [ft] | <i>ELEV</i> |
| 6 | Airport's reference temperature [$^{\circ}\text{C}$] | <i>Tref</i> |
| 7 | Airport magnetic declination [$^{\circ}$] | <i>DMG</i> |
| 8 | Most used takeoff runway | <i>TRWY</i> |
| 9 | Most used takeoff runway - Takeoff Runway Available [m] | <i>TORA</i> |
| 10 | Most used takeoff runway - Takeoff Distance Available [m] | <i>TODA</i> |
| 11 | Most used takeoff runway – Accelerate Stop Distance Available [m] | <i>ASDA</i> |

| | | |
|----|---|-------------|
| 11 | Most used landing runway | <i>LRWY</i> |
| 12 | Most used landing runway – Landing Distance Available [m] | <i>LDA</i> |
| 13 | Average takeoff delay [min] | <i>ATD</i> |
| 14 | Average landing delay [min] | <i>ALD</i> |
| 14 | City population | <i>POP</i> |
| 15 | Airport catchment radius [km] | <i>CRAD</i> |
| 16 | City buying power index | <i>B</i> |
| 17 | Gross domestic product [US\$] | <i>GDP</i> |

The whole MDO framework is integrated using the modeFrontier® application, produced by the Italian software company *ESTECO*®. This platform, developed in *Java* ® language, allows users to choose the optimization strategy based on the design space boundaries and on the required reliability and robustness. The platform includes advanced algorithms for direct optimization, using deterministic, stochastic and heuristic methods for both single and multiobjective problems [139]. This application is capable of handling different standalone modules, written in different languages or third part tools, allowing efficient streamlining of teamwork within multidisciplinary engineering processes. For that, input and output variables in such modules are configured to be recognized inside the application, which are used within the logic of the optimization framework.

In this research, the Aircraft and Network frameworks are coded into two distinct modules using *MATLAB*® application. These modules are integrated and called modeFrontier® in the optimization process. For convenience, the Aircraft Design Check routine is embedded in the Aircraft Design module. Fig. 3.3 displays the workflow of the framework.

Constraints (*h*), specific to the Aircraft Framework, are adopted in the optimization cycle as follows:

1. ICAO takeoff noise certification Chapter 4 compliant [140].
2. Fuel storage – all mission fuel must be accommodated in the wing fuel tanks.
3. Airplane stall beginning in the inner wing.
4. Longitudinal modes determined and checked against certification requirements (minimum Level 3) [141].
5. Static margin considering tail sizing and wing positioning.
6. Critical angles and clearance boundaries considered on landing gear and engines design.

The constraints I and II are built into the flow constructed modeFrontier framework. Constraints III, IV, V and VI, however, are embedded into the Aircraft Module applied during the discipline's calculations (to be explained in Session 3.1). The output of the Aircraft Framework execution is

the aircraft definition vector, composed of the main geometric and operational characteristics of the aircraft design under analysis. This includes design parameters, calculated parameters (from the aircraft design process) and aircraft fixed parameters. This vector is saved in a file, to be accessed during the execution of the Network module. The list of parameters included in the aircraft definition vector is shown in Table 3.7.

Table 3.7: Aircraft definition parameters

| Aircraft definition parameter | Symbol | Source |
|--|------------------|---|
| Maximum Operational Empty Weight [kg] | <i>OEW</i> | Aircraft Framework Module (calculated) |
| Maximum Zero Fuel Weight [kg] | <i>MTW</i> | Aircraft Framework Module (calculated) |
| Maximum Taxi Weight [kg] | <i>MZFW</i> | Aircraft Framework Module (calculated) |
| Maximum Takeoff Weight [kg] | <i>MTOW</i> | Aircraft Framework Module (calculated) |
| Maximum Fuel Capacity (kg) @ 0.81 kg/l fuel density | <i>MAXFUEL</i> | Aircraft Framework Module (calculated) |
| Design Range (full capacity @ 100 kg) | <i>RANGE</i> | Design parameter |
| Maximum certified Mach | <i>MMO</i> | Fixed parameters |
| Maximum certified Indicated Airspeed [kt] | <i>VMO</i> | Aircraft Operational and Certification fixed parameters |
| Maximum certified Altitude [ft] | <i>Ceiling</i> | Aircraft Operational and Certification fixed parameters |
| Number of Passengers (single class) | <i>Npax</i> | Design parameter |
| Number of crew members (pilots + flight attendants) | <i>Crew</i> | Aircraft Framework Module (calculated) |
| Number of aisles | <i>Naisles</i> | Aircraft fixed parameters |
| Number of Seat Abreast | <i>Nseat</i> | Design parameter |
| Seat width [m] | <i>SeatW</i> | Aircraft fixed parameters |
| Fuselage length [m] | <i>lf</i> | Aircraft Framework Module (calculated) |
| Forward fuselage length [m] | <i>lco</i> | Aircraft Framework Module (calculated) |
| Tailcone length [m] | <i>ltail</i> | Aircraft Framework Module (calculated) |
| Fuselage width ratio | <i>fush2w</i> | Aircraft Framework Module (calculated) |
| Fuselage width [m] | <i>fusw</i> | Aircraft Framework Module (calculated) |
| Fuselage diameter [m] | <i>fusd</i> | Aircraft Framework Module (calculated) |
| Fuselage height [m] | <i>fush</i> | Aircraft Framework Module (calculated) |
| Fuselage external height [m] | <i>fusdz</i> | Aircraft Framework Module (calculated) |
| Fuselage wet area [m] | <i>fuswetS</i> | Aircraft Framework Module (calculated) |
| Aircraft maximum lift coefficient on clean configuration | <i>CLMAX</i> | Aircraft Framework Module (calculated) |
| Aircraft maximum lift coefficient at takeoff configuration | <i>CLMAX TO</i> | Aircraft Framework Module (calculated) |
| Aircraft maximum lift coefficient at landing configuration | <i>CLMAX LD</i> | Aircraft Framework Module (calculated) |
| Wing Reference Area [m^2] | <i>wS</i> | Design parameter |
| Wing Aspect Ratio | <i>wAR</i> | Design parameter |
| Wing Taper Ratio | <i>wTr</i> | Design parameter |
| Wing semi-span [m] | <i>wb</i> | Aircraft Framework Module (calculated) |
| Wing quarter-chord sweepback angle [°] | <i>wSweep1/4</i> | Design parameter |

| | | |
|--|-----------------|--|
| Wing leading edge sweepback angle [°] | <i>wSweepLE</i> | Aircraft Framework Module (calculated) |
| Wing Twist Angle [°] | <i>wTwist</i> | Design parameter |
| Wing Wet Area [m^2] | <i>wSwet</i> | Aircraft Framework Module (calculated) |
| Kink Semispan position | <i>KinkPos</i> | Design parameter |
| Airfoil Incidence @ wing root [°] | <i>incroot</i> | Aircraft fixed parameters |
| Airfoil Incidence @ wing kink [°] | <i>inckink</i> | Aircraft Framework Module (calculated) |
| Airfoil Incidence @ wing tip [°] | <i>in_tip</i> | Aircraft Framework Module (calculated) |
| Airfoil thickness ratio @ wing root | <i>tcroot</i> | Aircraft Framework Module (calculated) |
| Airfoil thickness ratio @ wing kink | <i>tckink</i> | Aircraft Framework Module (calculated) |
| Airfoil thickness ratio @ wing tip | <i>tctip</i> | Aircraft Framework Module (calculated) |
| Airfoil chord length @ central fuselage [m] | <i>chordc</i> | Aircraft Framework Module (calculated) |
| Airfoil chord length @ wing root [m] | <i>chordr</i> | Aircraft Framework Module (calculated) |
| Airfoil chord length @ wing kink [m] | <i>chordk</i> | Aircraft Framework Module (calculated) |
| Airfoil chord length @ wing tip [m] | <i>chordt</i> | Aircraft Framework Module (calculated) |
| Wing mean aerodynamic chord length [m] | <i>CMA</i> | Aircraft Framework Module (calculated) |
| Wing leading edge position | <i>xle</i> | Aircraft Framework Module (calculated) |
| Flap length on semi-span [%] | <i>bflap</i> | Aircraft Framework Module (calculated) |
| Flap area [m^2] | <i>sflap</i> | Aircraft Framework Module (calculated) |
| Takeoff flap deflection [°] | <i>flapTO</i> | Aircraft fixed parameters |
| Landing flap deflection [°] | <i>flapLD</i> | Aircraft fixed parameters |
| Aileron position on wing semi-span [%] | <i>ailpos</i> | Aircraft Framework Module |
| Fuselage length [m] | <i>lf</i> | Aircraft Framework Module (calculated) |
| Forward fuselage length [m] | <i>lco</i> | Aircraft Framework Module (calculated) |
| Tailcone length [m] | <i>ltail</i> | Aircraft Framework Module (calculated) |
| Fuselage width ratio | <i>fush2w</i> | Aircraft Framework Module (calculated) |
| Rear spar position on mean aerodynamic chord [%] | <i>rspars</i> | Aircraft Framework Module (calculated) |
| Vertical Tail Area [m^2] | <i>vS</i> | Aircraft Framework Module (calculated) |
| Vertical Tail aspect ratio | <i>vAR</i> | Design Parameter |
| Vertical Tail tapper ratio | <i>vTR</i> | Design Parameter |
| Vertical tail sweep angle [°] | <i>vSweep</i> | Aircraft Framework Module (calculated) |
| Horizontal tail Area [m^2] | <i>hS</i> | Aircraft Framework Module (calculated) |
| Horizontal tail aspect ratio | <i>hAR</i> | Design Parameter |
| Horizontal tail tapper ratio | <i>hTR</i> | Design Parameter |
| Horizontal tail sweep angle[°] | <i>hsweep</i> | Aircraft Framework Module (calculated) |
| Winglet Aspect ratio [m^2] | <i>WL_AR</i> | Aircraft Framework Module (calculated) |
| Winglet tapper ratio | <i>WL_TR</i> | Aircraft Framework Module (calculated) |
| Winglet sweep angle | <i>WL_sweep</i> | Aircraft Framework Module (calculated) |
| Winglet cantlever angle [deg] | <i>WL_cantl</i> | Aircraft Framework Module (calculated) |
| Winglet twist angle [deg] | <i>WL_twist</i> | Aircraft Framework Module (calculated) |
| Maximum Takeoff Thrust @ sea level / ISA conditions [lbft] | <i>MAXRATE</i> | Aircraft Framework Module (calculated) |
| Engine by-pass ratio | <i>BPR</i> | Design Parameter |
| Engine Fan Diameter [m] | <i>eDiam</i> | Design Parameter |

| | | |
|--|--------------------|--|
| Engine Fan Pressure Ratio | <i>FPR</i> | Design Parameter |
| Engine Overall Pressure Ratio | <i>OPR</i> | Design Parameter |
| Engine Turbine Inlet Temperature [K] | <i>TIT</i> | Design Parameter |
| Engine length [m] | <i>le</i> | Aircraft Framework Module (calculated) |
| Engine minimum clearance to ground [m] | <i>eCLR</i> | Aircraft Framework Module (calculated) |
| Engine pylon height [m] | <i>epydz</i> | Aircraft Framework Module (calculated) |
| Engine wet area [m^2] | <i>eSwet</i> | Aircraft Framework Module (calculated) |
| Total aircraft wet area [m^2] | <i>totSwet</i> | Aircraft Framework Module (calculated) |
| Engine position flag | <i>ePOS</i> | Design Parameter |
| Horizontal tail position flag | <i>hpos</i> | Design Parameter |
| Winglet presence flag | <i>WingletPres</i> | Design Parameter |
| Slat presence flag | <i>SlatPres</i> | Design Parameter |
| Horizontal tail position | <i>HTP</i> | Design Parameter |

According to the explanations provided in Session 2.2, genetic algorithms are considered the most suitable optimizers for the multiobjective problem proposed in this research, especially due to its robustness, ability in dealing with global minima or maxima in poor-known search space and handling several types of variables. Genetic algorithms designed for multiobjective optimization frameworks (such as MOGA and NSGA-II) are available in modeFrontier® and therefore will be used as main optimizers in this research.

The design of experiments (*DOE*), used as search space by the optimization algorithm, is based on the Latin Hypercube sampling methodology. As discussed in Session 2.1, such method guarantees relatively random uniform distribution, with minimum number of samples over each of the design variable dimension [60]. This is also an embedded feature of the modeFrontier ® application.

The outputs produced by the Network Framework (Net Present Value, Network Direct Operational Cost, Number of Aircraft and Network Profit) may be selected as objective functions (*J*) to be used in the multi objective optimization process. In genetic algorithms, they represent fitness functions, which are evaluated in each by the optimizer, influencing the characteristics of each population generation. Although in Fig. 3.3, all output variables are illustrated as objective functions, some of them may be excluded from the analysis, depending on the nature of the optimization (to be explained in Session 4).

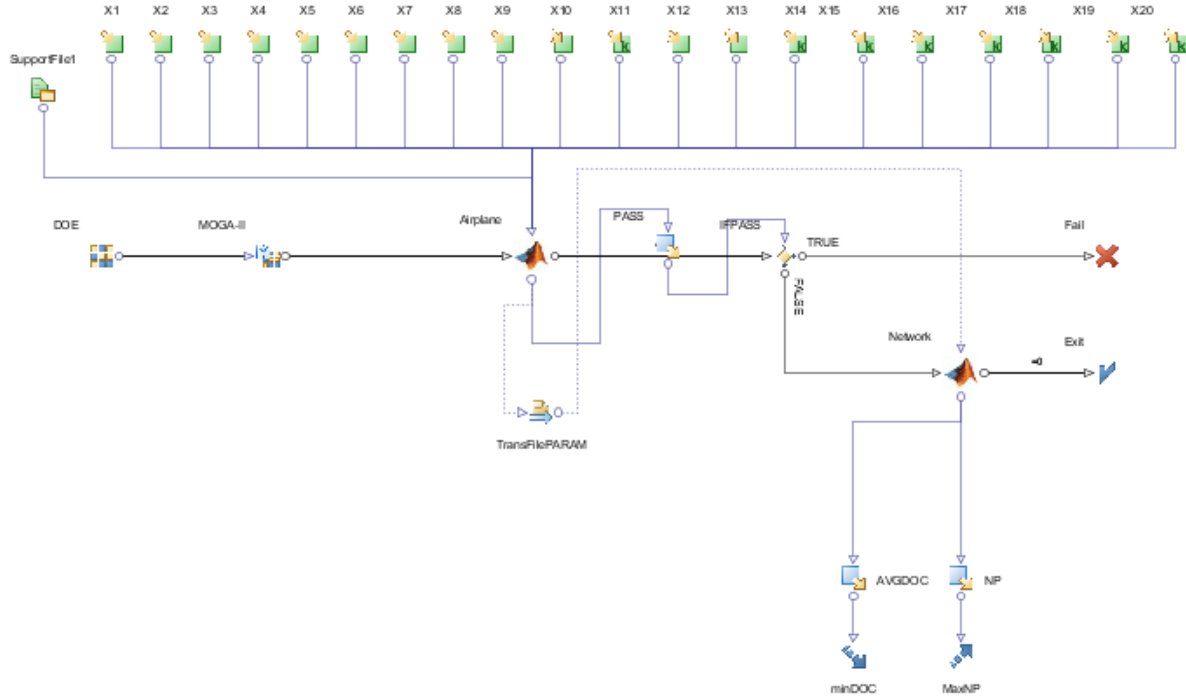


Figure 3.3: Proposed MDO workflow elaborated with *modeFrontier*®.

The following sessions describe in detail the Aircraft and Network frameworks calculation methodologies related to the disciplines involved. As mentioned previously, each framework is implemented as a single MATLAB ® code module.

3.1 The aircraft framework

The definition of airplane geometry is one of most important deliverables in the conceptual design phase and is the final objective of the Aircraft Framework module. It usually involves the use of a set of input parameters in order to determine the basic layout and dimensions of the passenger section of fuselage, fuselage nose and tail cone, wing, horizontal and vertical tails, engine nacelle and pylon [48].

Considering the traditional approaches developed by Roskam [24], Torenbeek [23], and Raymer [142] and the more recent one proposed by Isikveren [46], the one proposed by Roskam was considered here as it is more straight-forward and is widely used by aircraft manufacturers. In all these methods, the initial parameter to be determined is the total wetted area, which is required

for aerodynamic drag coefficient and therefore for initial weight estimation. However, thanks to the improvement in computer power, higher levels of details for geometry modeling became standard procedure in the conceptual design phase.

The Aircraft Framework is implemented in a single *MATLAB®* module composed of several calculation routines in which computations related to the disciplines are executed and a final certification design check is performed. This module has the main objective to generate the aircraft definition parameters according to design techniques related to the following disciplines: Aerodynamics, Propulsion, Weight Estimation, Noise computations and Design Check.

In the conceptual design phase, a reasonable estimation of airplane's Maximum Takeoff Weight (*MTOW*) and Operational Empty Weight (*OEW*) is fundamental to the aircraft dimensions determination process and is at the core of the Aircraft Framework module.

Figure 3.4 shows the block diagram related to the execution of this module. The main idea is to size the aircraft via an iterative loop which primary objective is to estimate the MTOW and OEW. All aircraft design related definitions parameters are derived from such process. After the weight estimation loop, noise computations are performed considering certification standards [143] and then the airplane design check is performed in order to allow the Network Framework computations or not consider the design.

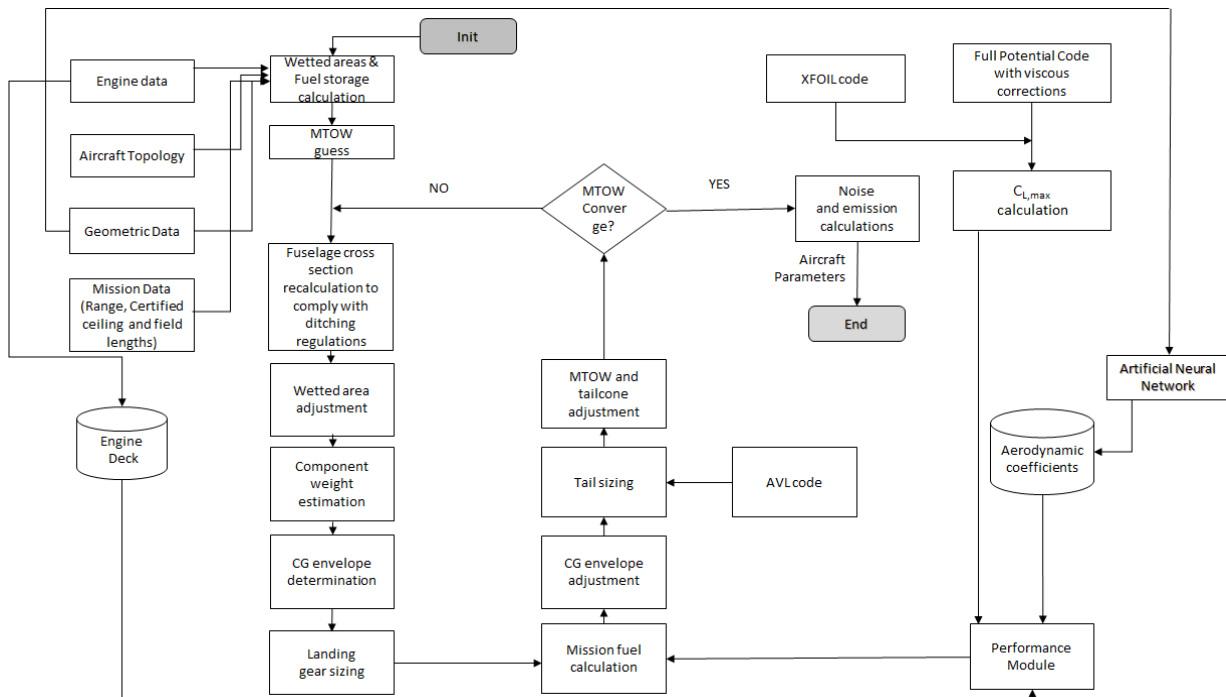


Figure 3.4: Flowchart of Aircraft Framework calculations

3.1.1 MTOW and OEW estimation

The weight estimation loop is the core of the Aircraft Framework module through an iterative calculation process. According to Fig. 3.4, the initial airplane dimensions estimation is used to calculate an initial guess of airplane weight based on its wetted area, according to the methodology proposed by Roskam [144], in the so called Class I method. This initial guess is then used in the calculation of airplane's component weight breakdown, according to the methodologies developed by Roskam [144] and Torenbeek [23], in the so called Class II method.

In this method, the calculation of pylons, fuselage, empennage (vertical and horizontal tails), systems, landing gear and engines are done separately and then added together to compose the Operational Empty Weight (*OEW*). These component weights are then used on the determination of the *OEW*'s related center of gravity (*CG*).

With the *OEW* determined, the MTOW and Maximum Landing Weight (*MLW*) are then calculated using the mission performance module, used in the Network Framework, where the trip fuel is determined. The following operational profile assumptions are considered in the mission performance calculations:

- Standard atmosphere.
- Takeoff and Landing airports at sea level.
- Payload related to 100% of passenger's capacity (@100kg each).
- Mission distance equal to the design range.
- Alternate airport distance equal to 200 nm.
- Speed and Altitude profiles defined according to mission performance module logic.

The information derived from the above process is then used to estimate the moments of inertia of the airplane and the center of gravity shift with fuel consumption required for the stability and control analysis performed in the tail sizing refinement process. The resulting MTOW is iteratively refined until the difference between two consecutive iterations is lower than 5kg tolerance, which then defines the weight convergence. Since in this study the structures discipline is not developed, the Zero Fuel Weight (*MFW*) is estimated as a fraction the *MLW* (herein assumed as 98%), following Roskam's methodology [145] [24]. In addition to the above explanations, the following

considerations are necessarily related to sizing and weight estimation of some specific components:

Wing's weight estimation

The wing weight is estimated by sizing the wingbox to withstand aerodynamic loads calculated with a full potential code in some few maneuvers in the flight envelope and the secondary structure being estimated by empirical formulae, according to the methodology proposed by Isikveren [146].

Engine's weight estimation

Most of the jet engines weight estimation methods developed in academia are derived from empirical formulae based on geometric data from first and second generations of turbojet engines, presenting by-pass ratios. Some examples are the work developed by Reymer [35], Loftin [49] and Boeing [147]. Such methods are most times not applicable to the current generation of turbofan engines, with high by-pass ratios, much different in manufacturing technologies and design (notably equipped with larger fan diameters, improved combustion cameras and complex associated accessories). It is not uncommon to observe significantly different results, using the traditional weight estimation formulae, when compared with actual engine weight data. For example, applying the classical method developed by Reymer [35] to the GE-90/77B engines (used in the Boeing 777 series), an estimated engine weight, 46% larger than the actual value is found. In order to improve such kind of results, studies dedicated to turbofan engines were later conducted by Tong et al. [148], Lolis [149] and Greitzer [150], mainly focusing on single component weight modeling, producing more suitable results, within 15% error margin. In this research, we propose a new method for engine weight estimation considering the main thermodynamic parameters commonly used in high-bypass turbofan engines, as an expansion of the conventional modeling proposed by Reymer [35] and Loftin [49]. Thus, the following parametrization is proposed:

$$W_E = \frac{T1 \cdot (BPR/\overline{BPR})^a \cdot (OPR/\overline{OPR})^b \cdot (T_{net}/\overline{T_{net}})^c \cdot (eDiam/\overline{eDiam})^d \cdot (l_e/\overline{l_e})^e \cdot (FF/\overline{FF})^f}{T2 \cdot (OPR/\overline{OPR}) \cdot (T_{net}/\overline{T_{net}}) \cdot (eDiam/\overline{eDiam}) \cdot (l_e/\overline{l_e}) \cdot (FF/\overline{FF})} + T3 \quad (4)$$

The coefficients and exponents of Eq. 4 are obtained by optimization using a genetic algorithm with the minimization of mean square error related to known engines [151]. These engines belong

to a database that comprised of over 25 engines with considerable thrust variation among them, covering a large variety of turbofan designs [152]. Table 3.8 shows the coefficients and parameters obtained with the optimization process. Table 3.9 shows the average parameters used for normalization. Table 3.10 contains weight estimation errors for some known turbofan engines.

Table 3.8: Engine weight equation exponents and coefficients

| Coefficient/exponent | Value |
|----------------------|-----------|
| T1 | 2587.2461 |
| T2 | 50.1920 |
| T3 | 154.6179 |
| a | -0.1965 |
| b | -0.0718 |
| c | 1.0435 |
| d | 0.2493 |
| e | -0.3444 |
| f | -0.1455 |

Table 3.9: Engine weight equation normalization parameters

| Parameter | Value |
|-------------------|----------|
| BPR | 4.6911 |
| OPR | 25.4000 |
| $eDiam$ [m] | 1.7906 |
| \bar{l}_e [m] | 3.3276 |
| T_{net} [kN] | 148.1217 |
| \bar{FF} [kg/s] | 464.7333 |

Table 3.10: Weight error estimation for typical turbofan/jet engines

| Engine | Deviation [%] |
|------------------------|---------------|
| CF6-50C | 2.55 |
| JT8D-219 | 0.74 |
| GE CF-34-10A | 6.48 |
| R&R RB211-535C | 0.97 |
| Trent 800-875 | 3.12 |
| Pratt & Whitney PW2040 | 0.44 |
| GE-90/77B | 0.31 |
| R&R Tay 620 | 2.65 |

Landing gear sizing

Although the landing gear design is not normally determined in the airplane's conceptual design phase, in this research, a detailed nose and main landing gear positioning and dimensions are developed inside the weight estimation loop in order to provide a more accurate weight value for such components. For that, the methodology developed by Roskam [145] with improvements proposed by Currey [153] is adopted.

The process consists of determining gear position based on airplane balance on the ground from airplane attitudes, *CG* limit locations (derived from the component weight estimation process) and estimations of gear static and dynamic loads. The following aspects are considered in the calculation process:

- Engine clearance to ground (0.3m) considered in the landing gear main strut sizing.
- Wheels of the main landing gear must be accommodated inside the wing-fuselage fairing.
- Wake from the main landing gear wheels must avoid hitting and shadowing the inner flaps.
- Nose and main landing gears designed with single wheel axis and mounting.
- Nose and main landing gear wheels equipped with tires designed for 225 mph speed limit
- Main landing gear wheels chosen by minimum weight design criteria [153].
- Nose landing gear wheels chosen by lower radius design criteria [153].

Figure 3.5 shows the single wheel landing gear configuration used in all designs. Fig. 3.6 illustrates the main landing gear design clearances considering engine, inner flaps and fuselage geometries.



Figure 3.5: Single wheel nose and main landing gear configuration

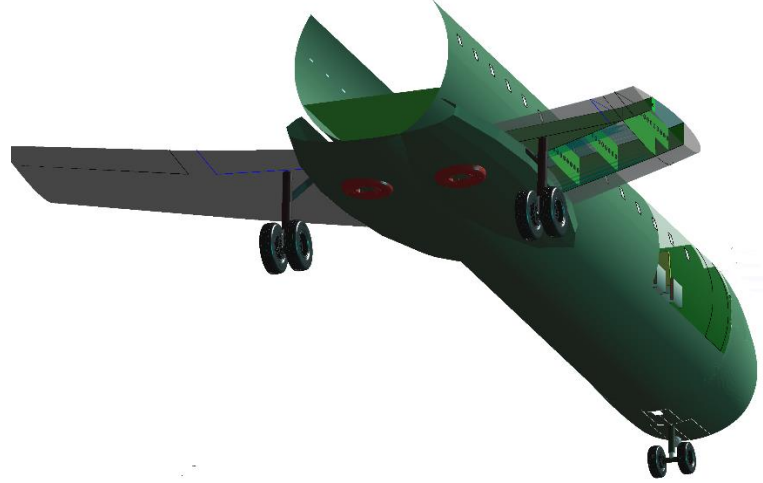


Figure 3.6: Main landing gear design clearances considering inner flaps and fuselage geometries

Fuselage and cabin sizing

The code developed for fuselage and cabin sizing is based on the methodology described in the work of Sholz [154] [155] and Marckwardt [156] on aircraft preliminary design.

In such method, the fuselage is modeled as a long cylinder with constant ellipsoid cross section. The code considers as inputs the total number of passengers, seat width, aisle width, cabin height, number of aisles and number of seats abreast (maximum 6), in order to calculate the dimensions of the minor and major axis of the ellipsoid's cross section (outer dimensions, considering fuselage thickness) and total fuselage length. These are key parameters used in the wet area computation adopted in the MTOW/OEW determination loop, using Roskam's formulae [145]. Although cargo revenue is not considered in this research, space for cargo containers in the fuselage lower floor is also considered in the fuselage cross-section computations. Figure 3.7 shows typical layouts produced by such methodology. In all designs, the following assumptions are made during the cross-section calculations:

- Single class configuration (economy).
- Space for two LD3-45/AKH container (1.46m x 1.49m x 1.13m) [157] in the lower cargo compartment, mostly used in the A320 aircraft.

- Passenger's dimensions defined by the 95% of American male, defined by NASA [158].

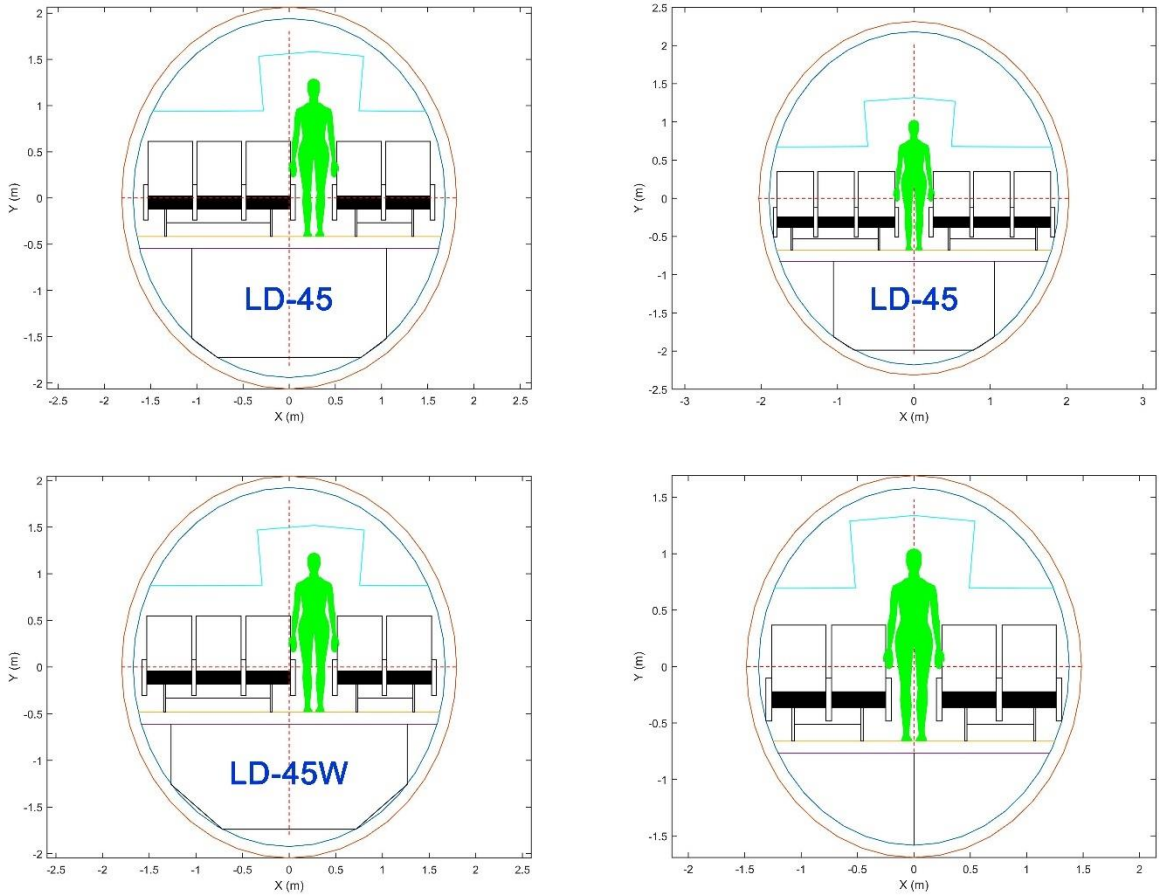


Figure 3.7: Typical fuselage cross section computation

Horizontal and vertical tail sizing

The code developed for horizontal and vertical stabilizer areas sizing considers a higher fidelity method than that offered by the tail volume approach, as described in the classical aircraft preliminary design literature (Roskam [144], Raymer [142] and Torenbeek [23]). A methodology based on static stability and controllability criteria was developed and integrated into MTOW interactive process, based on Mattos and Secco's work [159].

The incorporation of a more sophisticated methodology for the tail plane sizing determines a more complex task in the interactive process for MTOW calculation. The determination of the CG location, and its allowable variation along the flight envelope, is needed not only for the tail plane area calculation, but for the positioning of the wing, and the main and nose landing gears, which

are also dependent on this process. The allowable center of gravity variation is calculated regarding the design mission, depending on the associated fuel consumption (as function of wings geometry) and mass distribution along the fuselage, including passengers' uneven distributions and people movements along the cabin in cruise phase. In addition, the CG location guides the wing placement in the chosen configuration [159] [142], as shown in Fig. 3.8.

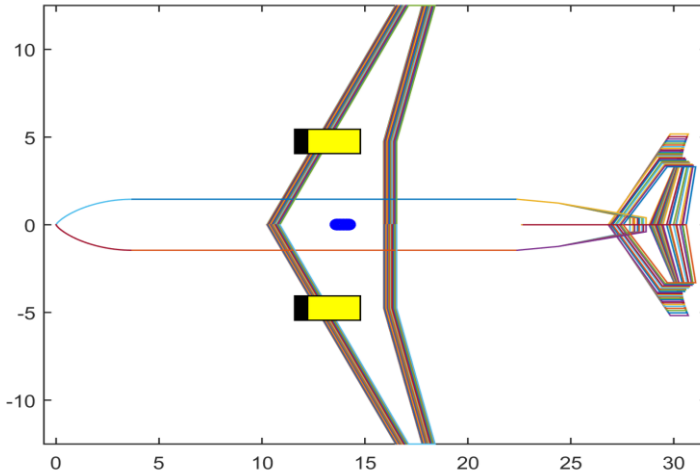


Figure 3.8: Example of wing and tail placements considering the allowable CG variation (blue) for a certain design

Two criteria are adopted for the vertical stabilizer sizing: lateral static stability and controllability. They are evaluated separately in which the geometry of the largest area is taken as solution. The lateral stability criteria is set in order to fulfill a value that incorporates a desired variation of yawing moment coefficient with yaw angle ($C_{n\beta}$), calculated according to Roskam's methodology [160]. The lateral controllability criteria is set in order to fulfill the one engine failure takeoff minimum control speeds certification requirements, according to FAA's regulations for commercial transport aircraft [161].

The horizontal stabilizer area is obtained considering the evaluation of both longitudinal static stability and controllability criteria at the same time. The static longitudinal stability criteria is determined through the check of the pitch moment coefficient ($C_{m\alpha}$) sign or the location of the aircraft neutral point, also according to Roskam's methodology [160]. The longitudinal controllability criteria is determined via classical tail volume analysis, as described in the classical literature [144] [142] [23]. According to Scholz [162], the relationship between the area ratio (hS/wS) and the distance from the CG to the neutral point (static margin) for both criteria may be

combined into a single graph, where the integrated analysis is performed, as shown in Fig. 3.9. The permitted areas of focus are settled between the limit lines of controllability and stability requirements. Between these lines, the required CG range (green dashed line) can thus be fitted in order to determine smallest horizontal tail surface area [159].

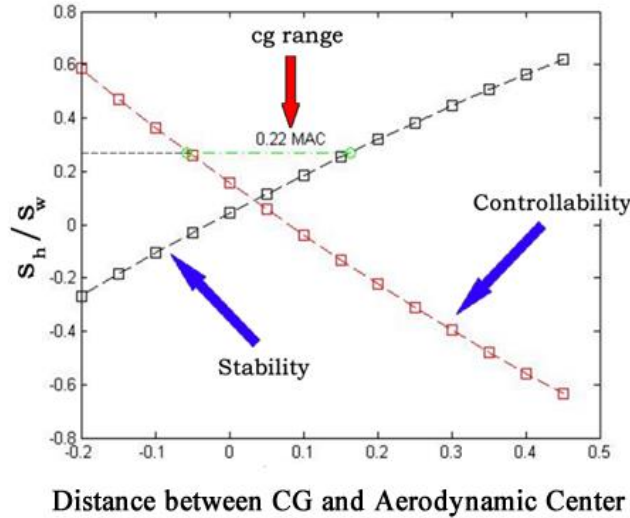


Figure 3.9: Scholz method to determine the minimum horizontal tail area

The stability derivatives needed for the above calculations (C_{ma} and $C_{m\alpha}$) and the other ones necessary for the stability and control analysis, were obtained using the Aerodynamic Vortex Lattice (AVL) open application, developed by the Massachusetts Institute of Technology [163]. This application uses the aircraft's main geometric characteristics to model a flow simulation, using an extended vortex lattice model for the lifting surfaces, together with a slender-body model for fuselages and nacelles, in order to determine the main aerodynamic coefficients and associated stability derivatives of the aircraft. The application also has a flight dynamic analysis mode that combines a full linearization of the aerodynamic model about a steady flight state. Inertia properties, necessary inputs for AVL's dynamic model, were estimated via Roskam's methodology [160] also using the main geometric characteristics of the aircraft. An example of AVL model is shown in Fig.3.10.

With AVL results, the flight quality evaluation is performed on the resulting airplane considering the longitudinal and lateral responses to small perturbations. This is done according to Stevens et al. methodology [164] where a frequency response examination is performed on the poles resulting from the eigenvector of the stability derivatives matrix. In the longitudinal

movement, the short period oscillations mode is considered, while in the lateral-directional movement, Dutch-roll mode is investigated. The damping constant (ζ_d) and response frequency (ω_n) associated with these two modes are checked against the MIL-STD-1797B flight quality requirements [164] [165], as shown in Fig. 3.11. The design under analysis is then considered accepted if minimum Level 2 classification is achieved in both modes. This means that flight qualities are adequate to accomplish the mission flight phase, but some increase on pilot workload may be expected. If not, a new horizontal and vertical stabilizer cycle needs to be initiated until convergence.

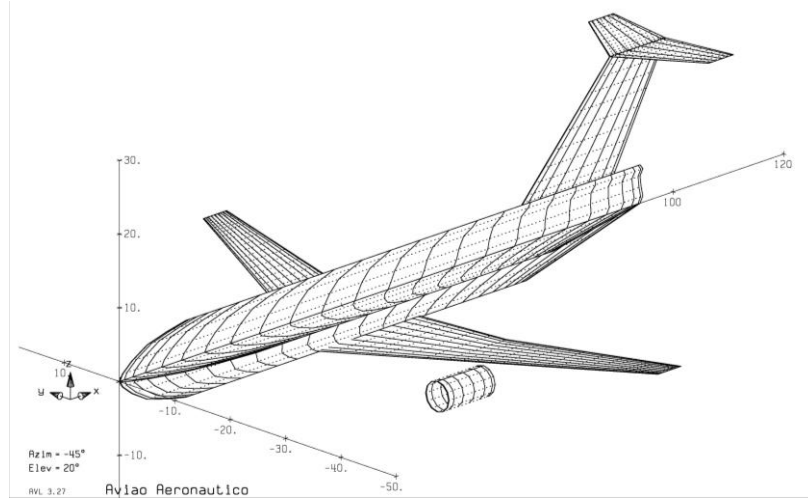


Figure 3.10: AVL model for the calculation of stability derivatives

Short-Period Damping Ratio Limits

| Level | Cat. A & C Flight Phases | | Cat. B Flight Phases | |
|-------|--------------------------|----------|----------------------|----------|
| | Minimum | Maximum | Minimum | Maximum |
| 1 | 0.35 | 1.30 | 0.30 | 2.00 |
| 2 | 0.25 | 2.00 | 0.20 | 2.00 |
| 3 | 0.15* | no limit | 0.15* | no limit |

*May be reduced at altitude > 20,000 ft with approval.

Limits on $\sigma_{n,\alpha}^2 / (n/\alpha)$

| Level | Cat. A Phases | | Cat. B Phases | | Cat. C Phases | |
|-------|-----------------------------|----------|---------------|----------|------------------------------|----------|
| | Min. | Max. | Min. | Max. | Min. | Max. |
| 1 | 0.28 $\omega_n \geq 1.0$ | 3.60 | 0.085 | 3.60 | 0.16 $\omega_n \geq 0.7$ | 3.60 |
| 2 | 0.16 $\omega_n \geq 0.6$ | 10.0 | 0.038 | 10.0 | 0.096 $\omega_n \geq 0.4$ | 10.0 |
| 3 | 0.16 | no limit | 0.038 | no limit | 0.096 | no limit |

There are some additional limits on the minimum value of n/α and the minimum value of ω_n for

Dutch-Roll-Mode Specifications

| Level | Flight Phase Category | Class | min | min | min |
|-------|-----------------------|-------------|-----------|------------------------|----------------|
| | | | ζ_d | $\zeta_d \omega_{n_d}$ | ω_{n_d} |
| 1 | A | I, IV | 0.19 | 0.35 | 1.0 |
| | | II, III | 0.19 | 0.35 | 0.4 |
| | B | all | 0.08 | 0.15 | 0.4 |
| 2 | C | I, II-C, IV | 0.08 | 0.15 | 1.0 |
| | | II-L, III | 0.08 | 0.15 | 0.4 |
| 3 | all | all | 0.02 | 0.05 | 0.4 |

Figure 3.11: Flight quality requirements for Dutch Roll and short period [164]

3.1.2 Aerodynamics

This module, developed in *MATLAB®* code, computes the total drag and lift coefficients required for performance calculations mission performance module, to be detailed in Session 3.2.1.

For that, a surrogate model based on an artificial neural network (*ANN*) is employed for the estimation of aerodynamics coefficients of the wing, according to the methodology proposed by Secco and Mattos [166] [58]. Among many architectures evaluated, a three-layer feed-forward ANN, with hyperbolic transfer function, was found to be best suited for non-linear problems with dozens of variables as with the present case. This type of network can approximate any function to any desired degree of accuracy, provided it has enough neurons in the hidden layers.

Regarding estimation of total drag coefficients, three dedicated ANNs were designed to estimate the three drag components, zero-lift, induced, and wave drag. According to Secco and Mattos [58], this approach is considerably more accurate than employing a single ANN for the total drag estimation. A multi-layer neuron network type was used for the aerodynamic surrogate model, consisting of three layers on feed forward configuration (50-50-1), hyperbolic transfer function and back propagation algorithm. The ANN was trained with 110,000 different wing geometry airfoil configurations with wing reference areas ranging from 50 to 200 m².

For the generation of the ANN training database, a full potential aerodynamic code was used to evaluate the above-mentioned aerodynamic coefficients related the several wing geometries. According to Mattos et. all [12], the time-cost benefit makes this method very attractive for higher fidelity aerodynamic computations in MDO processes. Indeed, a study conducted by Mattos [167] shows that such methodology may bring equivalent aerodynamic estimations than Reynolds Average Navier-Stokes (*RANS*) solutions with much less computational efforts. Due to the extreme sensitiveness of transonic flow to airplane geometry, this module is also coupled with an integral boundary layer algorithm that calculates the viscous effects at prescribed stations along wingspan. Besides delivering satisfactory profile drag values, the viscous coupled calculation used is also be able to handle shock-boundary layer interactions.

Input for the computations of the ANN are environmental conditions, wing and airfoil parameters, as listed in Table 3.11 and Figures 3.12 and 3.13, respectively. An additional 3-4% on total CD is applied to consider miscellaneous drag. Induced drag is adjusted for the presence of winglets according to the study conducted by Mattos et al. [168].

Table 3.11: Inputs for the ANN computation

| ANN Input Parameters | Symbol |
|---|------------|
| Mach number | M |
| Pressure Altitude (ft) | H_p |
| Angle of attack | α |
| Wing Aspect Ratio | wAR |
| Wing Taper Ratio | wTR |
| Wing semi-span (m) | wb |
| Wing leading edge sweepback angle (deg) | $wSweepLE$ |
| Inner wing panel dihedral | δ_1 |
| Outer wing panel dihedral | δ_2 |
| Kink Semispan position | $KinkPos$ |

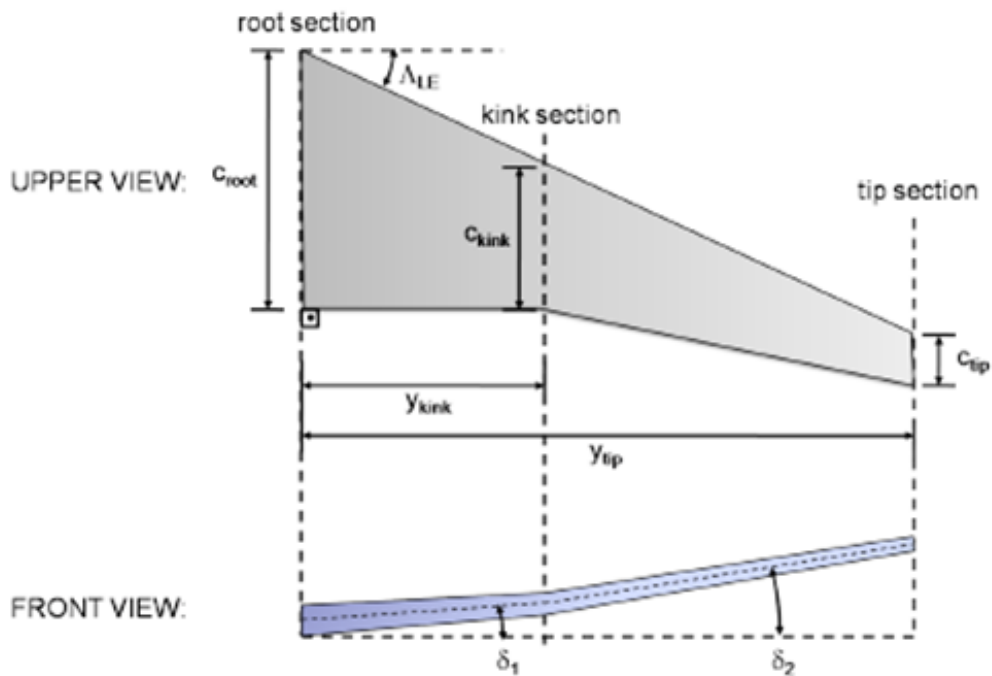


Figure 3.12: Wing geometric parameters [58]

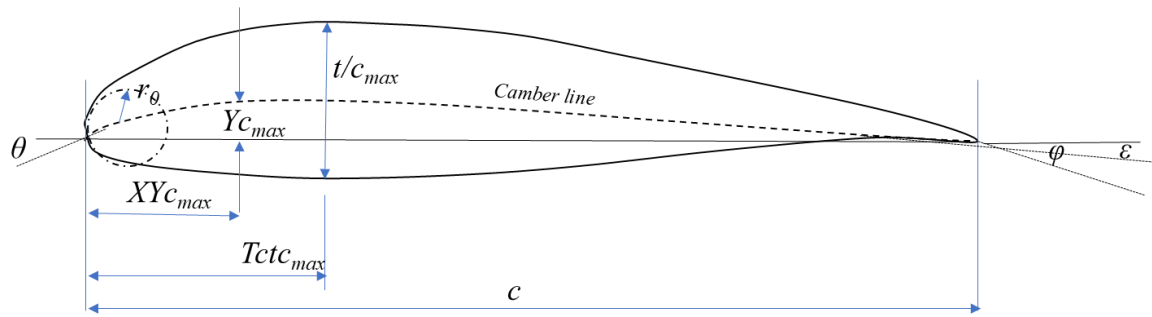


Figure 3.13: Airfoil geometric parameters

Three fixed airfoils for the root, kink and tip stations are used in all wings of the airplanes generated in each optimization cycle. Such airfoils are optimized for Mach 0.78 cruise speed, with maximum L/D = 23. Their coordinates are read from a specific database (Aero Database).

Since the airfoils geometric parameters are needed as input for the ANNs [166], a polynomial fitting, according to Sobieski methodology [169] is applied to the provided coordinates in order to determine such parameters. There is then a need for an optimization problem to fit Sobiesczky polynomials to these geometries. This was carried out with the *fsolve* optimization tool from MATLAB® [170] [171] [172]. Fig.3.14a shows the original airfoil coordinates and the obtained polynomial fittings. The three airfoils parametric coefficients, calculated from the polynomial fitting, are presented in Table 3.12.

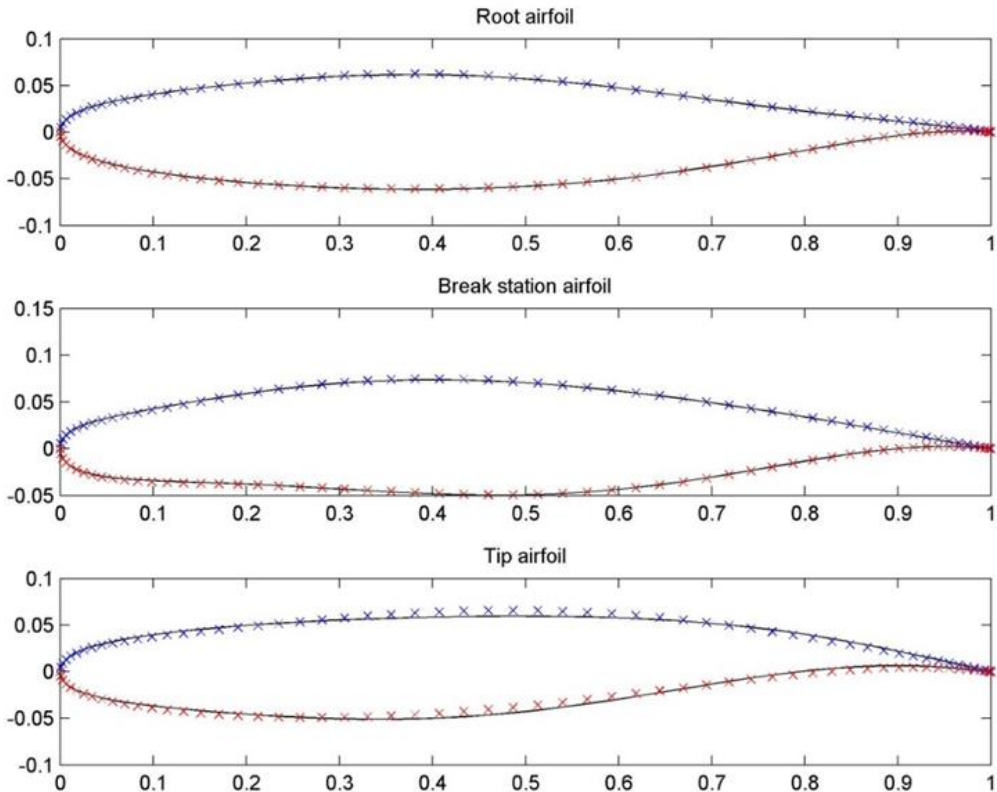
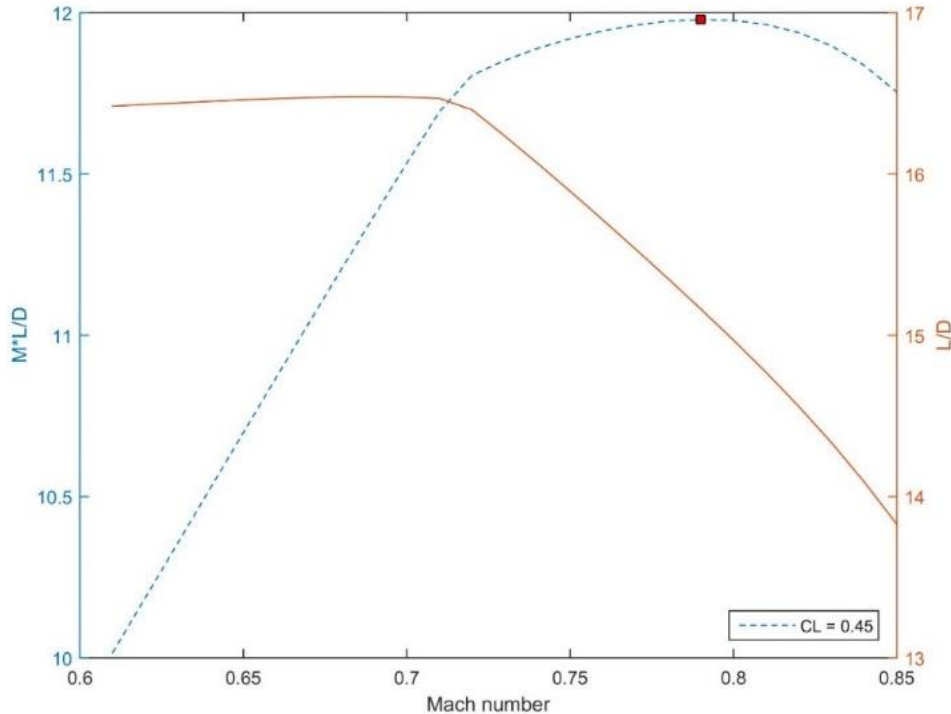


Figure 3.14a: Airfoil coordinates and polynomial fittings.

Table 3.12: Airfoil geometric parameters

| Parameters | Symbol | Root | Kink | Tip |
|---|-------------------|---------|--------|--------|
| Leading edge radius | r_0 | 1.5 | 1.5 | 1.5 |
| Airfoil thickness ratio [%] | t_c | 13.5 | 11.3 | 11.3 |
| Thickness line angle at trailing edge [°] | φ | -0.1 | -0.1 | -0.1 |
| Maximum thickness chord-wise position | $t_{c_{max}}$ | 0.3738 | 0.3545 | 0.3630 |
| Camber line angle at leading edge [°] | θ_c | 0.1 | 0 | 0.1 |
| Camber line angle at trailing edge [°] | ε | -0.1 | -0.1 | -0.1 |
| Maximum camber | $Y_{C_{max}}$ | -0.0404 | 1.2095 | 1.3791 |
| Camber at maximum thickness chord-wise position | $T_c t_{c_{max}}$ | -0.0638 | 0.5663 | 0.8571 |
| Maximum chamber chord-wise position | $X Y_{C_{max}}$ | 0.6188 | 0.7283 | 0.7033 |

Fig 3.14b shows the aerodynamic characteristics of the basic airplane using such airfoils on its wings. The aerodynamic efficiency (L/D) and performance efficiency ($M.L/D$) parameters are displayed as function Mach numbers ranging from 0.62 to 0.85 (limiting speed where the ANN is trained).

**Figure 3.14b:** ML/D and L/D curves for the optimized airfoils (basic airplane)

An important consideration about the observed $M.L/D$ variation is its “flat” behavior against a broad range of Mach numbers. This is a highly desirable characteristic once allows the airline to operate the airplane without performance degradation for distinct flight profiles, wide ranges of weight and cruise altitude. Fig. 3.14c contains some pressure coefficient (C_p) distributions for stations along the wing semispan of the basic airplane, at the design point (Mach 0.78, $\alpha = 1.46^\circ$ and $C_L=0.45$). It may be observed that the C_p distribution strongly resembles an isentropic recompression in all stations. To assure a good off-design behavior as seen in Fig. 3.14b, the drag coefficient increase from a subsonic condition was constrained for some lift coefficients.

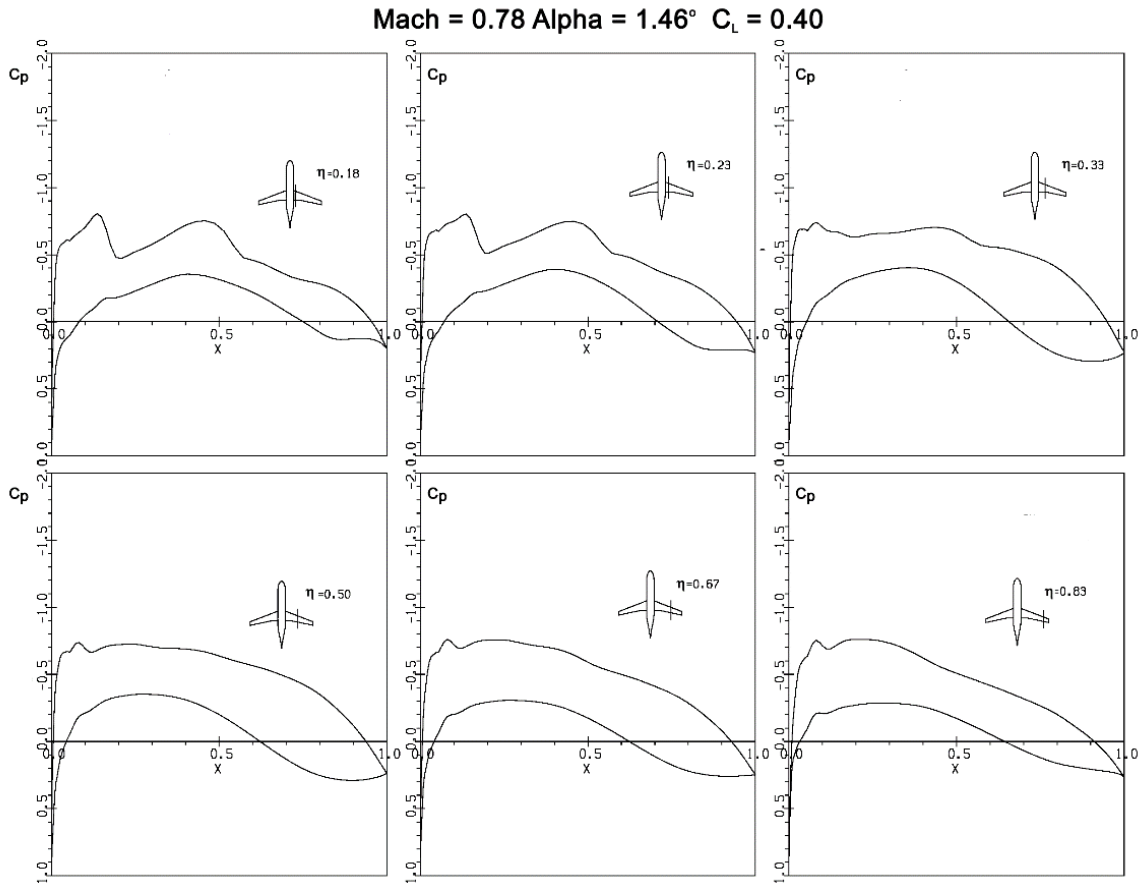


Figure 3.14c: Pressure distributions for the reference airplane at design point

Table 3.13 shows a comparison between the ANN and the full potential code methodology, for the basic aircraft, at design conditions. It may be observed that the overall drag differs by one drag count only, with the wave drag coefficient recorded the highest difference, about three drag counts. This represents typically the error obtained with flight test data and those from large subsonic wind tunnels. If the flow is subsonic over the entire airplane surface, the average estimation error of the

ANN lies below 0.1 drag counts. Despite the complexity of the airflow at the cruise condition over the test case airliner, ANNs could predict the drag coefficients.

Table 3.13: Predicted and calculated coefficient values by ANN and full potential code at design point of the basic aircraft

| Predicted coefficient (counts) | ANN | Full potential code | Deviation |
|--------------------------------|--------|---------------------|-----------|
| C_{D0} | 0.0065 | 0.0066 | 1.5% |
| $C_{D\text{ ind}}$ | 0.0055 | 0.0056 | 1.8% |
| $C_{D\text{ wave}}$ | 0.0069 | 0.0066 | 4.5% |
| C_D | 0.0189 | 0.0188 | 0.53% |
| C_L | 0.3670 | 0.3820 | 3.9% |

Finally, a verification of the accuracy and capability of the ANN estimation of the drag divergence is shown in Fig. 3.15. Two airplane configurations were selected from the database, run via full potential code with viscous corrections (CFD), not part of the ANN training set, presenting different drag behavior over Mach number, evaluated at a pressure altitude of 35000ft. It may be observed that the delay of the drag divergence with the increase of the wing sweep angle was correctly captured by the drag-predictor ANN for the two configurations. The comparison shows that the delay of the drag divergence with the increase of the wing sweep angle was correctly captured by the drag-predictor ANN.

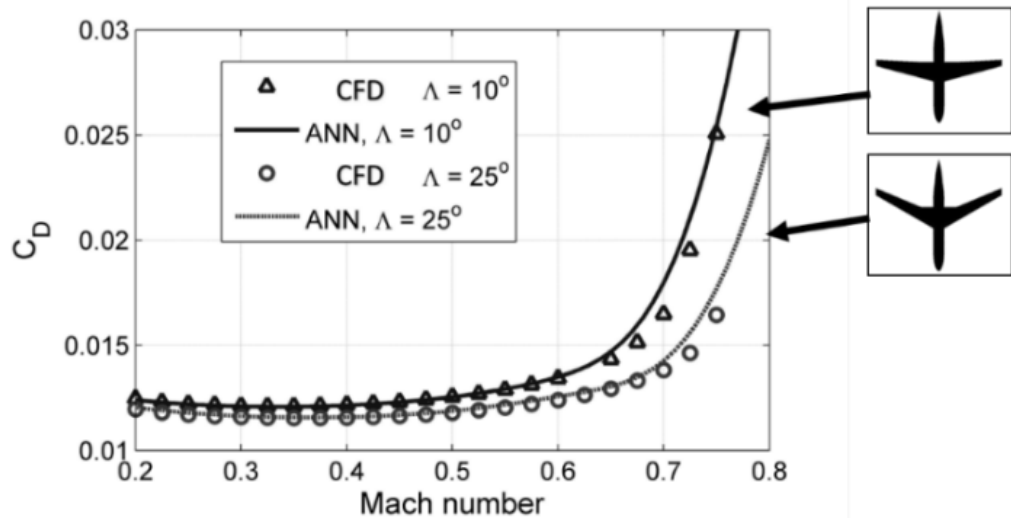


Figure 3.15: Comparison between ANN overall drag predictions and CFD results

CL_{max} computation

High-lift performance has an enormous impact on sizing, economics and safety of any airplane [173]. Navier-Stokes analysis is very time consuming due to the complex nature of the flow in combination with complex geometries.

Several analytical methods that account for both stall effects and enable the prediction of the maximum lift coefficient were discussed and a trade-off between the methods was conducted by Singh [174]. In his study, it was found that both the pressure difference rule and the so-called Critical Section are good options in terms of accuracy and versatility. It has validated both the pressure difference rule and critical section method against wind-tunnel experiments, both for wing only samples and wing + fuselage models. The approximation of clean maximum lift coefficient is shown to be in good agreement, which is about 3% error.

Therefore, the Critical Section Method was used in this module to estimate airplane's clean maximum lift coefficient (CL_{MAX}). For that, an XFOIL ® panel code [175], combined with a wing-fuselage full potential code with viscous corrections according to the methodology proposed by Mattos [167], was used to determine the maximum lift coefficient on the set of wing sections of the wing design under analysis. According to this method, stall is reached when the lift coefficient distribution along the semispan, obtained from the full potential code, locally equals the wing section's maximum lift coefficient. The pressure difference rule on the other hand, determines wing stall by implementing an empirical chordwise pressure difference criterion. Thus, wing stall is established when the wing section's chordwise pressure difference, at an angle of attack, equals to the critical pressure difference which is empirically derived and depends on both Mach and Reynolds numbers [167].

High lift devices

High-lift systems have a major influence on the sizing, economics, and safety of transport airplanes. Although high-lift systems are complex and costly, they are necessities that allow airplanes to take off and land on runways of acceptable length without penalizing the cruise efficiency significantly [176]. In this module, the methodology described in the US Airforce DATCOM [177] is used to determine the CL_{MAX} , for the takeoff, landing and approach flaps configurations. The basic high lift devices geometric configurations adopted in all designs are:

- One slot flap
- Slat present
- Flap length: 75% wingspan.

3.1.3 Propulsion

This module, developed in *MATLAB* ® code, computes the net thrust (T) and fuel flow (FF) parameters required for performance calculations mission performance module (Session 3.2.1) and Noise Module (Session 3.1.4).

During the conceptual design phase, engine performance is usually determined based on a desired thrust and an average specific fuel consumption value [26]. However, whenever vehicle trajectory simulations need to be performed, sophisticated engine models are necessary to predict both steady state and transient engine behavior. In such models, engine performance fidelity is highly dependent on the modeling aerodynamic, thermodynamic and mechanical component behaviors.

The aerothermodynamic turbofan engine model employed in this module is based on Loureiro's work [178], derived from the generic engine deck formulations proposed by Benson [179] and adopted by NASA in the *EngSim* Project [180]. The model uses a closed formulae approach to calculate thermodynamic input and output states on each engine's component in a generic mounting configuration.

The input parameters used in such model correspond to the engine design parameters, listed in Table 3.2. They are by-pass ratio (BPR), fan pressure ratio (FPR), overall pressure ratio (OPR), inlet turbine temperature (TIT), fan diameter ($DFAN$) and cruise altitude design point. In addition, the operational parameters necessary for computations at each flight calculation point are pressure altitude, Mach number, ISA deviation and throttle position (IT). The outputs from the calculation are net thrust (T) and fuel flow (FF). Two calculation steps are built in this methodology:

1. The design step: where all engine characteristics are determined at a given design point defined by a given cruise Mach number, cruise altitude and 95% of maximum throttle setting.
2. The analysis step: where it is possible to calculate the engine thrust and fuel flow from the geometric characteristics obtained in the design step.

A special consideration shall be given to the turbofan compressor efficiency computation, which is performed as an intermediate step of the net thrust determination. In this work, a numerical interpolation, via multi-dimensional look-up table, is performed via generic compressor map used in the Gas Turbine Simulation Program (GSP) developed by National Aerospace Laboratory of Netherlands (NLR) [181]. This map was selected since it provides more realistic performance calculations during transitory operations, such as on climb and descent phases, rather than using fixed efficiency as stated in Benson's model (assumed to be 80%). This last model produces, for example, throttle settings different than zero for idle thrust during the descent and therefore increasing the fuel flow at this phase, which is not realistic. In the GSP formulation, the compressor efficiency (η) is calculated as a function of compressor pressure ratio (PR), corrected mass flow (W_c) and corrected rotor speed (N_c), as shown in Fig.3.16.

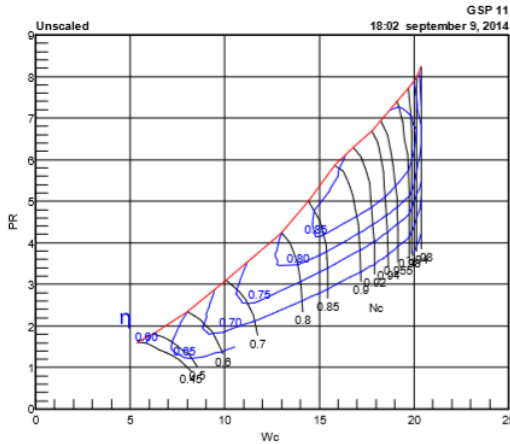


Figure 3.16: Generic compressor map [181]

$$\text{Where } W_c, N_c, PR \text{ are given by:} \quad W_c = \frac{m_c \sqrt{\theta}}{\delta} \quad (5) \quad N_c = \frac{N}{\sqrt{\theta}} \quad (6) \quad PR = \frac{P_{t_{in}}}{P_{t_{out}}} \quad (7)$$

3.1.4 Noise

This module, developed in *MATLAB* ® code, computes the noise levels at the aircraft certification measuring points, recorded in the Aircraft Definition database.

According to Fig. 3.17, after the aircraft dimensions are defined as product of the weight estimation loop, the aircraft noise estimations are performed according to type certification regulations. For that, airplane noise shall be assessed in three defined measurement points along

the flight path, according to international standards defined by Annex 16 of the Convention of the International Civil Aviation Organization [143].

These measurement points, illustrated in Fig. 3.16 as green dots where microphones are set, are determined with the objective to capture the effects of airplane performance (fly-over point), engine design (sideline point) and airframe characteristics (approach point) on the resulting noise signature. According to Annex 16, the accumulative level (sum of the measured sound level in these three performance points, measured in terms of *Equivalent Perceived Noise - EPNdB*) shall be used as baseline for the noise classification of the aircraft (the so-called “Chapters 2,3,4 and 14”). This information is essential to determine the capability of the aircraft to operate at certain airports, according to specific noise constraints.

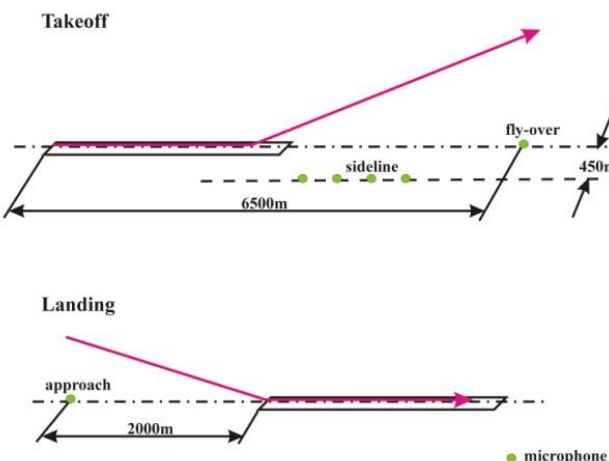


Figure 3.17: Noise measuring points for airplane certification (Source: Magalhães [182])

Airplane noise models have been used to estimate the noise level at certification points since the 70's and vary on complexity of details [183]. The so-called type-1 models, according to classification proposed by Zaporozhets et al. [184], are the foundation for the basic noise computations of any aircraft type, which consists of a spectral analysis of the acoustic field around the aircraft due to the aggregated contributions of each of its noise source evaluated separately. These models consider the distance from the airplane to the receiver (r), the frequency (F) and directivity (Θ) of the sound source, engines throttle setting (IT) and airplane configuration (flaps and landing gear) to measure the sound level in terms of Sound Pressure Level (SPL). The equation used to predict the complete airplane noise is defined below:

$$\text{SPL}_{\Sigma}(F) = 10 \cdot \log_{10} [\sum_i 10^{0.1 \cdot \text{SPL}_i(F)}] \quad (8)$$

Where $SPL_i(F)$ is the basic spectrum contribution of each noise source corrected for directivity, frequency shift, relative movement of the source, interference of sources, atmospheric attenuation and absorption and ground reflection.

Semi-empirical type-1 models were the first to be developed and are based on correlations of key design parameters and measured noise from airframe and engine components. Considering this approach, the most complete model is NASA's Airplane Noise Operations Prediction Program (ANOPP) [183], which provides closed formulae for such computations including corrections for directivity, spectral and speed variations, besides atmospheric abortions. In this research, the methodology proposed by Magalhães [182] [48], based on the ANOPP model equations, is used to estimate noise and airframe noise levels at certification points.

With the objective to accomplish this calculation, a complete flight path simulation shall be performed in order to achieve the certification points. Takeoff and approach noise assessment are derived from simple flight mechanics' modeling, according to a Roskam's methodology [24]. The takeoff flight path consists of an integration of airplane acceleration on the ground, followed by an integration of rate of climb data up to 3000ft above the runway. No thrust reduction (cut-back) was considered in the flight path for simplicity. The approach flight path consists of calculating a standard -3deg flight path approach in the landing configuration from 1500ft down to 50ft above the runway [182].

The complete airplane noise model consists of the integration of the flight-path generation with the engine and airframe noise estimation functions. Once the SPLs for the whole trajectories were obtained, they were converted into Effective Perceived Noise Levels (*EPNLdB*) for the noise certification points.

3.1.5 Airplane design performance check

As mentioned previously, once the aircraft design is completed, it is necessary to check if its performance is adequate according to specific certification requirements predicted in FAR25 [161], before running the mission/network calculations. The idea is to have an initial estimation

about operational performance of the aircraft under evaluation to avoid potentially unfeasible designs for airlines.

In this research, the methodology proposed by Loftin, in his work developed for NASA [49] about the operational suitability of aircraft designs, is adopted. The method is based on the so-called Design-Diagram check, where the analysis of the influence of the wing loading (W/S) and thrust-to-weight ratio (T/W) in a set of operational characteristics of the aircraft is performed. The idea of this method is to compare the pair ($MTOW/S$, T/W) of the aircraft under analysis with the function $W/S=f(T/W)$ associated with certain operational conditions. Fig. 3.18 shows a graphical example of such methodology, considering some basic performance checks.

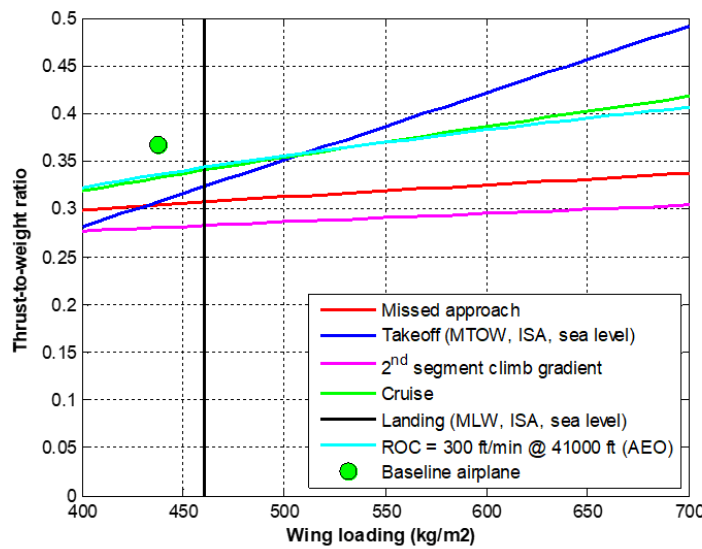


Figure 3.18: Design Diagram check

Class-I methods (direct formulae) are used to check each performance condition, based on Roskam's [24] and Torembeek's [23] methodologies. If the selected aircraft design does not satisfy any of the check, the aircraft is considered a failure in the MDO cycle and is not considered in the optimization process. The following checks are considered:

Takeoff field length

The balanced field length takeoff capability is verified at Maximum Takeoff Weight ($MTOW$) and Maximum Takeoff Thrust (T_{max}) considering the design takeoff field length ($TOFL$), sea level

airport and standard atmospheric conditions. The following equation, derived from Roskam's methodology [24], is used:

$$ToW_{req} = \frac{2,34 \left(\frac{MTOW}{wS} \right)}{CL_{MAX_{TO}} \cdot (T_{OFL})} \quad (9)$$

If the ratio of $T_{max}/MTOW$ is less than ToW_{req} , the aircraft design under evaluation is not selected.

Landing field length

The landing field length landing capability is verified at Maximum Landing Weight (MLW), considering the design landing field length (LFL), a sea level airport and standard atmospheric conditions. The following equation, derived from Roskam's methodology [24], is used:

$$WoS_{req} = \frac{0,119 \cdot LFL \cdot CL_{MAX_{LD}}}{(MLW/MTOW)} \quad (10)$$

If the ratio of $MTOW/wS$ is less than WoS_{req} , the aircraft design under evaluation is not selected.

Second segment climb

The climb capability is verified according to FAR25.121 requirements for the second segment on the gross takeoff flight path, considering the following configuration:

- One engine failed
- Maximum thrust applied in the remaining engine
- Minimum climb gradient: 2.4% (2 engines aircraft)
- Takeoff flaps applied
- Landing gear retracted
- 1.2 Stall speed at the configuration
- No ground effects
- Maximum Takeoff Weight
- Standard atmospheric conditions
- Sea level airport

The following equations, derived from Roskam's [24] and Torembeek's [23] methodologies, are used:

$$ToW_{req} = 2 \cdot \left(\frac{CD}{CL} + \sin(0.024) \right) \quad (11)$$

$$CD = CD_{wing} + CD_0 + CD_{ubridge} + CD_{rudder} + CD_{flap} + CD_{windmill} \quad (12)$$

$$CL = \frac{CL_{MAXTO}}{1.44} \quad (13)$$

Where:

- CD_{wing} is the total wing drag coefficient, obtained from the ANN described in session 3.1.2
- CD_0 is the zero lift drag coefficient [24]
- $CD_{ubridge}$ is the zero lift drag increase due to wing-fuselage interference [24]
- CD_{rudder} is drag increase due to rudder deflection [24]
- CD_{flap} is drag increase due to takeoff flap extended [24]
- $CD_{windmill}$ is the drag increase due to wind milling of the failed engine [23]

If the ratio of $T/MTOW$ is less than ToW_{req} , the aircraft design under evaluation is not selected.

Landing climb

The climb capability is verified according to FAR25.119 requirements applied to the go-around maneuver in the final approach phase, considering the so-called "Landing Climb configuration" as follows:

- All engines operating
- Maximum thrust applied in all engines
- Minimum climb gradient: 3.2%
- Landing flaps applied
- Landing gear extended
- 1.3 Stall speed at the configuration
- No ground effects
- Maximum Landing Weight
- Standard atmospheric conditions

- Sea level airport

The following equations, derived from Roskam's [24] methodology, are used:

$$ToW_{req} = \left(\frac{CD}{CL} + \sin(0.032) \right) \quad (14)$$

$$CD = CD_{wing} + CD_0 + CD_{0ubridge} + CD_{flap} + CD_{gear} \quad (15)$$

$$CL = \frac{CL_{MAX\ LD}}{1.69} \quad (16)$$

Where:

- CD_{wing} is the total wing drag coefficient, obtained from the ANN described in session 3.1.2
 CD_0 is the zero lift drag coefficient [24]
 $CD_{0ubridge}$ is the zero lift drag increase due to wing-fuselage interference [24]
 CD_{flap} is drag increase due to takeoff flap extended [24]
 CD_{gear} is drag increase due to landing gear extended [24]

If the ratio of $T/MTOW$ is less than ToW_{req} , the aircraft design under evaluation is not selected.

Approach climb

The climb capability is verified according to FAR25.121 requirements applied to the go-around maneuver in the final approach phase, considering the so-called "Approach Climb configuration" as follows:

- One Engine operating
- Maximum thrust applied in the remaining engine
- Minimum climb gradient: 2.1%
- Approach flaps applied
- Landing gear retracted
- 1.65 Stall speed at the configuration
- No ground effects
- Maximum Landing Weight

- Standard atmospheric conditions

The following equations, derived from Roskam's [24] and Torembeek's [23] methodologies, are used:

$$ToW_{req} = 2 \cdot \left(\frac{CD}{CL} + \sin(0.021) \right) \quad (17)$$

$$CD = CD_{wing} + CD_0 + CD_{ubridge} + CD_{rudder} + CD_{flap} + CD_{windmill} \quad (18)$$

$$CL = \frac{0.6 + CL_{MAX}}{2,72} \quad (19)$$

Where:

- CD_{wing} is the total wing drag coefficient, obtained from the ANN described in session 3.1.2
- CD_0 is the zero lift drag coefficient [24]
- $CD_{ubridge}$ is the zero lift drag increase due to wing-fuselage interference [24]
- CD_{rudder} is drag increase due to rudder deflection [24]
- CD_{flap} is drag increase due to the approach flap extended [24]
- $CD_{windmill}$ is the drag increase due to wind milling of the failed engine [23]

If the ratio of $T/MTOW$ is less than ToW_{req} , the aircraft design under evaluation is not selected.

Residual rate of climb

A minimum residual rate of climb of 300ft/s (1,524 m/s) is verified at maximum certified ceiling altitude, considering the best climb speed, weight at takeoff climb equivalent to 95% MTOW and maximum thrust at this altitude at standard atmosphere. The following equations are used:

$$ToW_{req} = 0,95 \cdot \left(\frac{1,524}{V_{best\ ROC}} + \frac{1}{L/D_{best\ ROC}} \right) \quad (20)$$

$$V_{best\ ROC} = \sqrt{\frac{2}{\rho \sqrt{CD_0 \cdot \pi \cdot wS \cdot e}} \cdot \frac{0.95 \cdot MTOW}{wS}} \quad (21)$$

$$\frac{1}{L/D_{best\ ROC}} = \sqrt{\frac{\pi \cdot w \cdot S \cdot e}{CD_0}} \quad (22)$$

Where the zero lift drag (CD_0) and Oswald Factor (e) of the airplane are estimated via Class-I formulas according to Torembeek's methodology [23].

If the ratio of $T/MTOW$ is less than ToW_{req} , the aircraft design under evaluation is not selected. In this case, the cruise thrust (T) is evaluated at maximum certified ceiling via propulsion model as described in Session 3.1.3, considering cruise speed equal to $V_{best\ ROC}$.

Maximum cruise speed

In this check, it is verified if the aircraft is capable of maintaining the Maximum Operational Mach (MMO) at the cruise altitude equal to the certified ceiling, standard atmosphere and associated weight at top of climb (W_{TOC}) considering taking off with MTOW. The following formulas are applied:

$$ToW_{req} = \left(\frac{CD}{CL} \right) \quad (23)$$

$$CD = CD_{wing} + CD_0 + CD_{0_ubridge} \quad (24)$$

$$CL = \frac{2 \cdot W_{TOC}}{\rho_0 \cdot a_0 \cdot \delta \cdot MMO^2} \quad (25)$$

Where:

CD_{wing} is the total wing drag coefficient, obtained from the ANN described in session 3.1.2

CD_0 is the zero lift drag coefficient [24]

$CD_{0_ubridge}$ is the zero lift drag increase due to wing-fuselage interference [24]

If the ratio of T/M_{TOC} is less than ToW_{req} , the aircraft design under evaluation is not selected. In this case, W_{TOC} is calculated via mission performance module (described in session 3.2.1) and the cruise thrust (T) is evaluated at maximum certified ceiling via propulsion model as described in Session 3.1.3, considering the cruise speed associated with MMO .

Drag divergence

In this check, the wave drag behavior is checked when the aircraft accelerates through a range of speeds toward the MMO. This would ensure smooth increase on drag rise along a selected speed range and therefore a minor impact on fuel consumption when flying at higher speeds. The test condition consists of the drag computation at Mach 0.7 and MMO, cruise altitude equal to the certified ceiling, standard atmosphere and weight at top of climb (W_{TOC}) considering taking off with MTOW. In this scenario, the drag rise at these two speeds should not exceed 2.5%. The following equation is therefore applicable:

$$\Delta D_{div} = \frac{CD_{MMO} - CD_{Mach\ 0.70}}{CD_{Mach\ 0.70}} \cdot 100 \quad (26)$$

The CD computation follows the same methodology applied to Maximum Cruise Speed check (Eq.23). If ΔD_{div} is more than 2.5%, the aircraft design under evaluation is not selected.

3.2 Network framework

As shown in Fig. 3.1, once the aircraft geometry is defined, the calculation flow is transferred to the Network Framework module, which is responsible for calculating the optimum airline network associated with such design and the necessary outputs used in the optimization process. Three calculation sub-modules are executed in the following sequence:

I) Network Optimization:

In this sub-submodule, the optimum airline network is determined considering selected airports in a given area of operations and is associated with the aircraft under analysis. In this process, a Linear Programming Model (*LPM*) is executed in a local optimization routine in order to determine the frequencies between the involved city pairs. A gravitational passenger demand model is used to estimate the daily passengers flow between the city pairs, based on the city/airports information extracted from the Airport and Econometrics Database (*AED*) and network fixed parameters.

II) Mission Performance:

Once the frequencies between city pairs are determined, this sub-module is responsible for computing the trip time, fuel burned and direct operational cost (*DOC*) for each route connection,

considering the aircraft under analysis at a given load factor. In this process, a realistic vertical flight path profile is simulated, considering the selection of optimum speeds and optimum altitudes along the flight path. All certification performance limitations at origin and destination airports, as well as payload-range envelope constraints, are considered to determine the takeoff weight in all computations.

III) Network Economics:

In this last sub-module, the outputs necessary to feed the optimization process are computed, considering the data generated in the other sub-modules. In this process, aggregated network key performance indicators, envisioning the airline's objective functions side, are determined. They are: Estimated Total Number of Aircraft, Network Total Direct Operational Costs (*NDOC*) and Total Network Profit (*NP*). In addition, in this sub-module, the Net Present Value (*NPV*) of the aircraft design and production cashflow is also calculated, envisioning the aircraft manufacturer's objective function side.

The calculation methodologies employed in each of these three sub-modules are described below:

3.2.1 Network optimization

The optimization algorithm in this sub-module is derived from the Linear Programming Model (*LPM*) proposed by Jaillet et al. [103] for generic network determination considering passengers fractional flow. A *MATLAB*® code was developed to set up and solve this problem using the LPM solver available for this application. The mathematical formulation of the problem is presented in the next paragraphs.

Let X_{iltj} be the fraction of the passenger's demand flow f_{ij} from origin i to destination j , served by a two-stop connecting flight through cities l and t , Y_{ijk} the number of aircraft type k used in the route from city i to j , p the average fare per passenger, c_k the average operational cost (\$/nm) at design range, b_k the passenger capacity of aircraft k , the reference load factor $LFref$ and d_{ij} the distance between origin and destination airports.

The following integer linear programming model is proposed:

$$\text{Maximize } \sum_{i \neq j} \sum_k k_1 \cdot p - k_2 \cdot \frac{(c_k \cdot d_{ij})}{LFref * b_k} \quad (27)$$

subject to:

$$f_{ij} + \sum_{t \neq i,j} (f_{it} \cdot X_{ijt} + f_{tj} \cdot X_{tij} - f_{ij} \cdot X_{itj}) + \sum_{i,t \neq i,j} (f_{ij} \cdot X_{ltij} + f_{it} \cdot X_{ijlt} - f_{ij} \cdot X_{iltj}) \leq \sum_k L \text{Fref} \cdot b_k \cdot Y_{ijk} \quad (28)$$

$$\sum_{t \neq i,j} X_{ijt} + \sum_{l,t \neq i,j} X_{iltj} \leq 1 \quad (29)$$

, for all $i \neq j$

Where X_{ijt} , X_{iltj} are positive and Y_{ijk} integer positive for all $i \neq j$

The average operational costs (C_k) for each aircraft fleet, necessary for the optimization, correspond to the Direct Operational Cost (DOC) related to the design range of each aircraft under analysis (explained in item 3.2.2). The objective function (27) is set to maximize the network profit, based on the difference between the average fare (p) and the average cost per passenger. Constraint (28) states that the fractional flow on route ij cannot exceed the total capacity of the aircraft assigned, while constraint (29) ensures that the passenger flow from a direct flight from i to j is non-negative.

In this research, it is assumed that 50% of all passenger demand from i to j are derived from direct flights (X_{ij} and X_{ji}), 30% distributed equally among all one-stop flights (X_{ijt} , X_{tij} and X_{itj}) and 20% distributed equally among two-stop flights (X_{ltij} , X_{ijlt} and X_{iltj}), as shown in Fig. 3.19. Passengers demand between origin and destination (f_{ij}) is estimated via gravitational model, based on city pair distance and econometric parameters, as proposed by Wojan [15]. Let P be the city pair population product ($P = P_i P_j$), C the city pair airport catchment area product ($C = C_i \cdot C_j$), B the city pair combined Buying Power Index ($B = B_i + B_j$), G the city pair GDP product ($G = GDP_i \cdot GDP_j$) and d_{ij} the reference distance of the city pair. The following passenger demand model is proposed as follows:

$$f_{ij} = K_0 \cdot P^{K1} \cdot C^{K2} \cdot B^{K3} \cdot G^{K4} \cdot d_{ij}^{-K5} \quad (30a)$$

Or in log-linear format:

$$\ln(f_{ij}) = \ln(K_0) + K1 \cdot \ln(P) + K2 \cdot \ln(C) + K3 \cdot \ln(B) + K4 \cdot \ln(G) + K5 \cdot \ln(d_{ij}) \quad (30b)$$

In Equation 30, the exponents $K0, K1, K2, K3, K4$ and $K5$ are calibration constants, determined by log-linear regression. They may be easily calculated using the public econometric data available (P_i, C_i, B_i and GDP_i often published by economic agencies).

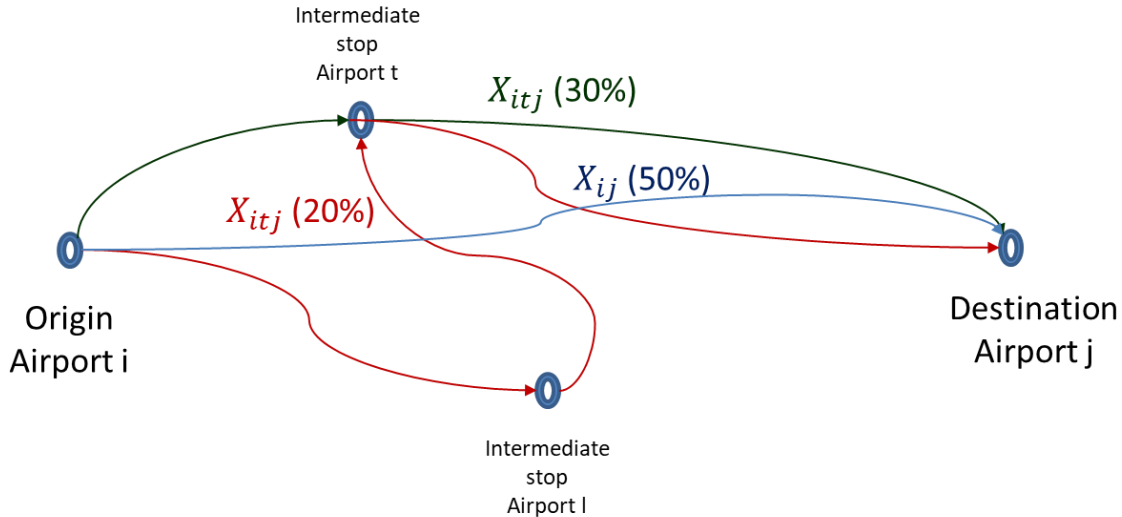


Figure 3.19: Two stop demand model and adopted shares

Route distances d_{ij} and average magnetic headings HDG_{ij} between city pairs are determined via haversine formulae proposed by Robusto [185] for loxodromic routes. The following equations are applicable:

$$a = \sin^2\left(\frac{LAT_j - LAT_i}{2}\right) + \cos(LON_i) \cdot \cos(LON_j) \cdot \sin^2\left(\frac{LON_j - LON_i}{2}\right) \quad (31)$$

$$c = 2 \cdot \arctan\left(\sqrt{\frac{a}{1-a}}\right) \quad (32)$$

$$d_{ij} = 1,03 \cdot R \cdot c \quad (33)$$

$$\Psi_{ij} = \arctan\left(\frac{\sin(LON_j - LON_i) \cdot \cos(LAT_j)}{\cos(LAT_j) \cdot \sin(LON_j) - \sin(LON_i) \cdot \cos(LAT_j) \cdot \cos(LON_j - LON_i)}\right) \cdot \frac{180}{\pi} + \frac{DMG_i + DMG_j}{2} \quad (34)$$

Where R is earth's average radius (assumed as 6.367 km or 3.438 nm)

It is worth mentioning that Eq.33 is computed differently than original great circle distance computation [185], since it has embedded a multiplication factor of 1.03 (3% bias) in order to adjust the computed value to airway-route differences.

Network parameters

In the complex network theory [186] the indicators reflecting the statistical features of network structure may be used as key performance parameters of airline networks. In recent studies, Bing [32] proposes six basic indicators to analyze topological structures of airline networks in China. In this research it is proposed to use Bing's methodology to evaluate the optimum network generated in each calculation. The network indicators computation is performed inside the Network Optimization routine. Considering an airline network defined as a number of connections (so called arcs) between a number of airports (so called nodes), the network indicators are defined and computed as follows:

- *Number of nodes (N)*

Corresponds to the total number of airports served in the network.

- *Average path length (L)*

Corresponds the average route distance (d_{ij}) of all arcs in the network, which is a property of the transport shortcut in the integral network. The shorter the average path length is, the less transit times are required between any two airports, bringing more convenience for the passengers.

- *Degree of nodes (DON)*

Corresponds to the number of airports j (for $j \neq i$) having direct flights with an airport i . In an aviation network, it refers to the number of airports having direct flights with an airport. A greater degree of a node means greater importance of airport i in the network.

- *Average degree of nodes (ADON)*

Average value of all airport's degrees of nodes.

- *Network density (ND)*

Corresponds to the ratio of actual arcs numbers to the maximum possible arcs in a network. In an aviation network, it describes the ratio of actual number of opened segments to the number of all possible segments. The density indicates the closeness of the air connections among all cities in the network.

- *Clustering index (C_i)*

Corresponds to the ratio of the actual arcs to the maximum possible arcs between an airport i and its adjacent airports. In an aviation network, the clustering coefficient of a node indicates the average cluster degree of the local network comprised of the airport and its adjacent airports. Higher clustering coefficient means greater cluster degree of the local network, and smaller impact of this node on the adjacent airports; on the contrary, lower value means more dependence of the adjacent airports on this node.

- *Average clustering (AC_i)*

Average value of all airport's clustering index.

According to Bing [32] the most important indicators that characterize the network topologic structure are the Average Path Length (which corresponds the air transport depth) and the Average Clustering Index (which corresponds the air transport width). They shall be analyzed together to determine the airline network performance. For example, the combination of a small average path length with big clustering coefficient means a better route capillarity between closer airports and therefore a stronger fault tolerance capability (or resilience).

3.2.2 Mission performance

This sub-module is the most important part of the Network Framework since it is where all calculations necessary to determine trip fuel (W_f) and trip time (TT) are performed. These variables are essential to compute direct operational cost (DOC) for each route determined by the network optimization module. Inputs from the Aerodynamics (CD) and Propulsion (net thrust - T and fuel flow - FF) sub-modules are necessary for solving the mass point equations at time integration steps, for given performance state (weight and environmental conditions at a given altitude) and operational flight profile constraints (i.e. 250kt airspeed restriction below 10,000ft pressure altitude).

According to Lewis [164], the vertical flight of any flight vehicle path may be constructed integrating the point-mass equations of motion regarding the variables V (true airspeed), γ (flight path angle) and H_p . The following system of differential equations are applicable:

$$T - D = W \cdot \sin(\gamma) + \frac{W}{g} \dot{V} \quad (35)$$

$$L + \frac{W}{g} \dot{\gamma} = W \cdot \cos(\gamma) \quad (36)$$

$$\dot{H}p = V \cdot \sin(\gamma) \quad (37)$$

Where the local net thrust (T) is computed at the propulsion submodule and aircraft's total drag (D) is derived from the CD computed at the aerodynamics sub-module. As previously mentioned, they are functions of pressure altitude (H_p), true airspeed (V) and atmospheric conditions, at a certain time t .

These equations may be linearized and simplified drastically if steady state ($\dot{V}=0$) and small flight path angles (where $\cos(\gamma) \sim 1$ and $\sin(\gamma) \sim \tan(\gamma) \sim \gamma$) are considered along all flight path.

In fact, a Boeing study [187] shows that in most of the commercial jet transport operations, the flight path angle is always less than 5° where these assumptions may be applied. Taking this into consideration, Eq. 33, Eq.34 and Eq. 35 may be collapsed into a single-direct formula for γ as follows:

$$\gamma = \left(\frac{\frac{T}{W} - \frac{C_D}{C_L}}{(1 + f_{ac})} \right) \quad (38)$$

Where

$$C_L = \frac{2 \cdot W}{\rho S V^2} \quad (39)$$

f_{ac} is the so-called acceleration factor, which the same Boeing study [187] recommends being computed as:

$$f_{ac} = \begin{cases} -0.1332M^2 \left(\frac{283.15 - \beta.Hp}{283.15 - \beta.Hp + \Delta ISA} \right) & , \text{for constant } M \text{ below tropopause} \\ 0 & , \text{for constant } M \text{ above tropopause} \\ 0.7M^2 \left(\phi - 0.1902 \frac{283.15 - \beta.Hp}{283.15 - \beta.Hp + \Delta ISA} \right) & , \text{for constant CAS below tropopause} \\ 0.7M^2\phi & , \text{for constant CAS above tropopause} \end{cases}$$

(40)

with

$$\phi = \frac{[(1+0.2M^2)^{3.5}-1]}{0.7M^2(1+0.2M^2)^{2.5}} \quad (41)$$

In this format, the true airspeed (V) is assumed to be known along all the profile, because of the operational speed schedule (explained in next paragraphs). The total distance and pressure altitude computed along the flight at a certain time t may be computed through the following equations :

$$S(t) = \int_0^t V \cdot dt \quad (42)$$

$$H\mathbf{p}(t) = \int_0^t V \cdot \gamma \cdot dt \quad (43)$$

The lateral flight path is assumed to be a straight loxodromic route between the origin and destination airports, where an average magnetic heading is maintained, and is calculated according to Eq. 33. The total trip time TT is obtained when S is equal to the total route distance, computed via Eq. 32. In addition, the total fuel consumption (W_f) is calculated as the resulting integration of the fuel flow (also obtained from the propulsion sub-module) along all flight path according to:

$$W_f = \int_0^{TT} FF \cdot dt \quad (44)$$

Environmental conditions (pressure, density and temperature) at each integration point, which steps are evaluated every one second along the trajectory, are calculated as per the International Standard Atmosphere isentropic model [188]. Zero wind, standard atmospheric pressure and 10°C ISA deviation from standard temperature are assumed in this study. Tropopause lower pressure altitude limit is assumed fixed at 11km pressure altitude. The mission profile computation

considers a realistic jet transport airliner operational profile as shown in Fig. 3.20, according to the following segments:

- *Segment A (Climb to 10,000 ft)*

From pressure altitude of 1,500 ft above the elevation of the most used runway for takeoff, the aircraft climbs maintaining maximum climb thrust and constant calibrated airspeed of 250 knots (respecting Air Traffic Control speed restriction rules [189]) until a pressure altitude of 10000 ft. Fuel and time quantity allowances, as shown in Table 3.5, are added to computations representing the aircraft maneuvering necessary for takeoff run, lift off and gear/flap configuration changes.

- *Segment B (Climb with constant CAS)*

At 10,000 ft pressure altitude, the aircraft then accelerates in a levelled segment to a calibrated airspeed of 280 knots and then climbs at maximum thrust maintaining this speed until the Mach-Crossover Altitude or Cruise Altitude, whichever is lower. The Mach-Crossover Altitude is the pressure altitude where the number of Mach reaches the prescribed climb cruise Mach number.

- *Segment C (Climb with constant Mach to cruise altitude)*

From the Mach-Crossover Altitude, the aircraft climbs at maximum thrust with constant number of Mach (calculated cruise Mach number) to the selected cruise altitude.

- *Segment D (Cruise at optimum altitude and mach number)*

The cruise altitude corresponds to the optimum cruise altitude adjusted to the suitable flight level as per the Reduced Vertical Separation Minima (RVSM) air traffic rules [190]. To select the correct flight level, the average magnetic course between origin and destination airports is considered. The optimum cruise altitude is calculated as the minimum of: maximum certified ceiling (fixed as 41,000 ft in this study), maximum specific range altitude (considering the selected cruise speed and takeoff weight), maximum altitude where the residual rate of climb is 300 ft/min, and the maximum altitude where 1.3 g buffet margin is achieved. The latest considers stall at 40° bank angle in clean configuration and is calculated according to [187]:

$$\delta_{max} = \left(\frac{W}{wS} \right) \frac{2}{CL_{MAX} \cdot \cos(\varphi) a_0^2 M^2} \quad (45)$$

$$H_{max, Buffet} = \begin{cases} 44330(1 - \delta_{max}^{0.1903}) & , \text{ below tropopause} \\ 11000 + 153.8462 \Delta ISA - 6341.5800 \ln(4.4771 \delta_{max}) & , \text{ above the tropopause} \end{cases} \quad (46)$$

The cruise segment is performed at constant number of Mach that is derived from the maximum value for the $M \cdot L/D$ ratio.

- *Segment E (Descent with constant Mach to Mach-Crossover Altitude)*

From top of descent, the aircraft descents at idle thrust with cruise Mach number to the Mach-Crossover Altitude, where a calibrated airspeed of 310kt is reached.

- *Segment F (Descent with constant CAS to 10,000 ft)*

From the Mach-Crossover Altitude, a constant calibrated airspeed of 310 kt is maintained in the descent flight at idle thrust to 10,000 ft pressure altitude where the airplane is decelerated in leveled flight to a calibrated airspeed of 250 kt.

- *Segment G (Descent to 1500 ft)*

From 10,000 ft pressure altitude, constant calibrated airspeed of 250 kt is maintained in the descent flight at idle thrust to 1500 ft pressure altitude above the landing runway elevation where the airplane initiates the approach and landing phase. Fuel and time allowances, as shown in Table 3.5, are added to computations representing the aircraft maneuvering necessary for approach, gear/flap configuration changes and landing.

The total fuel on board (*FOB*) is determined considering the minimum fuel required to comply with Brazilian regulations (RBAC 121.645 [191]) for jet transport aircraft, representing the sum of the following quantities:

- Fuel necessary to fly from origin to destination airport (W_f) considering the operational profile described before.
- The fuel required to fly from destination to alternate (or diversion) airport considering the given operational profile. In this study, the alternate airport is chosen as the closest airport from the destination airport in the network, considering that all airports in the company network have the capacity available and handling infrastructure to absorb the demand (W_f Alternate).
- Fuel burn related to 10% of the trip time determined in (I) to be used as contingency for route deviations and adverse weather conditions (W_f Contingency).
- Consideration of 30-min holding at 1500 ft height over the alternate airport elevation at suitable holding speed. In this study, the holding speed is selected as the maximum L/D speed or 1.3g margin to stall speed (ensuring a protection of 44° maximum bank angle to stall) in clean configuration, whichever is higher, considering weight estimated at the alternate airport.

Considering the statements above, the Eqs.47 to 51 are used in the mission performance calculation algorithm with the objective to determine trip fuel (W_f). They consider all elements necessary to determine the Takeoff Weight (TOW) and Landing Weight (LW) at each sector [192]:

$$TOW = OEW + FOB + PAYLOAD \quad (47)$$

$$TOF = W_f + W_{f\text{Alternate}} + W_{f\text{Contingency}} + W_{f\text{Holding}} \quad (48)$$

$$FOB = TOF + Wf_{taxi} \quad (49)$$

$$PAYLOAD = b.PAXWT.LF_{ref} + CARGO \quad (50)$$

$$LW = TOW - Wf - Wf_{app} \quad (51)$$

In addition, payload-range diagram related limitations shall be respected when considering mission performance calculations [192]. Equations 52 to 55 show the Takeoff Weight (TOW)

constraint equations related to Maximum Takeoff Weight ($MTOW$), Maximum Zero Fuel Weight ($MZFW$), Maximum Landing Weight (MLW) and Maximum Fuel Capacity ($MAXFUEL$) [192]:

$$TOW < MTOW \quad (52)$$

$$TOW < MZFW + FOB \quad (53)$$

$$TOW < MLW + Wf \quad (54)$$

$$FOB < MAXFUEL \quad (55)$$

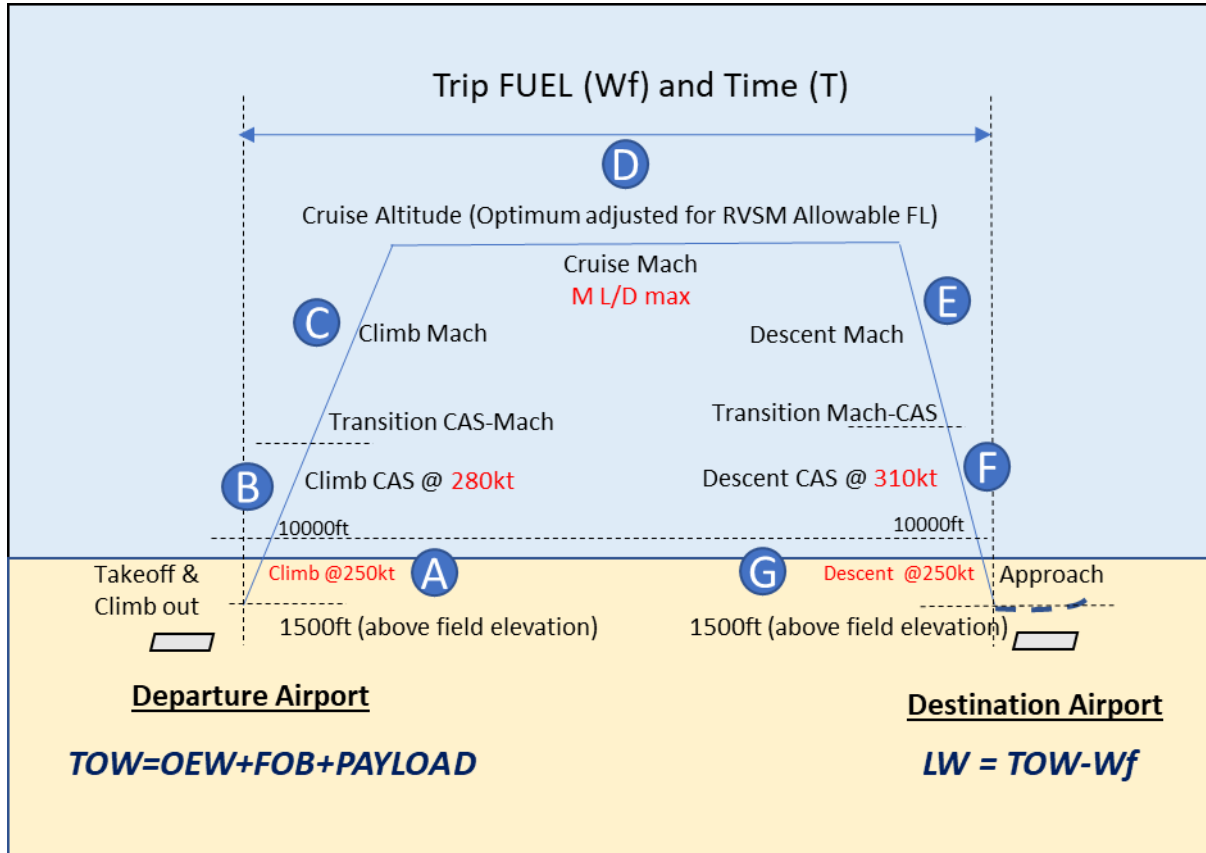


Figure 3.20: Mission Profile

Mission performance computations

Initially, a trip fuel (W_f) and time (TT) determination routine (or Flight Profile Computation) is elaborated considering that aircraft departs with a certain takeoff weight (TOW) at the origin airport and accomplishes the complete flight profile with climb, cruise and descent flight phases. The sum of associated phase distances shall be equal to the total route distance.

Since the calculation starts after the takeoff roll, climb distance to the selected cruise altitude is directly determined through Eq. 40. However, an interactive algorithm is necessary to be applied in order to determine the length of cruise and descent segments, as shown in Fig. 3.21.

The algorithm starts computing the top of descent over the destination airport, computing all cruise phase up to there. Then the descent distance is determined from this point and subtracted from the cruise phase, determining a new top of descent. A new computation cycle is then computed from this point and determining a new descent distance. The process is repeated until the difference between the descent points on subsequent runs is less than 0.5 nm.

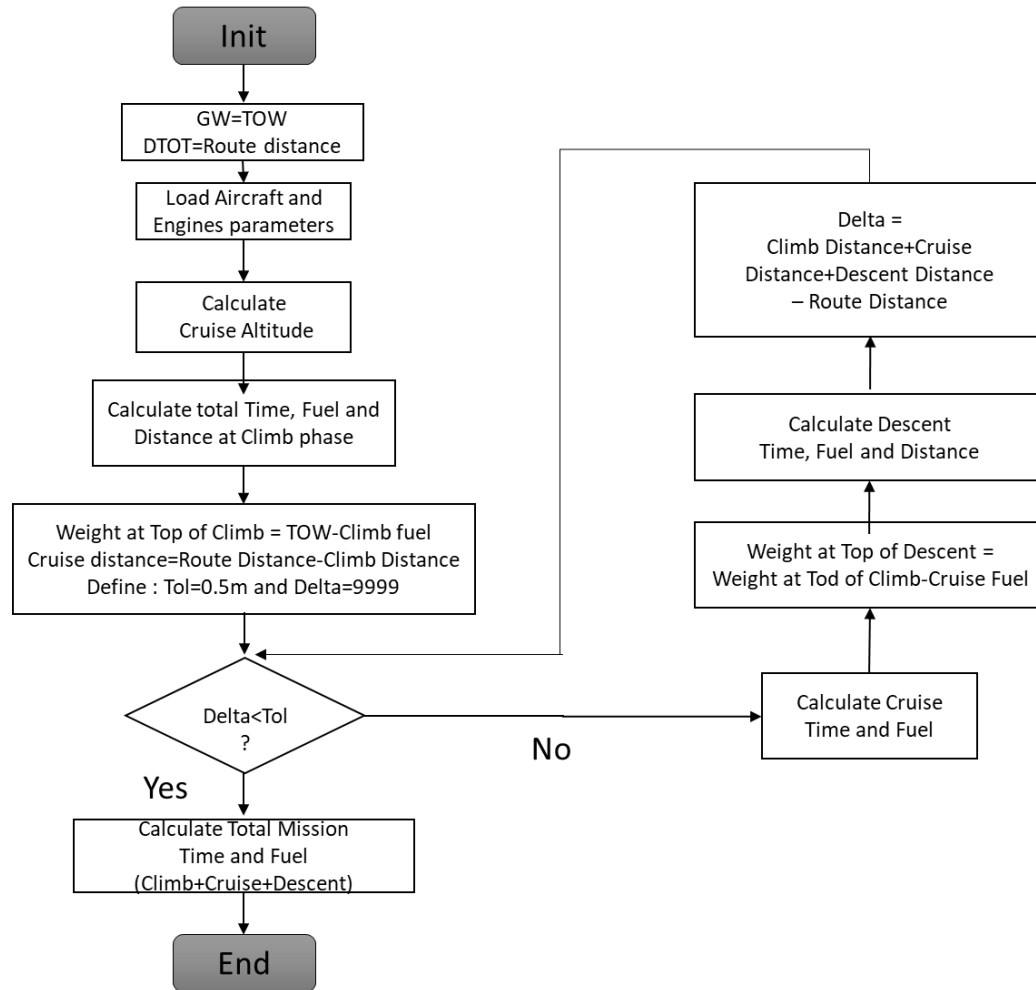


Figure 3.21: Flight profile workflow for calculation of trip fuel and time

The core of the mission calculation is also an interactive process in which the TOW is calculated via Flight Profile computation routine explained above. The process starts with an initial guess of

TOW correspondent to a ZFW and fuel on board (*FOB*) equal to the maximum fuel capacity (*MAXFUEL*). In each cycle, the FOB is reduced with the objective to respect the MZFW, MTOW and MLW limitations, related to the payload range envelope, as shown in Fig.3.22.

The TOW is also checked against the performance requirements for takeoff according to Session 3.15 (balanced field length and second segment climb). In this case, the current origin airport elevation and reference temperature are considered in computations. The MTOW is reduced accordingly in case any of these limitations are met.

The LW is checked against the performance requirements for landing according to Session 3.15 (landing field length, approach climb and landing climb). In this case, the current destination airport elevation and reference temperature are considered in the computations. The MLW is reduced accordingly in case any of these limitations are met. In all computations, the ZFW is a fixed part of the TOW and computed as the weight of a fraction of the maximum passenger capacity (average load factor) of the aircraft, as follows:

$$\text{PAYLOAD} = N_{pax} \cdot LF_{avg} \cdot PAXWT \quad (56)$$

It is worth mentioning that alternate fuel ($Wf_{\text{alternate}}$), necessary to compute the FOB, is computed considering the TOW as estimated landing weight minus a go-around fuel allowance at the destination airport.

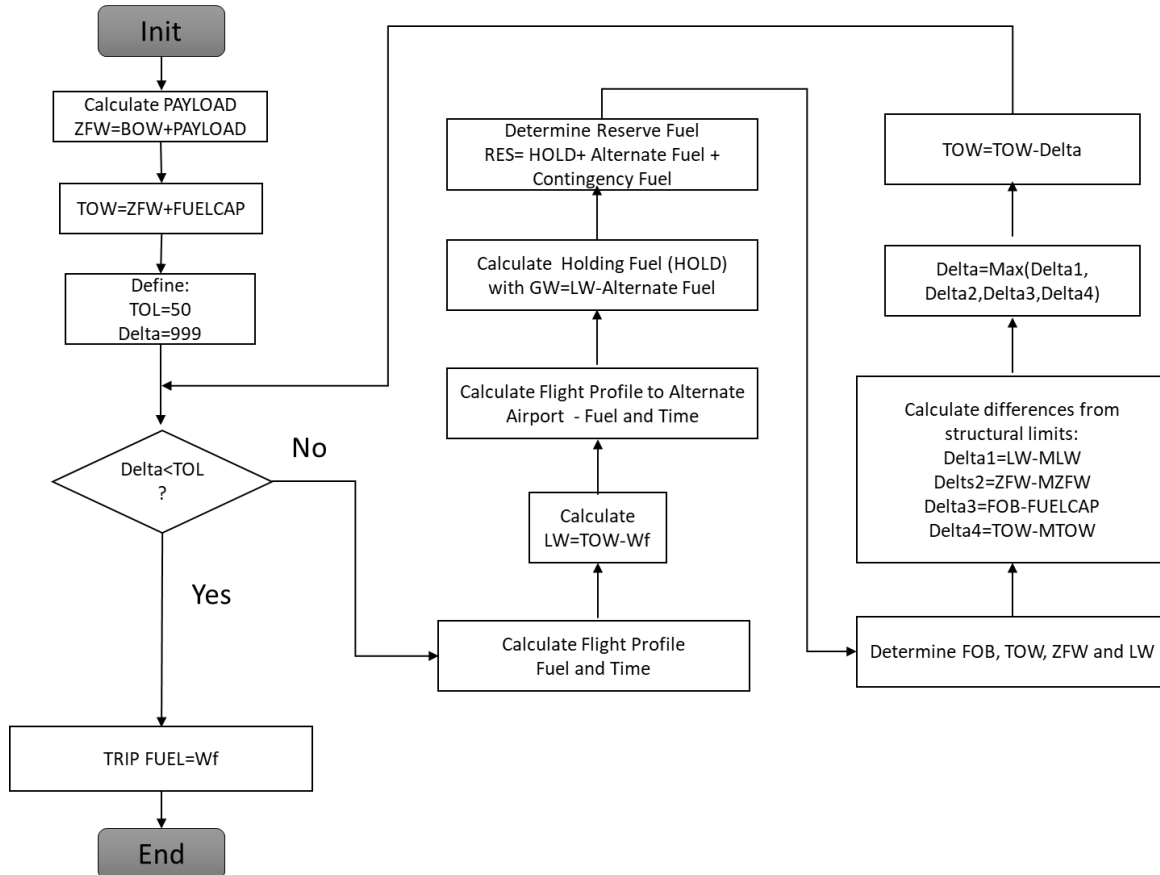


Figure 3.22: Complete mission calculation algorithm

Direct operational cost

The single-sector Direct Operational Cost (*DOC*) is also computed in the Mission Performance module and provided as input to the Economics sub-module, used in the total network operational cost computations. The methodology proposed by Roskam [193] is used to calculate the cost components of the *DOC*. The method involves the application of empirical formulae to compute five types of cost components as follows:

$$\mathbf{DOC} = C_{\text{fl}} + C_{\text{main}} + C_{\text{depr}} + C_{\text{fee}} + C_{\text{fin}} \quad (57)$$

Where:

- C_{fl} are flight operations related costs considering fuel consumption, oil consumption, crew salaries (as function of block time) and insurance.

- C_{main} are maintenance related costs considering airframe labor, airframe materials, engine labor and engine materials.
- C_{depr} are capital depreciation related costs for airframe, engines and systems parts.
- C_{fee} are fees related costs considering navigation and airport charges.
- C_{fin} are finance related costs considering aircraft/engines acquisition and leasing.

Inputs for such computations are crew hourly salaries, block time ($BLKT$), block fuel ($BLKF$), Maximum Takeoff Weight ($MTOW$), Operational Empty Weight (OEW), engine weight (Eq.4) and engine time between overhaul ($eTBO$). Block time and fuel are computed considering the total flight cycle (flight and ground phases) as follows:

$$BLKT = TT + TIT + TOT \quad (58)$$

$$BLKF = W_f + FFref \cdot (TIT \cdot \frac{LW}{MTOW_{ref}} + TOT \cdot \frac{TOW}{MTOW_{ref}}) \quad (59)$$

Where:

- $FFref$ is the reference fuel flow value assigned as 5kg/min, corresponding to the Embraer 145LR's taxi fuel flow.
- $MTOW_{ref}$ is the reference MTOW value assigned as 22,000kg corresponding to the Embraer 145LR's MTOW.

The taxi fuel component in block fuel is modeled as a function of landing and takeoff weights, normalized to reference values of MTOW and fuel flow, specifically to the Embraer 145LR model. This aircraft is adopted as reference due to the availability of the fuel flow data in the aircraft operations manual [194].

Crew hourly salaries (captains, first-officers and flight attendants) are also estimated as function of MTOW, based on a linear regression applied on the annual salaries database constructed by the American Airline Pilots Central [195]. The data used in the regression considers several legacy airlines and seven models of narrow body aircraft operating in North America. The hourly salary is derived in the computations considering monthly schedule of 75 flight hours for each crew member. Table 3.14 shows the results of the linear regression obtained with reasonable values of Pearson's coefficients (all greater than 0.95).

Table 3.14: Hourly crew salaries for narrow body aircraft operating in North America [195]

| Captain Salary | | | First Officer Salary | | | Flight Attendant Salary | | |
|----------------|-----------|-----------------|----------------------|-----------|-----------------|-------------------------|-----------|---------------------|
| Aircraft MODEL | MTOW [kg] | Salary [US\$/h] | MODEL | MTOW [kg] | Salary [US\$/h] | MODEL | MTOW [kg] | Hourly Pay [US\$/h] |
| MD80 | 64,000 | 240.51 | MD80 | 64,000 | 162.95 | MD80 | 64,000 | \$ 97.77 |
| Airbus 320 | 77,000 | 270.55 | Airbus 320 | 77,000 | 190.93 | Airbus 320 | 77,000 | \$ 114.56 |
| Boeing 737-800 | 68,000 | 272.31 | Boeing 737-800 | 68,000 | 207.46 | Boeing 737-800 | 68,000 | \$ 124.48 |
| CRJ700 | 32,999 | 98.88 | CRJ700 | 32,999 | 59.03 | CRJ700 | 32,999 | \$ 35.42 |
| CRJ200 | 24,041 | 102.88 | CRJ200 | 24,041 | 70.01 | CRJ200 | 24,041 | \$ 42.01 |
| Embraer 195LR | 47,790 | 207.51 | Embraer 195LR | 47,790 | 140.48 | Embraer 195LR | 47,790 | \$ 84.29 |
| Embraer 175LR | 37,500 | 102.76 | Embraer 175LR | 37,500 | 57.11 | Embraer 175LR | 37,500 | \$ 34.26 |
| Embraer 145LR | 22,000 | 90.87 | Embraer 145LR | 22,000 | 48.17 | Embraer 145LR | 22,000 | \$ 28.90 |
| Intercept | -2.4825 | | Intercept | -21.3571 | | Intercept | -12.8143 | |
| Slope | 0.0038 | | Slope | 0.0030 | | Slope | 0.0018 | |
| R ² | 0.96 | | R ² | 0.95 | | R ² | 0.95 | |

Therefore, the crew hourly salaries are calculated as:

$$\text{CAPSAL} = -2.4825 + 0.0038 \text{ MTOW} \quad (60)$$

$$\text{FOSAL} = -21.3571 + 0.0030 \text{ MTOW} \quad (61)$$

$$\text{FASAL} = -12.8143 + 0.0018 \text{ MTOW} \quad (62)$$

3.2.3 Network economics

In this sub-module, the key outputs related to all air transport networks and all airplane fleets k evaluated (in case of more than one type of aircraft are considered) are aggregated. The computation of the total network profit (NP) and total network DOC (NDOC) are done as function of route frequencies (Y_{ijk}), departure and arrival delays (DD_i and AD_j), average inflight delay cost per minute (ID_k) of each aircraft k , sector distance (d_{ij}), aircraft passenger capacity (b_k) and average ticket price (p) as follows:

$$\text{NDOC} = \sum_{k=1}^a \sum_{i=1}^N \sum_{j=1}^N Y_{ijk} \cdot (\text{DOC}_{ijk} + ID_k * (DD_i + AD_j)) , \text{for } i \neq j \quad (63)$$

$$\text{NP} = k_1 \cdot \frac{p}{\sum_{k=1}^3 \sum_{i=1}^N \sum_{j=1}^N d_{ijk}} - k_2 \cdot \frac{\text{NDOC}}{\sum_{k=1}^3 \sum_{i=1}^N \sum_{j=1}^N b_k \cdot LF_{ref} \cdot Y_{ijk}}, \text{ for } i \neq j \quad (64)$$

In addition, the fleet size required in each aircraft type k may be estimated as function of sector block time ($TB_{i,j}$) and average daily utilization (DU) according to:

$$TB_{ijk} = T_{ijk} + TIT + TOT + DD_i + DD_j, \text{ for } i \neq j \quad (65)$$

$$Nacft_k = \text{int}\left(\frac{\sum_{i=1}^N \sum_{j=1}^N TB_{i,j,k}}{DU}\right), \text{ for } i \neq j \quad (66)$$

The average inflight delay cost per aircraft type ID_k is estimated according to the methodology proposed by a Eurocontrol study [196]. In this method, tactical arrival management delay costs are determined as function of aircraft types. Based on the known MTOW for existing aircraft, it is possible to determine, via linear regression, the delay cost as a function of the MTOW related to the aircraft under analysis. Table 3.15 shows the results of the linear regression obtained, with a reasonable value of Pearson's coefficient (0.731). According to the linear regression, the inflight-delay cost per minute related to aircraft k (ID_k) is calculated as:

$$ID_k = 0,0012 \cdot MTOW_k \quad (67)$$

Where $MTOW_k$ is the MTOW associated with the aircraft type k of the analysis.

Table 3.15: Inflight delay costs as function of MTOW

| Aircraft MODEL | MTOW [kg] | Delay cost 30 min basis [\$] [196] | Delay cost [\$/min] |
|-----------------------|-----------|------------------------------------|---------------------|
| Airbus 319 | 75,000 | 2,516 | 83.9 |
| Airbus 320 | 78,000 | 2,827 | 94.2 |
| Airbus 321 | 93,500 | 3,268 | 108.9 |
| Boeing 737-300 | 61,234 | 2,406 | 80.2 |
| Boeing 737-400 | 62,822 | 2,737 | 91.2 |
| Boeing 737-800 | 79,010 | 2,917 | 97.2 |
| Embraer 190LR | 47,790 | 1,885 | 62.8 |
| Intercept | | | 0.0000 |
| Slope | | | 0.0012 |
| R^2 | | | 0.731 |

NPV calculation

The Economics sub-module is also responsible for computing the Net Present Value (NPV) of the total cashflow related to the design and production of the aircraft under analysis.

In this study, the methodology proposed by Mattos et al. [197] is used to determine the cashflow for the aircraft under analysis on each optimization cycle. In financial analysis, NPV refers to sum of all cashflows is computed along each year of the lifecycle of the project, which accounts for the time value of money. This is a commonly used method for evaluating and comparing capital projects or financial products with cash flows spread over time, as in loans, investments, payouts from insurance contracts plus many other applications.

In this study the cashflow is defined as the difference between sales revenue and the development (non-recurring) and production (recurring costs) of the aircraft. For all aircraft designs produced in the optimization, it is considered that the first five years in the lifecycle are related to the program development phase (with no sales where non-recurrent costs are dominant), forwarded by eleven years of production phase (where sales revenues and recurrent costs are dominant). It is also assumed that the minimum acceptable rate of return (*MAR*) is 5% per year, which may be interpreted as the minimum interest rate which the capital could be potentially applied in another financial investment. The following formulae is used to determine the total NPV:

$$NPV(t) = \sum_{t=1}^{16} \frac{FC_t}{(1+MAR)^t} \left\{ \begin{array}{l} t = \text{time (years or months)} \\ n = \text{project time} \\ MAR = \text{minimum acceptable rate of return} \\ FC_t = \text{Cash flow at period } t \end{array} \right. \quad (68)$$

$$NPV = \sum_{t=1}^{15} NPV(t) \quad (69)$$

The internal rate of return (*IRR*) of the project is also calculated. Its value is determined by equaling Eq.64 to zero and solving for MAR for which such condition is satisfied, according to the following equation:

$$0 = \sum_{t=1}^n \frac{FC_t}{(1+IRR)^t} \quad (70)$$

The higher a project's internal rate of return, the more desirable it is to undertake. IRR is uniform for investments of varying types and, as such, IRR can be used to rank multiple prospective projects on a relatively even basis. Assuming the costs of investment are equal among the various projects, the project with the highest IRR would probably be considered the best and be undertaken first.

The project is considered feasible in the event IRR is at least 30%, also representing a constraint of the optimization. In addition, the breakeven point (*BE*) of the project (in terms of number of years), where the accumulated NPV is zero, is also calculated and provided as output. The design is only considered if the BE is less than the middle of the life cycle (seven and a half years).

With the objective to determine the cashflow in each period *t*, it is necessary to calculate the non-recurring costs, production costs and sales revenue. These costs are modeled as function of Maximum Takeoff Weight (*MTOW*), wing area (*wS*), number of engines (*n_e*), maximum engine thrust (*MAXRATE*), fan diameter (*eDiam*) and number of passengers (*NPax*). It is worth mentioning that this method considers the design and production costs model applied to a 50-seat regional jet as baseline (Embraer ERJ145LR model). Therefore, in order to adjust the analysis, it is assumed that most of all recurring and non-recurring costs are proportional to the aircraft size. Considering this premise, the baseline related costs are adjusted proportionally to the ratio $MTOW/MTOW_{\text{baseline}}$ ($MTOW_{\text{baseline}} = 22,000\text{kg}$) with the objective to estimate the actual costs of the aircraft under analysis. Exemptions are made to administrative costs (which remain the same as in the ERJ145 program) and engine related costs (which are proportional to the maximum engine thrust of the aircraft under analysis).

In this study, the sales revenue considers the number of aircraft delivered per year proportional to the market forecast for regional airlines in South America [198]. For this it is considered the manufacturer's market share (*MMS*) as 60%. It is also assumed that the aircraft sales price is dependent on the market share and a discount of a certain percentage of the list price to airlines is always applied, as common practice among manufacturers [199]. Usually, the level of discount offered is a linear function of manufacturer's market share in such way that the largest is the market share, the largest is the discount. In this study, the final sales price (*SP*) of the aircraft produced in each computation cycle is determined as linear function of *MTOW* and a certain discount rate (*DESC*) according to the following equations:

$$SP = (1 - DESC) \cdot (3.3383 + 0.0013 \cdot MTOW) \quad (71)$$

$$DESC = 0.5 \cdot \frac{MMS}{100} \quad (72)$$

It is worth mentioning that Eq.71 coefficients are derived from a linear regression based on the Airbus narrow bodies price list, published in June 2018 [200]. It is also noticeable from Eq. 72 that, for the selected market share (60%), the discount rate applied in all aircraft will be 30%.

After the development and production cost structures alongside the size of market for the airplane under analysis are established, the NPV, IRR and Breakeven point for the analysis aircraft may be calculated. An example of application of such methodology is shown in Fig. 3.23, where the resulting NPV analysis for a 120-seater design along a fifteen-year aircraft program. In this case, 675 deliveries are demanded, 37.1% IRR, 4.5 years breakeven and 5.4 Billion US\$ are obtained.

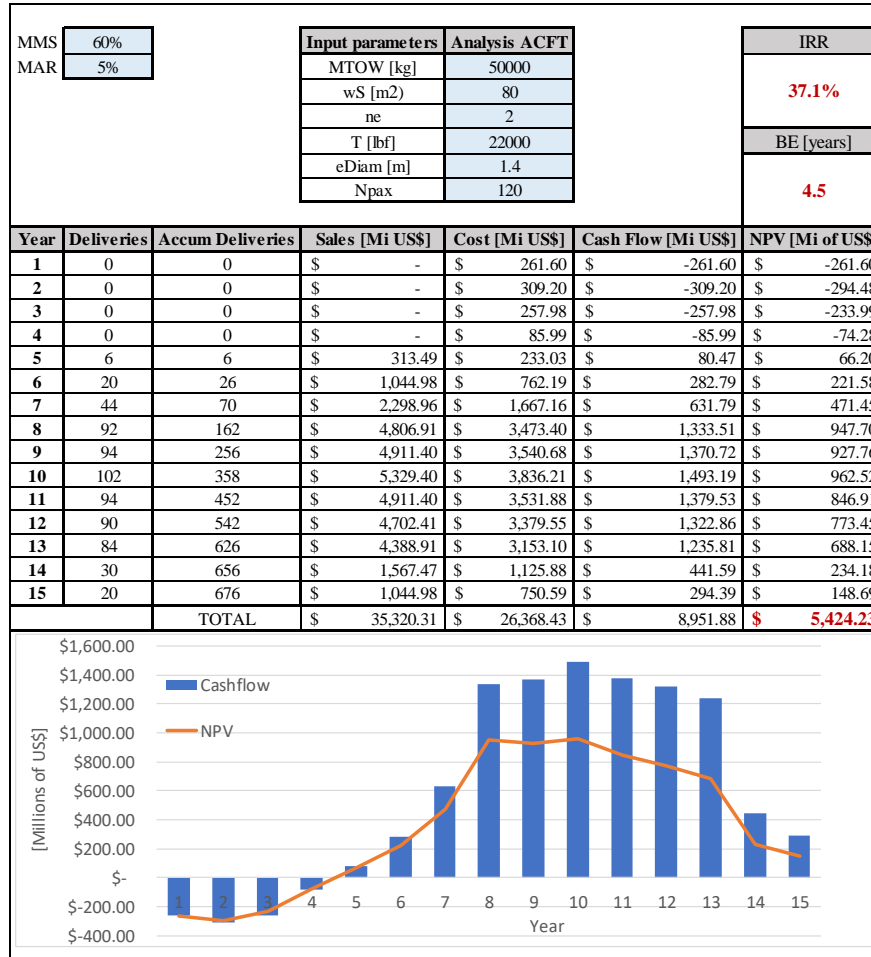


Figure 3.23: Cashflow NPV analysis of a 120-seat aircraft design

3.3 The optimization cycle

As shown in Fig. 3.3, the optimization cycle is implemented via ModeFrontier ® application, which integrates the Aircraft and Network framework (implemented in MATLAB ®) modules into a multiobjective-multidisciplinary optimization problem. In this study, two sets of objective functions (Y) will be explored in the simulations:

Set A: Airline operations optimization

- Minimization of Network Direct Operational Cost (NDOC)..
- Maximization of Network Profit (NP).

Set B: Airline operations and Aircraft Manufacturer optimization

- Maximization of Network Profit (NP)
- Maximization of NPV.

The optimization algorithm

The optimization cycle uses the MOGA-II Genetic Algorithm as optimizer module, embedded in the *ModeFrontier* ® application. This was selected due to its capacity to handle multiple types of variables (discrete and continuous), on a smart multi search elitism for robustness and directional crossover for fast converge, in a complex design space, as the one composed by the design parameters defined in this problem [201].

The first step in the algorithm is to determine an initial population. By default, it is created a population that is feasible with respect to bounds and/or constraints defined in the framework, using the appropriate design of experiments (DOE). After that the main interaction of the algorithm proceeds under the following steps

1. Parents for the next generation are determined using a defined selection function on the current population.
2. Children from the selected parents are generated by the genetic operators.

3. Children are scored by calculating their objective functions values and feasibility.
4. Current population and the children are combined into one matrix, composing an extended population.
5. Compute the rank and crowding distance for all individuals in the extended population. The crowding distance is a measure of the closeness of an individual to its nearest neighbors.
6. Trim the extended population to have the determined population size individuals by retaining the appropriate number of individuals of each rank.
7. The interaction continues executing all steps above until one of the following stopping conditions is met:
 - a. Maximum number of generations is exceeded.
 - b. Geometric average of the relative value of the spread is less than a tolerance.
 - c. The final spread is less than the mean spread of the past 3 generations.

It is worth to mention that the spread is a measure of the movement of the Pareto set. To calculate the spread, the algorithm first evaluates the standard deviation (σ) of the crowding distance measure of points that are on the Pareto front with finite distance. The algorithm then evaluates μ , which corresponds to the sum over the k objective function indices of the norm of the difference between the current minimum-value Pareto point for that index and the minimum point for that index in the previous iteration. The spread is then calculated as:

$$\text{spread} = (\mu + \sigma)/(\mu + k^*\sigma) \quad (71)$$

When the spread is small , the extreme objective function values do not change much between iterations (that is, μ is small) and when the points on the Pareto front are spread evenly (that is, σ is small).

At this point it is worth to mention that the MOGA-II algorithm represents an improvement of the original MOGA [86]. This new version considers four slightly different operators for reproduction: classical crossover, directional crossover, mutation, and selection. At each generation step, one of the four operators are chosen according to predefined operator probabilities and applied to the current individual. However, a new operator called evolutionary directional crossover, is introduced to accelerate the convergence. This compares the fitness of the individual i from generation t with the fitness of its parents belonging to generation $t - 1$. The new individual

is then created by moving in a randomly weighted direction that lies within the ones individuated by the given individual and his parents. Therefore, the directional crossover assumes that a direction of improvement can be detected comparing the fitness values of two reference individuals, used as selection function. According to Rigoni and Poles [202], the directional crossover operator has been demonstrated to help the algorithm convergence for a wide range of numerical problems. Table 3.17 shows the setting parameters used in the GA optimization process in this study.

Table 3.16: MOGA-II Optimization parameters setting

| | |
|--|-----|
| Maximum population size | 30 |
| Maximum number of generations | 300 |
| Probability of directional cross-over | 50% |
| Probability cross-over | 50% |
| Probability of Selection | 5% |
| Probability of Mutation | 1% |

Finally, it is proposed to use the Uniform Latin Hypercube (ULH) sampling to generate the Design of Experiment (DOE) used as starting point for the GA optimization. As explained in Session 2, the Design of Experiment (DOE) is a sampling methodology which maximizes the knowledge of experimental data, eliminating redundant observations allowing the analysts to extract as much information as possible through a limited use of runs. In the ULH method, the design space is constructed in such a way that each of the dimensions (design variables) is divided into equal levels and that there is only one sample at each level. A random procedure is used to determine the point locations. The test points locations are then uniformly distributed inside the DOI providing reasonable space-filling properties at reasonable computational costs.

4. Simulations and analysis

Considering the integrated MDO frameworks and methodologies described in Section 3, four types of simulations are conducted in progressive complexity levels. The final objective is to develop a complete analysis on the integrated optimization of a family of aircraft and complex network designs. With the objective to develop such analysis, simulations are conducted according to the following steps sequence:

- *Step I: Optimized Aircraft Design for a given Network*

Where the optimum aircraft design is obtained considering a given network connecting a limited number of airports, contained in certain geographical area.

•

- *Step II: Optimized Network for a given Aircraft Design*

Where the optimum network is designed for a given type of aircraft, considering a limited number of airports, contained in certain geographical area.

- *Step III: Integrated Network and Aircraft Design Optimization*

Where the optimum network and aircraft designs are determined considering a limited number of airports, contained in certain geographical area.

- *Step IV: Integrated Complex Network and Aircraft Fleet Optimization*

Where the optimum family of aircraft and associated networks for each aircraft are determined simultaneously considering a considerable number of airports, contained in certain geographical area.

In the following sessions, results and associated discussions for each simulation step will be presented.

4.1 Optimized aircraft design for a given network

The first step of simulations corresponds to the determination of the best aircraft design that fits on a given air transport network. In fact, this is one of the most important activities conducted by aircraft manufacturers during the conceptual project phase or even on marketing campaigns, when a family of aircrafts are evaluated in future customer's network [26].

In order to find the best aircraft, the airline operations optimization process is conducted in a dedicated *MATLAB*© code, where the network optimization module is switched off and replaced by a fixed (given) network routine. In this case two main objective functions are evaluated: maximization of Network Profit (*NP*) and minimization of Network Direct Operational Cost (*NDOC*). A comparison with the basic aircraft results on this network is also performed.

For that, a hypothetical air transport network is proposed as proof of concept, connecting five major Brazilian airports, which are: Porto Alegre/Salgado Filho - POA, São Paulo International/André Franco Montoro - GIG, Rio de Janeiro International/Tom Jobin - GIG, Brasilia International/Jucelino Kubitschek - BSB and Salvador/Antonio Carlos Magalhães - SSA, through all possible city pair connections (twenty in total), as shown in Fig. 4.1. The airport data used in mission analysis computations are extracted from the Brazilian Aeronautical Information Publication (AIP) [201]. Airport and city-econometric data related to such airports is displayed in Appendix B (Tables B.1 and B.2). The air transport network main characteristics indicators are shown in Table 4.1 and represents the operations of typical regional airline in southeast Brazil.

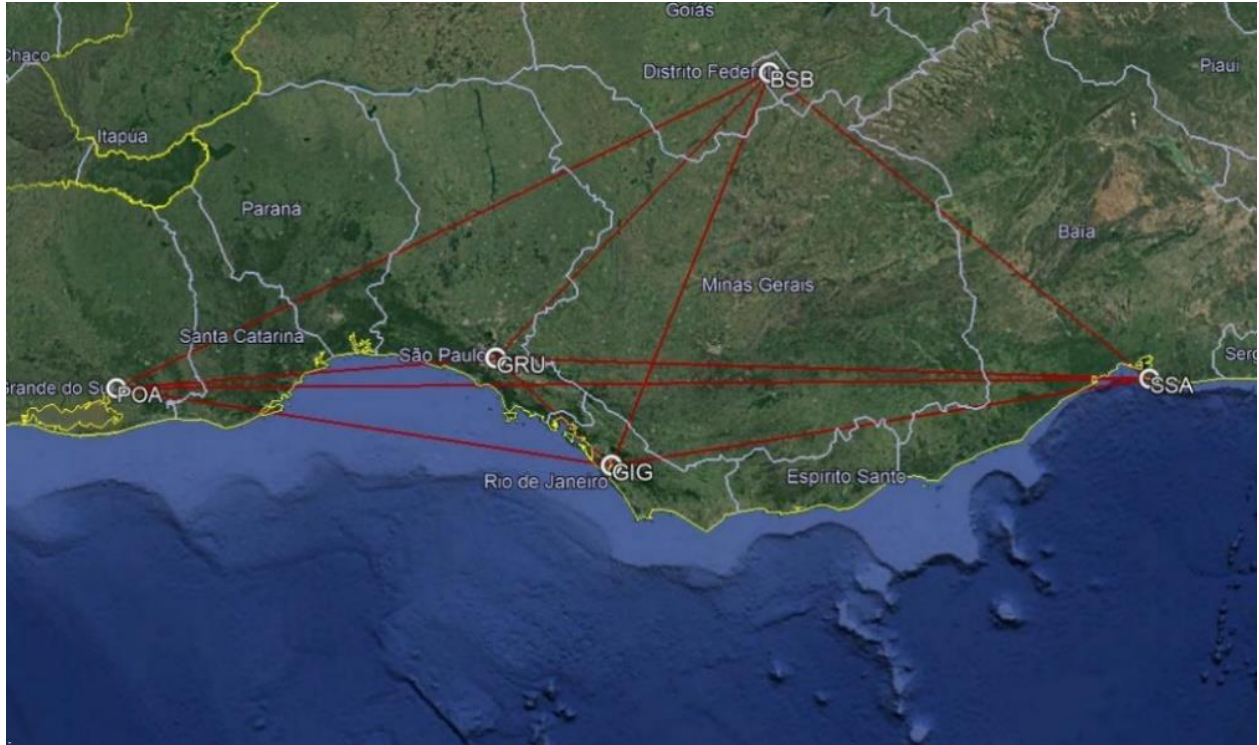


Figure 4.1: Five cities air transport network

Table 4.1: Five airports network indicators

| | |
|---------------------------------------|-------|
| Number of nodes (N) | 5 |
| Number of arcs | 20 |
| Average Degree of Nodes (DON) | 3.2 |
| Average path length (L) [nm] | 654.5 |
| Network Density (ND) | 1.0 |
| Average Clustering Index (ACi) | 0.8 |

This network is operated by a hypothetical regional airline with the following assumptions:

- The airline has 10% market share of domestic passengers
- No cargo operations are considered. All revenues come from passenger's demand.
- An average Load Factor (LF_{avg}) of 85% is applied in all route connections.
- One aircraft design is considered to operate in the network.
- An average fare of US\$120,00 is applied in all route connections. This value corresponds approximately to the average fare practiced by the top four Brazilian airlines in 2017, according to the Brazilian Airlines Association (ABEAR) [203].
- Additional 10% on tickets revenue is generated via ancillary services.
- Additional 30% on sector's DOC is applied to estimate associated administrative costs.

Appendix B also shows the respective route distances (calculated according to Eq.34) and magnetic headings between airports (calculated according to Eq.33), the last one necessary for the correct selection of cruise altitude. Average delays on each airport are considered by the model proposed by Newell [204] as function of runway configuration and capacity: for departure delays, which occur on ground, ten minutes for airports with two or more active runways (for GRU, GIG and BSB) and five minutes for airports with one active runway (POA and SSA). For arrival delays, associated with terminal holdings and enroute speed reductions, are assumed five minutes on airports with two or more active runways and three minutes for airports with one active runway. The city-econometric data (related to year 2017) were extracted from the Brazilian Geographic and Statistical Institute's (IBGE) website [205].

As previously mentioned, the route passengers demand (per day) is calculated via gravitational model proposed via Eq. 30. The model was calibrated considering the passenger's domestic demand data related to the twenty busiest route city-pairs in Brazil, extracted from the Brazilian Civil Authority (ANAC) statistical database [206]. The coefficients related to the proposed model (shown in Eq.30a and Eq.30b) were obtained via log-linear regression analysis, using demand data related to years 2014, 2015 and 2016 (the last three years with available consolidated data by the time of herein calculations were performed, in December 2017). All analyses were conducted using the Microsoft Excel ® Solver, which results are shown in Appendix A. The coefficients adopted in the model (A_0, A_1, A_2, A_3, A_4 and A_5) are calculated as the average of the correspondent

coefficients obtained from the 2014, 2015 and 2016 analyses. Table 4.2 shows the regression results of all analysis and average values.

It is worth mentioning that it is not uncommon to observe gravitational demand models being unable to capture local specific consumer behaviors or country's political-econometric influences and, as consequence, a degradation on model estimation accuracy [207]. In fact, it has been observed in years 2014, 2015 and 2016 a stagnation on passenger's demand in Brazil [206], possibly influenced by the economic recession scenario which the country passed through.

This may be reflected into lower values of Person's coefficient (Multiple R), approximately 0,6 in such years, what is considered acceptable in the econometric point of view [111], but other exogenous factors (usually not predicted in the classical gravitational model literature) may be present and should be investigated if a more accurate analysis is necessary. When considering the city-pair combinations related to the five airports network city-pairs only, the Person's coefficient is improved to 0.65. Table 4.3 shows the estimated passenger's demand for each city pair in the five airports network, calculated according to the above explained model.

Table 4.2: Passenger regression model coefficients, based on city-pair demand of the twenty busiest Brazilian domestic routes.

| Coefficient | 2014 Regression | 2015 Regression | 2016 Regression | Model |
|-------------------|-----------------|-----------------|-----------------|---------|
| <i>Ln(K0)</i> | 5.1453 | 3.5299 | 2.0559 | 3.5770 |
| <i>K1</i> | 0.3153 | 0.4011 | 0.5305 | 0.4157 |
| <i>K2</i> | -0.0370 | -0.0383 | -0.0412 | -0.0388 |
| <i>K3</i> | 0.4901 | 0.8548 | 1.4448 | 0.9299 |
| <i>K4</i> | -0.0931 | -0.1401 | -0.2598 | -0.1643 |
| <i>K5</i> | 0.2382 | 0.1163 | 0.0449 | 0.1331 |
| <i>Multiple R</i> | 0.60 | 0.55 | 0.57 | 0.65 |

Table 4.3: Route passenger's estimated demand per day (10% market share)

| Departure Airport (i) | Arrival Airport (j) | | | | |
|-----------------------|---------------------|-----|-----|-----|-----|
| | GRU | GIG | BSB | POA | SSA |
| GRU | 0 | 398 | 367 | 346 | 404 |
| GIG | 398 | 0 | 311 | 302 | 329 |
| BSB | 367 | 311 | 0 | 257 | 267 |
| POA | 346 | 302 | 257 | 0 | 280 |
| SSA | 404 | 329 | 267 | 280 | 0 |

The optimization is carried out according to the airline operations optimization objectives (maximization of the total network's profit (NP) and minimization the total network direct operational cost ($NDOC$)) according to the framework displayed in Figure 3.3. In order to reduce the computation time, some design variables were set as fixed parameters as shown in Table 4.4:

Table 4.4: Design variables set as fixed parameters

| i | Design Parameter (X_i) | Symbol | Fixed value |
|-----------------------|---|--------------------|---------------------|
| 11 | Engine fan pressure ratio | <i>FPR</i> | 1.6 |
| 14 | Design range, full pax @ 100kg, ISA conditions [nm] | <i>RANGE</i> | 1600 |
| 15 | Engine design point pressure altitude [ft] | <i>eHp</i> | 41000 |
| 16 | Engine design point Mach number | <i>eM</i> | 0.78 |
| 17 | Engine position flag | <i>ePos</i> | 1 (below wings) |
| 18 | Winglet presence flag | <i>WingletPres</i> | 1 (winglet present) |
| 19 | Slat presence flag | <i>SlatPres</i> | 1 (slats present) |
| 20 | Horizontal tail position | <i>HTP</i> | 1 (fuselage) |

The genetic algorithm MOGA-II, embedded in modeFrontier® application, was used as optimizer. A design of experiments (*DOE*) was created, also via modeFrontier ® application, with 30 individuals using the Uniform Latin Hypercube (*ULH*) technique to support the first generation of airplanes to be evaluated by the optimization algorithm. Appendix C shows the DOE and all design variables calculated by the GA for each individual generated and all designs generated by the optimization. The total computation time was 19.156 hours in a machine equipped with 2.7 GHz CPU, 4 Intel Core i7-7500U processors, with two cores. Each generation took an average of 3.806 min to be processed. The GA produced in total 302 generations, distributed in 20 populations. From those, 189 individuals presented feasible outputs (62.6%), 73 failed in the performance check, representing unfeasible outputs (24.2%) and 42 did not converge in the airplane calculation module (13.9%).

Fig. 4.2 shows the resulting individuals produced by the optimization, including non-dominant (gray points) and Pareto front (green points) in an $NDOC \times NP$ plot. The unfeasible designs and failed designs that arose during the computations are not shown in the figure. Tables 4.5a and 4.5b show important characteristics of the aircraft and network of the thirteen individuals present in the Pareto front resulting from the optimization. In the sake of comparison, the results regarding the geometry and performance of baseline aircraft in such network is also shown in this table.

Figure 4.3 shows the relative position of the baseline aircraft regarding the pareto front and two significant design extremes: #293 related maximum Network Profit ($12,06 \cdot 10^{-4}$ US\$/nm.pax), #289 related to minimum DOC (7.62 US\$/nm). They correspond to the different design concepts, as shown in Fig.4.4. From this graph it is noticeable that the basic aircraft reference plot is located quite below the Pareto front designs obtained from the optimization. This strongly suggests that the basic aircraft design, originally considering a single 1600 nm mission, could be improved much more when the fixed five-airports network is considered and airline operations optimizations objectives (min $NDOC$ and Max NP) is set as main goal.

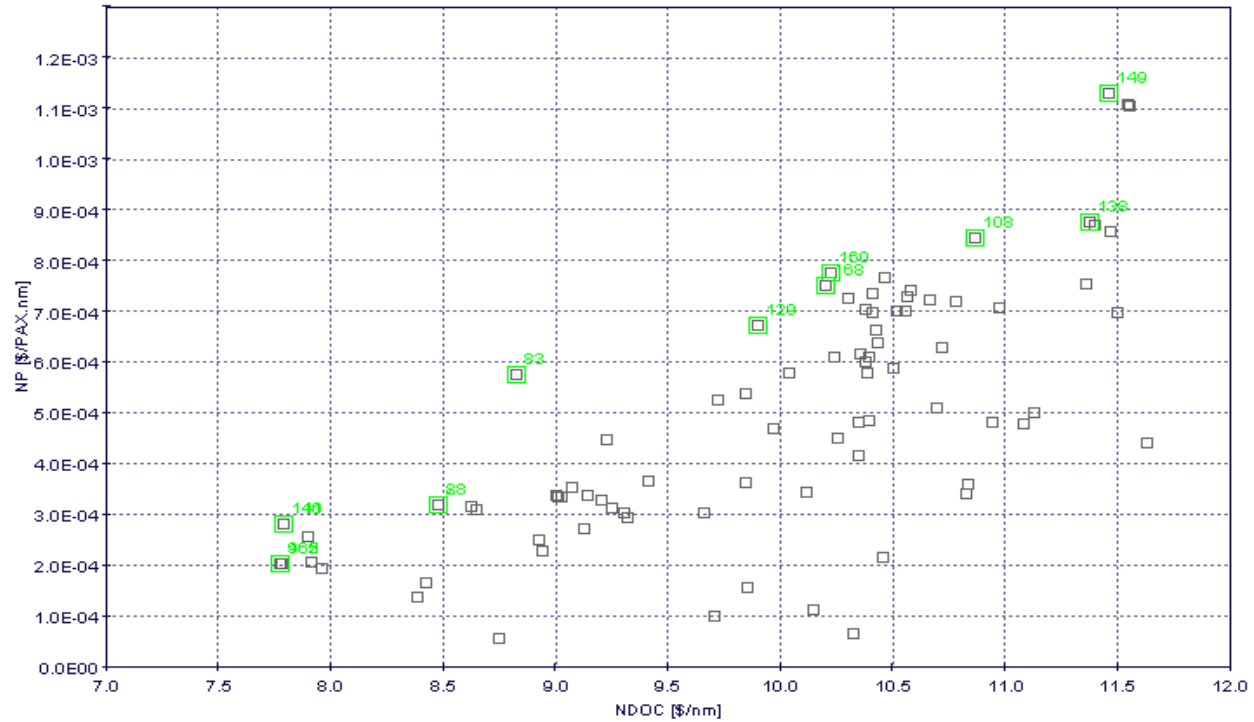


Figure 4.2: Optimization results – Fixed Network/Optimum Aircraft (5 airports)

Table 4.5a: Pareto Front individuals – Fixed Network/Optimum Aircraft
(Aircraft characteristics)

| ID# | OEW [kg] | MTOW [kg] | Avg CRZ Mach | N Pax | N Seat abr | wS [m ²] | w AR | w TR | w Sweep [°] | w Twist [°] | Kink Pos | BPR | eDiam [m] | OPR | ITT [K] | Total Noise [dB] | NPV [\$] x 10 ⁹ |
|------------------|----------|-----------|--------------|-------|------------|----------------------|------|-------------|-------------|-------------|-------------|-----|-------------|------|---------|------------------|----------------------------|
| BASE LINE | 21212 | 36831 | 0.797 | 78 | 4 | 72.7 | 8.6 | 0.29 | 26.5 | -4.5 | 0.34 | 5.0 | 1.36 | 28.5 | 1450 | 261.6 | 3.0 |
| 289 | 31137 | 17792 | 0.733 | 70 | 6 | 80.3 | 8.5 | 0.34 | 15.0 | -3.9 | 0.32 | 6.5 | 1.28 | 30.0 | 1466 | 236.7 | 2.2 |
| 110 | 32431 | 18680 | 0.748 | 75 | 4 | 77.5 | 7.7 | 0.33 | 23.4 | -2.5 | 0.34 | 5.8 | 1.28 | 26.4 | 1453 | 237.6 | 2.4 |
| 141 | 32746 | 18601 | 0.770 | 75 | 4 | 77.5 | 7.7 | 0.33 | 23.4 | -2.5 | 0.34 | 5.8 | 1.28 | 26.4 | 1453 | 243.6 | 2.4 |

| | | | | | | | | | | | | | | | | | |
|------------|-------|-------|-------|-----|---|-------|-----|------|------|------|------|-----|------|------|------|-------|-----|
| 288 | 34200 | 18735 | 0.772 | 83 | 6 | 77.5 | 7.6 | 0.45 | 24.3 | -5.0 | 0.35 | 5.9 | 1.33 | 29.7 | 1416 | 245.0 | 2.6 |
| 271 | 34764 | 19545 | 0.786 | 83 | 5 | 80.3 | 7.7 | 0.41 | 22.5 | -5.0 | 0.36 | 6.0 | 1.28 | 30.0 | 1424 | 243.8 | 2.6 |
| 244 | 34999 | 19283 | 0.775 | 87 | 6 | 80.3 | 8.1 | 0.31 | 19.5 | -3.7 | 0.33 | 6.1 | 1.28 | 30.0 | 1466 | 243.4 | 2.6 |
| 129 | 39944 | 21609 | 0.788 | 104 | 5 | 96.9 | 7.6 | 0.36 | 20.7 | -4.8 | 0.40 | 6.5 | 1.47 | 22.0 | 1435 | 245.5 | 3.2 |
| 168 | 44467 | 24287 | 0.787 | 111 | 5 | 105.1 | 7.6 | 0.30 | 15.0 | -3.5 | 0.40 | 6.4 | 1.47 | 29.3 | 1391 | 244.4 | 3.6 |
| 160 | 44304 | 24290 | 0.763 | 112 | 5 | 96.9 | 7.6 | 0.34 | 19.2 | -4.8 | 0.40 | 6.5 | 1.49 | 23.5 | 1429 | 242.6 | 3.5 |
| 258 | 45308 | 24129 | 0.786 | 119 | 6 | 110.7 | 8.5 | 0.34 | 15.0 | -3.9 | 0.32 | 6.5 | 1.54 | 26.6 | 1393 | 244.7 | 3.6 |
| 286 | 47597 | 26175 | 0.760 | 122 | 6 | 110.7 | 8.3 | 0.32 | 16.2 | -4.1 | 0.32 | 6.4 | 1.54 | 27.1 | 1422 | 246.2 | 3.8 |
| 292 | 47956 | 26332 | 0.764 | 124 | 6 | 113.4 | 8.0 | 0.30 | 19.2 | -3.7 | 0.32 | 6.4 | 1.49 | 25.9 | 1424 | 246.4 | 3.8 |
| 293 | 49144 | 26568 | 0.768 | 130 | 6 | 105.1 | 8.4 | 0.32 | 16.2 | -3.7 | 0.33 | 6.4 | 1.54 | 27.0 | 1422 | 244.9 | 3.9 |

Table 4.5b: Pareto Front individuals – Fixed Network/Optimum Aircraft
(Network characteristics)

| ID# | Number of flights | Estimated Number of Aircraft | Connected Arcs (n) | Average degree of nodes (ADON) | Average path length (L) [nm] | Network Density (ND) | Network Clustering Index (NCi) | N DOC [\$/nm] | NP [\$/PAXnm] x 10 ⁻⁴ |
|------------------|-------------------|------------------------------|--------------------|--------------------------------|------------------------------|----------------------|--------------------------------|---------------|----------------------------------|
| BASE LINE | 91 | 13 | | | | | | 8.65 | 1.86 |
| 289 | 104 | 16 | | | | | | 7.62 | 2.39 |
| 110 | 94 | 14 | | | | | | 7.70 | 2.98 |
| 141 | 94 | 14 | | | | | | 7.79 | 2.83 |
| 288 | 86 | 13 | | | | | | 8.22 | 4.67 |
| 271 | 85 | 12 | | | | | | 8.17 | 5.10 |
| 244 | 84 | 12 | | | | | | 8.33 | 6.04 |
| 129 | 70 | 10 | | | | | | 9.28 | 8.15 |
| 168 | 66 | 10 | | | | | | 10.22 | 7.55 |
| 160 | 66 | 10 | | | | | | 10.21 | 7.77 |
| 258 | 59 | 9 | | | | | | 10.42 | 9.93 |
| 286 | 59 | 9 | | | | | | 10.87 | 9.43 |
| 292 | 57 | 8 | | | | | | 10.96 | 10.68 |
| 293 | 56 | 8 | | | | | | 11.25 | 11.86 |

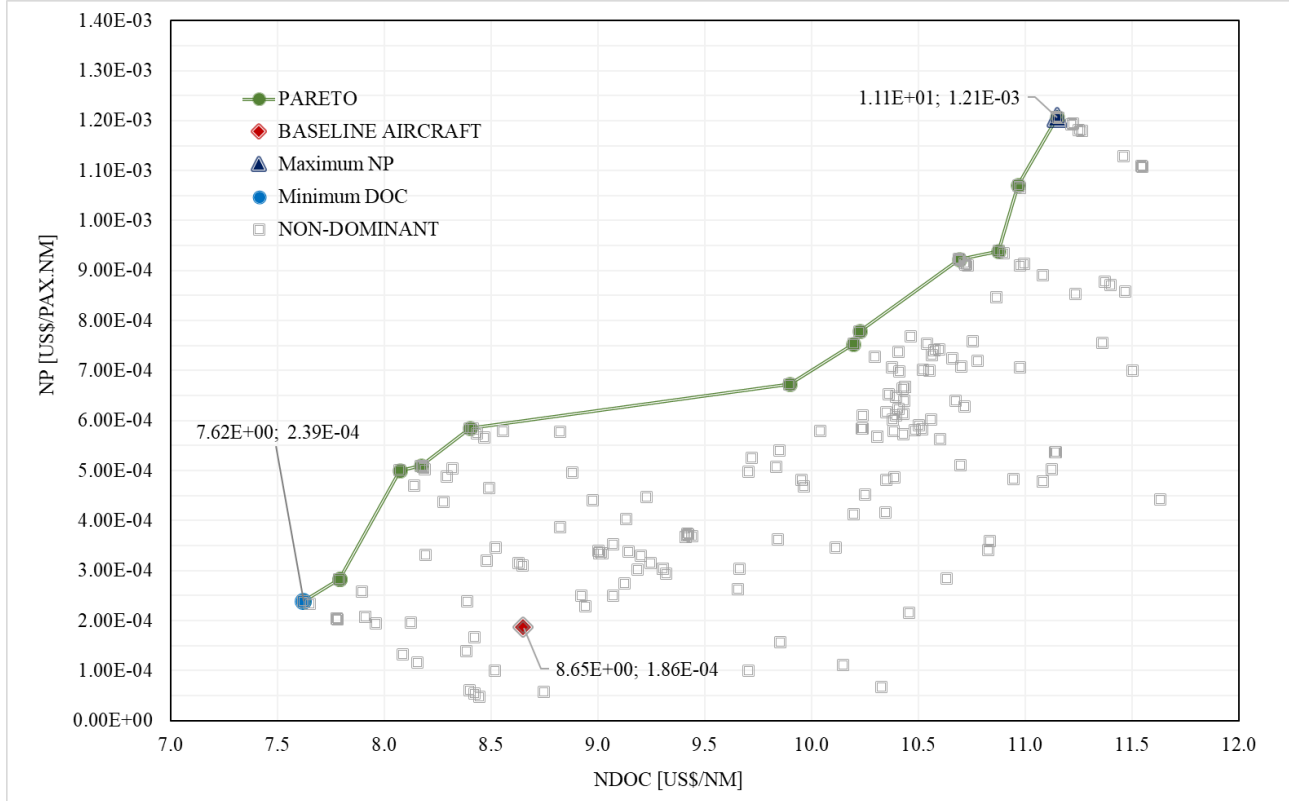


Figure 4.3: Pareto Front – Fixed Network/Optimum Aircraft (5 airports)

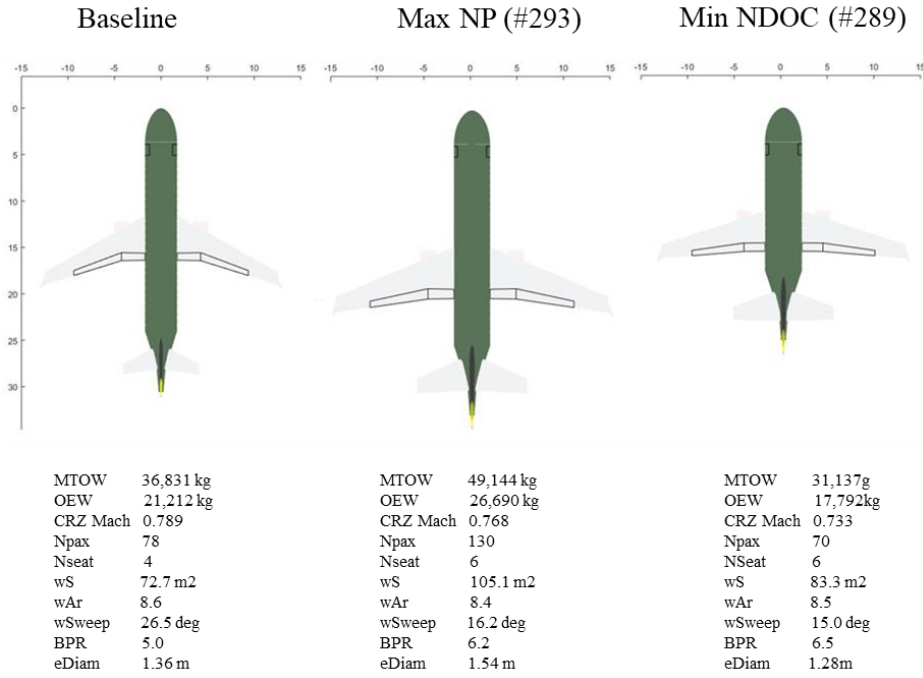


Figure 4.4: Baseline and extreme designs – Fixed Network/Optimum Aircraft (5 airports)

It is observed that the design associated to the minimum *NDOC* (ID#289) resulted on a cabin configuration corresponding to the minimum seating capacity (70 pax/ 6 seats abreast). Consequently, the *OEW* of this design about 7.6 tones lower than the baseline aircraft, which consequence is the reduction on fuel consumption. In this case a six seats abreast configuration is also selected, leading to a reduction on fuselage length and consequently a smaller wet area (essential parameter for the calculation of CD_0) and skin drag. One side effect on CD_0 reduction is also the reduction of average cruise Mach in order to keep the same maximum *M.CL/CD* ratio, considering the same airfoils are used in all designs (also in the baseline). Due to the lower cruise Mach, wave drag is also reduced, which results in the observed lower value of sweep angle (15.0°).

In addition, it was observed in this design a drastic increase engines by-pass ratio (6.5), which also presents a direct impact on engines' specific fuel consumption (*SFC*) reduction. All these components lead together to the reduction of mission fuel burn, and which has a direct impact on the minimization of the *DOC*. In fact, when comparing with the baseline aircraft, this design presents a reduction about -11.9% on *NDOC*, which is considered excellent in the operational point of view. However, due its lower seating capacity and therefore the necessity for a higher number of frequencies per day, the revenue per flight is reduced and therefore the network profit becomes marginal.

In the design related to the maximum Network Profit (ID#293), the optimization resulted on the biggest seating capacity aircraft (130 pax /6 seats abreast), seeking the highest revenue per leg. The immediate consequence is fuselage length increase and consequently a bigger wetted area. This growth leads to an increase about five tons in the *OEW*, when compared with the baseline aircraft, impacting directly on fuel consumption increase. With such additional structure, the wing area was increased significantly to (99.6m^2) in order to keep approximately the same wing loading, which impacts even also on the extra *TOW* contribution. In order to minimize such impact on fuel burn (influenced by the *NDOC* minimization objective), an increase on engines by-pass (6.2) and fan diameter (1.54 m) were also obtained, since both have direct impact on specific fuel consumption reduction. When comparing with the baseline aircraft, this design presents significant increase on *NP* (five times higher), mainly because of the revenue increase with the bigger number of passengers in the cabin. However, in this design, the *NDOC* is also increased (28.9%), as consequence of the unavoidable increasing fuel burn due to weight increase. The maximum *NPV* is achieved in this design, once this value is directly proportional to weight, engine

by-pass and wing area. Also, in this design, wing steep angle is reduced as a side effect of the lower cruise Mach and lower wave drag.

An aspect worth mentioning is that, in all designs in the Pareto front, the wing aspect ratio was kept within reasonable boundaries, reaching the highest value of 8.5 (basic aircraft's is 8.6). According to Mattos et. al [12], for this class of airplane, with passenger capacity topping 130 seats and up to 2000-nm range, no high-tech concepts such as extremely flexible wings or truss-braced configurations seem to be necessary, once lower aspect ratios are sufficient for short missions like the ones in this network evaluation. Wing sweepback angle higher than the baseline design are present in most of the Pareto front individuals, suggesting that the optimization is seeking for the minimization of wave drag to reduce the sector DOC. This is expectable once the airfoils are the same for all designs and therefore changes on wings platform characteristics (sweepback, twist, tapper ratio) are the remaining ways to improve the aerodynamic efficiency. It is also noticed that engine's by-pass ratios are significantly bigger than the baseline aircraft (above 5.7), suggesting a strong push for the optimization to seek more fuel-efficient turbofan engines, reducing fuel consumption and in line with the objective to minimize the *NDOC*.

The variation on aircraft size has direct influence on route daily frequencies. The bigger is the aircraft the less frequencies are necessary to exhaust the demand at for each city-pair served, considering that the same load factor (85%) is applied in all sectors. This effect is visualized on Table 4.6, where the necessary frequencies for each design extreme and the baseline design aircrafts are shown. Frequencies are highlighted in different green cell gradings (darkest corresponds to is the highest frequency).

Table 4.6: City-pair daily frequencies for extremes and baseline design aircrafts – Fixed Network/Optimum Aircraft

| Departure Airport (i) | Arrival Airport (j) | | | | | | | | | | | | | | |
|--------------------------|---------------------|-----------------------|---------------------|--------------|-----------------------|---------------------|--------------|-----------------------|---------------------|--------------|-----------------------|---------------------|--------------|-----------------------|---------------------|
| | GRU | | | GIG | | | BSB | | | POA | | | SSA | | |
| | Base Line | min NDOC (#289) | max NP (#293) | Base Line | min NDOC (#289) | max NP (#293) | Base Line | min NDOC (#289) | max NP (#293) | Base Line | min NDOC (#289) | max NP (#293) | Base Line | min NDOC (#289) | max NP (#293) |
| GRU | - | - | - | 6 | 7 | 4 | 5 | 6 | 3 | 5 | 6 | 3 | 6 | 6 | 4 |
| GIG | 6 | 7 | 4 | - | - | - | 4 | 5 | 3 | 4 | 5 | 3 | 4 | 5 | 3 |
| BSB | 5 | 6 | 3 | 4 | 5 | 3 | - | - | - | 3 | 4 | 2 | 4 | 4 | 2 |
| POA | 5 | 6 | 3 | 4 | 5 | 3 | 3 | 4 | 2 | - | - | - | 4 | 4 | 3 |
| SSA | 6 | 6 | 4 | 4 | 5 | 3 | 4 | 4 | 2 | 4 | 4 | 3 | - | - | - |

The Pearson's correlation matrix related to all design variables is shown in Fig. 4.5. The correlation coefficient, shown on each cell of the matrix, is a measure of the linear correlation between two pairs variables in the whole dataset, calculated as the covariance of the two variables in all designs divided by the product of their standard deviations. It ranges between +1 and -1, where 1 is total positive linear correlation, 0 is no linear correlation, and -1 is total negative linear correlation. From the graph it shall be noticed that the number of passengers (X12) strongly influences positively the Network Profit (due to the increased revenue), *NDOC* (due to the increase on aircraft weight and therefore fuel consumption) and on engines fan diameter (due to the necessity of more thrust due to the weigh increase). It is also observed the strong correlation between *NP* and *NDOC*, as expected, according to Eq.64.

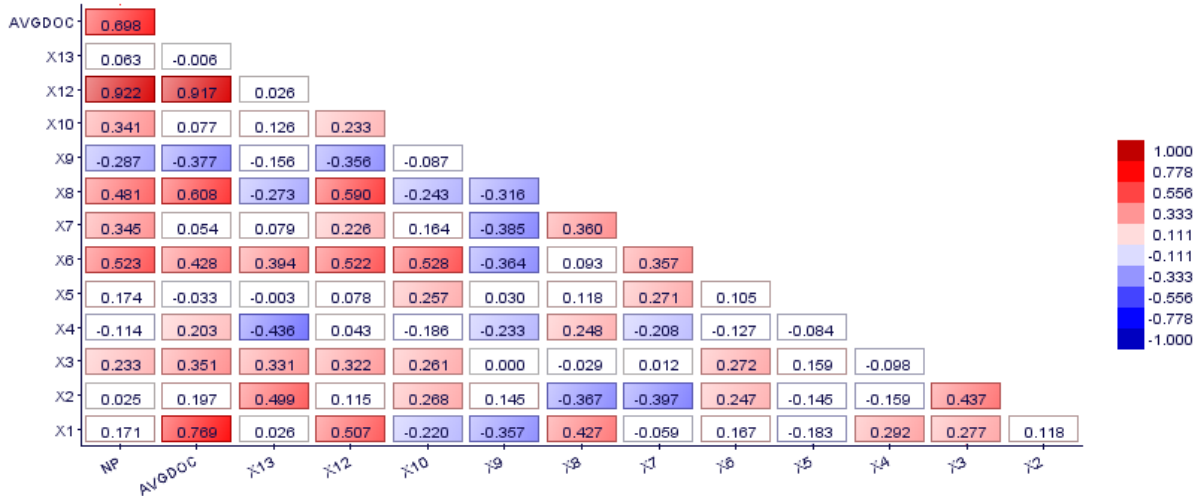


Figure 4.5: Pearson correlation matrix – Fixed Network/Optimum Aircraft (5 airports)

The final economic results for all design extremes, compared with the baseline aircraft, are shown on Tables 4.7a, 4.7b and 4.7c. Key parameters related to network, airline and aircraft manufactures perspectives are displayed.

From these tables it is possible to identify that the minimum *NDOC* scenario provides a -11.9% reduction when compared the baseline scenario. Despite of this, that the smaller aircraft capacity of this design (70 passengers) leads to a larger number of frequencies, and consequently the largest fleet (14 aircraft) of all extreme designs, in order to exhaust the required city-pair demands. As result, this network effect drives the total network costs and distance flown to be greater than the ones associated to maximum *NP* scenario. With that, the operational profit margin is increased by

78.1% when compared with the results using the baseline aircraft. Because of the reduced aircraft unit price (due to lower the MTOW), even though with a larger fleet, the necessary *CAPEX* on the airline side is -4.3% lower than the one required to acquire the baseline fleet.

In the maximum NP scenario, the larger aircraft capacity (130 passengers) leads to an opposite effect: lower frequencies and shorter total distances, reducing the total network costs by approximately -23%. Despite of a small increase on revenues (2.8%) the net effect is a significant increase on total profit, reaching an operational profit margin of approximately 11.5%, 27.5% greater than the baseline aircraft margin (8%). In this case a smaller fleet is obtained (8 aircraft) leading to the reduction of the fleet *CAPEX* by approximately -19.2%, when compared with the baseline aircraft fleet, although the aircraft unit price is increased approximately 31.4%. Although the biggest aircraft unit price, due to the combined effect of smaller fleet (and therefore smaller *CAPEX*) and higher annual profit, the return of investment is significantly reduced to 4.8 years, representing a -79.7% decrease when compared with the baseline fleet.

With the above results it may be concluded that the aircraft passenger's capacity has a significant impact on the number of frequencies and therefore the economic results for a fixed network. Although in the manufacturer side, airliners are usually designed for minimum *NDOC*, when considering the network effect, the maximization of profit demonstrated to be more appropriate when considering the airline perspective, considering also the return of fleet investment. It is important to mention that in both extremes (min *NDOC* and max NP) the annual profit is increased when comparing with the baseline fleet, and therefore any solution chosen in the Pareto front would provide a better profit for the airline.

Table 4.7a: Economic results for the minimum *NDOC* design (5 airports network)

| Key Parameter | Baseline Aircraft | Min <i>DOC</i> | Difference | |
|--------------------------------------|-------------------|-----------------|-----------------|--------|
| Total Distance flown [nm]/day | 57,141 | 59,604 | 2,463 | 4.3% |
| Total Passengers /day | 5,075 | 5,038 | -37 | -0.7% |
| Total Cost [US\$/]day | \$616,052.60 | \$575,432.82 | \$-40,619.78 | -6.6% |
| Total Revenue [US\$]/day | \$669,900.00 | \$665,016.00 | \$-4,884.00 | -0.7% |
| Profit [US\$/]day | \$53,847.40 | \$89,583.18 | \$35,735.78 | 66.4% |
| Annual Profit [US\$] | \$19,654,300.12 | \$32,697,859.82 | \$13,043,559.70 | 66.4% |
| Operational Profit Margin [%] | 8.7 | 15.6 | 6.8 | 78.1% |
| <i>NDOC</i> [US\$/nm] | 8.65 | 7.62 | -1.03 | -11.9% |
| NP (US\$/pax.nm)x1E-4 | 1.86 | 2.98 | 1.13 | 60.7% |
| NPV [US\$]x 10E9 | 3.0 | 2.3 | -0.7 | -23.0% |
| Aircraft Price [US\$ x 10E6] | 35.9 | 31.8 | -4.0 | -11.2% |
| Number of Frequencies | 91 | 94 | 3 | 3.3% |
| Estimated Number of Aircraft | 13 | 14 | 1 | 7.7% |
| Sectors per aircraft per day | 7 | 6 | -1 | -14.3% |
| CAPEX [US\$ x 10E6] | 466.1 | 445.9 | -20.2 | -4.3% |
| Return of Investment [years] | 23.7 | 13.6 | -10.1 | -42.5% |

Table 4.7b: Economic results for the maximum NP design (5 airports network)

| Key Parameter | Baseline Aircraft | Max NP | Difference | |
|-------------------------------|-------------------|-----------------|-----------------|--------|
| Total Distance flown [nm]/day | 57,141 | 34,078 | -23,063 | -40.4% |
| Total Passengers /day | 5,075 | 5,218 | 143 | 2.8% |
| Total Cost [US\$]/day | \$616,052.60 | \$474,277.49 | \$-141,775.11 | -23.0% |
| Total Revenue [US\$]/day | \$669,900.00 | \$688,776.00 | \$18,876.00 | 2.8% |
| Profit [US\$/day] | \$53,847.40 | \$214,498.51 | \$160,651.11 | 298.3% |
| Annual Profit [US\$] | \$19,654,300.12 | \$78,291,955.09 | \$58,637,654.97 | 298.3% |
| Operational Profit Margin [%] | 8.7 | 11.1 | 2.4 | 27.5% |
| NDOC [US\$/nm] | 8.65 | 8.40 | -0.25 | -2.9% |
| NP (US\$/pax.nm)x1E-4 | 1.86 | 5.85 | 3.99 | 214.8% |
| NPV [US\$]x 10E9 | 3.0 | 4.0 | 0.9 | 31.4% |
| Aircraft Price [US\$ x 10E6] | 35.9 | 47.1 | 11.2 | 31.4% |
| Number of Frequencies | 91 | 56 | -35 | -38.5% |
| Estimated Number of Aircraft | 13 | 8 | -5 | -38.5% |
| Sectors per aircraft per day | 7 | 7 | 0.0 | 0.0% |
| CAPEX [US\$ x 10E6] | 466.1 | 376.8 | -89.3 | -19.2% |
| Return of Investment [years] | 23.7 | 4.8 | -18.9 | -79.7% |

4.2 Optimized network for a given aircraft design

The second step of simulations corresponds to the determination of the optimum network topology considering a given aircraft design. Therefore, it is proposed to check the effectiveness of the proposed network optimization algorithm described in Session 3.2.1, which main objective is to maximize the network profit (US\$/pax.nm) in a nested sub-optimization process. The idea is to verify if the optimized network provides any kind of improvement on these objective functions.

For that, a *MATLAB*© code was prepared to run the optimization algorithm considering the five airports scenario (and associated passenger demands) associated to the fixed network simulation performed in Session 4.2. The MATLAB's *intlinprog* function, embedded with a dual-simplex algorithm [208], is used to solve the linear programming problem described in Session 3.2.1.

According to the proposed network optimization model, two input parameters (derived from the aircraft design in analysis) are necessary to run such simulations :i) airplane capacity (b) and ii) reference cost per distance unit (c). The aircraft capacity (b) is assumed to be the maximum cabin passengers ($NPax$) multiplied by the same average load factor use in the fixed network simulation (85%), while the reference cost per distance unit (c) is calculated according the DOC determination methodology described in Session 3.2.2.

The mission calculation routine is executed for each city-pair, in order to determine the trip and time parameters necessary for the associated city pair DOC computation. The following assumptions are considered in the mission profile calculations:

- ISA conditions
- Reference distances equal to the city-pair route distance in analysis
- Alternate airport selected as the closest airport to the destination airport of the city-pair in analysis.

The network optimization algorithm was then applied on the extreme aircraft designs obtained in the fixed network problem (maximum NP, minimum NDOC and maximum NPV) and basic aircraft design. Results from the optimization are shown on Figure 4.6, where the designs associated to the optimized networks are plotted in a NDOC x NP display, simultaneously with the Pareto front generated from the fixed network optimization, for the sake of comparison. Tables 4.10a and 4.10b show the resulting optimized frequencies between city pairs and the associated network parameters for each aircraft design considered. Figures 4.7a and 4.7b display the topologies of such networks (red lines correspond to the deactivated connections).

It may be noticed a significant improvement on the network profit in all designs. This is an expected effect when the number of connected city-pairs is reduced when compared the fixed (fully connected) network, mainly related to the lower profit sectors where demand and frequencies are diminished due to the gravitational model. Since an average and constant fare is applied in all sectors, sectors with lower frequencies lead to lower revenues (potentially minimum profit) and therefore are potential candidates to be eliminated by the algorithm.

With this, two groups of network topologies may be identified in Table 4.8: the one associated to the higher seating capacity aircraft (Maximum NP), and the other associated to the lower seating capacity aircraft (basic aircraft and minimum NDOC). City-pair daily frequencies are shown for each type of aircraft, again displayed with colored green cells gradient for better differentiation (darkest cells correspond to higher frequencies). From this table it may be observed that the POA-SSA and SSA-POA sectors are removed by the optimization in all designs, where the lower demands are strongly influenced by the largest route distances of the network. However, sectors BSB-SSA, SSA-BSB, BSB-POA and POA-BSB are removed from the Maximum NPV aircraft only, where lower sector frequencies associated to higher operational costs have influence on profitability. Since bigger aircraft present higher operational costs, longer routes with lower

demands may become unprofitable for the given average prices and therefore are switched off from the optimization.

As a result, an increase in NP is observed on these designs without such sectors. A side effect of sectors removal is the reduction of the average network path in all networks, what explains the increase of the associated NDOC in all designs.

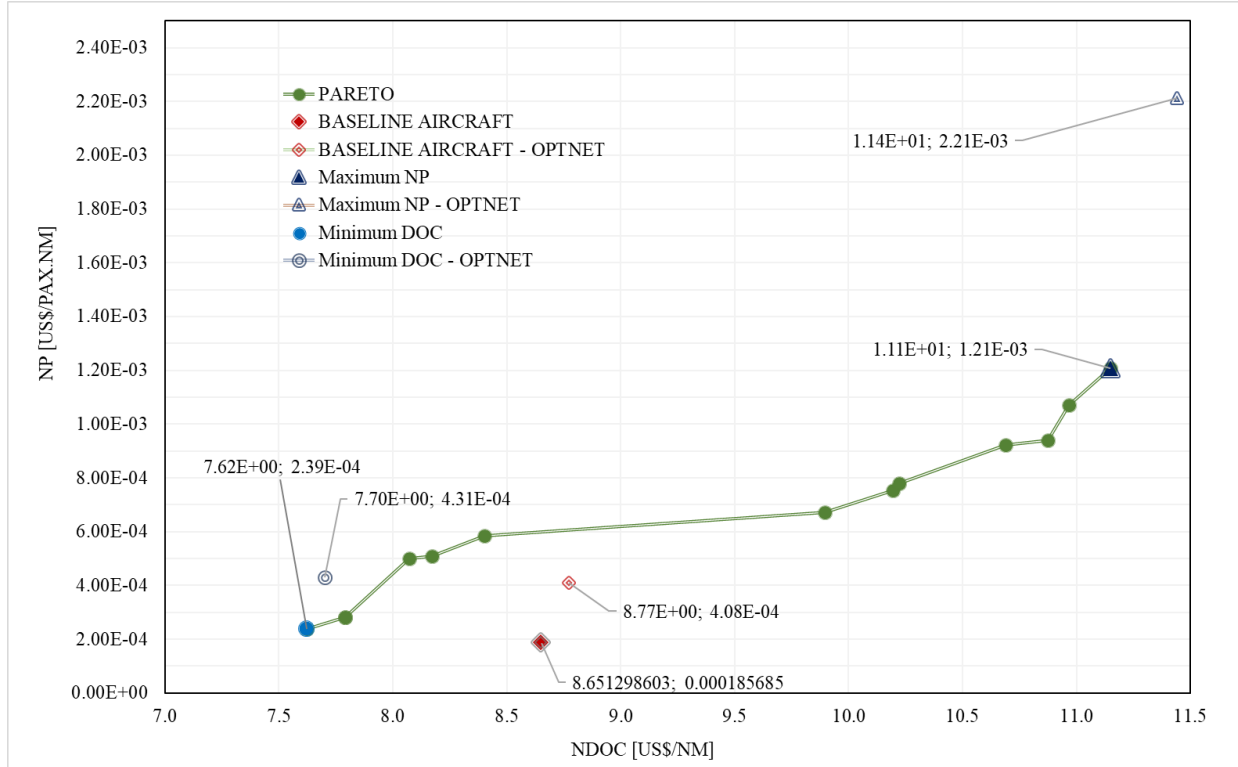


Figure 4.6: Results from the optimum network simulation

Table 4.8: Optimum network frequencies for Baseline Aircraft, Min DOC and Max NP designs

| BASIC AIRCRAFT and Min DOC (#289) | | | | | | | | | | | Max NPV(#293) | | | | | | | | | | | | | | |
|-----------------------------------|-----|-----------------|-----|-----|-----|-----|-----------------|-----|-----|-----|---------------|-----------------|-----------------|-----------------|-----|-----|-----|-----|-----------------|-----|-----|-----|-----|---|--|
| | | FIXED NETWORK | | | | | OPTIMUM NETWORK | | | | | | | FIXED NETWORK | | | | | OPTIMUM NETWORK | | | | | | |
| | | GRU | GIG | BSB | POA | SSA | GRU | GIG | BSB | POA | SSA | | | GRU | GIG | BSB | POA | SSA | GRU | GIG | BSB | POA | SSA | | |
| | | Arrival Airport | | | | | Arrival Airport | | | | | | | Arrival Airport | | | | | Arrival Airport | | | | | | |
| Departure Airport | GRU | - | 7 | 6 | 6 | 6 | - | 7 | 6 | 6 | 6 | Arrival Airport | Arrival Airport | GRU | - | 4 | 3 | 3 | 4 | - | 4 | 3 | 3 | 3 | |
| | GIG | 7 | - | 5 | 5 | 5 | 7 | - | 5 | 5 | 5 | | | GIG | 4 | - | 3 | 3 | 3 | 4 | - | 3 | 3 | 3 | |
| | BSB | 6 | 5 | - | 4 | 4 | 6 | 5 | - | 4 | 4 | | | BSB | 3 | 3 | - | 2 | 2 | 3 | 3 | - | 0 | 0 | |
| | POA | 6 | 5 | 4 | - | 4 | 6 | 5 | 4 | - | 0 | | | POA | 3 | 3 | 2 | - | 3 | 3 | 3 | 0 | - | 0 | |
| | SSA | 6 | 5 | 4 | 4 | - | 6 | 5 | 4 | 0 | - | | | SSA | 4 | 3 | 2 | 3 | - | 3 | 3 | 0 | 0 | - | |
| n | | 5 | | | | | 5 | | | | | | | 5 | | | | | 5 | | | | | | |
| N | | 20 | | | | | 18 | | | | | | | 20 | | | | | 14 | | | | | | |
| ADON | | 3.2 | | | | | 3.0 | | | | | | | 3.2 | | | | | 2.4 | | | | | | |
| L | | 654.5 | | | | | 584.2 | | | | | | | 654.5 | | | | | 537.4 | | | | | | |
| ND | | 1 | | | | | 0.9 | | | | | | | 1 | | | | | 0.7 | | | | | | |
| Aci | | 0.8 | | | | | 0.8 | | | | | | | 0.8 | | | | | 0.8 | | | | | | |

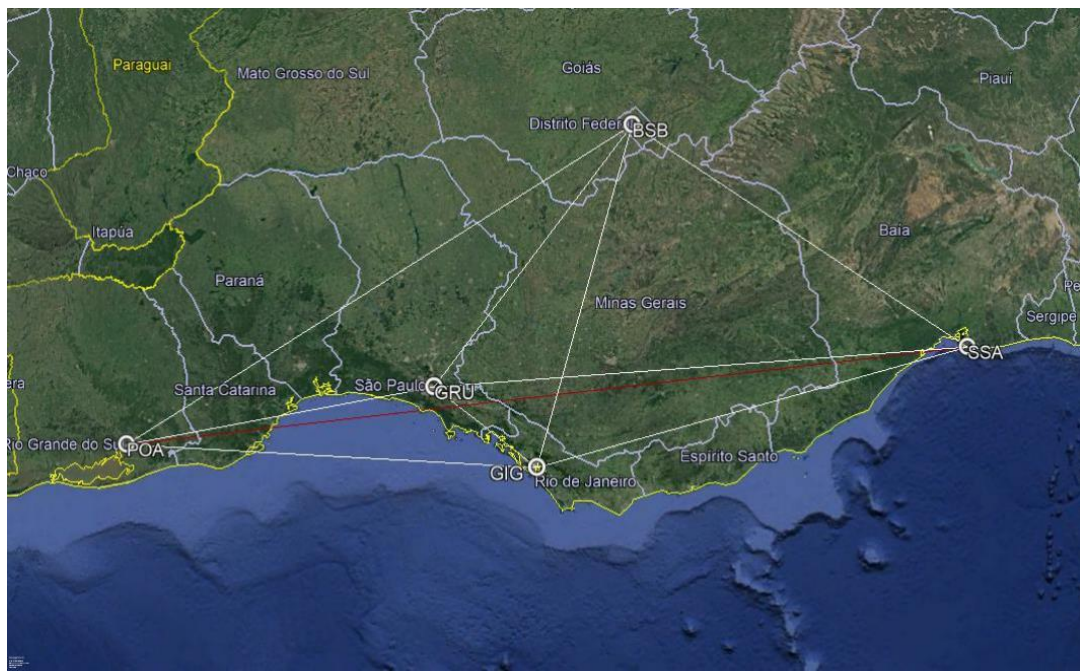


Figure 4.7a: Optimum network simulation results for baseline and min NDOC aircraft designs

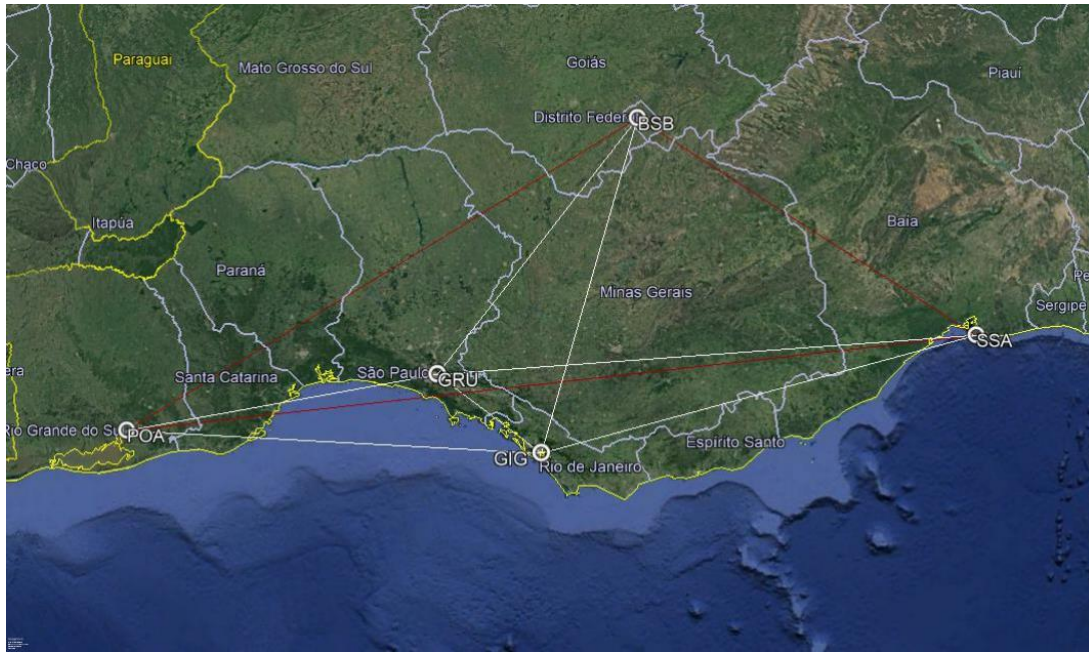


Figure 4.7b: Optimum network simulation results for max NP and max NPV aircraft designs

Tables 4.9a, 4.9b and 4.9c show the impact of the optimized network on the key airline econometric parameters, for the design extremes and baseline aircraft in analysis , when compared with the fixed network results.

Considering the lower capacity aircrafts (basic design and minimum NDOC) it is observed the annual profit increasing significantly (64.4% and 26.2% respectively), although not the maximum obtainable. In addition, the network optimization with these aircraft lead to reduction on fleet size and CAPEX (-11.5% and -3.2% respectively), representing about 71.7 Million US\$ savings for the baseline aircraft and 16.5 Million US\$ savings for the minimum DOC aircraft . As consequence, a significant drop on ROI is observed (-48.5% and -23.7% respectively).

For the higher capacity aircraft (maximum NP) it is observed slight drop in annual profit (-2.7%, -2.4 Million US\$), due to the largest reduction on connected network sectors, although providing the almost 9.5 times higher profit than the minimum NDOC design . However, the biggest benefit is the -25.2% reduction on fleet size and CAPEX, representing approximately 95.1 Million of US\$ savings for the airline and a - 23.2% reduction on ROI (from 4.8 to 2.7 years).

In both cases a significant increase in network profit is observed, when compared with the optimized aircraft designs in the fixed network case. This may be interpreted as a direct consequence of the sectors and fleet reduction resulted from the elimination of the marginal

profitable sectors. In all cases, the fleet reduction led to lower CAPEX and consequently the shorter return of investment. Therefore, the consideration of the network profit (NP, US\$/PAX. nm) maximization as objective in the optimization cycle demonstrated to bring extra financial benefits to airlines, associated to a CAPEX reduction as beneficial side effect.

Table 4.9a: Optimum network impact on economic parameters – basic aircraft design

| Key Parameter | Fixed Network | Optimum Network | Difference | |
|--------------------------------------|-----------------|------------------|-----------------|---------------|
| Total Distance flown [nm]/day | 57,141 | 46,846 | -10,295 | -18.0% |
| Total Passengers /day | 5,075 | 4,627 | -448 | -8.8% |
| Total Cost [US\$]/day | \$616,052.60 | \$ 522,219.75 | \$-93,832.85 | -15.2% |
| Total Revenue [US\$]/day | \$669,900.00 | \$ 610,764.00 | \$-59,136.00 | -8.8% |
| Profit [US\$]/day | \$53,847.40 | \$ 88,544.25 | \$34,696.85 | 64.4% |
| Annual Profit [US\$] | \$19,654,300.12 | \$ 32,318,650.81 | \$12,664,350.69 | 64.4% |
| Operational Margin [%] | 8.7 | 17.0 | 8.2 | 94.0% |
| NDOC [US\$/nm] | 8.65 | 8.77 | 0.12 | 1.4% |
| NP (US\$/pax.nm)x10E-4 | 1.86 | 4.08 | 2.23 | 120.0% |
| NPV [US\$]x 10E9 | | 3.0 | 0.0 | 0.0% |
| Aircraft Price [US\$ x 10E6] | | 35.9 | 0.0 | 0.0% |
| Number of Frequencies | 91 | 83 | -8 | -8.8% |
| Estimated Fleet size (# of aircraft) | 13 | 11 | -2 | -15.4% |
| Sectors per aircraft per day | 7 | 7 | 0.0 | 0.0% |
| CAPEX [US\$ x 10E6] | 466.1 | 394.4 | -71.7 | -15.4% |
| Return of Investment [years] | 23.7 | 12.2 | -11.5 | -48.5% |

Table 4.9b: Optimum network impact on economic parameters – minimum NDOC

| Key Parameter | Fixed Network | Optimum Network | Difference | |
|--------------------------------------|---------------|-----------------|--------------|-------------|
| Total Distance flown [nm]/day | 59,604 | 53,865 | -5,739 | -9.6% |
| Total Passengers /day | 5,038 | 4,870 | -168 | -3.3% |
| Total Cost [US\$]/day | \$575,432.82 | \$529,766.58 | \$-45,666.25 | -7.9% |
| Total Revenue [US\$]/day | \$665,016.00 | \$642,840.00 | \$-22,176.00 | -3.3% |
| Profit [US\$]/day | \$89,583.18 | \$113,073.42 | \$23,490.25 | 26.2% |
| Annual Profit [US\$] | 32,697,859.82 | \$41,271,799.87 | 8,573,940.05 | 26.2% |
| Operational Margin [%] | 15.6 | 21.3 | 5.8 | 37.1% |
| NDOC [US\$/nm] | 7.62 | 7.70 | 0.08 | 1.1% |
| NP (US\$/pax.nm)x10E-4 | 2.98 | 4.31 | 1.33 | 44.5% |
| NPV [US\$]x 10E9 | | 2.3 | 0.0 | 0.0% |
| Aircraft Price [US\$ x 10E6] | | 30.7 | 0.0 | 0.0% |
| Number of Frequencies | 94 | 96 | 2 | 2.1% |
| Estimated Fleet size (# of aircraft) | 14 | 14 | 0 | 0.0% |
| Sectors per aircraft per day | 6 | 7 | 1 | 14.3% |
| CAPEX [US\$ x 10E6] | 445.9 | 429.4 | -16.5 | -3.7% |
| Return of Investment [years] | 13.6 | 10.4 | -3.2 | -23.7% |

Table 4.9c: Optimum network impact on economic parameters – maximum NP

| Key Parameter | Fixed Network | Optimum Network | Difference | |
|-------------------------------|---------------|-----------------|---------------|--------|
| Total Distance flown [nm]/day | 34,078 | 22,946 | -11,132 | -32.7% |
| Total Passengers /day | 5,218 | 4,112 | -1,106 | -21.2% |
| Total Cost [US\$]/day | \$474,277.49 | \$334,016.23 | \$-140,261.26 | -29.6% |
| Total Revenue [US\$]/day | \$688,776.00 | \$542,784.00 | \$-145,992.00 | -21.2% |

| | | | | |
|---|---------------|-----------------|-----------------|--------|
| Profit [US\$]/day | \$214,498.51 | \$208,767.77 | \$-5,730.74 | -2.7% |
| Annual Profit [US\$] | 78,291,955.09 | \$76,200,236.34 | \$-2,091,718.75 | -2.7% |
| Operational Margin [%] | 11.1 | 62.5 | 51.4 | 460.7% |
| NDOC [US\$/nm] | 8.40 | 11.44 | 3.04 | 36.2% |
| NP (US\$/pax.nm)x10E-4 | 5.85 | 22.13 | 16.28 | 278.5% |
| NPV [US\$]x 10E9 | 4.0 | 0.0 | 0.0 | 0.0% |
| Aircraft Price [US\$ x 10E6] | 47.0 | 0.0 | 0.0 | 0.0% |
| Number of Frequencies | 56 | 44 | -12 | -21.4% |
| Estimated Fleet size (# of aircraft) | 8 | 6 | -2 | -25.0% |
| Sectors per aircraft per day | 7 | 7 | 0.0 | 0.0% |
| CAPEX [US\$ x 10E6] | 376.8 | 281.7 | -95.1 | -25.2% |
| Return of Investment [years] | 4.8 | 3.7 | -1.1 | -23.2% |

4.3 Integrated network and aircraft design optimization

The third step of simulations corresponds to the simultaneous optimization of the network topology and a single aircraft design, according to the optimization cycle proposed in Fig. 3.1 . The idea is to analyze the methodology's performance of the combined effect of the aircraft and networks in the complete MDO cycle. In order to conduct such simulation, the network optimization module (used in Session 4.2) was switched on in the *MATLAB* © code designed for simulations in Session 4.1. Also, the main objective functions related to the airlines operations optimization scenario are evaluated: maximization of Network Profit (NP) and minimization of Network Direct Operational Cost (NDOC).

The first simulation is performed considering the same five airports and operational scenario used in Session 4.1, with the objective to determine the net improvement from the previous simulation results (optimum aircraft/fixed network and optimum network/fixed aircraft). The genetic algorithm MOGA-II, embedded in modeFrontier® application, was also used as optimizer. A design of experiments (*DOE*) was created, also via modeFrontier ® application, with 30 individuals using the Uniform Latin Hypercube (*ULH*) technique to support the first generation of airplanes to be evaluated by the optimization algorithm. Appendix D shows the DOE and all design variables calculated by the GA for each individual generated and all designs generated by the optimization.

In this run, total computation time was 24.439 hours in a machine equipped with 2.7 GHz CPU,4 Intel Core i7-7500U processors, with two cores. Each generation took an average of 3.806 min to be processed. The GA produced in total 338 generations, distributed in 17 populations. From those, 239 individuals presented feasible outputs (70.7%) and 99 failed in the performance check, representing unfeasible outputs (29.3%). Fig. 4.8 shows the resulting individuals produced

by the optimization, including non-dominant (gray points) and Pareto front (green points) in an NDOC x NP plot. The unfeasible designs and failed designs that arose during the computations are not shown in the figure. Tables 4.10a and 4.10b show important aircraft and network characteristics of the fourteen individuals present in the Pareto front. In the sake of comparison, the results regarding the geometry and network of baseline aircraft (optimized and fixed) are also shown in these tables.

Figure 4.9 shows the relative position of the baseline aircraft regarding the pareto front from fixed and optimized networks. Again, significant design extremes may be identified: #384 related maximum Network Profit (130 pax / 6 seats abreast) and #396 related to minimum DOC (70 pax/ 5 seats breast). They correspond to the different design concepts, shown in Fig.4.10, side by side with the optimum aircraft design obtained at the fixed network scenario.

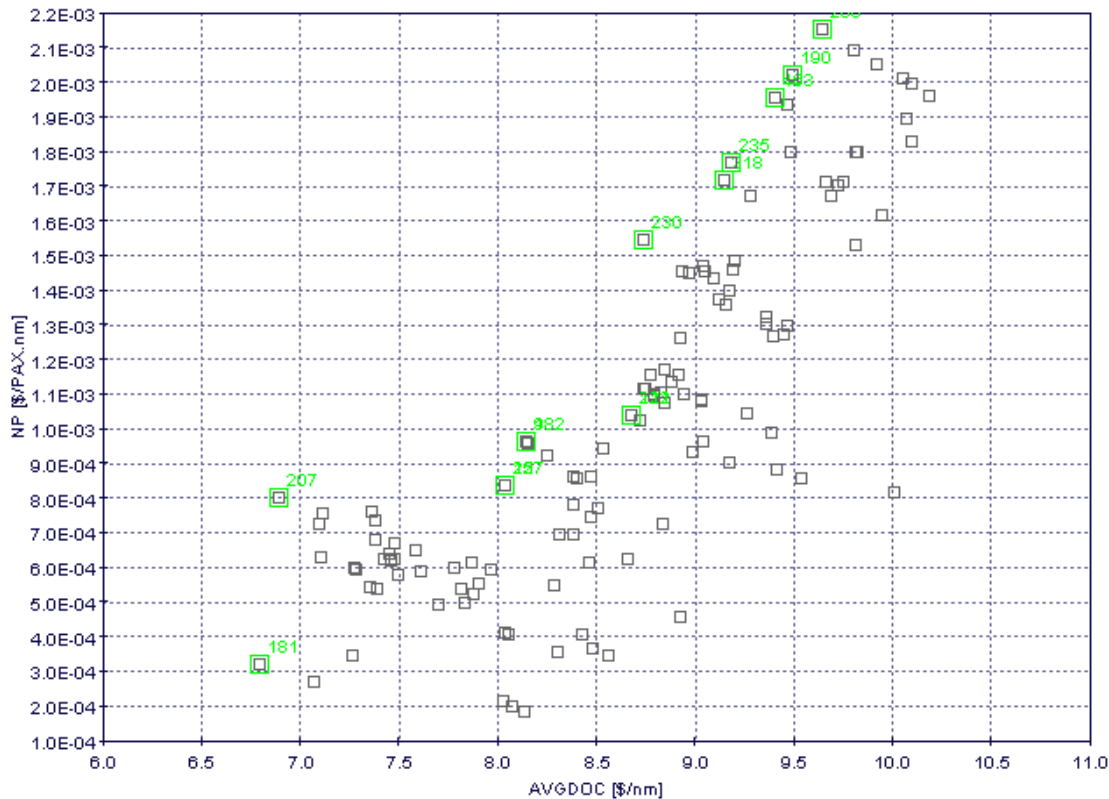


Figure 4.8: Optimization results – Integrated Aircraft and Network (5 airports)

Table 4.10a: Pareto Front individuals – Optimum Aircraft characteristics (5 airports)

| ID# | OEW [kg] | MTOW [kg] | Avg CRZ Mach | N Pax | N Seat | wS [m ²] | w AR | w TR | w Sweep [°] | w Twist [°] | Kink Pos | BPR | eDiam [m] | OPR | ITT [K] | Total Noise [dB] | NPV |
|------------------|--------------|--------------|--------------|-----------|----------|----------------------|------------|-------------|-------------|-------------|-------------|------------|-------------|-------------|-------------|------------------|------------|
| BASE LINE | 21212 | 36831 | 0.797 | 78 | 4 | 72.7 | 8.6 | 0.29 | 26.5 | -4.5 | 0.34 | 5.0 | 1.36 | 28.5 | 1450 | 261.6 | 3.0 |
| 396 | 31628 | 18362 | 0.758 | 70 | 5 | 77.5 | 8.6 | 0.37 | 27.3 | -3.2 | 0.35 | 6.2 | 1.29 | 27.9 | 1469 | 239.0 | 7.67 |
| 344 | 32880 | 18960 | 0.757 | 75 | 5 | 80.3 | 8.8 | 0.39 | 25.5 | -3.1 | 0.37 | 6.2 | 1.32 | 27.4 | 1392 | 239.9 | 7.89 |
| 366 | 33669 | 19256 | 0.779 | 78 | 5 | 74.8 | 8.7 | 0.38 | 24.9 | -3.6 | 0.38 | 6.3 | 1.35 | 27.5 | 1406 | 239.6 | 8.02 |
| 382 | 34618 | 19977 | 0.750 | 80 | 5 | 88.6 | 8.6 | 0.42 | 26.4 | -4.6 | 0.36 | 6.5 | 1.29 | 27.3 | 1405 | 240.1 | 8.36 |
| 304 | 34987 | 19974 | 0.754 | 81 | 6 | 88.6 | 8.3 | 0.42 | 27.3 | -4.9 | 0.34 | 6.4 | 1.28 | 27.8 | 1468 | 240.8 | 8.47 |
| 372 | 36297 | 20402 | 0.779 | 89 | 6 | 83.0 | 8.5 | 0.44 | 28.2 | -5.0 | 0.33 | 6.4 | 1.31 | 26.5 | 1439 | 242.4 | 8.53 |
| 294 | 37742 | 21164 | 0.772 | 93 | 6 | 88.6 | 8.6 | 0.41 | 28.5 | -4.6 | 0.34 | 6.5 | 1.30 | 26.9 | 1411 | 242.2 | 8.88 |
| 267 | 38337 | 21418 | 0.779 | 95 | 6 | 88.6 | 8.5 | 0.43 | 28.2 | -5.0 | 0.38 | 6.5 | 1.32 | 26.9 | 1438 | 242.3 | 9.03 |
| 332 | 42724 | 24378 | 0.792 | 101 | 6 | 94.1 | 8.8 | 0.41 | 29.4 | -4.8 | 0.37 | 6.0 | 1.51 | 27.8 | 1440 | 246.2 | 9.82 |
| 374 | 44475 | 24635 | 0.803 | 109 | 6 | 91.3 | 8.5 | 0.32 | 26.1 | -5.0 | 0.36 | 5.0 | 1.30 | 29.5 | 1440 | 244.2 | 10.01 |
| 395 | 43054 | 23575 | 0.791 | 112 | 5 | 88.6 | 8.1 | 0.42 | 29.7 | -2.9 | 0.38 | 6.5 | 1.41 | 28.1 | 1452 | 254.3 | 10.08 |
| 256 | 44655 | 24697 | 0.801 | 113 | 5 | 88.6 | 8.3 | 0.41 | 29.4 | -3.4 | 0.39 | 6.5 | 1.41 | 27.0 | 1447 | 244.6 | 10.23 |
| 300 | 44910 | 24789 | 0.801 | 114 | 5 | 88.6 | 8.3 | 0.40 | 29.7 | -3.4 | 0.39 | 6.5 | 1.41 | 27.0 | 1444 | 245.0 | 10.28 |
| 384 | 48423 | 25692 | 0.784 | 130 | 6 | 99.6 | 7.9 | 0.41 | 19.2 | -4.7 | 0.33 | 5.6 | 1.39 | 27.8 | 1467 | 251.7 | 11.39 |

Table 4.10b: Pareto Front individuals – Optimum Network characteristics (5 airports)

| ID# | Number of flights | Estimated Number of Aircraft | Connected Arcs (N) | Average degree of nodes (ADON) | Average path length (L) [nm] | Network Density (ND) | N DOC [\$/nm] | NP [\$/PAX nm] x 10 ⁻⁴ |
|--------------------------------|-------------------|------------------------------|--------------------|--------------------------------|------------------------------|----------------------|---------------|-----------------------------------|
| BASE LINE FIXED NETWORK | 91 | 13 | 20 | 3.2 | 654.5 | 1.0 | 8.65 | 1.86 |
| BASE LINE OPT NETWORK | 83 | 11 | 18 | 3.0 | 584.2 | 0.90 | 8.77 | 4.08 |
| 396 | 96 | 13 | | | | | 7.67 | 4.38 |
| 344 | 86 | 12 | | | | | 7.89 | 5.06 |
| 366 | 83 | 11 | | | | | 8.02 | 6.07 |
| 382 | 81 | 11 | | | | | 8.36 | 6.31 |
| 304 | 79 | 11 | | | | | 8.47 | 6.82 |
| 372 | 76 | 10 | | | | | 8.53 | 8.23 |
| 294 | 72 | 10 | | | | | 8.88 | 8.65 |
| 267 | 68 | 9 | | | | | 9.03 | 9.47 |
| 332 | 65 | 9 | | | | | 9.82 | 9.83 |
| 374 | 60 | 8 | | | | | 10.01 | 12.22 |
| 395 | 61 | 8 | | | | | 10.03 | 12.08 |
| 256 | 55 | 7 | | | | | 10.23 | 15.50 |
| 300 | 53 | 7 | | | | | 10.28 | 15.86 |
| 384 | 44 | 6 | 14 | 2.4 | 537.4 | 0.70 | 11.39 | 22.36 |

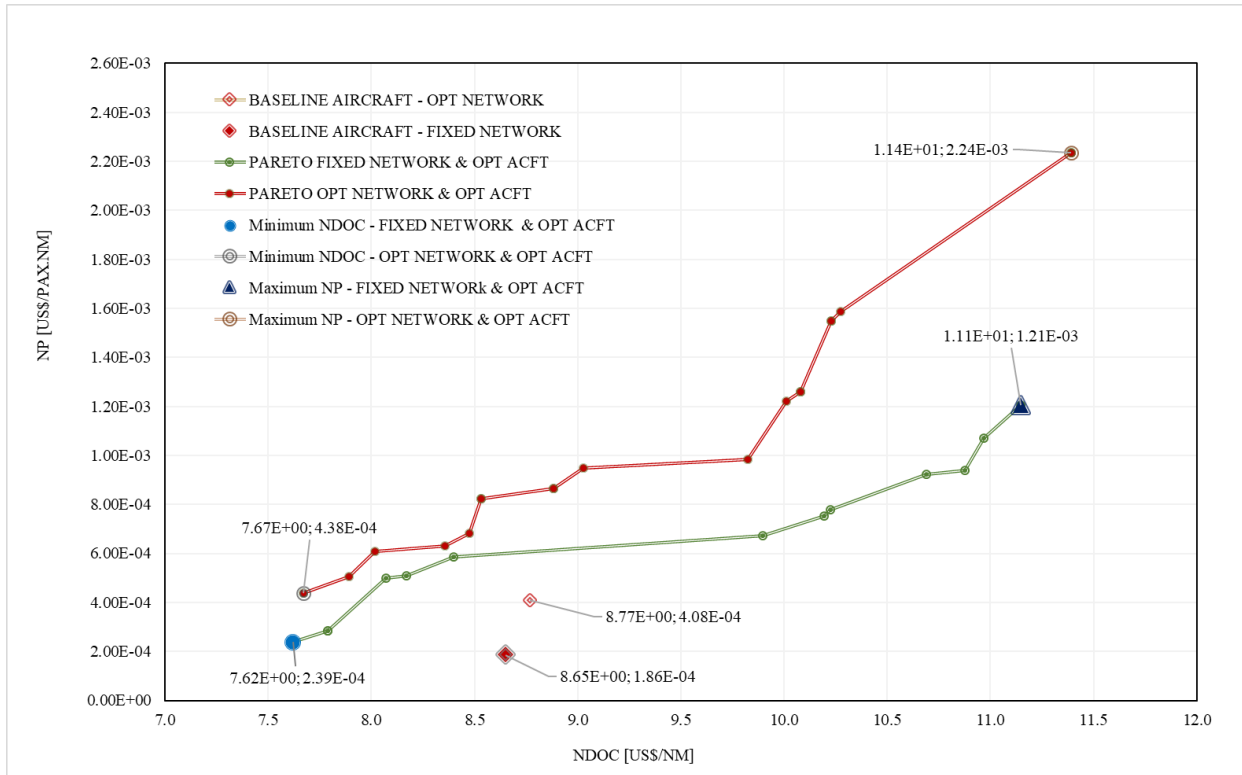


Figure 4.9: Integrated aircraft and network optimization Pareto front (5 airports)

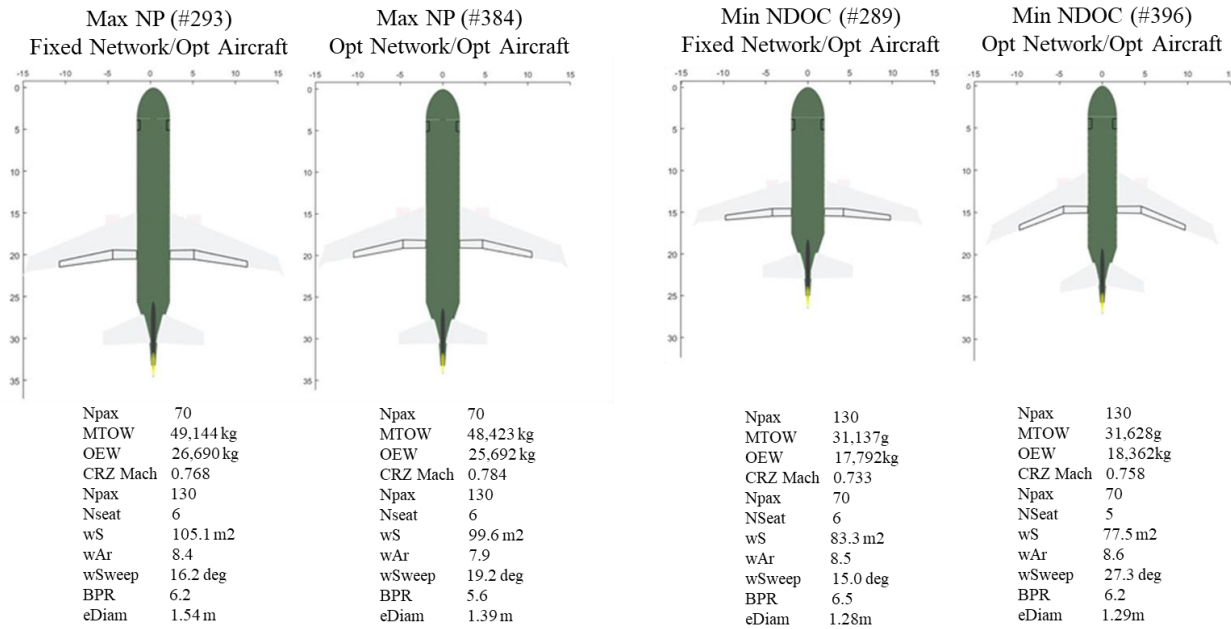


Figure 4.10: Extreme designs – Fixed Network x Optimum Network (5 airports)

From Fig. 4.9 it is observed that the Pareto front related to the integrated aircraft and network design represents a significant improvement on network profit values when compared with the fixed network /optimum aircraft and reference aircraft designs. However, it is also observed slight increase on NDOC (shifting the curve to the right), possibly due to reduction of the number connected city pairs which impacts on the total distance flown in the network, also observed in the optimized network simulation (Session 4.2). In addition, the aircraft produced in the integrated optimization were slightly heavier than the ones optimized form the fixed network case, which may have also contributed on the NDOC shift to the right.

From the aircraft design perspective, the two extreme aircraft designs obtained in the integrated optimization presented identical cabin capacity when compared with the optimum designs obtained in the fixed network case. The major difference between both scenarios is that the integrated designs present a cruise speed approximately 0.02 Mach higher than the fixed network/optimum aircraft. This fact explains the wing increased sweepback angle on these aircraft, which is demonstrated to be a suitable solution to reduce the wave drag, naturally increased at higher Mach numbers given the same airfoil profiles [23] [142]. Other interesting observation is the reduction of wings reference area in the integrated designs, which direct consequence is the skin drag reduction. These two aspects combined have negative impact on fuel flow, which is aligned with the DOC reduction objective.

In the network side, it is also observed the optimum network providing less city-pair connections when the aircraft size increases, since the demand is exhausted with reduced number of frequencies. In these cases, the longest sectors are switched off, due to the lower demand determined by the gravitational model, with consequent decrease of the average path length and network density. This effect is illustrated in Figures 4.11a, 4.11b and 4.11c showing the three different network topologies obtained in the Pareto front. It is noticeable the direct relationship between aircraft capacity and number of connections. City-pair daily frequencies from sample aircraft at each group are also displayed to illustrate such effects. Non-connected sectors are displayed in red lines and zeros in the frequency tables.

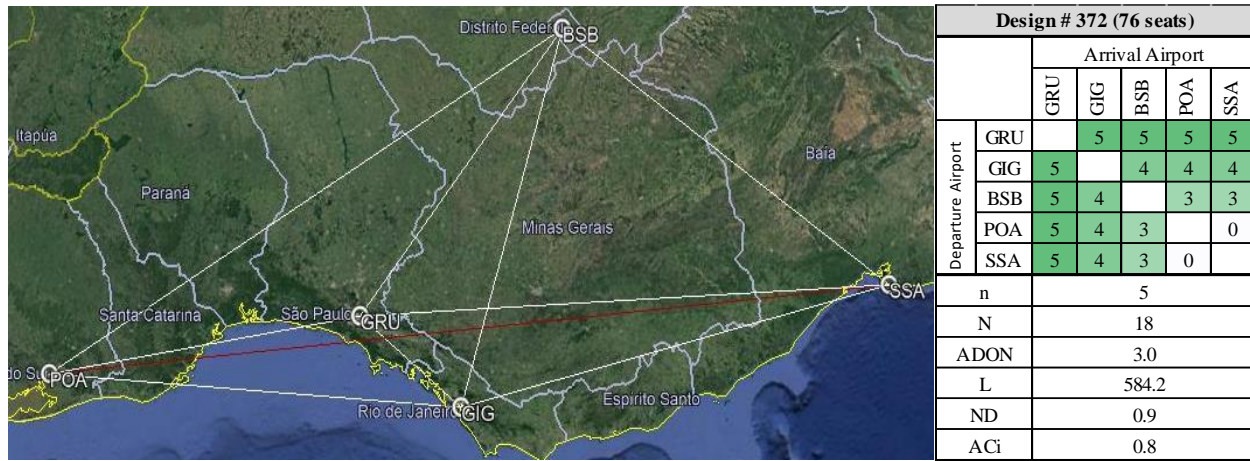


Figure 4.11a: Optimum Network type #1 - 70 to 109 seats aircraft (5 airports)

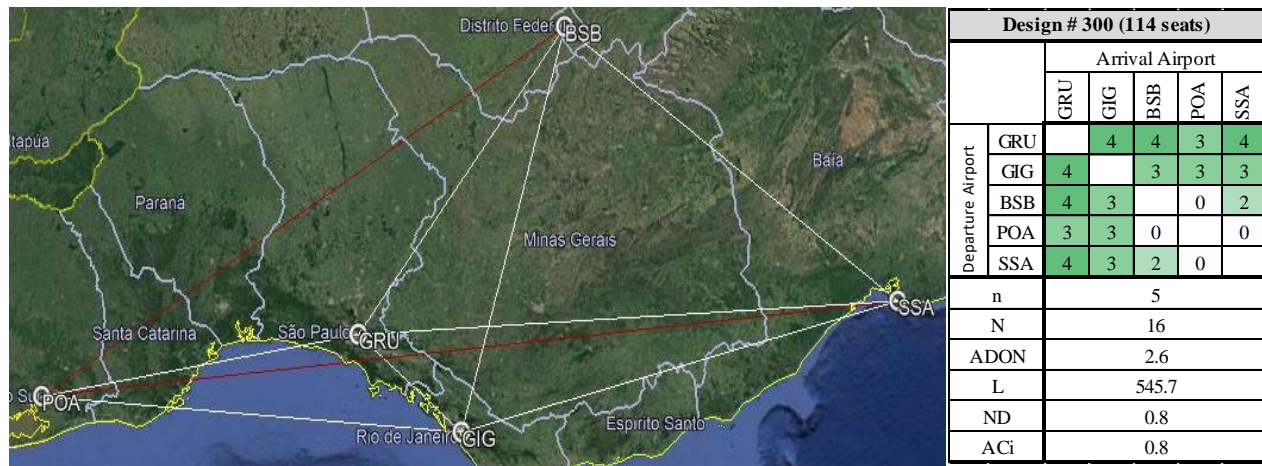


Figure 4.11b: Optimum Network type #2 – 113 and 114 seats aircraft (5 airports)

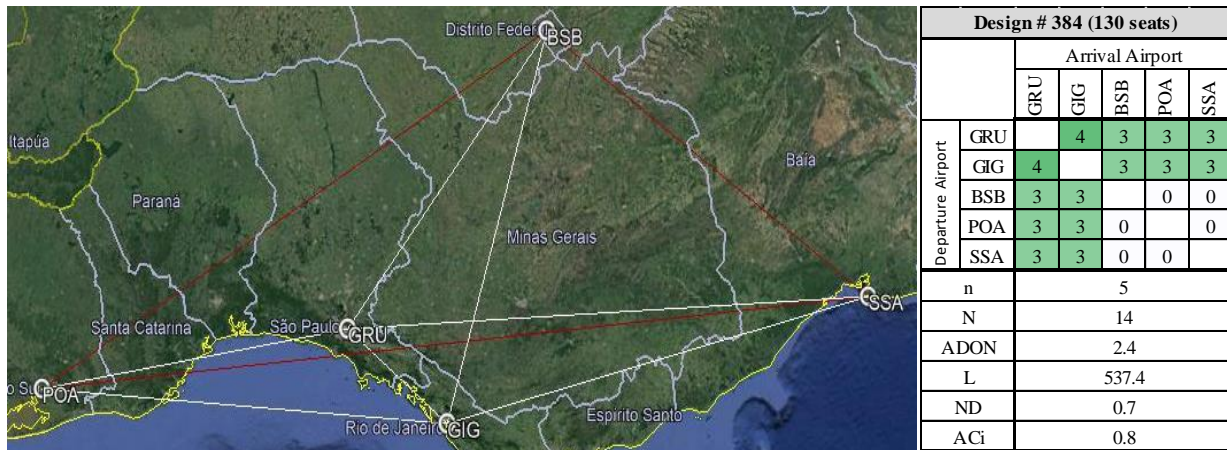


Figure 4.11c: Optimum Network type #3 – 130 seats aircraft (5 airports)

Tables 4.11a, 4.11b, 4.11c and 4.11d show the impact of the integrated optimum aircraft and network on the key airline economic indicators, compared with the fixed network/optimum and baseline aircrafts results.

It may be observed that the integrated design brought in both cases a slight increase in NDOC (0.7%) and significant in NP (282.4%), even transporting less passengers, when compared with the fixed network/optimum aircraft design. When compared with the baseline aircraft, these differences are even bigger (-11.3% on NDOC and 1104.1% on NP), showing the total improvement potential of the integrated optimization related to the conventional case of a given aircraft in a fixed network. As in the optimized network case, such improvement is caused by reduction of number of city-pairs connected (and associated frequencies) due to lower demands calculated by the gravitational model. Although the largest annual profit difference is obtained for the minimum NDOC case (9.2Million US\$/year), it must be again noted that the annual profit is also slightly lower in the NP scenario (-1.5%) than the optimum aircraft/fixed network.

Once again, it is observed a lower number of frequencies significantly impacting on the reduction of fleet size and consequently a lower CAPEX, with faster return of investments. The largest CAPEX difference is obtained in the maximum NP case (-98.4 Million US\$), confirming that the inclusion of such parameter as objective function to be minimized may bring an extra financial advantage to the airlines, specifically when defining their fleet acquisition plan. In addition, when compared with the baseline aircraft, the CAPEX difference reaches an expressive reduction in the maximum NP scenario (-40.3%), suggesting that the acquisition of the baseline aircraft may not represent a financial advantage for the airline, although producing some level of profit some level of profit.

Table 4.11a: Min NDOC - Integrated optimization x fixed network (5 airports)

| Key Parameter | Fixed Network/ Optimum Aircraft | Optimum Network/ Optimum Aircraft | Difference | |
|--------------------------------------|------------------------------------|--------------------------------------|----------------|-------------|
| Total Distance flown [nm]/day | 59,604 | 53,865 | -5,739 | -9.6% |
| Total Passengers /day | 5,038 | 4,866 | -172 | -3.4% |
| Total Cost [US\$]/day | \$575,432.82 | \$527,554.35 | \$-47,878.48 | -8.3% |
| Total Revenue [US\$]/day | \$665,016.00 | \$642,312.00 | \$-22,704.00 | -3.4% |
| Profit [US\$]/day | \$89,583.18 | \$114,757.65 | \$25,174.48 | 28.1% |
| Annual Profit [US\$] | 2,697,859.82 | 41,886,543.75 | \$9,188,683.92 | 28.1% |
| Operational Margin [%] | 15.6 | 23.0 | 7.4 | 47.4% |
| NDOC [US\$/nm] | 7.62 | 7.67 | 0.05 | 0.7% |
| NP (US\$/pax.nm)x10E-4 | 2.98 | 4.38 | 1.39 | 46.8% |
| NPV [US\$]x 10E9 | 3.0 | 2.3 | -0.1 | -2.7% |
| Aircraft Price [US\$ x 10E6] | 31.8 | 31.1 | -0.7 | -2.3% |
| Number of Frequencies | 94 | 96 | 2 | 2.1% |

| | | | | |
|---|-------|-------|-------|--------|
| Estimated Fleet size (# of aircraft) | 14 | 13 | -1 | -7.1% |
| Sectors per aircraft per day | 6 | 7 | 1 | 16.7% |
| CAPEX [US\$ x 10E6] | 445.9 | 404.5 | -41.4 | -9.3% |
| Return of Investment [years] | 13.6 | 9.7 | -4.0 | -29.2% |

Table 4.11b: Min NDOC - Integrated optimization x fixed network baseline (5 airports)

| Key Parameter | Fixed Network/ Baseline Aircraft | Optimum Network/ Optimum Aircraft | Difference | |
|---|-------------------------------------|--------------------------------------|-----------------|---------------|
| Total Distance flown [nm]/day | 57,141 | 53,865 | -3,276 | -5.7% |
| Total Passengers /day | 5,075 | 4,866 | -209 | -4.1% |
| Total Cost [US\$/day] | \$616,052.60 | \$527,554.35 | \$-88,498.26 | -14.4% |
| Total Revenue [US\$]/day | \$669,900.00 | \$642,312.00 | \$-27,588.00 | -4.1% |
| Profit [US\$]/day | \$53,847.40 | \$114,757.65 | \$60,910.26 | 113.1% |
| Annual Profit [US\$] | \$19,654,300.12 | \$41,886,543.75 | \$22,232,243.62 | 113.1% |
| Operational Margin [%] | 8.7 | 23.0 | 14.2 | 162.6% |
| NDOC [US\$/nm] | 8.65 | 7.67 | -0.98 | -11.3% |
| NP (US\$/pax.nm)x10E-4 | 1.86 | 4.38 | 2.52 | 135.8% |
| NPV [US\$]x 10E9 | 3.0 | 2.3 | -0.8 | -25.1% |
| Aircraft Price [US\$ x 10E6] | 35.9 | 31.1 | -4.7 | -13.2% |
| Number of Frequencies | 91 | 96 | 5 | 5.5% |
| Estimated Fleet size (# of aircraft) | 13 | 13 | 0 | 0.0% |
| Sectors per aircraft per day | 7 | 7 | 0 | 0.0% |
| CAPEX [US\$ x 10E6] | 466.1 | 404.5 | -61.6 | -13.2% |
| Return of Investment [years] | 23.7 | 9.7 | -14.1 | -59.3% |

Table 4.11c: Max NP - Integrated optimization x fixed network (5 airports)

| Key Parameter | Fixed Network/ Optimum Aircraft | Optimum Network/ Optimum Aircraft | Difference | |
|---|------------------------------------|--------------------------------------|-----------------|---------------|
| Total Distance flown [nm]/day | 34,078 | 22,946 | -11,132 | -32.7% |
| Total Passengers /day | 5,218 | 4,106 | -1,112 | -21.3% |
| Total Cost [US\$/day] | \$474,277.49 | \$332,310.22 | \$-141,967.27 | -29.9% |
| Total Revenue [US\$]/day | \$688,776.00 | \$543,576.00 | \$-145,200.00 | -21.1% |
| Profit [US\$]/day | \$214,498.51 | \$211,265.78 | \$-3,232.73 | -1.5% |
| Annual Profit [US\$] | 78,291,955.09 | \$77,112,008.75 | \$-1,179,946.34 | -1.5% |
| Operational Margin [%] | 11.1 | 63.6 | 52.4 | 470.3% |
| NDOC [US\$/nm] | 8.40 | 11.39 | 2.99 | 35.6% |
| NP (US\$/pax.nm)x10E-4 | 5.85 | 22.36 | 16.51 | 282.4% |
| NPV [US\$]x 10E9 | 4.0 | 4.0 | 0.0 | -0.1% |
| Aircraft Price [US\$ x 10E6] | 47.1 | 46.4 | -0.7 | -1.5% |
| Number of Frequencies | 56 | 44 | -12 | -21.4% |
| Estimated Fleet size (# of aircraft) | 8 | 6 | -2 | -25.0% |
| Sectors per aircraft per day | 7 | 7 | 0.0 | 0.0% |
| CAPEX [US\$ x 10E6] | 376.8 | 278.4 | -98.4 | -26.1% |
| Return of Investment [years] | 4.8 | 3.6 | -1.2 | -25.0% |

Table 4.11d: Max NP - Integrated optimization x fixed network baseline aircraft (5 airports)

| Key Parameter | Fixed Network/ Baseline Aircraft | Optimum Network/ Optimum Aircraft | Difference | |
|---|-------------------------------------|--------------------------------------|-----------------|---------|
| Total Distance flown [nm]/day | 57,141 | 22,946 | -34,195 | -59.8% |
| Total Passengers /day | 5,075 | 4,106 | -969 | -19.1% |
| Total Cost [US\$/day] | \$616,052.60 | \$332,310.22 | \$-283,742.38 | -46.1% |
| Total Revenue [US\$/day] | \$669,900.00 | \$543,576.00 | \$-126,324.00 | -18.9% |
| Profit [US\$]/day | \$53,847.40 | \$211,265.78 | \$157,418.38 | 292.3% |
| Annual Profit [US\$] | \$19,654,300.12 | \$77,112,008.75 | \$57,457,708.63 | 292.3% |
| Operational Margin [%] | 8.7 | 63.6 | 54.8 | 627.3% |
| NDOC [US\$/nm] | 8.65 | 11.39 | 2.74 | 31.6% |
| NP (US\$/pax.nm)x10E-4 | 1.86 | 22.36 | 20.50 | 1104.1% |
| NPV [US\$]x 10E9 | 3.0 | 4.0 | 0.9 | 31.3% |
| Aircraft Price [US\$ x 10E6] | 35.9 | 46.4 | 10.5 | 29.4% |
| Number of Frequencies | 91 | 44 | -47 | -51.6% |
| Estimated Fleet size (# of aircraft) | 13 | 6 | -7 | -53.8% |
| Sectors per aircraft per day | 7 | 7 | 0.0 | 0.0% |
| CAPEX [US\$ x 10E6] | 466.1 | 278.4 | -187.7 | -40.3% |
| Return of Investment [years] | 23.7 | 3.6 | -20.1 | -84.8% |

Ten airports network case

With the objective to check the robustness and performance of the integrated optimization framework in a wider scenario, a second simulation was performed considering ten airports in the airline network , under the same operational conditions. For that, the following five additional airports were included in the previous simulated network: CNF (Belo Horizonte/Tancredo Neves International), CWB (Curitiba/ Afonso Pena International) , FOR (Fortaleza/Pinto Martins International), REC (Recife/Teotônio Vilela International) and MAO (Manaus/Eduardo Gomes International). The airport geometric and econometric data, route distances and magnetic headings related to these new airports are displayed in Appendix B (Tables B.1, B2, B.3 and B.4). Calculated passenger's demand for all airports are displayed in Table 4.12.

Table 4.12: Route passenger's demand per day (10% market share) – 10 airports

| Departure Airport (i) | Arrival Airport (j) | | | | | | | | | |
|-----------------------|---------------------|-----|-----|-----|-----|-----|-----|-----|-----|-----|
| | BSB | CNF | CWB | FOR | GIG | GRU | MAO | POA | REC | SSA |
| BSB | - | 205 | 253 | 288 | 282 | 342 | 164 | 228 | 232 | 238 |
| CNF | 205 | - | 236 | 269 | 250 | 310 | 148 | 213 | 216 | 214 |
| CWB | 253 | 236 | - | 330 | 313 | 367 | 192 | 242 | 265 | 278 |
| FOR | 288 | 269 | 330 | - | 365 | 446 | 204 | 295 | 278 | 294 |
| GIG | 282 | 250 | 313 | 365 | - | 411 | 204 | 283 | 293 | 295 |
| GRU | 342 | 310 | 367 | 446 | 411 | - | 252 | 339 | 358 | 366 |
| MAO | 164 | 148 | 192 | 204 | 204 | 252 | - | 169 | 166 | 159 |
| POA | 228 | 213 | 242 | 295 | 283 | 339 | 169 | - | 237 | 247 |
| REC | 232 | 216 | 265 | 278 | 293 | 358 | 166 | 237 | - | 233 |
| SSA | 238 | 214 | 278 | 294 | 295 | 366 | 159 | 247 | 233 | - |

Two simulation scenarios were conducted: fixed network/optimum (all airports connected) aircraft and optimum network/ optimum aircraft, considering the same DOE and operational

conditions used in previous five-airports simulations. Appendix E and F show the DOE and all design variables calculated by the GA for each individual generated and all designs generated for both scenarios. The computational performance of such scenarios is shown in Table 4.13, together with the five-airports cases, for comparison. From this table, it is concluded that the computation time per cycle was increased more than three and a half times in the ten airports scenario, mostly influenced by the number of mission profiles calculated on each cycle. In fact, this value is function of the mission performance computation time (which takes approximately 8 seconds to run one route) and proportional to the factor $N(N-1)$, where N is the number of airports connected, achieving this limit at the fully connected network case. This leads the conclusion that possibly the computational costs may represent a challenge with an increasing number of airports in the network.

Table 4.13: Computational performance of all simulations

| Scenarios | | Number of Generations | Failed Designs | Average Population Size | Total Optimization time [h] | Average Calculation cycle time [min] | Average Mission computing time [min] |
|--------------------|---|-----------------------|----------------|-------------------------|-----------------------------|--------------------------------------|--------------------------------------|
| 10 Airports | Fixed network & Optimum aircraft | 295 | 90 (30.5%) | 16 | 71.865 | 14.6 | 12.0 |
| | Optimum network & Optimum aircraft | 277 | 61 (22.0%) | 15 | 73.841 | 16.0 | 5.5 |
| 5 Airports | Fixed network & Optimum aircraft | 302 | 73 (24.2%) | 15 | 19.156 | 3.8 | 2.7 |
| | Optimum network & Optimum aircraft | 338 | 99 (29.3%) | 17 | 21.439 | 4.8 | 2.3 |

Fig. 4.12 shows the relative position of the baseline aircraft regarding the pareto front produced from fixed and optimized networks. Once again, significant improvements are observed in both identified design extremes: maximum NP (130 pax / 6 seats abreast) and min NDOC (71 pax / 5 seats abreast) . The baseline aircraft with the related fixed network scenario is also shown for comparison. This confirms the effectiveness of the optimization framework in a larger scale network, also obtained in the five-airports case. Figures 4.13a, 4.13b and 4.13c show the integrated optimized network and aircraft characteristics for the pareto extremes and optimized baseline aircraft. As also observed in the five airports network case, the smaller capacity aircraft (baseline and minimum NDOC) develop more frequencies and more connected networks. For the higher capacity aircraft (maximum NP) unprofitable routes are switched off, leading to a lower density network.

And finally, Tables 4.13a, 4.13b, 4.13c and 4.14d show the impact of the integrated optimum aircraft and network on the key airline economic indicators, compared with the fixed and optimum network baseline aircraft results. As verified in the five-airports case, the integrated optimization

also brought a significant increase on network profit as consequence of the reduction of connecting sectors and decrease on fleet size. As in the five airports case, this leads the reduction of fleet's CAPEX and return of investment for airlines. The integrated optimization also demonstrated a potential to reduce the NDOC by -15% and increase the network profit up to 237,5% related to the baseline aircraft in fixed network (fully connected).

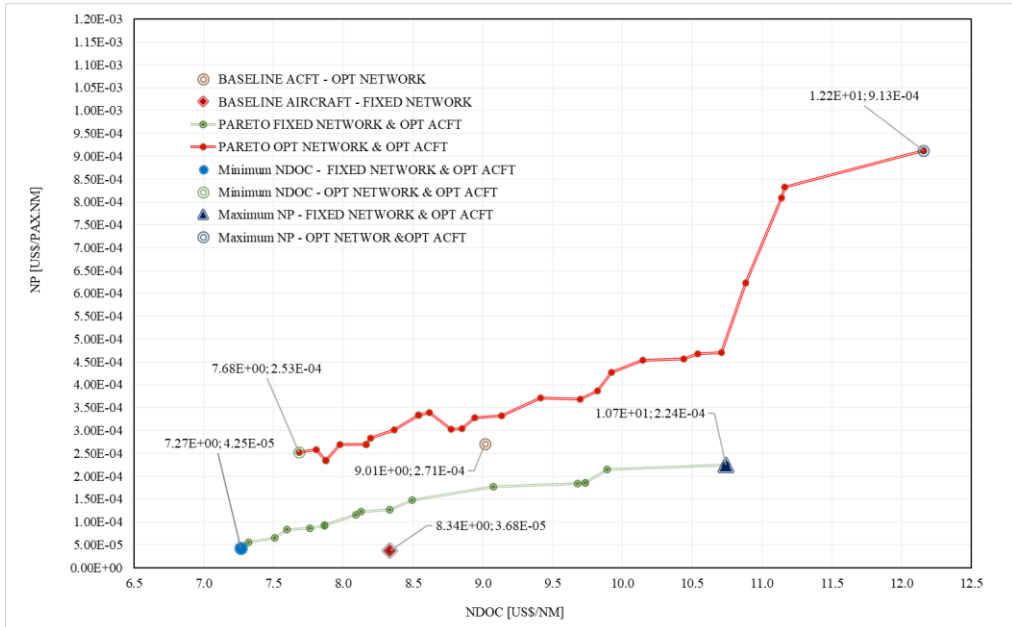


Figure 4.12: Integrated aircraft and network optimization Pareto front (10 airports)

| Network Frequencies and Characteristics | | | | | | | | | | | Aircraft Data | | |
|---|-----|-----------------|-----|-----|-----|-----|-----|-----|-----|-----|---------------|----------------------|--------|
| | | Arrival Airport | | | | | | | | | | | |
| | | BSB | CNF | CWB | FOR | GIG | GRU | MAO | POA | REC | SSA | Npax | 78 |
| Departure Airport | BSB | | 3 | 4 | 4 | 4 | 5 | 0 | 3 | 4 | 4 | Nseat | 4 |
| | CNF | 3 | | 4 | 0 | 4 | 5 | 0 | 3 | 3 | 3 | MTOW[kg] | 36,831 |
| | CWB | 4 | 4 | | 0 | 5 | 6 | 0 | 4 | 0 | 0 | wS [m ²] | 72.72 |
| | FOR | 4 | 0 | 0 | | 0 | 0 | 0 | 0 | 4 | 4 | wAR | 8.6 |
| | GIG | 4 | 4 | 5 | 0 | | 6 | 0 | 4 | 0 | 4 | wTR | 0.29 |
| | GRU | 5 | 5 | 6 | 0 | 6 | | 0 | 5 | 0 | 6 | wsweep [°] | 26.5 |
| | MAO | 0 | 0 | 0 | 0 | 0 | 0 | | 0 | 0 | 0 | wTwist [°] | -4.5 |
| | POA | 3 | 3 | 4 | 0 | 4 | 5 | 0 | | 0 | 0 | Kink | 0.34 |
| | REC | 4 | 3 | 0 | 4 | 0 | 0 | 0 | 0 | | 4 | BPR | 5.00 |
| | SSA | 4 | 3 | 0 | 4 | 4 | 6 | 0 | 0 | 4 | | eDiam [m] | 1.36 |
| n | | | | | | | | | | | | OPR | 28.5 |
| N | | | | | | | | | | | | eITT [K] | 1450 |
| ADON | | | | | | | | | | | | FPR | 1.46 |
| L [nm] | | | | | | | | | | | | Range [nm] | 1600 |
| ND | | | | | | | | | | | | TOT NOISE [dBA] | 261.6 |
| ACi | | | | | | | | | | | | CRZ MACH | 0.795 |



Figure 4.13a: Baseline - optimized network and aircraft characteristics (10 airports)

| NETWORK FREQUENCIES AND CHARACTERISTICS | | | | | | | | | | AIRCRAFT DATA | | Minimum NDOC Aircraft | | |
|---|-----------------|-----|-----|-----|-----|-----|-----|-----|-----|---|----------------------|-----------------------|--|--|
| | Arrival Airport | | | | | | | | | Npax | 71 | | | |
| Departure Airport | BSB | CNF | CWB | FOR | GIG | GRU | MAO | POA | REC | SSA | Nseat | 5 | | |
| BSB | 3 | 4 | 5 | 5 | 6 | 3 | 4 | 4 | 4 | 4 | MTOW [kg] | 31,440 | | |
| CNF | 3 | | 4 | 4 | 4 | 5 | 0 | 4 | 4 | 4 | wS [m ²] | 77.52381 | | |
| CWB | 4 | 4 | | 0 | 5 | 6 | 0 | 4 | 0 | 5 | wAR | 8.6 | | |
| FOR | 5 | 4 | 0 | | 6 | 0 | 0 | 0 | 5 | 5 | wTR | 0.33 | | |
| GIG | 5 | 4 | 5 | 6 | | 7 | 0 | 5 | 5 | 5 | wSweep [°] | 22.8 | | |
| GRU | 6 | 5 | 6 | 0 | 7 | | 0 | 6 | 6 | 6 | wTwist [°] | -4.3 | | |
| MAO | 3 | 0 | 0 | 0 | 0 | 0 | | 0 | 0 | 0 | Kink | 0.38 | | |
| POA | 4 | 4 | 4 | 0 | 5 | 6 | 0 | | 0 | 0 | BPR | 6.2 | | |
| REC | 4 | 4 | 0 | 5 | 5 | 6 | 0 | 0 | | 4 | eDiam [m] | 1.28 | | |
| SSA | 4 | 4 | 5 | 5 | 5 | 6 | 0 | 0 | 0 | 4 | OPR | 24.7 | | |
| n | 10 | | | | | | | | | eITT [K] | 1429 | | | |
| N | 62 | | | | | | | | | FPR | 1.6 | | | |
| ADON | 5.5 | | | | | | | | | Range [nm] | 1600 | | | |
| L | 640.7 | | | | | | | | | TOT NOISE [dBA] | 239.9 | | | |
| ND | 0.69 | | | | | | | | | CRZ MACH | 0.742 | | | |
| ACi | 0.90 | | | | | | | | | NDOC [US\$/nm] 7.68 NP (US\$/pax.nm)x1E-4 2.53 NPV [US\$x1E9] 2.3 | | | | |



Figure 4.13b: Min NDOC – integrated network and aircraft optimization (10 airports)

| NETWORK FREQUENCIES AND CHARACTERISTICS | | | | | | | | | | | AIRCRAFT DATA | | Maximum NP Aircraft | |
|---|-----------------|-----|-----|-----|-----|-----|-----|-----|-----|-----|----------------------|----------|---------------------|--|
| | Arrival Airport | | | | | | | | | | Npax | 130 | | |
| | BSB | CNF | CWB | FOR | GIG | GRU | MAO | POA | REC | SSA | Nseat | 6 | | |
| Departure Airport | BSB | 0 | 0 | 3 | 0 | 3 | 0 | 0 | 0 | 0 | | | | |
| | CNF | 0 | 0 | 0 | 0 | 3 | 0 | 0 | 0 | 0 | MTOW [kg] | 54,106 | | |
| | CWB | 0 | 0 | 0 | 3 | 3 | 0 | 0 | 0 | 0 | wS [m ²] | 107.9048 | | |
| | FOR | 3 | 0 | 0 | 3 | 4 | 0 | 0 | 0 | 3 | wAR | 9.5 | | |
| | GIG | 0 | 0 | 3 | 3 | 4 | 0 | 0 | 0 | 3 | wTR | 0.42 | | |
| | GRU | 3 | 3 | 3 | 4 | 4 | 0 | 3 | 3 | 3 | wSweep [°] | 26.1 | | |
| | MAO | 0 | 0 | 0 | 0 | 0 | 0 | 0 | 0 | 0 | wTwist [°] | -2.6 | | |
| | POA | 0 | 0 | 0 | 0 | 3 | 3 | 0 | 0 | 0 | Kink | 0.33 | | |
| | REC | 0 | 0 | 0 | 0 | 3 | 3 | 0 | 0 | 0 | BPR | 5.0 | | |
| | SSA | 0 | 0 | 0 | 3 | 3 | 3 | 0 | 0 | 0 | eDiam [m] | 1.6 | | |
| n | 10 | | | | | | | | | | OPR | 24.7 | | |
| N | 29 | | | | | | | | | | eITT [K] | 1471 | | |
| ADON | 2.6 | | | | | | | | | | FPR | 1.6 | | |
| L | 690.6 | | | | | | | | | | Range [nm] | 1600 | | |
| ND | 0.32 | | | | | | | | | | TOT NOISE [dBA] | 258.8 | | |
| ACi | 0.34 | | | | | | | | | | CRZ MACH | 0.790 | | |

NDOC [US\$/nm] 12.16
NP (US\$pax.nm)x1E-4 9.13
NPV [US\$xE9] 4.6



Figure 4.13c: Max NP – integrated network and aircraft optimization (10 airports)**Table 4.14a:** Min NDOC - Integrated optimization x fixed network baseline (10 airports)

| Key parameter | Fixed Network/ Baseline Aircraft | Optimum Network/ Optimum Aircraft | Difference | |
|--------------------------------------|-------------------------------------|--------------------------------------|------------------|--------|
| Total Distance flown [nm]/day | 315,903 | 187,269 | -128,634 | -40.7% |
| Total Passengers /day | 20,286 | 14,964 | -5,322 | -26.2% |
| Total Cost [US\$/]/day | \$3,111,230.45 | \$1,760,299.05 | \$-1,350,931.40 | -43.4% |
| Total Revenue [US\$]/day | \$3,347,190.00 | \$2,469,060.00 | \$-878,130.00 | -26.2% |
| Profit [US\$]/day | \$235,959.55 | \$708,760.95 | \$472,801.40 | 200.4% |
| Annual Profit [US\$] | 86,125,234.47 | \$258,697,746.28 | \$172,572,511.80 | 200.4% |
| Operational Margin [%] | 7.6 | 40.3 | 32.7 | 430.9% |
| NDOC [US\$/nm] | 8.34 | 7.68 | -0.65 | -7.8% |
| NP (US\$/pax.nm)x10E-4 | 3.68 | 2.53 | -1.15 | -31.3% |
| NPV [US\$]x 10E9 | 3.0 | 2.3 | -0.7 | -24.2% |
| Aircraft Price [US\$ x 10E6] | 35.9 | 31.9 | -3.9 | -10.9% |
| Number of Frequencies | 363 | 294 | -69 | -19.0% |
| Estimated Fleet size (# of aircraft) | 67 | 44 | -23 | -34.3% |
| Sectors per aircraft per day | 5 | 6 | 1 | 20.0% |
| CAPEX [US\$ x 10E6] | 2402.2 | 1405.0 | -997.2 | -41.5% |
| Return of Investment [years] | 27.9 | 5.4 | -22.5 | -80.5% |

Table 4.14b: Min NDOC - Integrated optimization x optimum network baseline (10 airports)

| Key parameter | Fixed Network/ Baseline Aircraft | Optimum Network/ Optimum Aircraft | Difference | |
|--------------------------------------|-------------------------------------|--------------------------------------|----------------|--------|
| Total Distance flown [nm]/day | 107,806 | 187,269 | 79,463 | 73.7% |
| Total Passengers /day | 11,760 | 14,964 | 3,204 | 27.2% |
| Total Cost [US\$/]/day | \$1,209,380.20 | \$1,760,299.05 | \$550,918.85 | 45.6% |
| Total Revenue [US\$]/day | \$1,552,320.00 | \$2,469,060.00 | \$916,740.00 | 59.1% |
| Profit [US\$]/day | \$342,939.80 | \$708,760.95 | \$365,821.15 | 106.7% |
| Annual Profit [US\$] | 125,173,026.12 | \$258,697,746.28 | 133,524,720.15 | 106.7% |
| Operational Margin [%] | 28.4 | 40.3 | 11.9 | 42.0% |
| NDOC [US\$/nm] | 9.01 | 7.68 | -1.33 | -14.7% |
| NP (US\$/pax.nm)x10E-4 | 2.71 | 2.53 | -0.18 | -6.5% |
| Aircraft Price [US\$ x 10E6] | 35.9 | 31.9 | -3.9 | -10.9% |
| NPV [US\$]x 10E9 | 3.0 | 2.3 | -0.7 | -24.2% |
| Number of Frequencies | 210 | 294 | 84 | 40.0% |
| Estimated Fleet size (# of aircraft) | 26 | 44 | 18 | 69.2% |
| Sectors per aircraft per day | 8 | 6 | -2 | -25.0% |
| CAPEX [US\$ x 10E6] | 932.1 | 1405.0 | 472.9 | 50.7% |
| Return of Investment [years] | 7.4 | 5.4 | -2.0 | -27.1% |

Table 4.14c: Max NP - Integrated optimization x fixed network baseline (10 airports)

| Key Parameter | Fixed Network/ Baseline Aircraft | Optimum Network/ Optimum Aircraft | Difference | |
|--------------------------------------|-------------------------------------|--------------------------------------|-----------------|--------|
| Total Distance flown [nm]/day | 315,903 | 63,065 | -252,838 | -80.0% |
| Total Passengers /day | 20,286 | 8,554 | -11,732 | -57.8% |
| Total Cost [US\$]/day | \$3,111,230.45 | \$918,908.15 | \$-2,192,322.30 | -70.5% |
| Total Revenue [US\$]/day | \$3,347,190.00 | \$1,411,410.00 | \$-1,935,780.00 | -57.8% |
| Profit [US\$]/day | \$235,959.55 | \$492,501.85 | \$256,542.30 | 108.7% |
| Annual Profit [US\$] | \$86,125,234.47 | \$179,763,173.57 | \$93,637,939.10 | 108.7% |
| Operational Margin [%] | 7.6 | 53.6 | 46.0 | 606.7% |
| NDOC [US\$/nm] | 8.34 | 12.16 | 3.82 | 45.8% |
| NP (US\$/pax.nm)x10E-4 | 3.68 | 9.13 | 5.45 | 148.1% |
| NPV [US\$]x 10E9 | 3.0 | 4.7 | 1.7 | 55.2% |
| Aircraft Price [US\$ x 10E6] | 35.9 | 51.5 | 15.7 | 43.8% |
| Number of Frequencies | 363 | 91 | -272 | -74.9% |
| Estimated Fleet size (# of aircraft) | 67 | 14 | -53 | -79.1% |
| Sectors per aircraft per day | 5 | 6 | 1.0 | 20.0% |
| CAPEX [US\$ x 10E6] | 2402.2 | 721.7 | -1680.5 | -70.0% |
| Return of Investment [years] | 27.9 | 4.0 | -23.9 | -85.6% |

Table 4.14d: Max NP - Integrated optimization x optimum network baseline (10 airports)

| Key Parameter | Fixed Network/ Baseline Aircraft | Optimum Network/ Optimum Aircraft | Difference | |
|--------------------------------------|-------------------------------------|--------------------------------------|-----------------|--------|
| Total Distance flown [nm]/day | 107,806 | 63,065 | -44,741 | -41.5% |
| Total Passengers /day | 11,760 | 8,554 | -3,206 | -27.3% |
| Total Cost [US\$]/day | \$1,209,380.20 | \$918,908.15 | \$-290,472.05 | -24.0% |
| Total Revenue [US\$]/day | \$1,552,320.00 | \$1,411,410.00 | \$-140,910.00 | -9.1% |
| Profit [US\$]/day | \$342,939.80 | \$492,501.85 | \$149,562.05 | 43.6% |
| Annual Profit [US\$] | 125,173,026.12 | \$179,763,173.57 | \$54,590,147.45 | 43.6% |
| Operational Margin [%] | 28.4 | 53.6 | 25.2 | 89.1% |
| NDOC [US\$/nm] | 9.01 | 12.16 | 3.14 | 34.9% |
| NP (US\$/pax.nm)x10E-4 | 2.71 | 9.13 | 6.42 | 237.5% |
| NPV [US\$]x 10E9 | 3.0 | 4.7 | 1.7 | 55.2% |
| Aircraft Price [US\$ x 10E6] | 35.9 | 51.5 | 15.7 | 43.8% |
| Number of Frequencies | 210 | 91 | -119 | -56.7% |
| Estimated Fleet size (# of aircraft) | 26 | 14 | -12 | -46.2% |
| Sectors per aircraft per day | 8 | 6 | -2.0 | -25.0% |
| CAPEX [US\$ x 10E6] | 932.1 | 721.7 | -210.4 | -22.6% |
| Return of Investment [years] | 7.4 | 4.0 | -3.4 | -46.1% |

4.4 Integrated complex network and aircraft fleet optimization

A classical approach adopted by aircraft manufacturers during sales campaigns is to offer airlines derivations of a certain aircraft type to supply different demand characteristics of proposed aerial networks to be flown. In this process, the aerial networks are set by the airlines and then aircraft manufactures conduct studies with a family of aircrafts, differed by passenger's capacity, which would be, in theory, enough to attend the demand characteristics of each network. For example, the Airbus 320CEO family presents the seating capacities across models varying within a range from 107 seats (A318) to 220 seats (A321) [209], commonly offered to attend regional or continental networks up to 2,200 nm range. In such families, design differences are set to minimal to keep communality on maintenance, operations and production costs. Normally wing geometries,

cockpits and fuselage cross sections are kept the same and engines are offered in one type variant with multiple maximum thrust selections. Of course, fuselage length is increased according to seating capacity.

As stated in Chapter 1, the major concern of such approach is that aircraft types are generally not optimized for specific airline networks, since their designs are already developed for a certain mission profile that might be very different from airline's reality. As result, the aircraft selected leads, most of the times, to a sub-optimum solution for maximum network profit. In addition, as shown in topics 4.1, 4.2 and 4.3, the maximum profit not necessary happens when all network demand is exhausted, since the aircraft design influences on the operational costs, turning unprofitable some sectors. Other factors such as ticket price, fuel cost, load factor and potential demand may have influence of the optimum network and maximum profit solution.

Under such considerations, the fourth and last step of simulations corresponds to the determination of the optimum aerial networks simultaneously with the optimum three aircraft type fleet (or family), operating within a certain geographical area. The objective functions are selected according to the Airline Operations and Aircraft Manufacturer's optimization set defined as maximization of network profit (NPV), from the airline side and the maximization of manufacturers programs cashflow (NPV), from the manufacturer's side.

Brazil represents a significant aviation market in the world with 112.5 million of passengers transported in 2017, 90.6 million in domestic flights, according to ANAC [210]. The revenue of the major airlines reached US\$ 11.8 billion considering an exchange rate of 3.20 Dollar/Real [210]. In this simulation it is proposed to expand the number of airports to twenty, considering the same geographical area of operations (Brazilian continental territory).

These twenty airports selected are the busiest in the country in terms of annual passenger's movements, according to ANAC [210]. They are: AJU (Aracaju/Santa Maria), BEL(Belém/Val de Caes), BSB(Brasília/Jucelino Kubitscheck Intl), CGH (São Paulo/Congonhas), CNF(Belo Horizonte/Confins), CWB(Curitiba/Afonso Pena Intl), FLN (Florianópolis/Hercílio Luz Intl), FOR (Fortaleza/Pinto Martins), GIG (Rio de Janeiro/Tom Jobim -Galeão Intl), GRU (São Paulo/André Franco Montoro- Guarulhos Intl), GYN (Goiânia/Santa Genoveva), MAO (Eduardo Gomes/Manaus Intl), MCZ (Maceió/Zumbi dos Palmares), NAT (Natal/São Gonçalo do Amarante Intl), POA(Porto Alegre/Salgado Filho Intl), REC (Recife/Guararapes Intl), SDU (Rio de Janeiro/Santos Dumont), SLI (São Luiz/Marechal Cunha Machado Intl), SSA (Salvador/Antônio Carlos Magalhães Intl) and VIX (Vitória/Goiabeiras). The airport geometric and econometric data,

route distances and magnetic headings related to these new airports are displayed in Appendix B (Tables B.1, B2, B.3 and B.4). In this simulation the following operational assumptions are made:

- Average Market Share: 20%
- Average Fuel Price : 1.413 US\$/kg (assuming fuel density of 0.81 kg/l), corresponding to the average fuel price practiced in the Brazilian airports in 2017(ABEAR [203])
- Average ticket price: 120,00 US\$, approximately the average fare applied by the top four Brazilian airlines in 2017 (ABEAR [203]).

The estimated passenger's demand for all airports are displayed in Table 4.15, according to the gravitational model developed applied in previous simulations (items 4.1, 4.2 and 4.3). It is assumed that the total demand at each city pair is split between the three aircraft fleet, proportionally to each design seating capacity, in such way that the aircraft fleet with the largest seating capacity captures the largest share of the demand in each route.

Table 4.15: Estimated Passengers Demand per day (20% Market share) - 20 airports

| Dep Apt (i) | Arrival Airport (j) | | | | | | | | | | | | | | | | | | | |
|-------------|---------------------|-----|-----|------|-----|-----|-----|------|-----|-----|-----|-----|-----|-----|-----|-----|------|-----|-----|-----|
| | AJU | BEL | BSB | CGH | CNF | CWB | FLN | FOR | GIG | GRU | GYN | MAO | MCZ | NAT | POA | REC | SDU | SLI | SSA | VIX |
| AJU | 0 | 324 | 420 | 723 | 385 | 464 | 302 | 450 | 524 | 637 | 345 | 351 | 307 | 328 | 434 | 343 | 594 | 321 | 347 | 220 |
| BEL | 324 | 0 | 411 | 718 | 383 | 465 | 295 | 444 | 525 | 633 | 333 | 278 | 381 | 352 | 429 | 394 | 596 | 256 | 401 | 223 |
| BSB | 420 | 411 | 0 | 834 | 443 | 537 | 357 | 627 | 623 | 734 | 325 | 427 | 503 | 479 | 514 | 525 | 707 | 420 | 533 | 273 |
| CGH | 723 | 718 | 834 | 0 | 720 | 760 | 517 | 1084 | 910 | 0 | 668 | 736 | 861 | 822 | 781 | 898 | 1033 | 734 | 917 | 438 |
| CNF | 385 | 383 | 443 | 720 | 0 | 485 | 318 | 586 | 507 | 631 | 362 | 398 | 462 | 444 | 468 | 484 | 577 | 393 | 477 | 222 |
| CWB | 464 | 465 | 537 | 760 | 485 | 0 | 297 | 691 | 622 | 678 | 429 | 473 | 551 | 524 | 458 | 574 | 705 | 473 | 600 | 290 |
| FLN | 302 | 295 | 357 | 517 | 318 | 297 | 0 | 450 | 407 | 460 | 286 | 300 | 359 | 341 | 284 | 374 | 460 | 303 | 384 | 188 |
| FOR | 450 | 444 | 627 | 1084 | 586 | 691 | 450 | 0 | 795 | 955 | 512 | 496 | 517 | 452 | 642 | 525 | 901 | 425 | 599 | 339 |
| GIG | 524 | 525 | 623 | 910 | 507 | 622 | 407 | 795 | 0 | 796 | 504 | 543 | 626 | 600 | 604 | 654 | 0 | 537 | 658 | 299 |
| GRU | 637 | 633 | 734 | 0 | 631 | 678 | 460 | 955 | 796 | 0 | 588 | 649 | 759 | 724 | 692 | 791 | 904 | 647 | 808 | 385 |
| GYN | 345 | 333 | 325 | 668 | 362 | 429 | 286 | 512 | 504 | 588 | 0 | 343 | 411 | 392 | 412 | 429 | 572 | 342 | 438 | 223 |
| MAO | 351 | 278 | 427 | 736 | 398 | 473 | 300 | 496 | 543 | 649 | 343 | 0 | 413 | 385 | 434 | 428 | 616 | 307 | 431 | 233 |
| MCZ | 307 | 381 | 503 | 861 | 462 | 551 | 359 | 517 | 626 | 759 | 411 | 413 | 0 | 365 | 514 | 363 | 710 | 376 | 441 | 263 |
| NAT | 328 | 352 | 479 | 822 | 444 | 524 | 341 | 452 | 600 | 724 | 392 | 385 | 365 | 0 | 487 | 353 | 680 | 345 | 445 | 255 |
| POA | 434 | 429 | 514 | 781 | 468 | 458 | 284 | 642 | 604 | 692 | 412 | 434 | 514 | 487 | 0 | 534 | 684 | 439 | 560 | 275 |
| REC | 343 | 394 | 525 | 898 | 484 | 574 | 374 | 525 | 654 | 791 | 429 | 428 | 363 | 353 | 534 | 0 | 742 | 388 | 475 | 277 |
| SDU | 594 | 596 | 707 | 1033 | 577 | 705 | 460 | 901 | 0 | 904 | 572 | 616 | 710 | 680 | 684 | 742 | 0 | 609 | 746 | 339 |
| SLI | 321 | 256 | 420 | 734 | 393 | 473 | 303 | 425 | 537 | 647 | 342 | 307 | 376 | 345 | 439 | 388 | 609 | 0 | 407 | 229 |
| SSA | 347 | 401 | 533 | 917 | 477 | 600 | 384 | 599 | 658 | 808 | 438 | 431 | 441 | 445 | 560 | 475 | 746 | 407 | 0 | 271 |
| VIX | 220 | 223 | 273 | 438 | 222 | 290 | 188 | 339 | 299 | 385 | 223 | 233 | 263 | 255 | 275 | 277 | 339 | 229 | 271 | 0 |

Therefore considering the above assumptions, for a given city-pair ij , the total passenger demand f_{ij} (between origin airport i and destination airport j) and given three fleet aircraft capacities (b_1 , b_2 and b_3), the share of the demand to be transported to for each fleet k (f_{ij}^k) is assumed as follows:

$$f_{ij}^1 = \frac{b_1}{b_1+b_2+b_3} f_{ij} \quad (73)$$

$$f_{ij}^2 = \frac{b_2}{b_1+b_2+b_3} f_{ij} \quad (74)$$

$$f_{ij}^3 = \frac{b3}{b1+b1+b3} f_{ij} \quad (75)$$

This demand distribution ensures the highest capacity aircraft fleet will capture the biggest share of the calculated demand between city-pairs.

Since the calculations now consider three aircraft types, each one with its own network and respective network mission analysis calculated properly, it is proposed to adapt the MDO framework described in Chapter 3, with the objective to minimize the computational costs. In fact, the total computational time for all twenty sectors would increase proportionally to the factor $3N(N-1)$ if using the original framework. This would correspond to approximately 12,7 times the total processing time related to the ten airports case. In addition to the aircraft design module takes approximately 7-10 minutes to run, which increases significantly the amount of time in each computational cycle. The adapted optimization framework is shown in Fig.4.14 in which the main idea is to replace the aircraft design module per three aircraft databases, each one corresponding to a group of aircraft. All designs in such databases shall be compliant to the Airplane Design Performance Check described in Session 3.1.5

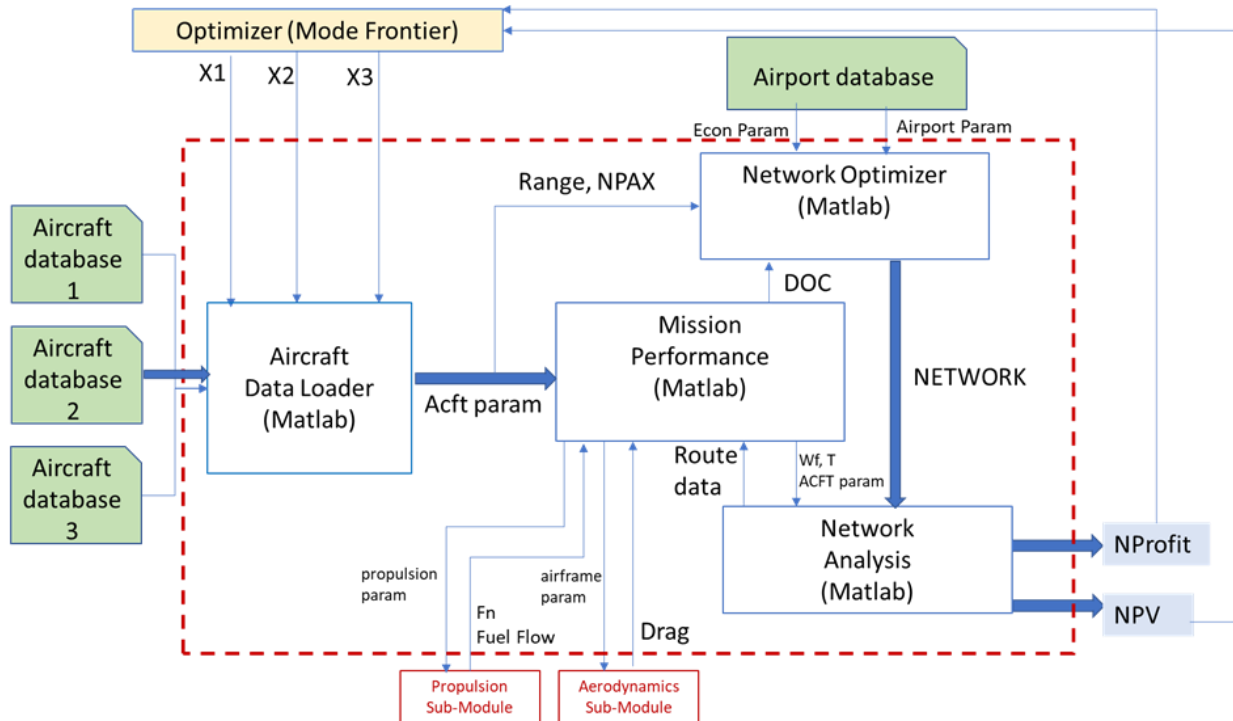


Figure 4.14: Airplane/Network optimization adapted optimization framework (20 airports)

In such way, four MATLAB®-coded sub-modules (three of them derived from the original MDO framework) are embedded into a new Network module, described as follows:

- I. Aircraft data loader – in this module, the aircraft definition parameters (Table 3.7) are retrieved from three selected airplane databases and delivered to the Mission Performance and Network Optimizer modules.
- II. Network optimizer: in this module, the optimum networks related to three airplane types are determined simultaneously based on airport and econometric information (retrieved from a database), aircraft maximum passenger capacity, aircraft design range and associated DOC, as described in Session 3.2.1
- III. Mission performance: in this module the mission fuel burn, trip time, and Direct Operational Cost (DOC) related to origin- destination sectors are calculated, as described in Session 3.2.2
- IV. Network analysis: in this module, fuel burn, trip time and DOC for all sectors are calculated and integrated to calculate the total network profit (NP) and Manufacturer's Cashflow Net Present Value (NPV), as described in Session 3.2.3

These sub-modules are then embedded into new Network module, integrated in a ModeFrontier® optimization framework as shown Fig.4.15. Three constraints are inserted in order to ensure solutions with aircrafts presenting IRR greater than 30%.

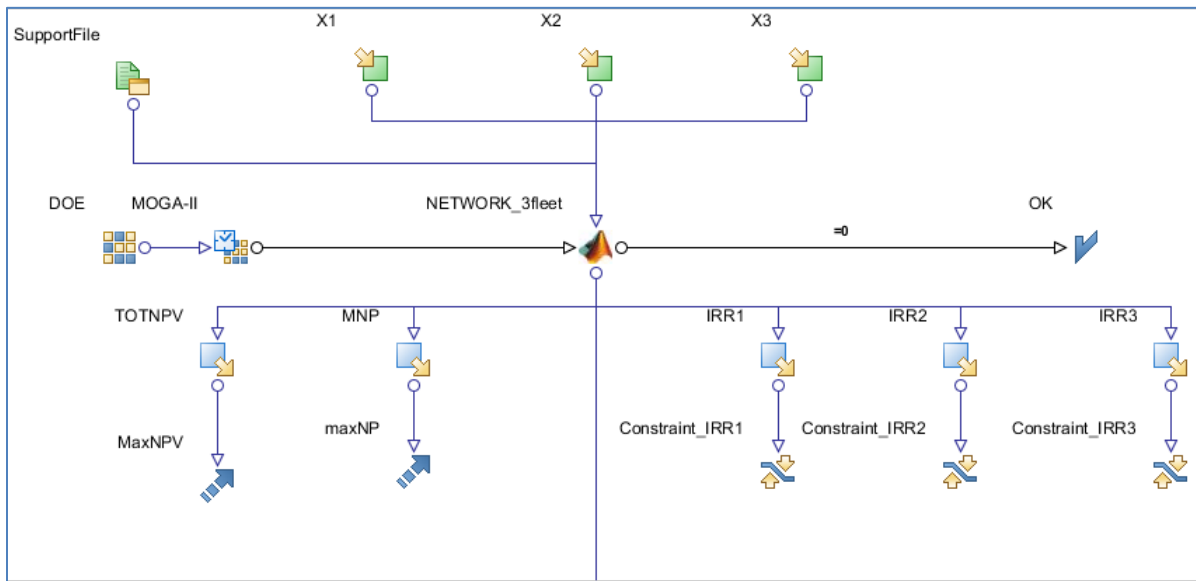


Figure 4.15: ModeFrontier® optimization framework – 20 airports

The aircraft databases, accessed via Support files shown in Fig 4.15, are constructed according to three ranges of passenger capacity. The first one considers airplanes with capacity ranging from 44 to 70 seats and is comprised of 7 individuals. The second database hosts airplanes transporting between 71 and 110 passengers and it has 24 configurations. Finally, the third database has 15 types of airplanes featuring between 111 and 180 seats. Thus, there are 2,520 potential three aircraft fleet combinations to be explored in the design space. Each aircraft in the databases is represented by the same aircraft definition parameters listed in Table 3.7 and designed following the methodology that was described in the preceding sections. However, in this case, the aircraft and engine design parameters are generated randomly within the allowed interval variation. Therefore, the airplanes that compose the databank feature different engine characteristics and configurations as well as different wing planform and airfoils. Fuselage seating abreast and passenger accommodation are other parameters that make the airplanes different from each other. For this, a specific *MATLAB* ® code, adapted from the former airplane module, is then used to generate the parameters for each aircraft and save them into the databases.

Fig.4.16a shows two kinds of DOCs: the cost per nautical mile flown (DOC1) and the cost per nautical mile per passenger. The tendency is clear that the larger the wing area, and therefore the passenger capacity, the larger the DOC1 is. DOC2 presents an inverse behavior to that registered for DOC1. Appendix G shows the characteristics of all 46 aircraft designs loaded in the databases. Some of the designs in the database are shown in Figure 4.16b.

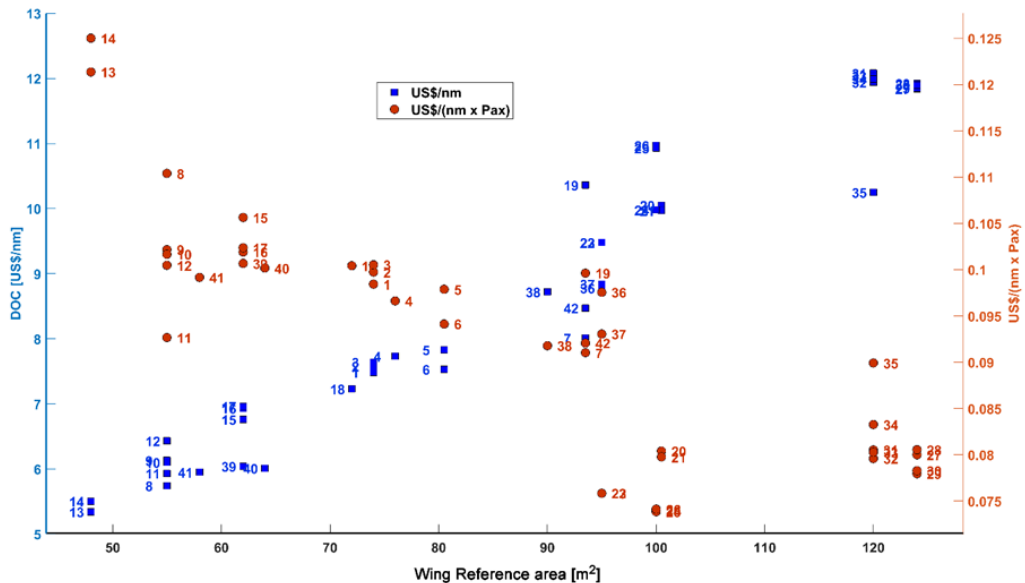


Figure 4.16a: US\$/nm and US\$(nm x Pax) as function of wing reference area
(databases aircraft)

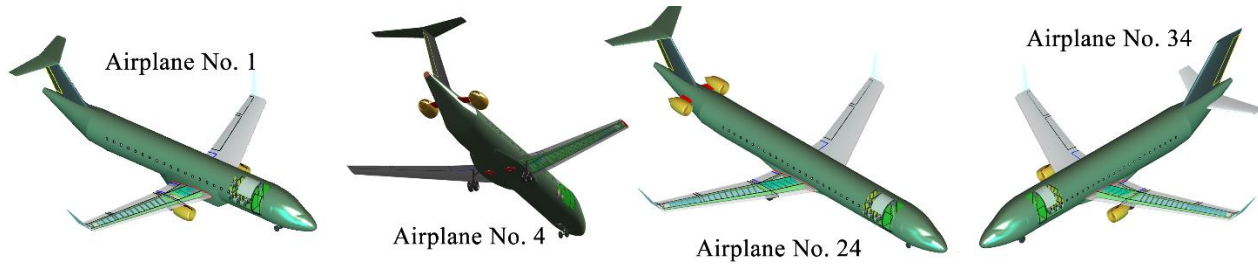


Figure 4.16b: Some airplanes that compose the database (not in same scale).

The Network Optimizer module provides the design variables (X_1 , X_2 , and X_3) generated via genetic algorithm (MOGA-II). These are continuous variables, corresponding to the position of an aircraft design (defined as a set of aircraft definition parameters) in each database. They vary in a range from 0% to 100%, meaning the relative position in each database the aircraft design is located. The GA parameters are set as follows: 50% probability of crossover, 5% probability of selection and 1% probability of mutation. A uniform Latin hypercube (ULH) is also used as sampling method to generate the starting points for the GA optimization. In this simulation, twenty individuals are initially created to compose the starting population of the process.

Once the designs are selected from the databases, the aircraft loader module reads the aircraft definition parameters and deliver them to the network optimization and mission performance modules for their calculations. The main difference is that now, three optimized networks are calculated simultaneously to exhaust the estimated demands between city pairs. The main assumption for the network optimization algorithm is that total daily passengers demand for each city pair is equally distributed among the three aircraft fleets. Once the networks are determined, the Mission Performance is run for each fleet to determine the trip fuel/time and associated DOC for each sector.

Finally, the Network Analysis module integrates fuel burn, trip time and DOC in all three networks, necessary to calculate the total network profit (NP), according to Eq.64. At this point, the total cash flow net present value (NPV) is also calculated through the summation of the values obtained for each aircraft type, determined according to Session 3.2.3. These two outputs are then provided as objective functions to the optimization module in each calculation cycle.

Simulation results

In this simulation, total computation time was 190.434 hours (7.93 days) in the same machine where the previous simulations were conducted. Each generation took an average of 56.3 min to be processed, due to the larger number of mission computations, significantly bigger than the previous single-fleet simulations. The GA produced in total 204 generations, distributed in 10 populations. From those, 113 individuals presented feasible outputs (55.4%) and 54 failed at the 30% IRR constraints (26.5%). Appendix H shows all simulation results, including key economic and network parameters.

Fig. 4.17 shows the individuals resulted from the optimization run considering the objective functions Network Profit (NP) and manufacturer's cash flow net present value (NPV), this time represented by the summation of the NPVs related to each of the three different designs. Individuals that maximize both NP and NPV are marked in green, composing the Pareto front. The unfeasible individuals, marked as yellow crosses, are the ones that failed in the 30% IRR limitation in any of the three aircraft designs and therefore excluded in the GA analysis. In addition, de individual marked in blue represents the single fleet baseline aircraft results for NP and NPV in its optimized network.

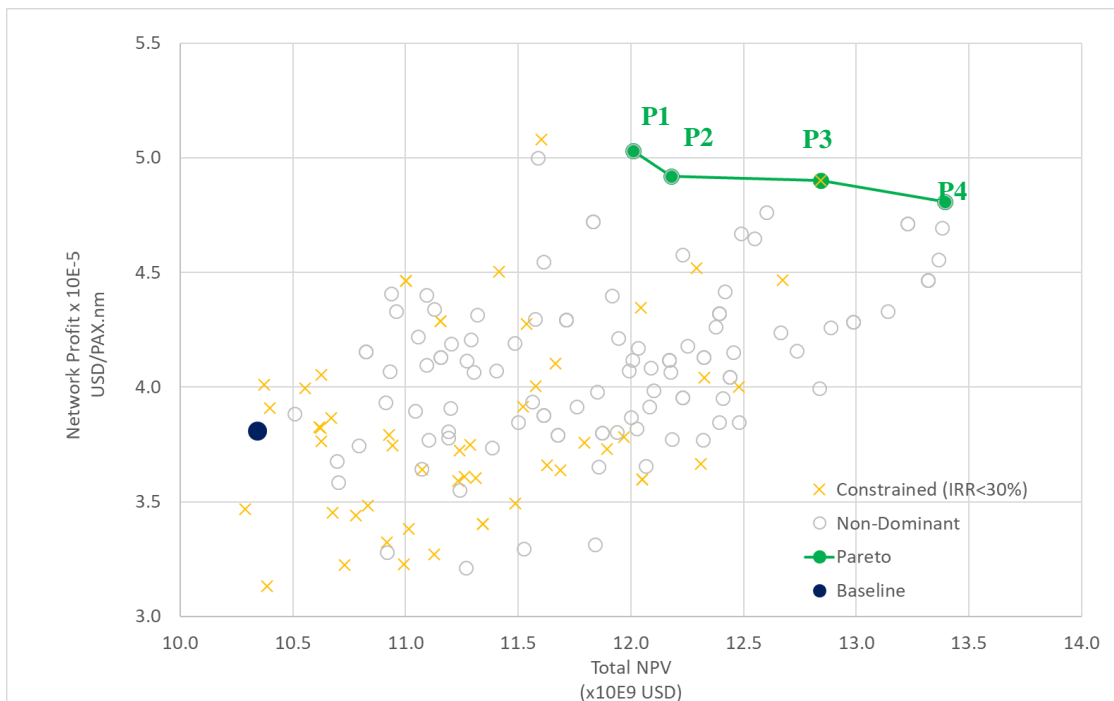


Figure 4.17 : Pareto front and dominated individuals (20 airports)

Table 4.16 shows relevant network and design characteristics related to the four individuals in the Pareto front (designs P1,P2,P3 and P4) resulted from the optimization task. As observed in previous simulations, two remarkable design extremes are identified: Maximum Network Profit (designs P1: 60 seats/4 abreast, 100 seats/5 abreast and 133 seats/6 abreast) and Maximum NPV (design P4: 60 seats/4 abreast, 105 seats/5 abreast and 174 seats/6 abreast). It is possible to identify common capacity aircraft (60-seater in fleet#1) in the extreme designs. The main difference in the Pareto front individuals is performed by fleet#2, with aircraft seating capacities between 77 to 105 seats.

Table 4.16: Individuals selected in the Pareto front (20 airports)

| Design ID | | NPax | NSeat | Design Range [nm] | MTOW [kg] | Wing Area [m ²] | Wing AR | D _e [m] | BPR | Network Number of connected arcs | Network Density | NPV [\$] x10 ⁹ | All Networks Profit [\$ /pax nm] x10 ⁵ |
|-------------------|-----|------|-------|-------------------|-----------|-----------------------------|---------|--------------------|-----|----------------------------------|-----------------|---------------------------|---|
| BASELINE AIRCRAFT | | 78 | 4 | 2000 | 38790 | 72.7 | 8.6 | 1.42 | 5.0 | 166 | 0.44 | 10.3 | 3.8 |
| P1 | AC1 | 60 | 4 | 1600 | 32344 | 70.0 | 9.3 | 1.44 | 5.5 | 166 | 0.44 | 12.0 | 5.0 MAX NP |
| | AC2 | 100 | 5 | 1000 | 45029 | 96.0 | 9.6 | 1.18 | 3.0 | 178 | 0.47 | | |
| | AC3 | 133 | 6 | 1950 | 58348 | 114.0 | 8.8 | 1.70 | 6.2 | 246 | 0.65 | | |
| P2 | AC1 | 60 | 5 | 1600 | 32344 | 70.0 | 9.3 | 1.44 | 5.5 | 166 | 0.44 | 12.2 | 4.9 |
| | AC2 | 77 | 5 | 1700 | 39512 | 91.5 | 8.3 | 1.34 | 4.9 | 172 | 0.45 | | |
| | AC3 | 144 | 5 | 1600 | 68601 | 128 | 9.0 | 1.62 | 5.6 | 278 | 0.73 | | |
| P3 | AC1 | 50 | 4 | 1400 | 24224 | 48.3 | 9.3 | 1.17 | 6.2 | 168 | 0.44 | 12.8 | 4.9 |
| | AC2 | 110 | 5 | 1900 | 50213 | 106.1 | 9.0 | 1.54 | 6.4 | 226 | 0.59 | | |
| | AC3 | 174 | 6 | 1600 | 68601 | 128.0 | 9.0 | 1.62 | 5.6 | 272 | 0.72 | | |
| P4 | AC1 | 60 | 4 | 1600 | 31390 | 70.0 | 9.3 | 1.47 | 5.9 | 170 | 0.45 | 13.4 MAX NPV | 4.8 |
| | AC2 | 105 | 5 | 1600 | 49229 | 99.20 | 9.3 | 1.48 | 5.5 | 220 | 0.58 | | |
| | AC3 | 174 | 6 | 1550 | 69530 | 124.6 | 9.4 | 1.57 | 5.3 | 270 | 0.71 | | |

The Pearson's correlation matrix is shown in Fig. 4.18 considering some key design variables related to fleet#2 (the largest database) and objective functions. As expected, the higher positive coefficients related to the MTOW are registered on dependencies related to wing area, design range and number of passengers. Engine diameter (proxy for engine size) is also positively influenced by number of passengers and wing area, which confirms the trend for bigger engines for bigger aircraft. It is noticeable that Network Profit presents the strongest negative dependency on range and positive dependency on number of passengers, meaning that the model captured the payload-range tradeoff as determinant characteristics on the airline profit. On the NPV side, the strongest positive dependencies are found in the variables related to the increase of the weight such as MTOW, number of passengers and wing area, according to predicted by the calculation module. These observations are also applicable to fleets #2 and #3.

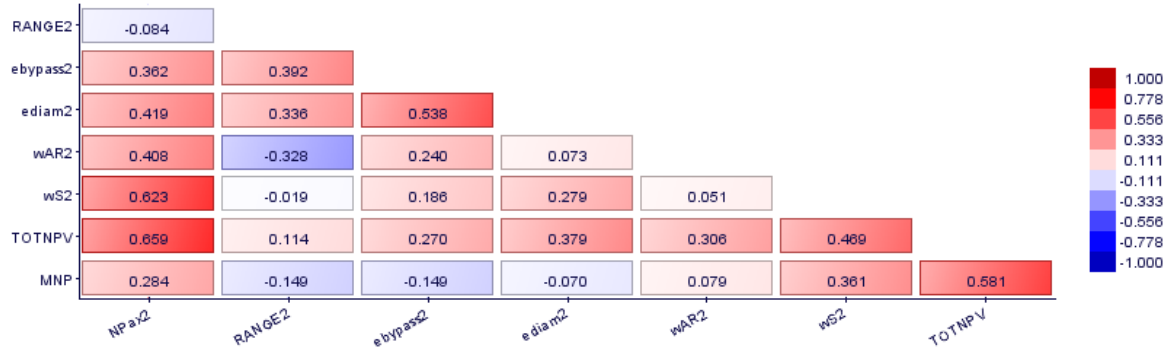


Figure 4.18: Aircraft Design #2 correlation Matrix (20 airports)

In Appendix I the complete pictorial information related to the integrated optimized network frequencies, route system, and some relevant aircraft characteristics related to the extremes and baseline designs are shown. For better visualization, network frequencies are displayed in shaded green cells (the darker are the cells, the higher are the associated number of frequencies).

From these pictures, it is noticed that the network optimization resulted on connecting routes between higher population density and wealth concentrations in all cases, especially in the southeast and some parts of the northeast areas of the country. For each network, the potential airport hubs are identified where the sum of the number of arrivals and departures and airport frequencies, or accumulated demands, are higher. They appear, consistently, at the most populated areas in Southeast (GRU, GIG, CGH and SDU) and at the higher population concentrations at Northeast area (FOR and SSA). Brasilia (BSB) also appears as natural hub in the central part of the country, which demand is mainly influenced by the proximity to the southern populated areas, associated to its higher econometric variables (GDP and BPI).

As concluded from the previous simulations, the longer route connections (POA-MAO and MAO-POA), were not computed as profitable and therefore excluded from all networks. As explained previously, this is mainly caused by the lower demand computed by the gravitational model, resulted from the combination of longer distances and relatively smaller population areas, when compared with other cities in the country. It may be also observed that the connections BSB-MAO, GYN-MAO, BSB-BEL and GYN-BEL demonstrated to feasible for the aircraft in fleet#3 Maximum NPV only (174 pax /6 abreast), where the highest revenue is in place. It is worth to mention that in actual Brazilian airlines networks, it is frequently observed the above mentioned locations connected with other cities of the country, which suggests that the adopted gravitational

demand model may be capturing extra demands or other exogenous aspects (such as government's incentives, national expansion plans, etc..) may be present. As expected, in both extremes the network's density and clustering increase proportionally to the seating capacity aircraft, since they capture the most part of the demand, bringing more frequencies to the system.

In both fleets #2 and #3 extremes an increase of aircraft capacity is observed, when compared with the baseline aircraft. With the objective to accommodate more passengers in the cabin, aircraft designs with wider fuselages are obtained providing 5 and 6 seat row configurations. In addition, an aircraft with capacity of 60 passengers and shorter range (1600 nm) arose from the optimization as solution for fleet #1 in most individuals of the Pareto front, meaning that this configuration may be more profitable in shorter connections than the baseline aircraft. Tables 4.19a , 4.19b and 4.19c show the results for both extremes networks, compared with a single fleet of baseline aircraft optimum network and between both extremes scenarios.

Table 4.17a: Results for the Maximum NP scenario (20 airports)

| Key Parameter | Optimum Network/ Baseline Aircraft | 3 Aircraft Family network | Difference | |
|---|---------------------------------------|------------------------------|-------------------|--------------|
| Total Distance flown [nm]/day | 495,827 | 502,694 | 6,867 | 1.4% |
| Total Passengers /day | 62,160 | 72,652 | 10,492 | 16.9% |
| Total Cost [US\$/day] | \$ 7,032,026.10 | \$ 7,753,043.82 | \$ 721,017.72 | 10.3% |
| Total Revenue [US\$]/day | \$ 8,205,120.00 | \$ 9,590,064.00 | \$ 1,384,944.00 | 16.9% |
| Profit [US\$]/day | \$ 1,173,093.90 | \$ 1,837,020.18 | \$ 663,926.28 | 56.6% |
| Annual Profit [US\$] | \$ 428,179,272.95 | \$ 670,512,364.93 | \$ 242,333,091.98 | 56.6% |
| Operational Margin [%] | 16.7 | 23.7 | 7.0 | 42.0% |
| NDOC [US\$/nm] | 10.9 | 12.9 | 1.94 | 17.8% |
| NP (US\$/pax.nm)x10E-5 | 3.8 | 5.0 | 1.2 | 32.2% |
| NPV [US\$x 10E9] | 10.3 | 12.0 | 1.7 | 16.1% |
| Aircraft Price [US\$ x 10E6] | 35.9 | 31.8/ 43.3/55.4 | - | - |
| Estimated Fleet size (# of aircraft) | 126 | 124 (24/38/62) | -2 | -1.6% |
| CAPEX [US\$ x 10E6] | 4523.4 | 5845.3 | 1321.9 | 29.2% |
| Return of Investment [years] | 10.6 | 8.7 | -1.8 | -17.5% |

Table 4.17b: Results for the Maximum NPV scenario (20 airports)

| Key Parameter | Optimum Network/ Baseline Aircraft | 3 Aircraft Family network | Difference | |
|---|---------------------------------------|------------------------------|-------------------|--------------|
| Total Distance flown [nm]/day | 495,827 | 520,400 | 24,573 | 5.0% |
| Total Passengers /day | 62,160 | 78,820 | 16,660 | 26.8% |
| Total Cost [US\$/day] | \$ 7,032,026.10 | \$ 8,374,551.94 | \$ 1,342,525.84 | 19.1% |
| Total Revenue [US\$]/day | \$ 8,205,120.00 | \$ 10,332,960.00 | \$ 2,127,840.00 | 25.9% |
| Profit [US\$]/day | \$ 1,173,093.90 | \$ 1,958,408.06 | \$ 785,314.16 | 66.9% |
| Annual Profit [US\$] | \$ 428,179,272.95 | \$ 714,818,942.56 | \$ 286,639,669.60 | 66.9% |
| Operational Margin [%] | 16.7 | 23.4 | 6.7 | 40.2% |
| NDOC [US\$/nm] | 10.91 | 13.4 | 2.50 | 22.9% |
| NP (US\$/pax.nm)x10E-5 | 3.8 | 4.8 | 1.00 | 26.3% |
| NPV [US\$x 10E9] | 10.3 | 13.4 | 3.0 | 29.5% |
| Aircraft Price [US\$ x 10E6] | 35.9 | 30.9/47.1/64.7 | - | - |
| Estimated Fleet size (# of aircraft) | 126 | 122 (22/42/58) | -4 | -3.2% |
| CAPEX [US\$ x 10E9] | 4523.4 | 6412.1 | 1888.7 | 41.8% |
| Return of Investment [years] | 10.6 | 9.0 | -1.6 | -15.1% |

Table 4.17c: Difference between Maximum NPV and Maximum NP scenarios (20 airports)

| Key Parameter | 3 Aircraft Family – Max NP | 3 Aircraft Family – MaxNPV | Difference | |
|--------------------------------------|----------------------------|----------------------------|-----------------|-------|
| Total Distance flown [nm]/day | 495,827 | 520,400 | 17,706 | 3.5% |
| Total Passengers /day | 62,160 | 78,820 | 6,168 | 8.5% |
| Total Cost [US\$/day] | \$ 7,032,026.10 | \$ 8,374,551.94 | \$ 621,508.12 | 8.0% |
| Total Revenue [US\$/day] | \$ 8,205,120.00 | \$ 10,332,960.00 | \$ 742,896.00 | 7.7% |
| Profit [US\$/day] | \$ 1,173,093.90 | \$ 1,958,408.06 | \$ 121,387.88 | 6.6% |
| Annual Profit [US\$] | \$ 428,179,272.95 | \$ 714,818,942.56 | \$44,306,577.62 | 6.6% |
| Operational Margin [%] | 16.7 | 23.4 | -0.3 | -1.3% |
| NDOC [US\$/nm] | 10.9 | 13.4 | 0.56 | 4.3% |
| NP (US\$/pax.nm)x10E-5 | 3.8 | 4.8 | -0.22 | -4.4% |
| NPV [US\$]x 10E9 | 10.3 | 13.4 | 1.4 | 11.5% |
| Aircraft Price [US\$ x 10E6] | 35.9 | 30.9/47.1/64.7 | | |
| Estimated Fleet size (# of aircraft) | 126 | 122 (22/42/58) | -2 | -1.6% |
| CAPEX [US\$ x 10E9] | 4523.4 | 6412.1 | 566.8 | 9.7% |
| Return of Investment [years] | 10.6 | 9.0 | 0.3 | 2.9% |

The Maximum NP solution leads to configurations presenting lower operational costs, mainly driven by lower fuel consumption. This is consequence of a relative decrease of TOW when compared with the maximum NPV extreme and also on slight increase on wing areas, aspect ratios and wing sweep angles revealing a trend from the algorithm to improve the specific range (therefore reducing trip fuel) and lower average cruise speeds (average Mach number). Engines also present increased bypass ratios (reaching a maximum of 6.2), towards the reduction of specific fuel consumption. In this scenario the Network Profit is increased by 32.2% when compared with the baseline aircraft network, bringing an annual profit about 663 Million US\$ to the airline. However, due to the fleet mix, the CAPEX is 29.2% higher than the baseline, representing an extra expenditure of 1.3 Billion US\$ on fleet investment.

The Maximum NPV solution leads to designs associated to higher sales revenues in the manufacturer's side, which means a larger number of aircrafts in the total fleet at higher sales prices. According to the proposed production and developments costs model, higher sales prices mean bigger aircraft and then higher MTOWs. This impacts significantly on fleet CAPEX, representing an increase of 41.8% related to the baseline, corresponding to approximately an extra 1.9 Billion US\$ fleet investment, more than three times the one required on the Maximum NP scenario. It is also observed that the maximum NPV also lead to a higher year profitability once more airplanes with higher capacity were inserted into the networks and therefore capturing the majority share of the demand. Heavier aircraft mean increasing the operational costs. In fact, although in this scenario the NPV is increased by 29.5%, there is a 19.1% increase on network direct operational cost, when compared with the baseline aircraft network. Due to the higher

profitability of both scenarios, the return of investment of the new fleets also was reduced by -1.8 (maximum NP) and -1.6 years (maximum NPV), when compared with the single aircraft baseline fleet.

As observed in previous simulations, when comparing both extreme scenarios it is possible to check that Maximum NPV scenario produces the highest maximum annual profit for the airline (6.6% more than the maximum NP, equivalent to an extra 44 Million US\$), due to the bigger capacity aircraft employed in the networks, although Network profit is -4.4% lower. This phenomenon produces an extra CAPEX to 566.8 Million US\$ to the airline, 9.7% more than the maximum NP scenario. This extra investment, would be compensated after 12.8 years, considering the difference of profits on both extremes.

This means that not always the biggest net profit corresponds to the best financial solution, since it depends pretty much on the fleet to be acquired and investment plan to be adopted. In this study we consider that the airline has plans to acquire all the fleet through a solid investment plan. In a more realistic scenario, however, airlines may elect a fleet leasing strategy in which acquisition may be performed in the end of a period. In this case, the leasing acquisition strategy would be included in the above financial analysis.

Finally, it is worth mentioning that in all fleets the wing aspect ratio relays within the range from 8.8 to 9.6 in the Pareto front. In fact, according to Mattos et. al [26], this is a reasonable range for this class of regional airplanes (passenger capacity topping 174 seats and maximum 2000-nm range), with no high-tech concepts such as extremely flexible wings or truss-braced configurations, which is the case. In addition, engines in all designs present increased parameters (eDiam, BPR, FPR, OPR) pressure when compared with the ones related to the baseline aircraft. This suggests also improvements towards the engines specific fuel consumption, and therefore a push for lower operational costs and therefore in accordance to higher profit objectives.

Sensitivity analysis

According to ABEAR [203], Brazilian airports historically present the most expensive JET-A1 prices in the world, representing and impact in the range of 40% to 50% on total operational costs of airlines. In fact, the average fuel price practiced in the Brazilian airports in 2017 corresponded to approximately 1.413 US\$/kg (considering fuel density of 0.81kg/l) [203], more than the double of the world average (0.65 US\$/kg, according to IATA [211]).

Considering such potential impact on DOC (and consequently profitability), a sensitivity analysis was carried out with the above 20-airport scenario to verify the impact of the fuel price on network topology and associated profitability. For that, the network optimization algorithm was run on the maximum network profit fleet (Design P1 of the Pareto front – 60,105 and 126 seating capacity designs), considering different scenarios of fuel price (taking the US\$1.413 as reference) and market shares. Table 4.18 shows the annual profit and network characteristics results considering the values of 50%, 100% and 150% of reference fuel price at three different market shares (15%, 20% and 25%). A minimum two connections per city pair for each aircraft type was set as constraint to better visualize the network effects.

From this table, two extreme scenarios are observed: the “Low Profit” (15% share/150% reference fuel price) and the “High Profit” (25% share/50% fuel price), corresponding to the shaded cells. It must be noted that the annual profit difference between both is approximately ten times in magnitude, showing how sensitive is the profitability of the network to fuel price and market share. The market share presents more influence on network density and clustering, as consequence of its parameter dependence on the overall demand: the higher is the market share the higher is the demand captured and more frequencies developed at all nodes (airports) of the network. In the other side, fuel price seems to provide a significant impact on the average degrees of node, which reflects on the number of route connections of each node of the network. In fact, since this parameter influences directly on direct operational costs (and therefore the profit of each route), more routes are disconnected from the network when the fuel price is increased.

Fig.4.19 illustrates graphically the combined impact such parameters on annual profit and network density. Fig.4.20a and Fig 4.20b show the 3-fleet network topologies regarding two “Low Profit” and “High Profit” scenarios. It is noticeable the significant increase of route connections of the last one, enabled by the lower operational costs and higher revenue capacity.

Table 4.18: Impact of fuel price and market share on airline profitability and network parameters

| Market Share | | 15% | | | | | | | | | |
|----------------------|----|----------------|--------|--------|--------|----------------|--------|--------|--------|----------------|--|
| % Ref Fuel Price | | 50% | | | 100% | | | 150% | | | |
| Fleet | | ACFT#1 | ACFT#2 | ACFT#3 | ACFT#1 | ACFT#2 | ACFT#3 | ACFT#1 | ACFT#2 | ACFT#3 | |
| N | | 37 | 51 | 67 | 31 | 37 | 53 | 29 | 31 | 39 | |
| L [nm] | | 451.7 | 628.0 | 785.5 | 373.6 | 451.7 | 650.0 | 352.4 | 373.6 | 478.0 | |
| ADON | | 1.9 | 2.5 | 3.4 | 1.6 | 1.9 | 2.6 | 1.4 | 1.6 | 1.9 | |
| ND | | 0.10 | 0.13 | 0.18 | 0.08 | 0.10 | 0.14 | 0.08 | 0.08 | 0.10 | |
| ACi | | 0.17 | 0.17 | 0.17 | 0.17 | 0.17 | 0.17 | 0.17 | 0.17 | 0.17 | |
| Total PAX | | 22670 | | | 17566 | | | 13892 | | | |
| Total Distance [nm] | | 205385 | | | 125489 | | | 80890 | | | |
| Annual Profit [US\$] | \$ | 143,929,476.87 | | | \$ | 108,663,541.07 | | | \$ | 107,393,958.55 | |

| Market Share | 20% | | | | | | | | |
|----------------------|---------------------|--------|--------|-------------------|--------|--------|-------------------|--------|--------|
| % Ref Fuel Price | 50% | | | 100% | | | 150% | | |
| Fleet | ACFT#1 | ACFT#2 | ACFT#3 | ACFT#1 | ACFT#2 | ACFT#3 | ACFT#1 | ACFT#2 | ACFT#3 |
| N | 94 | 120 | 158 | 70 | 94 | 120 | 66 | 70 | 100 |
| L [nm] | 533.9 | 649.7 | 808.9 | 415.0 | 533.9 | 649.7 | 399.1 | 415.0 | 560.9 |
| ADON | 4.7 | 6.0 | 7.9 | 3.5 | 4.7 | 5.3 | 3.3 | 3.5 | 5.0 |
| ND | 0.25 | 0.32 | 0.42 | 0.18 | 0.25 | 0.32 | 0.17 | 0.18 | 0.26 |
| ACi | 0.34 | 0.34 | 0.34 | 0.34 | 0.38 | 0.34 | 0.34 | 0.34 | 0.34 |
| Total PAX | 64248 | | | 52539 | | | 40203 | | |
| Total Distance [nm] | 561672 | | | 348049 | | | 237174 | | |
| Annual Profit [US\$] | \$ 521,349,365.49 | | | \$ 409,435,826.90 | | | \$ 284,780,928.95 | | |
| Market Share | 25% | | | | | | | | |
| % Ref Fuel Price | 50% | | | 100% | | | 150% | | |
| Fleet | ACFT#1 | ACFT#2 | ACFT#3 | ACFT#1 | ACFT#2 | ACFT#3 | ACFT#1 | ACFT#2 | ACFT#3 |
| N | 160 | 202 | 250 | 120 | 160 | 204 | 104 | 122 | 170 |
| L [nm] | 543.6 | 653.4 | 784.9 | 430.3 | 543.6 | 658.8 | 388.7 | 436.3 | 570.0 |
| ADON | 7.9 | 10.0 | 12.4 | 5.9 | 7.9 | 10.1 | 5.1 | 6.0 | 8.4 |
| ND | 0.42 | 0.53 | 0.66 | 0.32 | 0.42 | 0.54 | 0.27 | 0.32 | 0.45 |
| ACi | 0.65 | 0.65 | 0.65 | 0.65 | 0.65 | 0.65 | 0.65 | 0.65 | 0.65 |
| Total PAX | 119625 | | | 95514 | | | 77712 | | |
| Total Distance [nm] | 1024770 | | | 661902 | | | 456319 | | |
| Annual Profit [US\$] | \$ 1,116,961,459.61 | | | \$ 785,540,343.98 | | | \$ 567,545,852.62 | | |

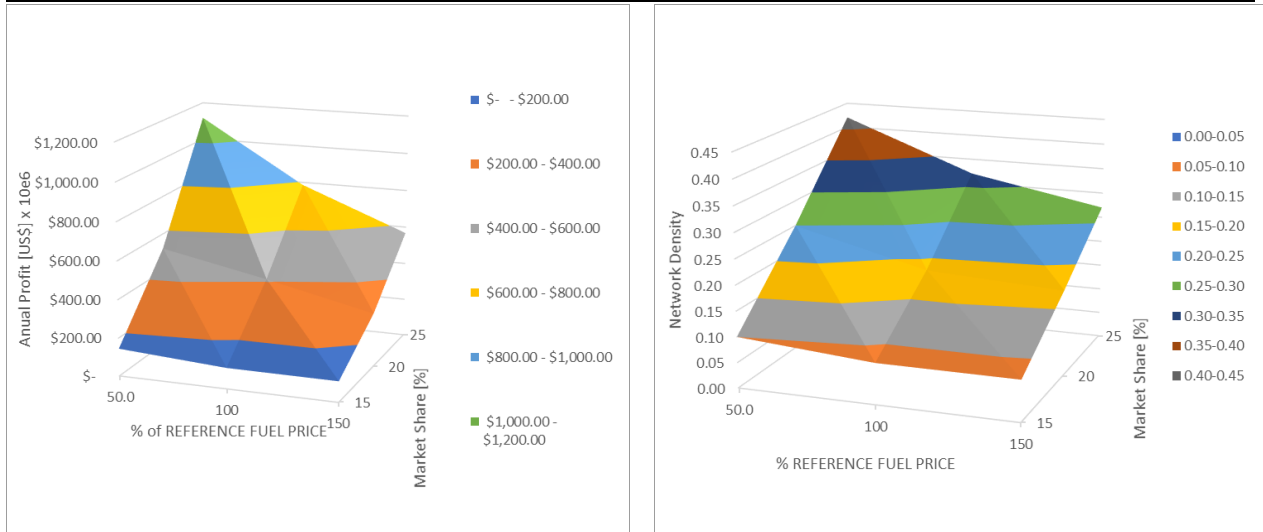


Figure 4.19: Effect of fuel price and market share on Annual Profit and Network Density



Figure 4.20a: Minimum Annual Profit scenario (15% Market Share /150% reference fuel price)
impact on max NP 3-fleet network topology

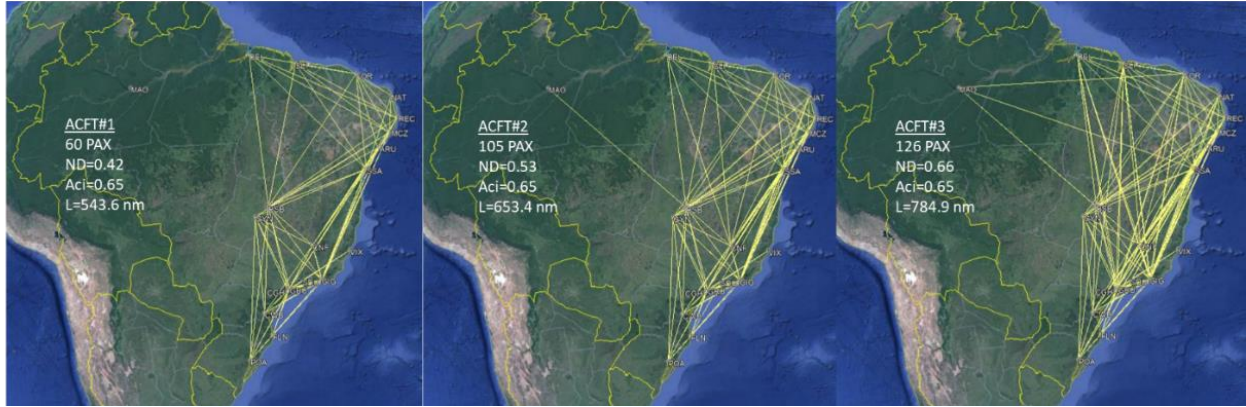


Figure 4.20b: Maximum Annual Profit Scenario (25% Market Share /150% reference fuel price) impact on max NP 3-fleet network topology

5. Conclusions

In this research, an innovative Multidisciplinary Design Optimization (MDO) framework was developed with the objective to optimize a highly detailed airplane design simultaneously with the associated airline network, for a given area of operations and associated demand, in a multiobjective-multivariable problem. Initially, a “hybrid MDF-CO” framework was proposed to sort this problem, where aircraft design and network computation frameworks (modules) are executed independently in sequenced blocks and wrapped into a genetic algorithm in the optimization process (MOGA-II algorithm).

In the aircraft design module, several design parameters (86 in total) were used to represent the airplane in finest detail with accurate aerodynamic, stability and control, and propulsion characteristics, necessary for the mission analysis of each route segment considered in the analysis network. The accurate calculation of a realistic mission profiles was performed thanks to the application of an ANN for aerodynamic coefficient estimation and a robust generic turbofan propulsion model (which includes a 4D compressor efficiency mapping methodology). A Weight Estimation sub-module was also part of the aircraft framework whose main objective is to estimate the mass of several aircraft components, in order to determine with reasonable accuracy, the MTOW and OEW of the aircraft generated in each cycle; moreover, parameters are also necessary in mission analysis computation. For the sophisticated methodologies for engine weight

estimation, fuselage sizing, landing gear sizing, tail sizing and center of gravity envelope were developed and applied.

After the execution of the aircraft design module, prior to running the network optimization module, performance and noise certification characteristics are checked to ensure of the feasibility produced by the design in each computation cycle. The network optimization framework was executed only if the design is evaluated to be feasible (check passed), otherwise this design is aborted and a new one is produced to continue with the optimization process.

In the network computation module, disciplines related to network optimization, mission performance and airline economics are integrated. The network optimization module is performed first in a sub-optimization framework using an elaborated gravitational demand model to predict passenger flows between city-pairs and a Mixed Integer Linear Program (MILP) algorithm to determine the necessary route frequencies for each city pair, considering the maximization of profit as objective function. Each route passengers demand (per day) was calculated via gravitational model and calibrated considering the passenger's domestic demand data related to the twenty busiest route city-pairs in Brazil, extracted from the Brazilian Civil Authority (ANAC) statistical database. A fixed load factor (85%), fuel price and ticket price were used in all sectors. Once the routes and frequencies were determined, the mission computation module runs a detailed mission calculation routine, considering typical airline flight planning dispatch calculation methodologies, with the objective to determine trip fuel, time and direct operational costs for each sector determined.

Finally, the airline economics module was developed to aggregate all sector parameters into network econometric results, computing the output parameters to be used as objective functions in the optimization. The computed output parameters produced by the simulation are: total network profit (NP - US\$/pax.nm), network direct operational costs (NDOC - US\$/nm), net present value of total development/production cash flow of the aircraft (NPV) and estimated number of aircraft (fleet size). Two sets of objective functions were studied, according to the optimization scope: airline operations optimization (considering NP and NDOC as objective functions) and airline/OEM optimization (considering NP and NPV as objective functions). Under this scope, four types of simulation scenarios were evaluated to apply the above described methodology. Their implementation and derived conclusions of each scenario are listed below:

Optimized Aircraft Design for a given network

This scenario corresponds to the determination of the best aircraft design that fits a given air transport network, with the objective to test the proposed MDO framework regarding aircraft design module. In this case, two main objective functions are evaluated: maximization of Network Profit (NP, corresponding to the total profit obtained per transport momentum unit expressed in PAX. nm) and minimization of Network Direct Operational Cost (NDOC). A comparison with the basic aircraft (78-seater regional jet) results on this network was performed.

Through this first simulation, two significant extreme designs could be identified in the Pareto front: The one corresponding to maximum NP and the other corresponding to Minimum NDOC and corresponding to significantly different design geometries. The minimum NDOC design corresponds to a lowest seating capacity (70 pax/6 seats abreast), with lower passenger capacity, lower cruise speed and consequently lower fuel consumption (which has a significant impact on mission DOC). In fact, this design presents a reduction of -11.9% in the NDOC when compared with the baseline aircraft. On the other hand, the design corresponding to the maximum NP corresponds to the biggest seating capacity aircraft (130 pax /6 seats abreast), seeking the highest revenue per leg. This growth leads to an increase of about five tons in the OEW, when compared with the baseline aircraft, impacting directly on fuel consumption increase. With such additional structure, the wing area was increased significantly to keep approximately the same wing loading, which impacts even also on the extra TOW contribution and consequently bigger fuel consumption. Due to this extra capacity, a significant 214% increase in NP is demonstrated, when compared with the baseline. However, due to the extra weight, an increase in NDOC is also observed.

It must be observed that the bigger aircraft obtained in the maximum NP design reduces the number of frequencies to exhaust the calculated demand. Because of this, the fleet size related to this aircraft design is reduced when compared with the basic aircraft fleet. Although the price of this aircraft is higher than the baseline, the fleet reduction brings a beneficial CAPEX reduction for the airline. This represents a financial advantage in case the fleet acquisition plan considers the full purchase of the fleet. In the evaluated scenario, an extra 89 Million USD in cash for the airline may be obtained selecting the Maximum NP design. In the NDOC design fleet, there is also a CAPEX advantage in a lower magnitude, mostly driven by the lower unit price. In this case, the total number of frequencies is slightly increased due to the smaller capacity of this design (70 pax) when compared with the baseline (78 pax).

Optimized network for a given aircraft design

The second simulation corresponds to the determination of optimum network topology considering a certain aircraft type, also a quite common request from airlines to aircraft manufacturers when evaluating the most profitable networks for certain aircraft types. For that, an adapted MILP model was used to determine the maximum Network Profit in a nested sub-optimization process, considering the aircraft capacity and DOC calculated for each sector. The same airports and operational conditions from the fixed network problem were considered. Also, the algorithm was applied to the extreme aircraft designs obtained in the previous run.

As a result of the optimization, sectors are removed in both maximum NP and minimum NDOC cases, where the lower demands are strongly influenced by the largest route distances of the network. However, specifically in the Maximum NPV design, where lower sector frequencies associated with bigger aircraft are present, certain routes become unprofitable due to the larger DOC and therefore are also switched from the network.

Consequently, a significant increase in NP is observed in these designs, even without certain sectors, when compared with the fixed network case fully connected. A side effect of sectors removal is the reduction in the average network path in all networks, which explains the slight increase in the associated NDOC in all designs. Another significant and interesting consequence of such kind of optimization is the reduction of the fleet CAPEX for the airline, once less sectors lead to the reduction of the fleet size. Such reduction is more significant in the higher capacity aircraft fleet (maximum NP design), reaching 25% in the proposed scenario. This compensates, by far, for the slightly lower annual profit of this design, a result of the lower number of frequencies.

Integrated network and aircraft design optimization

The third simulation run corresponds to the merging of the first two optimizations, where both aircraft design and network topologies were integrated in the proposed MDO cycle. Still in this case, the maximization of Network Profit (NP) and minimization of Network NDOC were performed and compared with the baseline aircraft. Simulations with five and ten airports, in the same operational area than previous runs, were conducted to check the robustness of the process and the impact of the number of airports on the computational cost. From the results, it was

observed that doubling the number of airports increased the computational time per cycle by approximately 3.3 times, suggesting that the inclusion of more airports in the network may impact significantly on the total computational time and therefore a more efficient computational process should be investigated for a wider scale network.

In both scenarios, a significant improvement on Network Profit (NP) was observed when compared with the fixed network/optimum aircraft and reference aircraft designs. However, the aircraft produced in the integrated optimization were slightly heavier than the ones optimized from the fixed network case, although they presented identical cabin capacity. The major difference between both scenarios is that the integrated designs presented a slightly higher cruise speed than the fixed network case.

It is interesting to note that the optimum network provides less city-pair connections when the aircraft size increases, since the demand is exhausted with reduced number of frequencies. As in the other simulations, the longest sectors are switched off, due to the lower demand determined by the gravitational model, with consequent decrease in the average path length and network density. Interestingly, the integrated design brought in both cases, significant increase in NP even transporting less passengers, when compared with the fixed network/optimum aircraft design. It must be noted, however, that the annual profit is slightly lower in the NP scenario than the correspondent in the optimum aircraft/fixed network. Also, a slight increase in NDOC is presented as a result of the reduction in the number of connected city pairs impacting on the total distance flown in the network.

Once again, a lower number of frequencies significantly impacting on the reduction of fleet size and consequently a lower CAPEX is observed, with faster return of investments. The largest CAPEX difference is also obtained in the maximum NP case confirming that the inclusion of such parameter as objective function to be minimized may bring an extra financial advantage to the airlines, specifically when defining their fleet acquisition plan. In addition, when compared with the baseline aircraft, the CAPEX reduction is even bigger, suggesting that the acquisition of the baseline aircraft may not represent a financial advantage for the airline, although producing some level of profit.

As a general conclusion, in single aircraft and network optimization, it may be observed that the fully connected network topology is not the optimum solution since this may lead to unprofitable sectors. All simulations demonstrated that the optimum networks are less connected (network density between 0.3 and 0.45) in which the Maximum Network Profit is associated with

higher capacity aircraft. In these cases, a lower fleet CAPEX is obtained and may represent an advantage if the airline has intention to acquire all the fleet through a solid investment plan. On the other hand, lower capacity aircraft are related to the minimum NDOC scenario, not representing the maximum annual profit. Therefore, this classical optimization approach should not be considered if airline's main objective is to maximize profit.

It may be concluded, from all simulations described above, that the proposed Flight Operations Optimization strategy (NP maximization and NDOC minimization set as objective functions) in the integrated aircraft and network optimization framework, brings not only the solution to the best network economic performance (near the highest annual profit) in airline operations, but also leads naturally to an optimized total number of aircraft in the fleet. This may be interpreted as result from the removal of the unprofitable sectors, having direct impact on aircraft size, fleet's CAPEX and consequent faster return of investment.

Integrated complex network and aircraft fleet optimization

In the last run of simulation, the complex network scenario where a fleet of three aircraft types and associated networks were optimized simultaneously was considered. The same operational area studied now considered a twenty key Brazilian airports network for each aircraft fleet. This combination would significantly increase the total computing time, estimated approximately 13 times more than the single aircraft optimization in ten airports. Considering that machine performance is therefore a significant factor, with the increased number of sectors and aircraft to optimize simultaneously, it was proposed to drop the aircraft design optimization process from the framework (where each design cycle takes approximately 7-10 min to run) and replace it with a database of 50 aircraft, composed of several topologies and seating configuration in the range of 44 to 180 seats and 4 to 6 abreast. This database was split into three subsets, based on seating configurations, which are accessed via genetic algorithm which determines the best fleet configuration for the associate optimum network in each cycle. With that, the networks for a selected triplet of aircraft are optimized simultaneously. It is important to mention that in this process, the total demand for each city pair was assumed to be split proportionally between the 3 selected aircraft type proportionally to their seating capacity. Therefore, the bigger the aircraft capacity, the bigger demand the fleet captures.

With this configuration, a new MDO cycle is proposed not considering the optimization variables and the position of the selected triplets of aircraft on each database. In addition, the objective functions were selected according to the Airline Operations and Aircraft Manufacturer's optimization set and maximization of network profit (NPV), from the airline side and the maximization of manufacturers' programs cashflow (NPV), from the manufacturer's side. In this case, a minimum return of investment (IRR) of 30% was set as limitation for the optimization. The complete cycle took approximately 5 times more than the single aircraft configuration in ten airports, representing a reduction of approximately 46% on the expected computational time if the complete aircraft design cycle was included.

In analogy on previous analysis, the simulation produced two remarkable design extremes in the Pareto front: Maximum Network Profit (designs P1: 60 seats/4 abreast, 100 seats/5 abreast and 133 seats/6 abreast) and Maximum NPV (design P4: 60 seats/4 abreast, 105 seats/5 abreast and 174 seats/6 abreast). Interestingly, it was possible to identify common capacity aircraft (60-seater in fleet#1) in both designs, corresponding to a different regional aircraft segment, with less capacity with the baseline aircraft, meaning that the baseline aircraft may not be the best regional aircraft for the Brazilian Scenario.

It was observed that the network optimization resulted in connecting routes between higher population density and wealth concentrations in all fleets, especially in the southeast and some parts of the northeast areas of the country. For each network, the potential airport hubs are identified where the sum of the number of arrivals and departures and airport frequencies, or accumulated demands, are higher. As concluded from the previous simulations, the longer route connections were not computed as profitable and therefore excluded from all networks. This is mainly caused by the lower demand computed by the gravitational model, which resulted from the combination of longer distances and relatively smaller population areas, when compared with other cities in the country.

However, different from the single aircraft and network simulations, where full city-pair demands were captured, in the 3-fleet case, the Maximum NP solution leads to configurations presenting lower operational costs, mainly driven by lower fuel consumption and therefore smaller aircraft are obtained in the fleet. This is a result of a relative decrease in TOW and a slight increase in wing areas, aspect ratios and wing sweep angles revealing a trend from the algorithm to improve the specific range (and lower average cruise speeds. Engines also present increased bypass ratios, towards the reduction of specific fuel consumption.

On the other hand, the Maximum NPV solution leads to designs associated with higher sales revenues, totally aligned with manufacturer's objectives, which means a larger number of bigger aircraft in the total fleet at higher sales prices. This increases the fleet CAPEX, representing an increase more than three times the one required on the Maximum NP scenario. However, interestingly, it was observed that the Maximum NPV solution produces the highest maximum annual profit for the airline, due to the bigger capacity aircraft employed in the networks.

Finally, a sensitivity analysis was performed in order to check how the annual profit and network topology respond to fuel price and market share. The 3-fleet simulation with twenty airports was also used, but in this case, varying the market share in a range of 15% and 25% and fuel price in a range of 50% to 150% of the reference fuel price (2017 average). It was observed that the market share presents more influence on network density and clustering, as a result of its parameter dependence on the overall demand: the higher the market share, the higher the demand captured and more frequencies developed at all nodes (airports) of the network. On the other hand, fuel price seems to provide a significant impact on the average degrees of node, which reflects on the number of route connections of each node of the network. In fact, since this parameter directly influences direct operational costs (and therefore the profit of each route), more routes are disconnected from the network when the fuel price is increased.

The annual profit difference between both the maximum profit scenario (higher market share and lowest fuel price) and the minimum profit scenario (lowest market share and highest fuel price) was approximately ten times in magnitude, showing how sensitive the profitability is to these two parameters.

Final remarks

This research study proposed new ways to evaluate optimization of aircraft and network designs, beyond the classical approach of minimizing DOC of one or more aircraft types in a fixed network. Here we proposed an innovative MDO approach where network and aircraft were designed simultaneously. Two different approaches for objective functions were selected to consider the profitability of the networks under airlines and aircraft manufacturers' objectives. In all cases, it was demonstrated that the fully connected networks with higher capacity aircraft is not always the best profitable solution. The maximization of Network Profit (NP) parameter set as one of the objective functions, lead to solutions close to the maximum annual profit, but with a

significant advantage for the airline in terms of minimization of fleet investment (CAPEX), in case of full fleet acquisition. On the other hand, maximization of the aircraft manufacturer's NPV leads to the maximization of the OEM profit, maximizing the fleet investment for the airline. In all cases, the annual profitability of the airline is always higher than the minimum DOC solution.

Airlines and aircraft manufacturers could, together, take advantage of the proposed methodology to better optimize the fleet, network and aircraft designs.

6. Areas of improvements and future work

Given the innovative aspect of this research, some model simplifications were performed to better develop the concepts proposed herein and expedite the computational time. Improvements on the methodology are suggested to provide even more realistic and faster results in the proposed MDO framework, for both aircraft and network modules. Future research may be expanded in the following topics:

- i. Although a sophisticated wing design optimization is adopted (an ANN surrogate model is used for drag and lift determination), only three fixed airfoil profiles were considered on relevant wing stations (tip, kink and root). An airfoil profile sub-optimization module, applied in more than three wing sessions, is suggested to be developed to better optimize the resulting wing.
- ii. The propulsion module could be expanded to consider a turboprop engine thermodynamic model. This would enable the analysis to be conducted in short range regional aviation scenarios. Also, a turbine efficiency map (as done with the compressor case) could be introduced in the engine thermodynamic models, either on turbofan or turboprop selections.
- iii. The flight profile could consider COST INDEX speed profile instead of fixed speeds for climb, cruise and descent phases. In this case, the speeds are optimized for minimum DOC during the aircraft operations, depending on the cost structure of each route flown by an airline.
- iv. The flight profile could consider step climb segments in cruise phase to fly as close as possible to the optimum altitude (minimum DOC based), as performed realistically in long range flights.
- v. The mission analysis could consider different fuel reserve policies, rather than ICAO rules.

- vi. Computation of Obstacle Climb limit of takeoff performance computations for each airport.
- vii. Adoption of a 4D atmospheric model (i.e. NOAA's) in order to estimate wind speed, direction and static air temperature at every point of the flight path, instead of using a fixed ISA deviation. This would significantly improve the performance computations, impacting on total flight time and fuel consumption.
- viii. A structural sub-optimization module may be developed, considering aeroelasticity aspects for aircraft design.
- ix. Airspace constraints could be inserted in flight path, both in lateral and vertical profiles. Airways tracking, speed and altitude limits related to the operational area shall be considered. This will lead to a more realistic flight profile instead of the great circle direct-to routing. Machine Learning methods could be used to determine the location of such constraints analyzing data from actual flights conducted in each city pair. ADS-B data is suggested to be used in such analysis.
- x. Actual demand data could be considered in the network optimization module to provide realistic calculations at a defined time snapshot.
- xi. Improvements on the gravitational demand model should be considered, including other types of variables, trying to capture specific exogenous factors.
- xii. Improvement on the NPV calculation model, considering market forecast models (such as the one proposed by Camarotti [212]) that influence aircraft price list.
- xiii. Adoption of parallel computing methods to improve the computation cost (calculation cycle).
- xiv. Code translation to an open source platform (i.e. Python), rather than MATLAB® and ModeFrontier® applications.

References

- [1] IATA, International Air Transport Association, "Economic performance of the airline industry," International Air Transport Association, Montreal, Canada, 2018.
- [2] IATA, International Air Transport Association, "Profitability and the air transport value chain," International Air Transport Association, Montreal, Canada, 2013.
- [3] R. Doganis, Flying Off Course IV: Airline Economics and Marketing, Routledge, 2009.
- [4] ICAO, International Civil Aviation Organization, "Group on International Aviation and Climate Change," ICAO, 2009, Montreal.
- [5] ICAO, International Civil Aviation Association, "Intergovernmental Panel on Climate Change (IPCC). Special Report on Aviation and Global Atmosphere. Special report from group I and III," ICAO, Montreal, Canada, 1999.
- [6] J. Fregnani and B. Mattos, "Aviation and Electrical Road Vehicles.," in *16th AIAA Aviation Technology, Integration, and Operations Conference*, Washington D.C., United States of America, 2016.
- [7] IATA, International Air Transport Association, "Operational Fuel Efficiency," International Air Transport Association, Montreal, Canada, 2015.
- [8] IATA, International Air Transport Association, "Technology Rodamap," International Air Transport Association, Montreal, 2013.
- [9] ICAO, International Civil Aviation Organization, "Resolution A39-3: Consolidated statement of continuing ICAO policies and practices related to environmental protection – Global Market-based Measure (MBM) scheme," ICAO, Montreal, 2018.
- [10] ATAG, Air Transport Action Group, "Beginner's Guide to Aviation Efficiency," Geneva, Switzerland, 2014.
- [11] The Boeing Company, "Jet Transport Performance Methods," Boeing Commercial Aircraft, Seattle, 2015.
- [12] B. Mattos, J. Fregnani and P. Magalhães, Conceptual Design of Green Transport Airplane, Book Series: Frontiers in Aerospace Science ed., Sharja: Benthan Books, 2018.
- [13] D. J. Caetano and N. D. F. Gualda, "A Flight Schedule and Fleet Assignment Model," in *12th World Conference on Air Transport Research*, Lisbon (Portugal), 2010.
- [14] T. Grosche, F. Rothlauf and A. Heinzl, "Gravity models for airlines passenger volume estimation," *Journal of Air Transport Management*, pp. 175-183, 2007.
- [15] O. Wojan, "Airline Network Structure and the Gravity Model," University of Hamburg and Lufthansa Technik AG, Hamburg, 2000.
- [16] W. E. O'Connor, An introduction to airline economics, Westport, United States of America: Greenwood Publishing Group, 2001.
- [17] D. Klabjan, "Large-scale models in the airline industry," *Column generation*, pp. 163-197, 2005.
- [18] A. Rabetanety, J. Calmet and C. Schoen, *Airline Schedule Planning Integrated Flight SCHEDULE Design and Product Line Design*, Karlsruhe: University of Karlsruhe, 2006.
- [19] C. Hane, C. Barnhart, C. Johnson, E. Marsten, R. Nemhauser and G. Sigismondi, "The fleet assignment problem: solving a large-scale integer program," Georgia Institute of Technology, 1995.
- [20] H. Gurkan, S. Gurel and M. Akturk, "An integrated approach for airline scheduling, aircraft fleeting and routing with cruise speed control," *Transportation research Part C-Emerging Technologies*, vol. 68, pp. 38-57, 2014.
- [21] M. Streetly, All the World's Aircraft: In Service Yearbook 17/18, London, UK: IHS Markit, 2018.
- [22] P. Magalhães and B. Mattos, "Conceptual optimal design of environmentally friendly airliners: a review of available methodologies and their integration into a consistent framework for everyday use," in *16th AIAA/ISSMO Multidisciplinary Analysis and Optimization Conference*, 2015.
- [23] E. Torenbeek, Advanced Aircraft Design, Wiley & Sons, 2013.
- [24] J. Roskam, Airplane Design Part I - Preliminary Sizing of Aircraft, DARcorporation, 1999.
- [25] P. Shmollgruber, Enhancement of the conceptual aircraft design process through certification constraints management and full mission simulations, Toulouse: Université Fédérale Toulouse Mid-Pyrénées, 2018.

- [26] B. S. Mattos, J. A. Fregnani and P. C. Magalhães, Conceptual Design of Green Transport Airplane., Book Series: Frontiers in Aerospace Science ed., vol. 3, Bentham Books, 2018.
- [27] M. Kruse, T. Wunderlich and L. Heirich, "A conceptual study of a transonic NLF transport aircraft with forward swept wings," in *30th AIAA Applied Aerodynamics Conference*, New Orleans, USA, 2018.
- [28] C. P. Taylor, "Integrated transportation system design optimization," Boston, United States of America, 2007.
- [29] G. Bower and I. Kroo, "Multiobjective Aircraft Optimization for minimum cost and emissions over specific route networks," in *8th AIAA ATIO*, 2008.
- [30] B. S. Mattos and N. R. Secco, "An Airplane Calculator Featuring a High-Fidelity Methodology for Tailplane Sizing," *Journal of Aerospace Technology and Management*, vol. 5, pp. 371-386, 2013.
- [31] P. J. Lederer and R. S. Nambimandom, "Airline Network Design," *Operations Research*, pp. 7865-804, 1998.
- [32] D. Bing, "Reliability Analysis for Aviation Airline Network Based on Complex Network," *Journal of Aerospace Technologies Management*, vol. 6, no. 2, pp. 193-201, 2014.
- [33] S. Sobieski, "Multidisciplinary design optimization: An emerging new engineering discipline," NASA-TM-107761, 1993.
- [34] J. R. Martins and A. B. Lambe, "Multidisciplinary design optimization: a survey of architectures," *AIAA journal*, pp. 2049-2075., 2013.
- [35] D. Raymer, Aircraft Design: A conceptual approach. 5th Edition and RDSWin STUDENT, Washington,D.C: American Institute of Aeronautics and Astronautics, 2012.
- [36] L. Schimt, "Structural Design by Systematic Synthesis. 2nd Conference on Electronic Computation," New York, 1960.
- [37] R. Haftka, "Automated Procedure for Design of Wing Structures to Satisfy Strength and Flutter Requirements," Hampton,VA, 1973.
- [38] H. Ashley, "On Making Things the Best — Aeronautical Uses of Optimization," *Journal of Aircraft*, vol. 19, no. 1, pp. 5-28, 1982.
- [39] B. Grossman, R. Haftka, P. Kao, D. Polen and M. Rais-Rohani, "Integrated Aerodynamic-Structural Design of a Transport Wing," *Journal of Aircraft*, vol. 27, no. 12, pp. 1050-1056, 1990.
- [40] R. Haftka, J. Sobieski and S. Padula, "On options for interdisciplinary analysis and design optimization," *Structural optimization*, vol. 4.2, pp. 65-74, 1992.
- [41] E. Cramer, J. Dennis, P. Frank, R. Lewis and G. Shubin, "Problem Formulation for Multidisciplinary Optimization," *SIAM Journal on Optimization*, pp. 754-776, 1994.
- [42] R. J. Balling and J. Sobieszczanski-Sobieski, "Optimization of coupled systems - A critical overview of approaches," *AIAA Journal*, vol. 34, 1996.
- [43] N. Alexandrov and M. Hussaini, Multidisciplinary design optimization: State of the art, vol. 80, SIAM, 1997.
- [44] J. Sobieski and R. Haftka, "Multidisciplinary aerospace design optimization: survey of recent developments," *Structural Optimization*, vol. 14.1, pp. 1-23, 1997.
- [45] I. Kroo and R. Shevell, Aircraft design: Synthesis and analysis, Desktop Aeronautics Inc., 2001.
- [46] A. T. Isikveren, "Quasi-Analytical Modelling and Optimisation Techniques for Transport Aircraft Design," Royal Stockholm of Technology (KTH), Stockholm, 2002.
- [47] R. Henderson, "Multidisciplinary Design Optimization of Airframe and Engine for Emissions Reduction," Master Thesis, University of Toronto, Toronto, 2009.
- [48] P. Magalhães and B. Mattos, "Conceptual optimal design of environmentally friendly airliners: a review of available methodologies and their integration into a consistent framework for everyday use," in *16th AIAA/ISSMO Multidisciplinary Analysis and Optimization Conference, AIAA AVIATION Forum*, Dallas,TX, 2015.
- [49] L. K. Loftin, Subsonic aircraft: Evolution and the matching of size to performance (NASA reference publication), National Technical Information Service, 1980, p. 441.
- [50] N. Queipo, R. Hafka, W. Shyy, T. Goel and R. Vaidyanathan, "Surrogate-based analysis and optimization," *Progress in Aerospace Science*, vol. 41, no. 1, pp. 1-28, January 2005.
- [51] S. Arlinghaus, PHB Practical Handbook of Curve Fitting, Boca Raton, United States: CRC Press, 1984.
- [52] G. Box and N. Draper, Response Surfaces, Mixtures, and Ridge Analyses, Second Edition ed., Willey, 2007.

- [53] J. Park and I. Sandberg, "Universal approximation using radial-basis-function networks," *Neural Computation*, vol. 3(2), pp. 246-257, 1991.
- [54] C. Cortes and V. Vapnik, "Support-vector networks," *Machine Learning*, vol. 20, no. 3, pp. 273-297, 1995.
- [55] J. Bandler, R. Biernacki, S. Chen, P. Grobelny and R. Hemmers, "Space mapping technique for electromagnetic optimization," *Transactions on Microwave Technology*, vol. 42, no. 12, pp. 2356-2544, 1994.
- [56] N. V. Queipo, R. Haftka, S. Shyy, T. Goel, R. Vaidyanathan and P. K. Tucker, "Surrogated Based Analysis and Optimization," *Progress in Aerospace Sciences*, pp. 1-28, 2005.
- [57] I. Cardenas, "On the use of Bayesian networks as a meta-modeling approach to analyse uncertainties in slope stability analysis," *Georisk: Assessment and Management of Risk for Engineered Systems and Geohazards*, vol. 17, no. 4, pp. 53-65, 2019.
- [58] N. R. Secco and B. S. Mattos, "Artificial Neural Networks Applied to Airplane Design," in *53rd AIAA Aerospace Sciences Meeting, AIAA SciTech Forum*, 2015.
- [59] R. Fisher, *The design of experiments*, Edinburgh,UK: Macmillan, 1937.
- [60] B. Tang, "Orthogonal array-based Latin hypercubes," *Journal of the American statistical association*, vol. 824, pp. 1392-1397, 1993.
- [61] I. Sobol, "Distribution of points in a cube and approximate evaluation of integrals," *U.S.S.R Comput. Maths. Math. Phys.*, vol. 7, pp. 8-112, 1967.
- [62] M. McKay, R. Beckman and W. Conover, "A Comparison of Three Methods for Selecting Values of Input Variables in the Analysis of Output from a Computer Code," *Technometrics*, vol. 21, no. 2, pp. 239-245, 1979.
- [63] J. R. Martins and A. Lambe, "Extensions to the Design Structure Matrix for the Description of Multidisciplinary Design, Analysis, and Optimization Processes," *Structural and Multidisciplinary Optimization*, vol. 2, no. 46, pp. 273-284, 2012.
- [64] N. P. Tedford and J. R. Martins, "Benchmarking multidisciplinary design optimization algorithms," *Optimization Engineering*, pp. 159-183, 2003 2009.
- [65] J. R. Martins, "A Short Course on Multidisciplinary Design Optimization - University of Michigan," 2016. [Online]. Available: <http://mdolab.engin.umich.edu/>.
- [66] J. Arora, "Introduction to optimum design - PhD Thesis," Standford University, Pallo Alto, United States of America, 2005.
- [67] J. Nocedal and S. Wright, *Numerical Optimization*, 2nd Edition ed., Springer, 2006.
- [68] K. Leoviriyakit, "Wing Planform Optimization via an Adjoint Method.PhD Dissertation," Standford,United States, 2005.
- [69] Y. Nestorov, *Introductory Lectures on Convex Optimization. A Basic Course*, New York, United States of America: Springer, 2004.
- [70] M. R. Hestenes and E. Stiefel, "Methods of Conjugate Gradients for Solving Linear Systems," *Journal of Research of the National Bureau of Standards*, December 1952.
- [71] R. Tappeta and J. Renauld, "Multiobjective Collaborative Optimization," *Journal of Mechanical Design*, vol. 119, pp. 403-401, 1997.
- [72] K. Miettinen, *Nonlinear Multiobjective Optimization*, Kluwer Academic Publishers, 1998.
- [73] S. Sobieski, J. B. Jaroslaw and D. R. Agustine, "Structural otimization by multi-level decomposition," *AIAA Journal*, pp. 1775-1782, 1985.
- [74] C. Coello, G. Lamont and D. Veldhuizen, *Evolutionary Algorithms for Solving Multi-Objective Problems*, Urbana, United States of America: Springer, 2007.
- [75] S. Kirkpatrick, C. Gelatt and M. Vecchi, "Optimization by Simulated Annealing," *Science*, vol. 220, pp. 671-680, 13 May 1983.
- [76] J. Kennedy and R. Eberhart, "Particle Swarm Optimization," in *Proceedings of IEEE International Conference on Neural Networks. IV. pp. 1942–1948.* , Perth, Australia, 1995.
- [77] M. Boyandi and Z. Michalewitz, "A locally convergent rotationally invariant particle swarm optimization algorithm," in *Swarm Intelligence*, vol. 8, Springer, 2014, pp. 159-198.
- [78] B. Mattos, *Notas de Aula do Curso AP-266 "Projeto de Otimização Multidisciplinar"*. Aula 3, Sao José dos Campos, Brasil: Instituto Tecnológico de Aeronáutica, 2016.

- [79] M. Dorigo and M. Birattari, "Ant Colony Optimization," in *Encyclopedia of Machine Learning*, Boston, United States, Springer, 2010.
- [80] M. Zlochin, M. Birattari, N. Meuleau and M. Dorigo, "Model-based search for combinatorial optimization: A critical survey," *Annals of Operations Research*, vol. 131, pp. 373-395, 2004.
- [81] J. Holland, *Adaptation in natural and artificial systems*, Michigan University Press, 1975.
- [82] M. D. McKay, R. J. Beckman and W. J. Conover, "A comparison of three methods for selecting values of input variables in the analysis of output from computer code," *Technometrics*, pp. 55-61, 2000.
- [83] J. Roberts, M. Agnello, J. Silveira, P. Prado and J. Freire Junior, "GAtoolbox: a Matlab-based Genetic Algorithm," in *THE 12th LATIN-AMERICAN CONGRESS ON ELECTRICITY GENERATION AND TRANSMISSION - CLAGTEE*, 2017.
- [84] L. V. Cabral, P. Paglione and B. S. Mattos, "Multi-Objective Design Optimization Framework for Conceptual Design of Families of Aircraft," in *44th AIAA Aerospace Sciences Meeting and Exhibit*, Reno, 2006.
- [85] L. Siqueira, B. S. Mattos and V. Loureiro, "The Suited Airliner for an Existing Airline Network," in *50th AIAA/ASME/ASCE/AHS/ASC Structures, Structural Dynamics, and Materials Conference*, California, 2009.
- [86] J. Fregnani and B. Mattos, "An Example of Genetic Algorithms Applied to Multidisciplinary Design Optimization," *Journal of the Brazilian Air Transportation Society*, vol. 1, no. 1, 2018.
- [87] C. M. Fonseca and P. J. Fleming, "Genetic Algorithms for Multiobjective Optimization: Formulation, Discussion and Generalization," in *Proceedings of the Fifth International Conference*, San Mateo (CA), 1993.
- [88] A. Zalzala and P. Fleming, *Genetic Algorithms in Engineering Systems*, The Institute of Electric Engineers, 1997.
- [89] J. Shaffer, "Multiple objective optimization with vector evaluated genetic algorithms," in *Proceedings of the First International Conference on Genetic Algorithms and Their Applications*, 1985.
- [90] C. Fonseca and P. Fleming, "Genetic Algorithms for Multiobjective Optimization: Formulation, Discussion and Generalization," *Icgaa*, vol. 93, 1993.
- [91] J. Horn, N. Nafpliotis and D. Goldberg, "A niched Pareto genetic algorithm for multiobjective optimization. Proceedings of the First IEEE Conference on," in *IEEE World Congress on Computational Intelligence*, Orlando, United States, 1994.
- [92] T. Murata and H. Ishibuchi, "MOGA: multi-objective genetic algorithms," in *Proceedings of 1995 IEEE International Conference on Evolutionary Computation*, Perth, Australia, 1995.
- [93] E. Zitzler and L. Thiele, "Multiobjective evolutionary algorithms: a comparative case study and the strength Pareto approach," in *IEEE Transactions on Evolutionary Computation*, 1999.
- [94] R. Sarker, K. Liang and C. Newton, "A new multiobjective evolutionary algorithm," *European Journal of Operational Research*, vol. 140, no. 1, pp. 12-23, 2002.
- [95] D. Kalyanmoy, A. Patrap, S. Agarwal and T. Meyarivan, "Fast and Elitist Multiobjective Genetic Algorithm: NSGA-II," *Transactions of Evolutionary Computation*, vol. 6, no. 2, p. IEEE, 2002.
- [96] K. Deb, *Multi-objective optimization using evolutionary algorithms*, Reston, USA: AIAA, 2009.
- [97] K. Deb, A. Pratap, S. Agarwal and T. Meyarivan, "A fast and elitist multiobjective genetic algorithm: NSGA-II," in *IEEE Transactions on Evolutionary Computation*, 2002.
- [98] D. Zinng, M. Nemee and T. Pulliman, "A Comparative Evaluation of Genetic and Gradient-Based Algorithms Applied to Aerodynamic Optimization," *Shape design in aerodynamics REMN*, vol. 17, pp. 103-126, 2008.
- [99] T. Aykin, "The hub location and routing problem," *European Journal of Operational Research*, vol. 83, pp. 200-219, 1993.
- [100] L. Young and R. Kornfield, "Examination of the Hub-and-Spoke Network: A Case Example Using Overnight Package Delivery," in *41st Aerospace Sciences Meeting and Exhibit*, American Institute of Aeronautics and Astronautics, Reston, Virginia, 2003.
- [101] J. F. Campbell, "Integer Programming formulations of discrete hub location programming," *European Journal of Operational Research*, pp. 387-405, 1994.
- [102] R. K. Ahuja, T. L. Magnanti, J. B. Orlin and M. R. Reddy, "Applications in Network Optimization," in *Handbooks of Operations Research and Management Science*, Kanpur (India), 1995, pp. 1-83.

- [103] P. Jaillet, G. Song and G. Yu, "Airline Network Design and Hub Allocation Problems," *Location Science*, vol. 4, pp. 195-212, 1996.
- [104] A. D. Evans, A. Schafer and L. Dray, "Modelling Airline Network Routing and Scheduling under Airport Capacity Constraints," in *26th Congress of International Council of the Aeronautical Science*, Anchorage, 2008.
- [105] D. J. Caetano and N. D. Gualda, "An exact model for airline flight network optimization based on transport momentum and load factor," *Transportes*, pp. 14-26, 2017.
- [106] H. Sawai, "Reorganizing a new generation airline network based on an ant-colony optimization-inspired small-world network.,," in *Congress on Evolutionary Computation*, 2012.
- [107] J. Pita, C. Barnhart and A. Antunes, "Integrated flight scheduling and fleet assignment under airport congestion," *Transportation Science*, vol. 47, no. 4, pp. 477-492, 2012.
- [108] Z. Dong, C. Yu and H. Hyk, "An integrated flight scheduling and fleet assignment method based on a discrete choice model," *Computers & Industrial Engineering*, vol. 98, pp. 195-210, 2016.
- [109] E. Taaffe, "Trends in airline passenger traffic: A geographic case study," *Annals of the Association of American Geographers*, vol. 49, no. 4, pp. 393-408, 1959.
- [110] E. Taaffe and L. King, "Geography in an Urban Age: Networks of cities," Association of American Geographers, Washington,DC, 1966.
- [111] A. Kanafani, *Transportantion Demand Analysis*, McGraw-Hill, 1983.
- [112] R. Ceha and H. Ohta, "Prediction of Future Origin Destination Matrix of Air Passengers by Fratar and Gravity Models," *Computers & Industrial Engineering*, vol. 33, no. 3-4, pp. 845-848, 1997.
- [113] R. Piermartini and L. Rousová, "Liberalization of Air Transport Services and Passenger Traffic. Staff Working Paper ERSD-2008-06," World Trade Organization, Economic Research and Statistics Division, Geneve, 2008.
- [114] T. Hazdeline, "Border effects for domestic and international Canadian passenger air travel," *Journal of Air Transport Management*, vol. 15, pp. 7-13, 2009.
- [115] D. Bhadra and J. Kee, "Structure and dynamics of the core US air travel markets: a basis empirical analysis of domestic passenger demand," *Journal of Air Transport Management*, vol. 14, pp. 27-39, 2008.
- [116] O. Olariaga, N. Bolívar, R. Gutiérrez and O. Galeana, "Gravitational analysis of the air transport network. Application to the case of Colombia," *Transportation Research Procedia*, vol. 33, pp. 51-58, 2017.
- [117] N. Davendralingam and W. Crossley, "Robust Optimization of Aircraft Design and Airline Network Desing Incorporating Econometric Trends," in *11th AIAA Aviation Technology*, 2010.
- [118] W. A. Crossley and M. Mane, "System of Systems Inspired Aircraft Sizing Applied to Commercial Aircraft / Airline Problems," in *AIAA 5th Aviation, Technology, Integration, and Operations Conference (ATIO)*, Arlington, 2005.
- [119] Nusawardhana and W. A. Crossley, "Concurrent Aircraft Design and Variable Resource Allocation in Large Scale Fleet Networks," in *9th AIAA Aviation Technology, Integration, and Operations Conference (ATIO)* , 2009.
- [120] G. Roth and W. Crossley, "Commercial transport aircraft conceptual design using a genetic algorithm based approach," in *7th AIAA/USAF/NASA/ISSMO Symposium on Multidisciplinary Analysis and Optimization, Multidisciplinary Analysis Optimization Conferences*, St. Louis, 1998.
- [121] J. Cavalcanti, B. S. Mattos and P. Paglione, "Optimal Conceptual Design of Transport Aircraft," in *11th AIAA/ISSMO Multidisciplinary Analysis and Optimization Conference* , Portsmouth, 2006.
- [122] L. Versiani, P. Paglione and B. Silva de Matos, "Multi-Objective Design Optimization Framework for Conceptual Design of Families of Aircrafts," in *44th AIAA Aerospace Sciences Meeting*, 2006.
- [123] C. Taylor and O. Week, "Integrated Transportation Network Design Optimization," in *47th AIAA Conference*, 2006.
- [124] M. Mane, W. Crossley and A. Nusawardhana, "SYystems-of-sytems Inspired Aircraft Sizing and Airline Resource alocation via Decomposition," *Journal of Aircraft*, pp. 1222-1235, 2007.
- [125] A. Nusawardhana and W. Crossley, "Allocating Variable Resources over a Finite Time Horizon to Combine Aircraft Sizing and Airline Planning," in *AIAA 5th ATIO Conference*, Reston, United Sates, 2005.

- [126] L. Siqueira, V. Loureiro and B. Silva de Mattos, "The Suited Airliner for an Existing Airline Network," in *11th AIAA*, 2009.
- [127] M. Braun, K. Wicke and A. Koch, "Analysis of Natural Laminar Flow Aircraft based on Airline Network Design and Fleet Assignment," in *11th AIAA Aviation Technology, Integration, and Operations (ATIO) Conference, Aviation Technology, Integration, and Operations (ATIO) Conferences*, Virginia Beach,VA, 2011.
- [128] N. Davendralingam and W. Crossley, "Robust Approach for concurrent aircraft desing and airline network design," *Journal of Aircraft*, vol. 51, no. 6, pp. 1773-1783, 2014.
- [129] N. Davendralingam and W. Crossley, "Concurrent aircraft design and network design incorporating passenger demand models," in *9th AIAA Aiation Technology*, 2009.
- [130] J. Hwang, S. Roy, J. Martis and W. Crossley, "Simultaneous aircraft allocation and mission optimization using a modular adjoint approach," in *56th AIAA/ASCE/AHS/ASC Structures, Structural Dynamics, and Materials Conference, AIAA SciTech Forum*, Kissimee,FL, 2015.
- [131] J. Hwang and J. Martins, "Parallel allocation-mission optimization of a 128-route network," in *16th AIAA/ISSMO Multidisciplinary Analysis and Optimization Conference, AIAA AVIATION Forum*, Datals,TX, 2015.
- [132] J. T. Hwang and J. R. Martins, "Allocation-mission-design optimization of next-generation aircraft using a parallel computational framework," in *57th AIAA/ASCE/AHS/ASC Structures, Structural Dynamics, and Materials Conference, AIAA SciTech Forum*, San Diego, 2016.
- [133] S. Roy, K. Moore, J. Hwang, J. Gray, W. Crossley and J. Martins, "A mixed integer efficient global optimization algorithm for the simultaneous aircraft allocation-mission-design problem," in *58th AIAA/ASCE/AHS/ASC Structures, Structural Dynamics, and Materials Conference, AIAA SciTech Forum*, Grapevine, Texas, 2017.
- [134] S. Roy, "A Mixed Integer Efficient Global Optimization Framework: Applied to the Simultaneous Aircraft Design, Airline Allocation and Revenue Management Problem - Doctoral Dissertation," Pardue University, 2017.
- [135] S. Roy and W. Crossley, "An EGO-like Optimization Framework for Simultaneous Aircraft Design and Airline Allocation," in *57th AIAA/ASCE/AHS/ASC Structures, Structural Dynamics, and Materials Conference*, San Diego,CA, 2016.
- [136] S. Roy, W. Crossley, K. Moore, J. Gray and J. Martins, "Next generation aircraft design considering airline operations and economics," in *2018 AIAA/ASCE/AHS/ASC Structures, Structural Dynamics, and Materials Conference, AIAA SciTech Forum*, (AIAA 2018-1647), Kissimee,FL, 2018.
- [137] K. Wilcox and S. Wakayama, "Simultaneous Optimization of a Multiple-Aircraft Family," *Journal of Aircraft*, vol. 40, no. 4, pp. 616-622, 2003.
- [138] J. Fregnani, B. Mattos and J. Hernandes, "An Innovative Approach for integrated Airline Network and Aircraft Family Optimization," in *AIAA Aviation 2019*, Dallas, United States, 2019.
- [139] ESTECO, "Optimization with modeFrontier," ESTECO, May 2017. [Online]. Available: <http://www.esteco.com/modefrontier/optimization-modefrontier>. [Accessed May 2017].
- [140] Federal Aviation Administraion, FAA, "14CFR36 Noise Standards and Airworthiness Certification Am.29," FAA, Washington, 2013.
- [141] Department of Defense, DOD, "Flying Qualities of Piloted Aircraft MIL-HDBK-797," US Department of Defense (DOD), Washington, 1992.
- [142] D. Raymer, "Enhancing Aircraft Conceptual Design using Multidisciplinary Optimization - Doctoral Thesis," Royal Institute of Technology, 2002.
- [143] ICAO, International Civil Aviation Organization, Annex 16 to the Convention of International Civil Aviation - Volume I. Aircraft Noise, Montreal: ICAO, 2008.
- [144] J. Roskam, Airplane Design Part II - Preliminary configuration, Lawrence: DAR Corporation, 2003, p. 209.
- [145] J. Roskam, Airpalne Design Part V - Component Weight Estimation, Lawrence, USA: DAR Corporation, 2003.
- [146] A. T. Isikveren, "Quasi-analytical modelling and optimisation techniques for transport aircraft design," Stockholm, Sweden, 2002.

- [147] E. Onat and G. Klees, "A method to estimate weight and dimensions of large and small gas turbine engines," Boeing Military Airplane Development, Seattle, USA, 1979.
- [148] M. Tong, I. Halliwell and L. Ghosn, "A computer code for gas turbine engine weight and disk life estimation," in *ASME Turbo Expo 2002: Power for Land, Sea, and Air*, 2002.
- [149] P. Lolis, "Development of a preliminary weight estimation method for advanced turbofan engines - PhD Thesis," CRANFIELD UNIVERSITY SCHOOL OF ENGINEERING, Cranfield, UK, 2004.
- [150] E. Greitzer, "Design methodologies for aerodynamics structures weight and thermodynamic cycles, Final_Report, Vol. 2.," Massachussets Intitute of Technology, Boston, USA, 2010.
- [151] MathWorks, "Genetic Algorithm," MathWorks, December 2017. [Online]. Available: <https://www.mathworks.com/discovery/genetic-algorithm.html>. [Accessed December 2017].
- [152] Jane's, "Jane's Aero Engines," IHS Markit, December 2017. [Online]. Available: <https://janes.ihs.com/>.
- [153] N. Currey, Aircraft Landing Gear Design: Principles and Practices, Reston, USA: AIAA, 1988.
- [154] D. Sholz, "Script for aircraft design. Lecture Notes," Hamburg University of Applied Sciences. Department of Automotive and Aeronautical Engineering,, Hamburg, Germany, 1999.
- [155] Bishop GmbH, "PresTo-Cabin. A preliminary sizing tool for passenger aircraf cabin - Documentation and user manual," Aero, Hamburg, Germany, 2015.
- [156] K. Marckwardt, "Documents for the lecture aircraft design," Hamburg University of Applied Sciences, Department of Automotive Engineering, Hamburg, Germany, 1998.
- [157] IATA, International Air Transport Association, "ATA ULD Regulations Manual (Unit Load Devices)," International Air Transport Association, Montreal, Canada., 2018.
- [158] National Aeronautics and Space Administration, "NASA STD 3000B (Volume I). Man Systems Integration Standards," National Aeronautics and Space Administration, Cape Canaveral (FL), USA, 1995.
- [159] B. Mattos and N. Secco, "An Airplane claculator featuring a high-fidelity methodology for tailplane sizing," *Journal of Aerospace Technology and Management*, pp. 371-386, 4 5 2013.
- [160] J. Roskam, Methods for estimating stability and control derivatives of conventional subsonic airplanes, Kansas: DAR, 1971.
- [161] Federal Aviation Administration, FAA, "14CFR25 Airworthiness Standards: Transport Cathegory Airplanes. Subpart B," FAA, Washington, USA, 2017.
- [162] D. Scholz, "PreSTO - Aircraft Preliminary Sizing Tool - From Requirements to the Three-view Drawings," in *EWADE 2011 - 10th Workshop on Aircraft Design Education*, Naples, Italy, 2011.
- [163] Massachussets Institute of Technology, MIT, "Aerodynamics Vortex Lattice Software.," [Online]. Available: <https://acdl-web.mit.edu/software>. [Accessed 10 01 2019].
- [164] B. Stevens, F. Lewis and E. Johnson, Aircraft control and simulation: dynamics, controls design, and autonomous systems, John Wiley & Sons, 2015.
- [165] J. Hodgkinson, Aircraft Handling Qualities. AIAA Education Series, Reston, USA: AIAA, 1998.
- [166] N. R. Secco and B. S. Mattos, "Artificial neural networks to predict aerodynamic coefficients of transport airplanes," *Aircraft Engineering and Aerospace Technology*, vol. 89, no. 2, pp. 211-230, 2017.
- [167] B. S. Mattos, "Numerischer Entwurf von transsonischen Flügeln und Tragflügelprofilen unter Anwendung des AF2-Algorithmus zur Lösung de vollständigen Potentialgleichung," Universität Stuttgart, Stuttgart, 1995.
- [168] B. S. Mattos, A. Puppin-Macedo and D. Silva Filho, "Considerations about Winglet Design," in *21st AIAA Applied Aerodynamics Conference*, 2003.
- [169] H. Sobieczki, "Parametric Airfoils and Wings," *Notes on Numerical Fluid Mechanics*, vol. 68, pp. 71-88, 1998.
- [170] M. Levenberg, "A Method for the Solution of Certain Problems in Least-Squares," *Quartely Applied Mathematics*, pp. 164-168, 1944.
- [171] D. Marquardt, "An Algorithm for Least-squares Estimation of Nonlinear Parameters," *SIAM Journal Applied Mathematics*, pp. 431-441, 1963.
- [172] M. J. Powell, "A Fortran Subroutine for Solving Systems of Nonlinear Algebraic Equations," in *Numerical Methods for Non-linea Algebraic Equations*, P. Rabinowitz, Ed., 1970.

- [173] G. W. Brune and J. W. McMasters, Applied Computational Aerodynamics, Vols. 125 - Progress in Aeronautical Series, P. A. Henne, Ed., Washington, D.C.: American Institute of Aeronautics and Astronautics, Inc., 1990.
- [174] B. Singh, "A Medium-Fidelity Method for Rapid Maximum Lift Estimation," Delft University, Delft, 2017.
- [175] M. Drela, "XFOIL - Subsonic Airfoil Development System," October 2018. [Online]. Available: <http://web.mit.edu/drela/Public/web/xfoil/>. [Accessed October 2018].
- [176] C. P. van Dam, "The aerodynamic design of multi-element high-lift systems," *Progress in Aerospace Sciences*, vol. 38, pp. 101-144, 2002.
- [177] D. E. Hoak, The USAF Stability and Control DATCOM. Chapter 8 - High Lift Systems and Maximum Lift, Air Force Wright Aeronautical Laboratories, 1978.
- [178] V. Loureiro, "Optimum design of transport airplanes with realistic engine model. Undergraduation Thesis," Technological Institute of Aeronautics (ITA), São Jose dos Campos, Brazil, 2008.
- [179] T. Benson, "An interactive educational tool for turbojet engines," in *AIAA 31st Joint Propulsion Conference Exhibit*, 1995.
- [180] National Aeronautics and Space Administration, "EngineSim Version 1.8a," Glenn Research Center, 01 06 2016. [Online]. Available: <https://www.grc.nasa.gov/WWW/K-12/airplane/ngnsim.html>. [Accessed 01 06 2016].
- [181] W. Visser, "Generic Analysis Methods for Gas Turbine Engine Performance: The development of the gas turbine simulation program GSP - Doctoral Thesis," TU Delft, Amsterdam, Netherlads, 2015.
- [182] P. Magalhães, "Multi-objective multi-disciplinary optimization applied to the conceptual design of airliners for minimal environmental impact. Masters Degree Thesis," Technological Institute of Aeronautics (ITA), São José dos Campos, 2014.
- [183] M. Smith, Aircraft Noise, Cambridge,UK: Cambridge University Press, 1989.
- [184] O. Zaporozhets, V. Tokarev and K. Attenborough, Aircraft Noise:Assessment, prediction and Control, Moscow, Russia: CRC Press, 2011.
- [185] C. C. Robusto, "The cosine-harvesine formula," *The Americal Mathematical Monthly*, vol. 64, no. 1, pp. 30-40, 1957.
- [186] M. Newman, "The Structure and Function of Complex," *SIAM Review*, vol. 45, pp. 167-225, 2003.
- [187] The Boeing Company, "Jet Transport Performance Methods," Boeing Commercial Aircraft, Seattle, USA, 1998.
- [188] ICAO, International Civial Aviation Organization, "Manual of the ICAO Standard Atmosphere - Doc.7488/3, Third Edition," Montreal, 1993.
- [189] ICAO, International Civial Aviation Organization, "Annex 11 to the Convention on International Civil Aviation - Air Traffic Services," Montral, 2001.
- [190] ICAO, International Civil Aviation Organization, "Manual of Implementation of a 300m (1000ft) vertical Separation Minimum between FL290 and FL410 - Doc 9574," Montreal, 2002.
- [191] Agência Nacional de Aviação Civil (ANAC), "Regulamento Brasileiro de Aviação Civil No.121 - Requisitos Operacionais: Operações Domésticas, Suplementares e de Bandeira," Brasília, 2010.
- [192] J. Fregnani, C. Muller and A. Correia, "A fuel tankering model applied to a domestic airline network," *Journal fo Advanced Transportation*, pp. 386-398, 2011.
- [193] J. Roskam, Airplane Design, Part VIII - Airplane Cost Estimation: Design, Development, Manufacturing and Operating, Ottawa, Canada: DAR Corporation, 1999.
- [194] Embraer, "Embraer 145 Aircraft Operations Manual - Vol.1," Empresa Brasileira de Aeronáutica, São José dos Campos, 2008.
- [195] Airline Pilots Central, "Airlines Pilots Central - Crew Salaries Database," 10 06 2018. [Online]. Available: <https://www.airlinepilotcentral.com/>. [Accessed 10 06 2018].
- [196] EUROCONTROL, "Standard Inputs for EUROCONTROL Cost-Benefit Analyses - Edition 8.0," Eurocontrol, Brussels, Belgium, 2018.

- [197] L. Siqueira, V. Loureiro and B. Silva de Mattos, "The Suited Airliner for an Existing Airline Network," in *50th AIAA/ASME/ASCE/AHS/ASC Structures, Structural Dynamics, and Materials Conference, Structures, Structural Dynamics, and Materials and Co-located Conferences*, Palm Springs, California, 2009.
- [198] Bombardier Commercial Aircraft , "Bombardier Commercial Aircraft Market Forecast 2009 - 2028," Bombardier Commercial Aircraft, Montréal, Canada, 2009.
- [199] D. Morrison, K. James and R. Hansman, "Game theory analysis of the impact of single-aisle aircraft competition on emissions," *Journal of Aircraft*, pp. 483-494, 2012.
- [200] Airbus SAS, "Airbus 2018 Price List - Press Release," 10 06 2018. [Online]. Available: <https://www.airbus.com/newsroom/press-releases/en/2018/01/airbus-2018-price-list-press-release.html>. [Accessed 10 06 2018].
- [201] C. A. Coello, G. A. Lamont and D. A. van Veldhuizen, *Evolutionary Algorithms for Solving Multi-Objective Problems*, Springer, 2007.
- [202] E. Rigoni and S. Poles, "NBI and MOGA-II, two complementary algorithms for Multi-Objective optimizations," in *Dagstuhl Seminar Proceedings. Schloss Dagstuhl-Leibniz-Zentrum für Informatik*, 2005.
- [203] Associação Brasileira de Empresas Aéreas, ABEAR, "Panorama da Aviação Brasileira. Dados e estatísticas," ABEAR, 2017. [Online]. Available: <http://panorama.abear.com.br/dados-e-estatisticas/tarifas/#c>. [Accessed 30 04 2017].
- [204] G. F. Newell, "Airport Capacity and Delays," *Transportation Science*, pp. 201-241, 1979.
- [205] Instituto Brasileiro de Geografia e Estatística, IBGE, "Estatística do IBGE - Download," 22 02 2017. [Online]. Available: <https://www.ibge.gov.br/estatisticas/downloads-estatisticas.html>. [Accessed 22 02 2017].
- [206] ANAC, Agencia Nacional de Aviação Civil, "Anuário do Transporte Aéreo - Banco de dados digital," Agencia Nacional de Aviação Civil (ANAC), 2014, 2015 and 2016. [Online]. Available: <http://www.anac.gov.br/assuntos/dados-e-estatisticas/mercado-de-transporte-aereo/anuario-do-transporte-aereo/dados-do-anuario-do-transporte-aereo>. [Accessed 30 Janeiro 2018].
- [207] A. Kanafani, *TRANSPORTATION DEMAND ANALYSIS*, New York: McGraw-Hil, 1983.
- [208] D. Bertsimas and J. Tsitsiklis, *Introduction to linear optimization*, Belmont, USA: Athena Scientific, 1997.
- [209] Airbus , "A320 AIRCRAFT CHARACTERISTICS - AIRPORT AND MAINTENANCE PLANNING," Airbus SAS Customer Services, Toulouse, France, 2019.
- [210] Agência Brasileira de Aviação Civil, "Anuário de Transporte Aéreo 2017," ANAC, Brasília, 2018.
- [211] IATA, International Air Transport Association, "IATA Fuel Jet Price Monitor," International Air Transport Association, [Online]. Available: <https://www.iata.org/publications/economics/fuel-monitor/Pages/index.aspx>. [Accessed 10 02 2018].
- [212] V. B. Camarotti, "Estudo de Drivers de Mercado, Metodologia e Desenvolvimento de Ferramenta Semi-Automática para Elaboração de Projeções de Mercado de Aviação de Linha," undergraduate thesis, Instituto Tecnológico de Aeronáutica, São José dos Campos, 2014.
- [213] NASA Glenn Research Center, "EngineSim Version1.8a," NASA, 2016. [Online]. Available: <https://www.grc.nasa.gov/WWW/K-12/airplane/enginesim.html>. [Accessed 30 January 2018].
- [214] Brazilian Airspace Control Department, "Aeronautical Information Publication (AIP) - AGA Part," Institute of Aeronautical Cartography, Rio de Janeiro, 2016.
- [215] H. Gurkan, S. Gurel and S. Altuk, "An integrated approach for airline scheduling, aircraft fleeting and routing with cruise speed control," *Transportation Research*, vol. Part C, pp. 38-57, 2016.
- [216] Y. Zang, "Solving Large-Scale Linear Programs by Interior-Point Methods under MATLAB environment," Baltimore, 1995.
- [217] A. K. Kundu, *Aircraft Design*, Cambridge University Press, 2010.
- [218] J. C. Medau, *Allocation of aircraft to flights considering aircraft operational, maintenance and performance restrictions*, São Paulo: University of São Paulo, 2017.
- [219] ICAO, Internationa Civil Aviation Organization, "Mitigation of Climate Change - Contributions of Working Group III to the Fourth Assessment of the Intergovernmental Panel on Climate Change (IPCC)," Cambridge University Press, New York, 2007.
- [220] Airbus Industries, "Getting to Grips with Fuel Efficiency," Airbus, Toulouse, France, 2003.

- [221] P. Nolte, "Quantitative Assessment of Technology Impact in Aviation Fuel Efficiency," in *Air Transport Operations Symposium*, Amsterdam, 2012.
- [222] J. Mankins, "Technology Readiness Levels," Office of Space Access and Technology, NASA, 1995.
- [223] Intergovernmental Panel on Climate Change, "Mitigation of Climate Change - Contribution of Working group III to the Fourth Assessment of the IPCC," Cambridge University Press, New York, 2007.
- [224] Wikipedia, "Fuel Economy in Aircraft," Wikipedia, the Free Encyclopedia, 11 May 2016. [Online]. Available: https://en.wikipedia.org/wiki/Fuel_economy_in_aircraft. [Accessed 28 May 2016].
- [225] P. C. Magalhães and B. S. Mattos, "Conceptual optimal design of environmentally friendly airliners: a review of available methodologies and their integration into a consistent framework for everyday use," in *16th AIAA/ISSMO Multidisciplinary Analysis and Optimization Conference*, Dallas, 2015.
- [226] B. Singh, "A Medium-Fidelity Method for Rapid Maximum Lift Estimation," Delft University, Delft, 2017.
- [227] Brazilian Airspace Control Department, DECEA, "Brazilian Aeronaautical Information Publication (AIP)," Ministério da Aeronáutica, Rio de Janeiro, Brazil, 2019.
- [228] W. O'Connor, An introduction to airline economics, Greenwo publishing group, 2001.
- [229] H. Schlichting and E. Truckenbrodt, Aerodynamics of the Airplane, McGraw-Hill Companies, 1970.